Development of clippase-based tools for studying ubiquitin and ubiquitin-like modification systems

Doctoral thesis

for

the award of the doctoral degree

of the Faculty of Mathematics and Natural Sciences

of the University of Cologne

submitted by

Susanne Kolek

in the year 2026

Table of content

Abstract

The post-translational modification by the small modifier ubiquitin regulates virtually all cellular processes and is indispensable for protein homeostasis, cell proliferation and cell survival. In recent years, a plethora of mass spectrometry-based methodologies have been developed to elucidate ubiquitin targets, their individual modified sites and cellular ubiquitin chain architectures. Further, studies aimed to get a holistic insight into the modifications by the ubiquitin-like proteins Nedd8, ISG15 and SUMO.
However, current studies employ either very complex strategies to discern between modifiers, which are often conflated due to their primary sequence similarities, or disregard their conflation altogether.
The characterization of several members of a novel class of deubiquitinating enzymes of bacterial origin paved the way to utilize them in mass spectrometry-based studies of ubiquitin and ubiquitin-like modification systems. These enzymes ‘clip’ within the modifiers C-terminus, leaving a GlyGly-remnant at the modification sites. Due to their unusual mode of action, these enzymes were termed clippases. One of the characterized enzymes is BpJOS from *Burkholderia pyrrocinia*, which exhibits exceptionally high activity against ubiquitin while acting promiscuously on all ubiquitin chain types. On top, BpJOS is inert against the modifier ISG15.
Based on the activity of BpJOS, two different mass spectrometry-based methodologies were developed to fill in the gaps left by the currently available, established protocols. First, the easy-to-apply method termed ‘Clippomics’ was conceptualized. This method allows for the distinguishment between ubiquitin and ISG15 sites in complex samples upon in-parallel treatment with the published ISG15-targeting clippase Lbpro. Moreover, BpJOS treatment alone enables specifically the identification of ubiquitin sites in presence of ISG15. By that, the shifts in the ubiquitome upon interferon-stimulation, as occurring under infection conditions, were studied. Both applications serve as proof-of-concepts for their use in ensuing studies, as the ‘Clippomics’ method makes further genetic manipulation for the distinguishment of ubiquitin and ISG15 dispensable and can be used on a wide array of samples.
Second, BpJOS was utilized for the investigation of ubiquitin chain linkages in *in vitro* studies. The ‘Ubi clipping with BpJOS’ methodology is inspired by the ‘Ub-clipping’ approach utilizing Lbpro. The clippase-generated GlyGly-remnants by treatment of ubiquitin chains allow for the in-depth characterization of present chain linkages and architectures. This process is optimized by the high activity of BpJOS against ubiquitin compared to the published Lbpro clippase.
Taken together, BpJOS was identified as a powerful, multi-faceted tool for the elucidation of ubiquitin and ubiquitin-like modifications. Both developed methodologies harbor great potential to significantly contribute to the research field of modification systems.

1 Introduction

1.1 Ubiquitin

Discovered in 1975, the 8.5kDa small protein ubiquitin was soon found to be a universal constituent of living cells (Goldstein et al., 1975). First wrongly assigned to be present in bacteria as well, it was discovered to be exclusively present in eukaryotes. In the ensuing years, ubiquitin was found to be covalently attached to histone H2A, whereby the first ubiquitin substrate was identified (Hunt & Dayhoff, 1977; Levinger & Varshavsky, 1980). Shortly after, ubiquitin was discovered to be covalently linked to ATP-dependent proteolysis factor 1 (APF-1), which was followed by its proteolytic breakdown (Ciechanover et al., 1980; Ciehanover et al., 1978). These findings established ubiquitin as a protein modifier and a cellular signaling platform. Ubiquitin is highly conserved across eukaryotic organisms and present in virtually all cellular compartments, cell types and tissues. This high degree of preservation and ubiquitous presence demonstrates its pivotal role in living cells. The crystal structure of ubiquitin was solved in 1987 and gave opportunity to biochemically study its functions as a modifier (Vijay-Kumar et al., 1987). The 76 amino acid ubiquitin protein harbors a compact globular fold, a flexible C-terminus and seven internal lysine residues (Figure 1B,C).

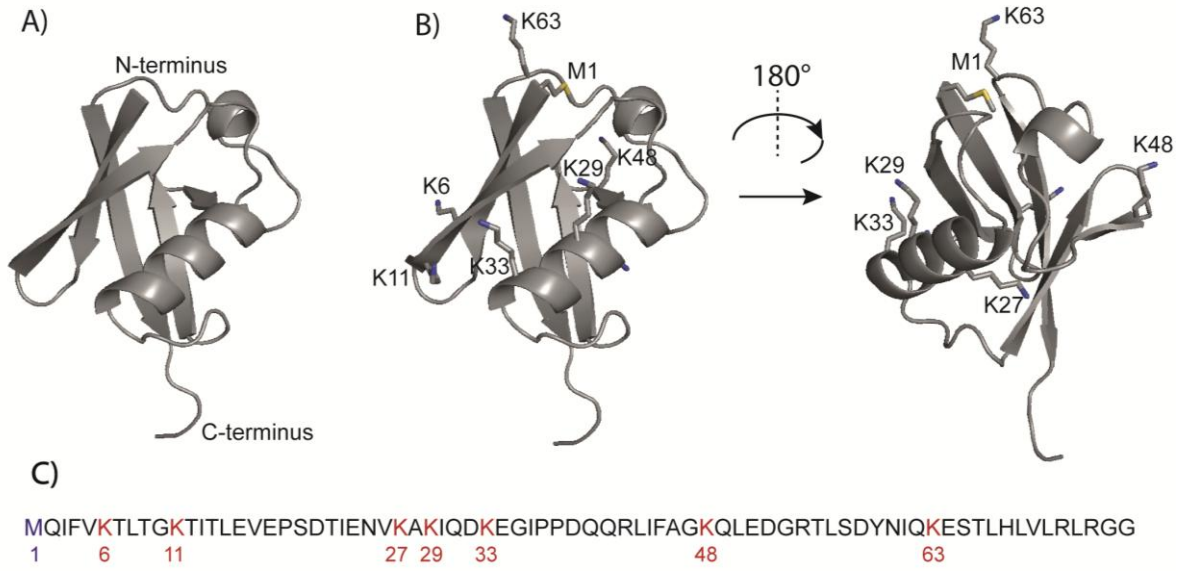

Figure 1: Crystal structure and primary sequence of ubiquitin. A) The structure of ubiquitin (PDB:1UBQ) is given in cartoon representation with the location of the N-terminus and C-terminus. **B)** The ubiquitin structure as shown in A) with additional presentation of its N-terminal Met1 and seven internal Lys residues shown as sticks and colored by atoms (nitrogen: blue, sulfur: yellow). **C)** Primary amino acid sequence of ubiquitin. The N-terminal Met1 is shown in blue, the seven Lys residues in red with their respective position.

Hershko and Heller first discovered the formation of polyubiquitin chains composed of ubiquitin linked to the amino group of another ubiquitin molecule in human erythrocytes. The degradation of the lysozyme substrate was facilitated by the presence of the polyubiquitin chains at the protein target (Hershko & Heller, 1985). Studies in yeast later demonstrated the formation of an array of polyubiquitin chains formed by the seven internal lysine residues in ubiquitin *in vivo* (Peng et al., 2003). In yeast and humans, four genes encode ubiquitin as ubiquitin tandems or ubiquitin-ribosomal protein fusions, which further exemplifies the high degree of conservation (Finley et al., 1989; Ozkaynak et al., 1987; Wiborg et al., 1985). These ubiquitin precursors are processed by specific enzymes originally termed Ubiquitin-specific processing proteases (UBPs). Nowadays, the processing enzymes are referred to as a specific class of deubiquitinases (DUBs). These enzymes cleave the fusion off and the ubiquitin tandems into single moieties (Bachmair et al., 1986; Finley et al., 1989). Thereby, monomeric ubiquitin moieties are provided to the cell as a substrate for modifications of other proteins. Ubiquitin is covalently attached to substrates and ubiquitin itself for the formation of polyubiquitin chains in a mechanism termed ubiquitination.

1.2 Ubiquitination

The tightly regulated process of ubiquitination controls a multitude of cellular functions and is essential for the maintenance of cellular physiology. Beyond the well-established role in protein degradation (Ciechanover et al., 1984; Ciechanover & Schwartz, 1998; Finley et al., 1984), it regulates the cell cycle (Goebl et al., 1988), DNA repair (Jentsch et al., 1987) and translational regulation (Hochstrasser & Varshavsky, 1990) amongst other functions.

Ubiquitination describes a post-translational modification by the covalent attachment of ubiquitin onto substrates and ubiquitin itself by ‘writer’ enzymes. The multi-step cascade is mediated by three major components of the ubiquitin system: the ubiquitin-activating enzyme E1, the ubiquitin-conjugating enzyme E2 and the ligation enzyme E3 (Hershko et al., 1983). First, the E1 enzyme catalyzes the adenylation of the ubiquitin C-terminus in an ATP-dependent process. The resulting ubiquitin-AMP product reacts with the catalytic cysteine of the E1 enzyme, which leads to a thioester formation (Haas & Rose, 1982; Figure 2). Upon recruitment of an E2 enzyme, the E1-loaded ubiquitin moiety is transferred onto the E2 catalytic cysteine via another thioester bond (Hershko et al., 1983). Lastly, the ubiquitin transfer onto a substrate or to another ubiquitin is mediated by E3 ligases by diverse mechanisms.

The human genome encodes two E1 enzymes (UBA1, UBA6), ~40 E2 and over 600 E3 enzymes (Middleton & Day, 2023). The E3 ligation enzymes are subdivided into several classes including RING/U-box (>300), HECT (28), RBR (14) and RCR (1) (Clague et al., 2015; Pao et al., 2018; Purser et al., 2023).

RING (really interesting new gene) ligases and RING-like U-box proteins, both hereon after referred to as RING ligases, act as a scaffold by bringing the ubiquitin-loaded E2 and the substrate in close proximity (Figure 2). Upon binding of the E2 to the E3, the E2 is allosterically activated for transferring ubiquitin onto the substrate (Ozkan et al., 2005). Therefore, RING ligases catalyze the direct ubiquitin transfer from the E2 and do not form ubiquitin intermediates in contrast to the remaining E3 ligase classes. One prominent subgroup of the RING E3 class are the multi-subunit complex Cullin-RING-ligases (CRLs; Feldman et al., 1997; Skowyra et al., 1997). CLRs are modular assemblies composed of a scaffold protein (Cullin 1-9), a RING finger subunit (RBX1/2) and interchangeable adaptor and substrate binding proteins (Ebadi et al., 2025).

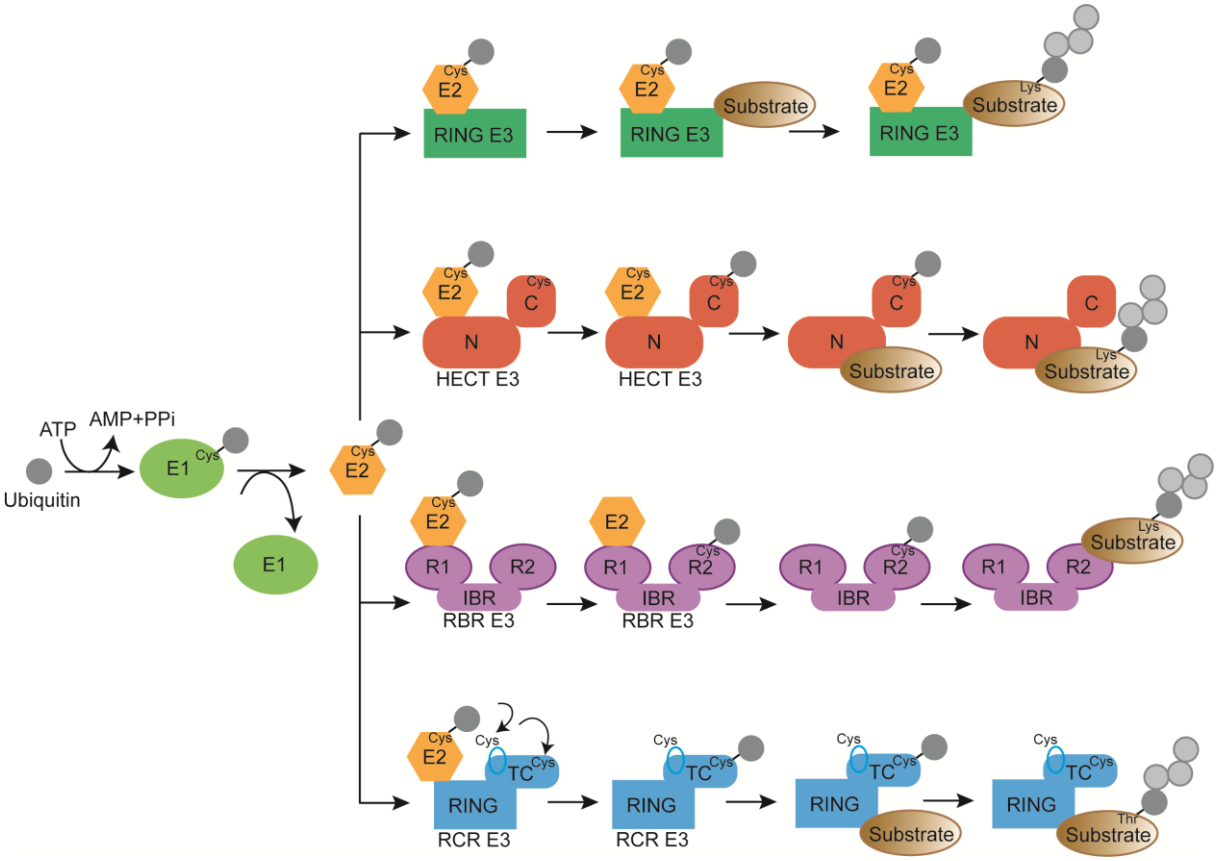

Figure 2: Overview of the ubiquitination cascade. Ubiquitin is activated by E1 enzymes (light green) under ATP hydrolysis. Activated ubiquitin-AMP reacts with the E1 catalytic cysteine and is subsequently transferred onto the catalytic cysteine of the ubiquitin conjugating enzyme E2 (yellow). The transfer of ubiquitin onto the substrate can occur in four basic pathways determined by the E2/E3 complex. RING E3 ligases (dark green) link the E2-bound ubiquitin and the substrate, thereby mediating direct ubiquitin transfer. HECT E3 ligases (red) bind the E2 at the HECT domain N-lobe (N), which transfers the ubiquitin onto the C-lobe (C). The substrate is then ubiquitinated by the HECT E3. For RBR ligases (purple), the RING1 (R1) domain binds the E2, which deposits the ubiquitin onto the RING2 (R2) domain. The domains are linked by an IBR (in-between-RING) domain. The RBR ligase binds the substrate with a domain close to the R2 and ubiquitinates it. RCR ligases (blue) bind the E2 at the RING domain, which is followed by the ubiquitin transfer on one cysteine residue within the TC (tandem cysteine) domain. Subsequently, the ubiquitin is relayed onto another cysteine before deposition onto a threonine residue within the substrate. The ubiquitination process can be iterated for the formation of polyubiquitin chains on the substrate.

The conserved HECT-domain in HECT (homologous to the E6AP carboxyl terminus) E3 ligases is comprised of the N-lobe, which binds the ubiquitin~E2 complex, and a C-lobe carrying the catalytic cysteine (L. Huang et al., 1999). The two lobes are connected by a flexible linker. Upon E2 interaction, the ubiquitin is transferred onto the catalytic cysteine in the C-lobe via trans-thiolation. Thereby, a ubiquitin~E3 thioester intermediate is formed. After release of the E2, ubiquitin is ligated to the recruited substrate by the HECT E3 (Kamadurai et al., 2013).
RBR (RING-IBR-RING) ligases exhibit some similarities to the activity by RING and HECT E3 ligases. They comprise two RING domains, RING1 and RING2, and a central in-between-RINGs (IBR) zinc-binding domain (Zheng & Shabek, 2017). Similar to RING E3 ligases, the RBR RING1 domain binds the ubiquitin~E2 conjugate. Subsequently, the ubiquitin is transferred from the E2 onto the catalytic cysteine in the RING2 domain forming a thioester intermediate as for HECT ligases (Wenzel et al., 2011). Lastly, the ubiquitin transfer is completed by ligation onto the substrate, which is bound at a substrate recognition domain. One well-studied RBR ligase is PARKIN, which regulates mitophagy and mitochondrial quality control (Walden & Martinez-Torres, 2012).
Usually, substrates are modified at lysine residues. However, in recent years several studies revealed non-lysine ubiquitination at cysteine residues (Okumoto et al., 2011), serine or threonine residues (Kelsall et al., 2019), even in ubiquitin itself (McCrory et al., 2022).
A newly discovered class of E3 ligases are the RCR (RING-Cys-Relay) type enzymes. They operate in an unconventional way as the ubiquitin is relayed from the E2 onto two conserved cysteine residues within their tandem cysteine (TC) domain. From the second cysteine residue the ubiquitin is transferred onto a threonine residue of the substrate (Pao et al., 2018). So far, the only member of this class is MYCBP2 with implications of being important for neural development (Mabbitt et al., 2020; Pao et al., 2018). Another just recently identified class of E3 enzymes are the RZ ligases, which utilize a non-canonical zinc-binding RZ (RNF213-ZNFX1 finger) domain to conjugate ubiquitin via an active-site cysteine residue (Kelsall, 2022; Otten et al., 2021).

Most E3 ligases target proteinaceous substrates for ubiquitination. However, apart from proteins, recent studies revealed an emerging role of ubiquitination of other biomolecules. For example, RNF213 ubiquitinates lipopolysaccharides (LPS) of intracellular *Salmonella* bacteria to restrict bacterial infection (Otten et al., 2021). Furthermore, the RBR ligase HOIL1 is able to target sugars for ubiquitination (Kelsall et al., 2022). Ongoing studies on novel ubiquitination substrates will uncover more targets in the foreseeable future.

The high complexity of writer enzymes in the ubiquitin system aligns with the great scope of targeted substrates and generated ubiquitin modifications. The ubiquitination process results in mono- or multi-mono-ubiquitination of the substrate, if one or multiple residues are modified by one ubiquitin moiety. When the monomeric ubiquitin modifier is subjected to another rounds of ubiquitin additions, polyubiquitin chains are formed.

1.3 Ubiquitin chains

The diverse molecular functions of ubiquitination are determined by its modification topology, often referred to as the 'ubiquitin code' (Komander & Rape, 2012). Mono-ubiquitination is known to serve as a recruiting factor in DNA damage response by ubiquitination of Proliferating cell nuclear antigen (PCNA), leading to the recruitment of Y family polymerases (Hoege et al., 2002). Responses to DNA damage were further attributed to mono-ubiquitination on histone H2A (Bergink et al., 2006). However, mono-ubiquitination of histones serves to regulate transcription and chromatin structure as well (J. Kim et al., 2009; W. Zhou et al., 2008). The simultaneous decoration of a substrate with multiple ubiquitin moieties at different residues, termed multi-mono-ubiquitination, was reported for several targets. One example is the epidermal growth factor receptor (EGFR), a receptor tyrosine kinase. EGFR undergoes multi-mono-ubiquitination for receptor internalization and lysosomal degradation upon ligand binding (Haglund et al., 2003).

The multitude of functions mediated by ubiquitination is expanded by the formation of different polyubiquitin chains (Figure 3). The seven internal lysine (Lys) residues and the N-terminal methionine (Met1) residue can typically be utilized for chain generation via formation of new (iso)peptide bonds. Due to the different linkage types, ubiquitin chains adopt different conformations. Chains linked by Lys6, Lys11 and Lys48 take up a closed conformation, while Met1 and Lys63-linked chains occupy an extended conformation (Komander & Rape, 2012).

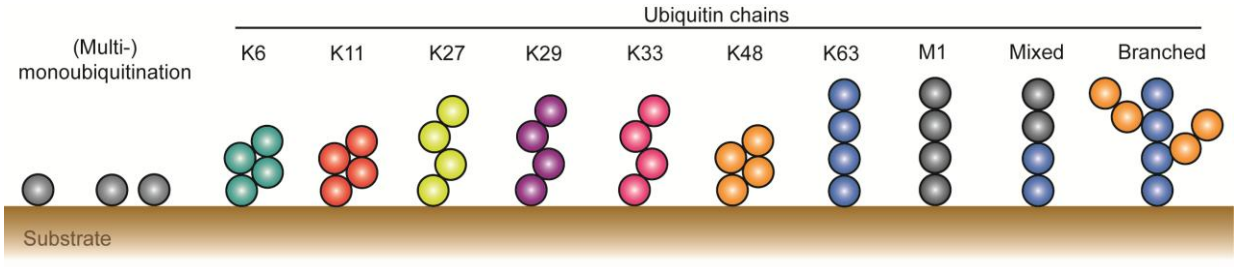

Figure 3: The different topologies of ubiquitin modification. Substrates can be modified with one or multiple ubiquitin moieties at different residues resulting in mono- or multi-mono-ubiquitination. Mono-ubiquitination can be expanded with additional ubiquitin molecules by modifications at the seven internal lysine residues (K6, 11, 27, 29, 33, 48, 63) or the N-terminal methionine residue (M1). By that, homotypic chains (linked by one type of linkage) or heterotypic chains can be formed. The latter chain type comprises different linkage types (mixed) or are made of branched ubiquitin chains, in which one ubiquitin moiety is linked to (at least) two other moieties.

Homotypic chains are composed of one linkage type, for example Lys48-linked ubiquitin molecules. Modifications by K48-linked chains are the most extensively studied chain as they were the first identified chain type while simultaneously being highly abundant in cells (Chau et al., 1989; Kaiser et al., 2011). Substrates decorated with K48-linked chains are typically targeted for proteasomal degradation. The recognition of K48-ubiquitin chains by receptor sites at the proteasomal 19S subunits Rpn10 and Rpn13 connects it to the ubiquitin proteasome system (UPS; Husnjak et al., 2008). By this system, misfolded or dysfunctional proteins are converted to and broken down by the proteasome (Grice & Nathan, 2016; Peth et al., 2010).

Modifications with K63-linked chains serve a plethora of signaling pathways, such as lysosomal degradation, endocytosis, kinase activation and innate immune signaling. Besides the aforementioned induction of DNA repair mechanisms by mono-ubiquitination of PCNA and histones, RNF8 builds K63-linked chains on H2AX upon genotoxic stress to facilitate the recruitment of repair factors (Huen et al., 2007; Ma et al., 2011). During endocytosis, ubiquitin chains on CD4 were shown to act as a sorting signal in the endosomal sorting machinery, whereby K63-linked ubiquitin modification resulted in its lysosomal degradation (Barriere et al., 2007). Moreover, during innate immune signaling via the Nuclear factor-κB (NF-κB) pathway, the signal transducer TRAF6 forms K63-ubiquitin chains and thereby activates the IκB kinase (IKK; Deng et al., 2000). IKK is composed of two catalytic subunits, IKKα and IKKβ, and a regulatory subunit named NF-κB essential modulator (NEMO). Upon activation, IKK phosphorylates the inhibitor of NF-κB, IκBα, leading to its proteasomal degradation by K48-linked ubiquitin chains. This triggers the activation of NF-κB proteins p50 and p65 to translocate to the nucleus and induces anti-apoptosis and inflammatory responses (Smit et al., 2013; Tokunaga & Iwai, 2009). The K63-linked chains formed by TRAF6 recruit the linear ubiquitin chain assembly complex (LUBAC; Goel et al., 2023). The LUBAC complex is composed of Heme-Oxidized IRP2 ubiquitin Ligase 1 (HOIL1), HOIL-1 interacting protein (HOIP) and Sharpin (Kirisako et al., 2006). Linear ubiquitination on NEMO facilitates IKK activation and thereby further drives the canonical NF-κB pathway. LUBAC is the only known ubiquitin ligase capable of producing linear chains in cells and is mainly associated with immune responses. Apart from NEMO, several other substrates of LUBAC have been identified, including the DUB CYLD (Elliott et al., 2016) and regulator of TNF-mediated apoptosis RIPK1 (Fuseya et al., 2020). Further implications for LUBAC are the antibacterial defense during infections by coating cytosolic bacteria with linear chains for autophagic clearance as shown for *Salmonella typhimurium* (van Wijk et al., 2017). This selective antimicrobial macroautophagy mechanism is referred to as xenophagy (Hu et al., 2020).
Besides linear chains, K6-linked and K27-linked chains formed by LRSAM1 are involved in the xenophagic clearance of *Salmonella,* demonstrating the various host coping mechanisms (Huett et al., 2012). Lysine-6 ubiquitin chains are also associated with mitophagy (Michel et al., 2017) but further functions are yet under investigation.

The most elusive linkage types remain K29- and K33-linked chains as limited data is available, but studies report on affiliations to epigenome integrity (Arroyo-Gomez et al., 2025) and protein trafficking (H. Huang et al., 2010).
Ubiquitin chains linked by K11-linked are highly upregulated in mitotic cells suggesting a role in cell cycle progression. In specific, the decoration of cell-cycle regulators with K11-chains targets them for proteasomal degradation (Matsumoto et al., 2010).

The abundance of the numerous ubiquitin modifications differs in tissues and cell types as shown by Kaiser et al. In tested HEK293 cells ~65% of ubiquitin was present as monoubiquitinated substrates, ~23% as free ubiquitin and ~11% as polyubiquitin chains. The reported chain type abundances revealed a ratio of K48>K63>K11 with the remaining linkages K6, K27, K29 and K33 amounting to less than 1% (Kaiser et al., 2011). A study conducted in yeast showed similar results with K48 and K63 linkages being predominant, and the abundance of other linkages were at a proportion of K29 > K11 > K6 > M1 ≅ K27 ≅ K33 (Tsuchiya et al., 2018).

To add to the complexity of ubiquitin chains, they can adopt other architectures like branched chains. For branched chains, one ubiquitin moiety is simultaneously linked to at least two other moieties (Figure 3). Studies showed that K11/K48-branched chains could accelerate the substrates turn over by proteasomal degradation compared to K48-chains alone. This was demonstrated by the stronger binding affinity of K11/K48 branches chains to the proteasomal subunit Rpn1 (Boughton et al., 2020). During NF-κB signaling, the E3 ligase HUWE1 generates K48 branches on K63 chains formed by TRAF6, yielding K48/K63 branched chains. The generated chains are protected from degradation by CYLD, which further amplifies NF-κB signaling (Ohtake et al., 2016).

In contrast to branched chains, mixed chains are composed of different linkage types without branching but by elongation of existing chains by another type. One example are K63/M1 mixed chains in innate immune signaling. Priming of Interleukin-1 receptor (IL-1R)-associated kinase (IRAK) with K63 chains is followed by chain extension via M1-linked chains produced by LUBAC, which facilitates the recruitment of the NF-κB machinery (Emmerich et al., 2013).

These findings demonstrate the multitude of possible ubiquitin chain topologies and their various implications for the cell. This collective knowledge of the various chain types will be expanded in the upcoming years by emerging, new approaches. Ubiquitin signaling in its diverse functions is mediated by defined interaction sites within the ubiquitin structure.

1.4 Ubiquitin recognition

Ubiquitin is recognized by binding partners through diverse ubiquitin-binding domains (UBDs). UBDs include the Ubiquitin Interacting Motif (UIM) and the Ubiquitin Binding Motif (UBM) amongst others. They are modules within proteins of the ubiquitin system,

which utilize the UBDs for ubiquitin interaction through several interaction sites (Randles & Walters, 2012). The small, globular ubiquitin structure constitutes a β-grasp fold consisting of five β-strand sheets, a central α-helix and another short α-helical segment (Vijay-Kumar et al., 1987). The β-sheets expose three hydrophobic residues on the surface (Leu8, Ile44, Val70; Figure 4A). This hydrophobic triad forms a hydrophobic area termed the Ile44-patch, which is contacted by the majority of UBDs. The adjacent positively charged His68 residue contributes to the interaction surface by providing an additional site for non-covalent bonds with UBDs (Komander & Rape, 2012).

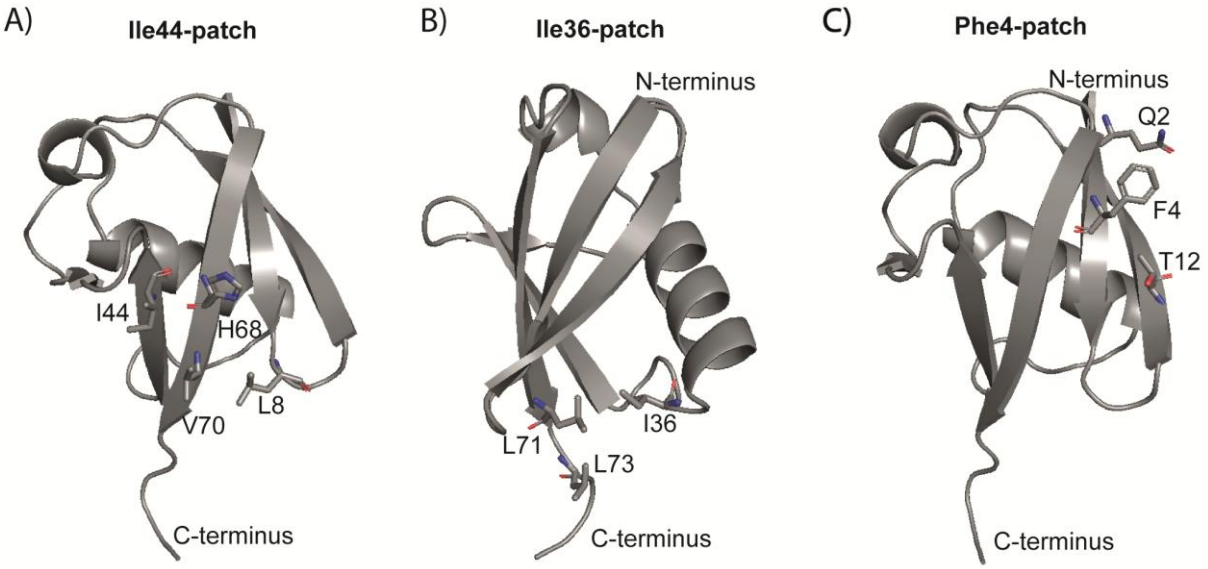

Figure 4: Interaction surface patches in ubiquitin. Given is the ubiquitin structure with three different interaction sites (PDB:1UBQ). The corresponding amino acids are shown as sticks and colored by atoms (nitrogen: blue, oxygen: red). **A)** The Ile44-patch. The constituents of the Ile44-patch include Leu8, His68 and Val70 besides Ile44. **B)** The Ile36-patch comprises Ile36, Leu71 and Leu73 located close to the C-terminus. **C)** The Phe4-patch is formed by Gln2, Phe4, and Thr12.

Another hydrophobic patch is located around Ile36 extending to Leu71 and Leu73 (Ile36-patch) close to the C-terminus (Figure 4B). This interaction site is recognized by several members of the ubiquitin machinery as shown for the DUB USP5 (Reyes-Turcu et al., 2006) and the HECT domain of NEDD4 (Kamadurai et al., 2009). Additionally, ubiquitin displays the Phe4-patch on its surface, which comprises Gln2, Phe4, and Thr12 (Figure 4C). Amongst other proteins, the Phe4-patch is contacted by the UBAN (ubiquitin binding in ABIN and NEMO) domain in NEMO besides the Ile44-patch for the recognition of linear chains during NF-κB activation (Rahighi et al., 2009). Apart from the Phe4-, Ile-36 and Ile44-patches, the TEK-box of ubiquitin is less often utilized as an interaction site. The TEK-box includes Thr12, Thr14, Glu34, Lys6, and Lys11, which are contacted by the Anaphase-Promoting Complex (APC/C), which targets substrates

for degradation during mitosis (Jin et al., 2008; Komander & Rape, 2012; Matsumoto et al., 2010).
Ubiquitin itself is highly conserved across species. Furthermore, the conserved ubiquitin β-grasp fold is present as ubiquitin-like folds in other modifiers, so-called ubiquitin-like proteins (Ubls).

1.5 Ubiquitin-like modifiers

Ubiquitin-like proteins (Ubls) are a family of small proteins, which share structural similarities based on the ubiquitin-like folds and joint evolutionary relationships with ubiquitin. The family is subdivided into type I and type II Ubls defined by their ability to be conjugated onto substrates (Cappadocia & Lima, 2018). Type II Ubls are mainly associated with multiprotein complexes and no substrates have been identified yet as reported for Hub1 and Esc2 (Cappadocia & Lima, 2018; Lüders et al., 2003; Novatchkova et al., 2005; Yashiroda & Tanaka, 2004). Hallmarks of type I Ubls are a C-terminal glycine (Gly) or double-glycine (GlyGly) motif often exposed after proteolytic processing and their conjugation through a cascading process mediated by E1, E2, and E3 enzymes (Cappadocia & Lima, 2018). In humans, type I Ubls include SUMO-1, -2, -3 and -4, NEDD8, ATG8, ATG12, UFM1, ISG15 and FAT10 (Figure 5).

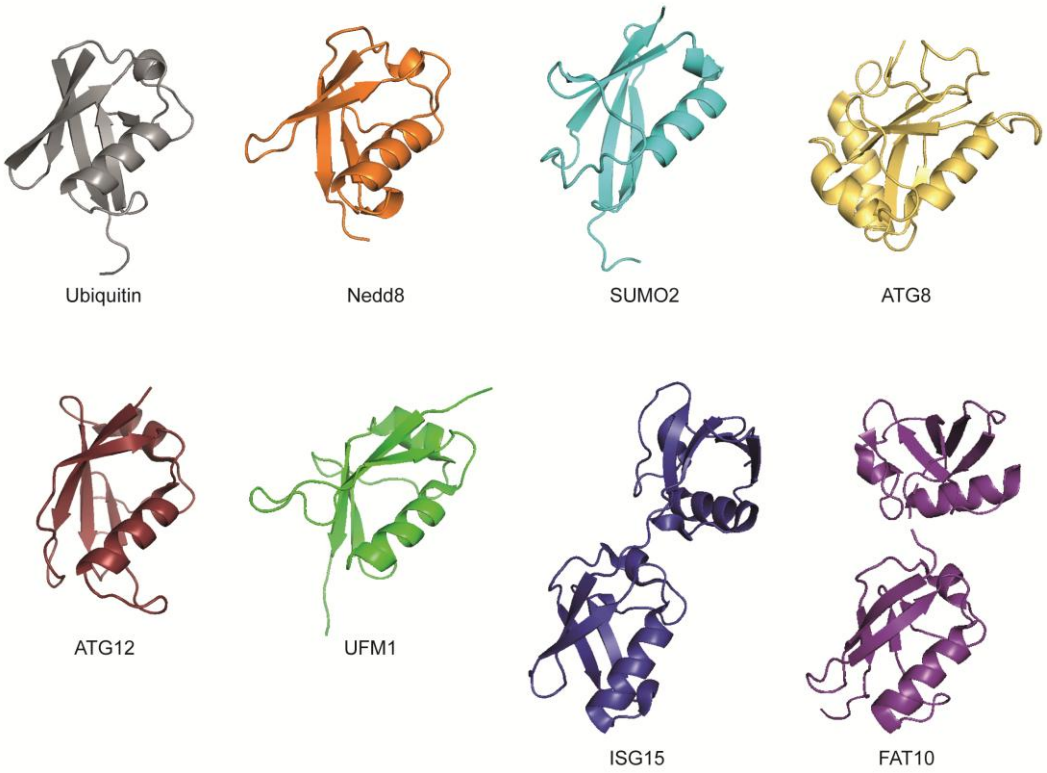

Figure 5: Structures of ubiquitin and ubiquitin-like modifiers. Given are the structures of ubiquitin and selected ubiquitin-like proteins (Ubls) displaying structural similarities based on the conserved ubiquitin-like folds. The numbers in brackets refer to the PDB identifier: human ubiquitin (1UBQ), human Nedd8 (1NDD), human SUMO2 (1WM2), yeast ATG8 (2KWC), human ATG12 (4GDK), human UFM1 (1WXS), human ISG15 (1Z2M), human FAT10 (7PYV).

Four isoforms of SUMO (Small Ubiquitin-like Modifier, 1-4) are encoded in humans, while SUMO4 was reported to be only present and processed under stress conditions (Wei et al., 2008). The existence of a SUMO5 protein is debated as one study showed its suggested involvement in the regulation of PML nuclear bodies, but the finding is not widely accepted and SUMO5 presence remains tentative (Liang et al., 2016). SUMO1 conjugation is associated with modulation of protein solubility and stability (W. Wang et al., 2023; W. Wang & Matunis, 2023). SUMO2 and SUMO3 share a 95% identity, are often referred to as SUMO2/3, and can be conjugated onto themselves, reminiscent of ubiquitin chains (Matic et al., 2008; Tatham et al., 2001). SUMOylation, the conjugation of SUMO moieties onto substrates, is involved in proteostasis through association with the ubiquitin pathway mediated by SUMO-targeted ubiquitin ligases (STUbLs; Uzunova et al., 2007; Weisshaar et al., 2008). Apart from proteasomal degradation, SUMOylation was shown to mediate DNA repair mechanisms and nucleo-cytoplasmic transport (Matunis et al., 1996; Z. Shen et al., 1996).

ATG8 (autophagy-related protein 8) in yeast corresponds to the GABARAP and the LC3 families in humans with a total of seven members (Cappadocia & Lima, 2018). The latter family includes the well-studied LC3B, which acts an adaptor protein for cargo recognition and facilitates autophagosome formation during autophagy (Ichimura et al., 2000; Rogov et al., 2014). Thereby, ATG8/LC3 is conjugated onto phosphatidylethanolamine (PEI) located in the autophagosome membrane. During the autophagic process, ATG12 complexes other autophagic-related components and drives autophagosome formation by promoting ATG8/LC3 lipidation (Metlagel et al., 2013; Phillips et al., 2008).

UFM1 (Ubiquitin-fold modifier 1), together with ubiquitin, SUMO, Nedd8, ISG15 and ATG8, is encoded as a preprotein, which is processed by specific proteases for its mature form. Only few targets of UFMylation are reported, of which most show an association with the endoplasmic reticulum (ER). Studies suggest that UFM1 plays a role in ER homeostasis and ribosome-associated quality control (RQC) at the ER (Komatsu et al., 2024).

FAT10 (Human leukocyte antigen F locus adjacent transcript 10) and ISG15 both are composed of two tandem β-grasp domains separated by a short, flexible linker resulting in proteins around double the size of ubiquitin (Figure 5). Substrate modification by FAT10 mediates various functions as it was reported to induce proteasomal degradation (Hipp et al., 2005), apoptosis (Raasi et al., 2001) and to be involved in the cell cycle (Y. C. Liu et al., 1999).

All modifiers share structural and sequence similarities to ubiquitin to varying degrees. However, solely ISG15 and Nedd8 harbor the same four amino acids within their C-terminus matching with those in ubiquitin (Figure 6).

Ubiquitin	1-56	SDYNIQKESTLHLVLRLRGG
Nedd8	1-56	ADYKILGGSVLHLVLALRGG
ISG15	1-137	GEYGLKPLSTVFMNLRLRGG

Figure 6: C-terminal sequences of mature ubiquitin, Nedd8 and ISG15. The C-terminal amino acid sequence of ubiquitin (57-76) aligned with the sequences of Nedd8 (57-76) and ISG15 (138-157) after processing into their mature forms. All three modifiers share their last four amino acids (LRGG, highlighted in the red box).

1.5.1 Nedd8

The small modifier Nedd8 (neural-precursor-cell-expressed developmentally down-regulated 8) is 60% identical and 80% homologous to ubiquitin (Kamitani et al., 1997). Maturation of the 81 amino acids preprotein is conducted by Nedd8-specifc protease NEDP1, which exposes the C-terminal GlyGly-motif used for the conjugation onto substrates. Neddylation is initiated by the Nedd8 E1 NAE (Nedd8 activating enzyme), which is a heterodimer consisting of AppBp1 and Uba3 (D. T. Huang & Schulman, 2005). The conjugation is facilitated by two Nedd8-specific E2 enzymes, UBC12 and UBE2F, via a trans-thiolation reaction. This is followed by the ligation carried out by E3 ligases such as DCN1 and the E3 ligase component RBX1 (D. T. Huang et al., 2009; Kamura et al., 1999; H. Zhou et al., 2017). Besides executing Neddylation, RBX1 catalyzes ubiquitination by ubiquitin Cullin-Ring Ligases (CRLs). The multi-unit complexes are assembled by Cullin proteins (1-9), which scaffold the substrate recruited by a substrate receptor (e.g. Skp1) bound at the Cullin N-terminus and the RING-containing protein RBX1/2 protein at the C-terminus (Duda et al., 2011). However, this process requires activation by Nedd8 itself: only upon neddylation at the Cullin WHB-domain in the C-terminus a conformational change is induced which shifts the CRLs complex from a closed to an open state (Duda et al., 2011). The E2~ubiquitin bound by RBX1/2 thereby comes in close proximity to the substrate mediated by the Cullin scaffold and the substrate gets ubiquitinated.
Proteins of the Cullin family are the primary canonical targets for neddylation. A study suggested that CRLs are responsible for 20% of intracellular ubiquitinated proteins targeted for proteasomal degradation demonstrating its significance for the cell (Soucy et al., 2010; Soucy et al., 2009). Apart from Cullins, studies report on 300-600 non-Cullin neddylation substrates identified by diverse techniques (J. Li et al., 2020). The identification of *bona fide* Nedd8 substrates remains a challenge as neddylation is potentially upregulated upon stress conditions. Studies propose a non-canonical neddylation pathway upon proteotoxic stress conditions, which displays increased cross-talk to the ubiquitination machinery (Meszka et al., 2022). These notions complicate the discrimination between canonical and non-canonical Nedd8 targets. Further, the formation of Nedd8 chains was shown primarily under stress conditions (Keuss et al., 2019; Meszka et al., 2022; Ohki et al., 2009). Reported neddylation

functions included the modulation of protein activity, e.g. E3 ligases apart from CRLs, cell-cycle control, altering protein stability and localization (J. Li et al., 2020; Vijayasimha & Dolan, 2021).
Nedd8 is recognized by its conserved Ile44-patch as for ubiquitin but lacks the Phe4-patch and harbors Ala72 within the C-terminus compared to R72 in ubiquitin. These characteristics aid interacting proteins to discern the two modifiers (Komander & Rape, 2012; L. Shen et al., 2005; Ye et al., 2011). Recognition by deneddylases NEDP1 and the COP9 signalosome remove the neddylation modification off substrates (L. Shen et al., 2005; Vijayasimha & Dolan, 2021).
Besides Nedd8, the modifier ISG15 can also be conjugated and deconjugated in a similar manner.

1.5.2 ISG15

ISG15, the product of interferon (IFN)-stimulated gene 15, is robustly expressed by IFNs, interleukin 1 beta (IL-1β), pathogenic infection and lipopolysaccharides (LPS) among other stimuli (Kang et al., 2022). The modifier exists as a 17kDa precursor protein, which is processed into its mature form with an exposed GlyGly-motif (Potter et al., 1999). Matured ISG15 can be present in an unconjugated (free) form or be conjugated onto substrates coming with different functions in the cell. The conjugation cascade is carried out by other interferon-stimulated gene (ISGs) proteins including E1 (Ube1L), E2 (UbcH8), and E3 enzymes (Herc5 or TRIM25). ISGylation can be reversed by the deISGylase USP18 (Dzimianski et al., 2019; Malakhov et al., 2002).
ISG15 is a key component of host responses to microbial infection, which has been extensively studied over the years (Dzimianski et al., 2019). The free form of ISG15 can act intracellularly or be secreted to enhance production of cytokines itself (Dos Santos & Mansur, 2017; Recht et al., 1991).
Especially the role of ISG15 in the antiviral immunity response is well studied as shown for infections with the Sindbis virus (Lenschow et al., 2005), Influenza B virus (Zhao et al., 2016) and HIV-1 (Okumura et al., 2006) amongst others. The ISG15 E3 ligase Herc5 mainly localizes at ribosomes, which causes ISGylation to predominantly occur co-translationally on newly synthesized proteins. Consequently, during viral infection, translated proteins such as ISGs and viral proteins are preferentially ISGylated (Dzimianski et al., 2019). The ISG15 modification on viral proteins work in a multitude of mechanisms: disrupting the oligomerization of proteins and protein function, interfering with the intrusion of host pathways or stalling viral replication altogether (Perng & Lenschow, 2018).
Besides viral infections, ISG15 also acts as a defense mechanism against infections by intracellular bacteria as shown for *Listeria monocytogenes*-infected mice (Yifeng Zhang et al., 2019). Host proteins are targeted by ISGylation to modulate protein stability or function to enhance robust immune response. For example, ISG15 modification of the interferon-induced transcription factor IRF3 prevents specific protein interactions, which would usually lead to its ubiquitination and subsequent

degradation (Shi et al., 2010). Similarly, ISGylation of the transcription factor STAT1 was shown to maintain levels of activated STAT1 and downstream signaling (Ganesan et al., 2016; Perng & Lenschow, 2018).
The primary sequence of ISG15 displays interspecies diversity reflecting in variations in the protein structure (Dzimianski et al., 2019). Moreover, the sequences of the two ubiquitin-like β-grasp domains of ISG15 share only about 30% identities with ubiquitin (Kang et al., 2022) and the ISG15 structure lacks the Ile44-patch conserved in ubiquitin and Nedd8.
However, as for Nedd8 and ISG15, conjugation of ubiquitin onto substrates is opposed by its deconjugation executed by a major class of enzymes, termed deubiquitinases (DUBs).

1.6 Deubiquitinases

The modification by ubiquitin is reversible and can be ‘erased’ by deubiquitinases, in short DUBs. In this process, the fate of the substrate is modulated by either disassembling, removing or shortening ubiquitin chains residing on substrates. One prominent example is the removal of K48-linked ubiquitin chains, which spares the substrate from proteasomal degradation (Figure 7).

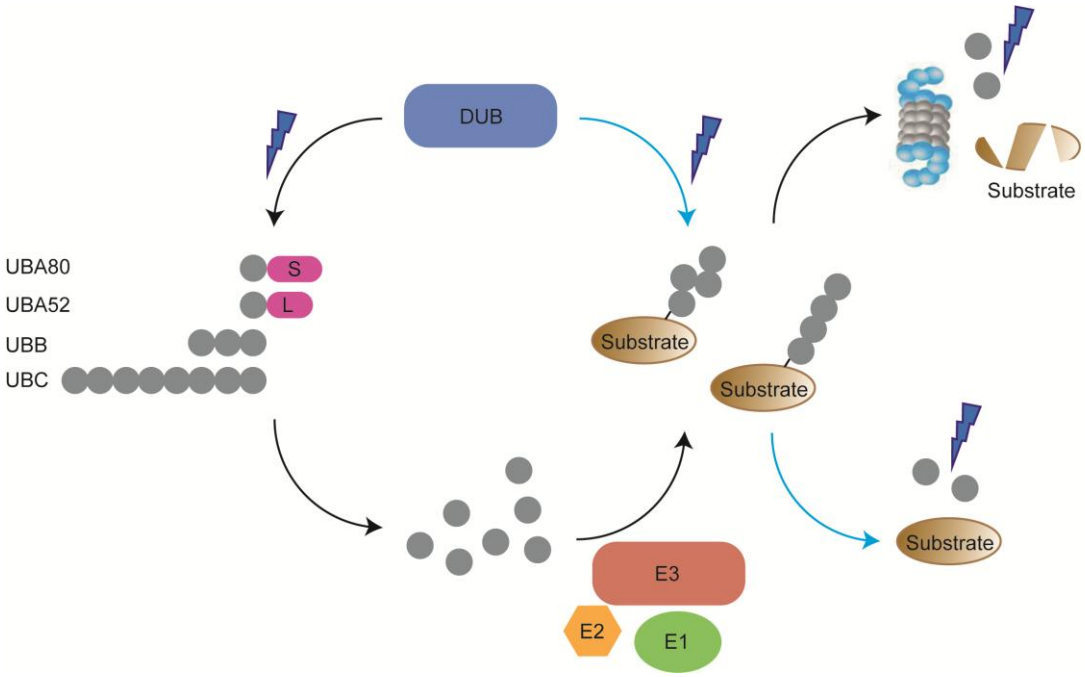

Figure 7: Ubiquitin recycling and ubiquitin signaling modulation is regulated by DUBs. DUB activities are represented by blue lightning bolts. Shortening or removal of ubiquitin chains can save substrates from proteasomal degradation (blue arrows). This mechanism stands representatively for a plethora of DUB-mediated signaling alternations. By this, free ubiquitin moieties are once again provided for the cell. In parallel, DUBs convert ubiquitin precursors, which are present as polyubiquitin or fusions to ribosomal proteins (S/L), into functional moieties ready for ubiquitination by the E1, E2 and E3 cascade. One possible fate of ubiquitinated substrates is the degradation by the proteasome (blue-grey structure). S, ribosomal protein eS31; L, ribosomal protein eL40.

Edited and removed chains are converted into single moieties, which contribute to the pool of free ubiquitin. Ubiquitin chains residing on proteasome-targeted substrates are removed before proteolysis, whereby ubiquitin is also recycled. Additionally, DUBs cleave ubiquitin precursors (UBA80, UBA52, UBB and UBC in humans) into functional, monomeric moieties. By all mechanisms, mono-ubiquitin is provided for the ubiquitin conjugation machinery to be utilized in another round of ubiquitination (Clague et al., 2015; Komander & Rape, 2012). Hence, DUBs are important regulators of the ubiquitin life cycle (Figure 7).

The human genome encodes around 100 DUBs, which can be classified into two major subgroups, metalloproteases and cysteine proteases (Komander et al., 2009; Pinto-Fernández et al., 2019). The only family of metalloproteases is the JAMM (JAB1/MPN/Mov34) family, which employs Zn^{2+} ions for hydrolysis of ubiquitin isopeptide bonds (Figure 8A; Shrestha et al., 2014). In contrast, cysteine proteases utilize a conserved active domain comprising a catalytic cysteine residue. The catalytically active triad is usually constituted of a Cys-His-Asp/Asn formation (Komander et al., 2009). Cysteine protease DUBs are subdivided into seven families: ubiquitin-specific proteases (USPs), ubiquitin carboxy-terminal hydrolases (UCHs), ovarian-tumor proteases (OTUs), motif interacting with Ub-containing novel DUB family proteases (MINDY), Machado-Joseph disease protein domain proteases (MJD), Zn-finger and UFSP domain protein (ZUFSP) and Viral tegument-like DUBs (VTDs; Figure 8A; Abdul Rehman et al., 2016; Clague et al., 2015; Erven et al., 2022; Hermanns et al., 2018).

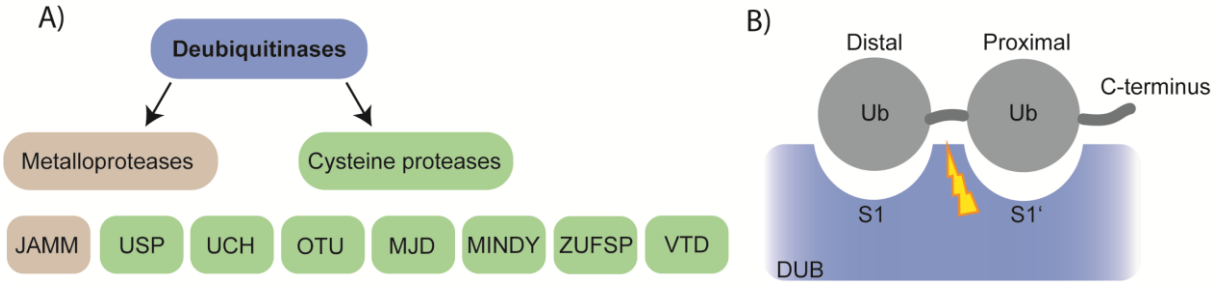

Figure 8: Deubiquitinase families and their ubiquitin binding sites. A) DUBs are divided into two classes (metalloproteases and cysteine proteases) and further categorized into seven families (JAMM, USP, UCH, OTU, MJD, MINDY and ZUFSP). **B)** Ubiquitin binding pockets determine the ubiquitin cleavage site (yellow lightning bolt), here represented by a di-ubiquitin chain. The distal moiety binds to the S1 pocket and the proximal moiety at the S1' site pocket.

Upon DUB activity, the peptide bond in linear chains or the isopeptide bond formed via the side chain of a lysine residue in ubiquitin chains or on substrates gets cleaved. A common denominator among DUBs is the recognition of the ubiquitin C-terminus via its two arginine residues (**R**L**R**GG, see Figure 6). The interaction is mediated by salt bridges formed between the arginine residues and acidic side chains of the DUBs

(Hermanns et al., 2020). Many DUBs also employ a conserved aromatic residue, termed the ‘gate-keeper motif’, which fits into the groove at Gly75 (RLR**G**G) in ubiquitin and would sterically clash with any other residue (Hermanns et al., 2020). These notions drive DUB specificity to cleave the scissile bond after the C-terminal GlyGly motif in ubiquitin.

The specificity of DUBs can be directed at specific substrates, as for most USP class DUBs, which regulate their targets in splicing, protein trafficking, or chromatin remodeling amongst other functions (Komander & Rape, 2012). Substrate recognition is mediated by specific interaction domains within the DUBs or through adaptor proteins.

In contrast, a plethora of DUBs exhibits chain linkage specificity. Ubiquitin chains are recognized at specific binding sites within the DUB (Figure 8B). The interaction domains can fit either one, two or more ubiquitins of chains at their respective binding sites. Linkage specificity is determined by contacting at least two moieties, which occurs according to the chain topology. Binding of two ubiquitin moieties at the S1 and S1’ binding pockets for the distal and proximal ubiquitin, respectively, positions the cleavage site to the catalytic center (Suresh et al., 2020). For example, linkage-specific DUBs include the K63-specific Zup1 of the ZUSPF family (Hermanns et al., 2018) or OTULIN of the OTU family, which specifically cleaves linear chains (Keusekotten et al., 2013).

The vast number of DUBs come with numerous physiological roles in the cell. Apart from salvaging substrates from proteasomal degradation, DUBs regulate protein stability by removing K63-linked chains from substrate to prevent lysosomal degradation (Lauwers et al., 2009). Receptor recycling of EGFR by the metalloprotease AMSH opposes the ubiquitin-dependent sorting of receptors to lysosomes (McCullough et al., 2004). Further, DUBs regulate chromatin remodeling (Mueller et al., 1985), subcellular localization (Komander et al., 2008), DNA damage responses (Hermanns et al., 2018), NF-κB signaling (Keusekotten et al., 2013) and several cell death pathways (Schwickart et al., 2010; S. Zhang et al., 2018), to name only few functions.

DUBs of the small MJD family with four members, hereon after referred to as Josephins, had early implications of repressing transcription (Shimohata et al., 2000). Moreover, it was reported that the most prominent member Ataxin-3 interacts with the E3 ligases CHIP and PARKIN, of which both are involved in maintaining cellular homeostasis (Durcan et al., 2012; Scaglione et al., 2011). Members JOSD2 and ATX3L were shown to prefer long K48- and K63-linked polyubiquitin chains and to be able to target ester-linkages, which are formed by ubiquitination on serine and threonine residues (Cesare et al., 2021; Grasty et al., 2019; Mao et al., 2005).

Besides eukaryotes, some bacteria have acquired proteins that are active in the ubiquitin system of the eukaryotic host cells.

1.7 Bacterial ubiquitin effectors

Invading intracellular bacteria are targeted by host immune responses to prevent further cellular damage. These bacteria can enter the host cell via phagocytosis or induced endocytosis (Weddle & Agaisse, 2018). Some of the intracellular, pathogenic bacteria reside in the cell inside membranous compartments of host origin (bacteria-containing vacuoles, BCV) or escape these structures into the cytosol (Figure 9). Amongst the cytosolic, 'naked' bacteria are *Shigella* and *Listeria* (Chang et al., 2020; Kortebi et al., 2017). Bacteria proliferating within the BCV include *Legionella*, *Chlamydia* and in some cases *Salmonella* (Fels et al., 2023; Sturgill-Koszycki & Swanson, 2000).

To defend against these pathogens, the bacteria and BCV-structures are targeted by several host E3 ligases, such as LUBAC, PARKIN and RNF213. These coat the bacteria with ubiquitin chains of different linkages to trigger downstream pro-inflammatory responses and xenophagy (Tripathi-Giesgen et al., 2021). By the latter system, the bacteria are conveyed to degradation within the lysosome.

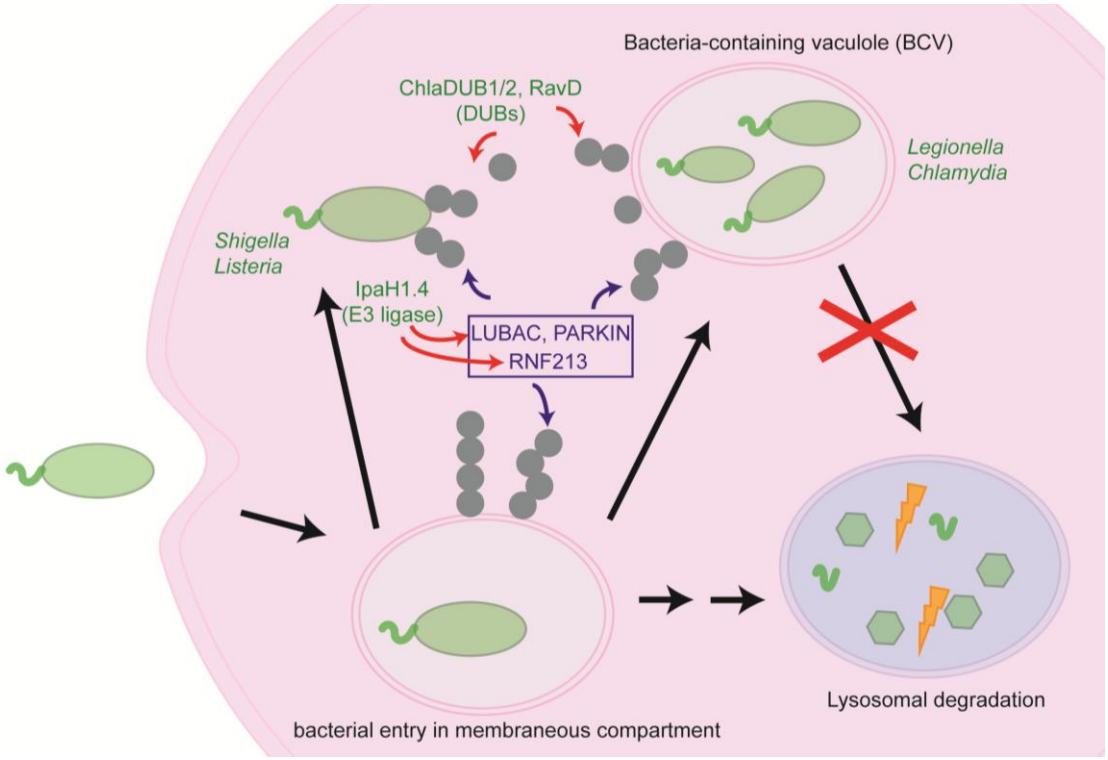

Figure 9: Defense mechanisms of intracellular, pathogenic bacteria. Bacteria can enter the cell by phagocytosis or similar pathways and either reside in the cytosol 'naked' (*Shigella, Listeria)* or within bacteria-containing vacuoles (BCVs; *Legionella, Chlamydia*) used for proliferation. Bacterial structures are coated with ubiquitin chains by host E3 ligases, such as LUBAC, RNF213 and PARKIN (blue arrows) to trigger immune responses and xenophagic clearance of bacteria in the lysosome (blue compartment with yellow lightning bolts). Bacterial defense responses (red arrows) lead to the secretion of effectors including DUBs like ChlaDUB1/2 from *Chlamydia* and RavD from *Legionella*, which remove the ubiquitin chains to prevent lysosomal degradation and ensure bacterial survival. The *Shigella* E3 ligase IpaH1.4 targets host RNF213 and LUBAC for degradation and thereby inhibits ubiquitin chain generation.

Despite not coding for ubiquitin themselves, many intracellular bacteria evolved ubiquitin-targeting effectors to hijack or counteract the hosts defense mechanisms. Some bacteria secrete E3 ligases into the cytosol to target host proteins themselves. The E3 ligase NleL encoded by enterohaemorrhagic *Escherichia coli* (EHEC) modulates host protein function as demonstrated by its interaction with the human E2 Ubch7 and its interference with signal transduction of MAP kinase JNK during infection (Lin et al., 2012; Sheng et al., 2017). One common mechanism is the targeting of host defense proteins for degradation. A recent study showed that the *Shigella flexneri* effector IpaH1.4 degrades the host E3 ligase RNF213, thereby counteracting the ubiquitin-dependent degradation of bacterial structures (Saavedra-Sanchez et al., 2025). Moreover, IpaH1.4 was shown to convey components of the LUBAC complex to proteasomal degradation, which prevents the formation of linear chains and downstream activation of immune responses (Jong et al., 2016).

Besides E3 ligases, numerous bacteria encode DUBs with the implication to disturb the host ubiquitin system (Hermanns & Hofmann, 2019). *Chlamydia trachomatis* expresses two DUBs, ChlaDUB1 and ChlaDUB2, which interfere with the Golgi apparatus and dampen NF-κB activation (Le Negrate et al., 2008; Pruneda et al., 2018). Another example for a bacterial DUB that inhibits NF-κB signaling is RavD from *Legionella pneumophila,* which specifically cleaves linear chains (Wan et al., 2019).

Apart from bacterial DUBs, a novel class of deubiquitinating enzymes also shows a destructive activity, so-called clippases.

1.8 Clippases

A few years ago, a novel class of de-modifying enzymes was discovered. The first member of this class was shown cleave ISG15 within its C-terminus, whereby the cleavage site is located N-terminally of the C-terminal GlyGly-peptide. Thereby, the small ‘clipped’ GlyGly-motif remains at the modified lysine residue of the substrate. Hence, his new class of enzymes was termed clippases (Swatek et al., 2019).

1.8.1 Lbpro

The first member to establish this class was Lbpro from Foot-and-mouth-disease virus (FMDV) uncovered by Swatek et al. (2018). Prior to the investigation of its cleavage mode, the viral leader protease Lbpro has been reported to regulate IFN pathways by ‘inhibiting’ ubiquitination of several cellular substrates (D. Wang et al., 2011). The observed catalytic activity of the Lbpro cysteine protease was at that time attributed to regular DUB activity. In-depth biochemical and structural characterization conducted by Swatek et al. revealed the unusual cleavage activity exhibited by Lbpro (Swatek et al., 2018). They identified Lbpro as a deISGylase, which clips within the ISG15

C-terminus (RLR↓GG, see Figure 6). Lbpro exerts ISG15-deconjugation *in vitro* and in FMDV-infected cells *in vivo.* Further, they found that Lbpro at higher concentrations exhibits cross-reactivity against ubiquitin and Nedd8. A structural analysis of Lbpro in complex with an ISG15 probe, in which the two C-terminal GlyGly were removed and the adjacent Arg155 was replaced with a Gly-like C-terminal propargyl warhead, was conducted (Swatek et al., 2018). Thereby, the canonical -RL(154)RGG C-terminus in ISG15 was replaced by a -RL(154)-warhead probe. The solved complex structure allowed for the identification of interaction sites employed by Lbpro. ISG15 was shown to be contacted at the hydrophobic Trp123 at its surface and the C-terminal Arg153, with implications that Arg155, which was missing in the probe, would be involved as well. Moreover, Leu154 was demonstrated to concert Lbpro activity against ISG15 as mutations at that site led to decreased cleavage ability (Swatek et al., 2018).

Lbpro clipping of the ISG15 C-terminus has two-fold consequences for the cell. It renders the C-terminally truncated ISG15 moiety unrecyclable for another modification round. Simultaneously, the remaining GlyGly-motif blocks the substrates lysine residue from further modification. This mechanism has likely evolved to counteract the host antiviral response with an elevated destructive effect compared to regular de-modifications (Swatek et al., 2018).
Based on the solved structure of Lbpro, a more ubiquitin-targeting variant Lbpro L102W, termed Lbpro Star (*), was engineered (Swatek et al., 2019). This variant was used for studies of ubiquitin chain architecture, which will be discussed in more detail in a later chapter.
Recently, more members of the novel class of clippases have been discovered.

1.8.2 Ubiquitin C-terminal clippases

For the identification of novel deubiquitinases in bacteria, bioinformatics-based predictions were paired with the biochemical testing of identified candidates (Hermanns et al., 2025). Screening of genomes of several intracellular bacteria by employing an established bioinformatics pipeline harbored an array of hits for predicted DUBs (Hermanns & Hofmann, 2023). All candidates showed sequence similarities to eukaryotic Josephin DUBs. The biochemical investigation of the candidates revealed that several candidates displayed unusual activities. They showed activity against di-ubiquitin chains in *in vitro* assays, but did not react with conventional activity-based probes (Hermanns et al., 2025). This finding implied that a different cleavage mode was employed compared to regular DUBs. Considering the finding of the Lbpro clippase, the Josephin-like candidates were tested for clippase activity (Hermanns et al., 2025). By that, the existence of a multitude of bacterial ubiquitin C-terminal clippases (UCCs) was uncovered.

Similar to Lbpro, UCCs clip within the ubiquitin C-terminus between Arg74 and Gly75 (RL**R**↓**G**G, Figure 10). These identified clippases include enzymes from *Simkania negevensis, Burkholderia pyrrocinia* and *Parachlamydia sp.* (Hermanns et al., 2025).

In total, eleven predicted enzymes with sequence similarities to eukaryotic Josephin DUBs were proven to be UCCs. In-depth biochemical characterizations demonstrated that different cleavage preferences are employed by the clippases as some exert ubiquitin-chain specificity while others are linkage-promiscuous (Hermanns et al., 2025).

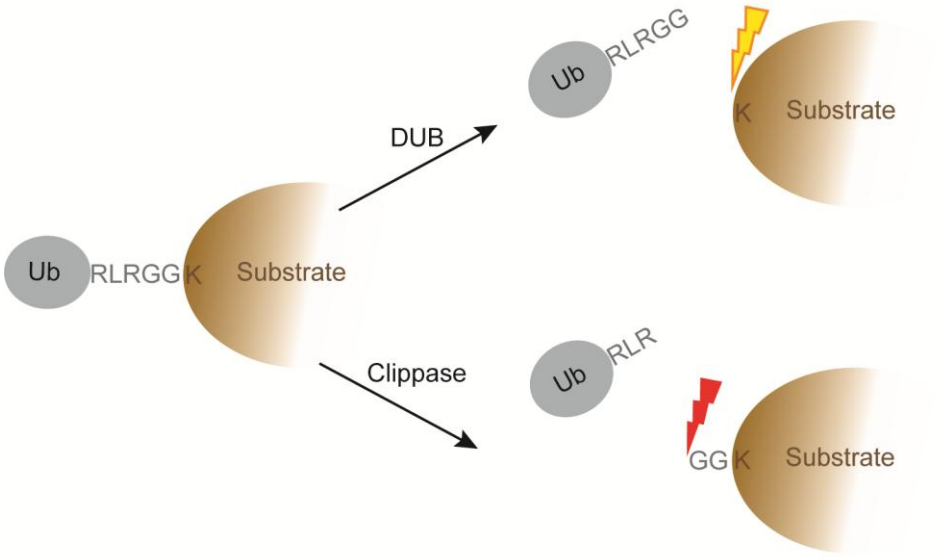

Figure 10: Clippases 'clip' within the modifier C-terminus. The unusual cleavage mode of clippases is represented at the example of ubiquitin and their de-modifiers DUBs. While DUBs remove the ubiquitin moiety complete off the substrate, clippases ‘clip’ before the C-terminal GlyGly-motif. The motif remains at the initially modified lysine residue of the substrate.

One of the validated clippases was BpJOS from *Burkholderia pyrrocinia.* Despite the lack of evidence for the invasion of human cells, *Burkholderia pyrrocinia* was reported to play a beneficiary role in plant defense responses and inhibit plant pathogenic fungi (A. Liu et al., 2020; Yu et al., 2023). The cause for the evolutionary emergence of the UCC activity in BpJOS is yet under debate.

The BpJOS clippase demonstrated a high activity against virtually all ubiquitin chain types *in vitro* (Hermanns et al., 2025). Structural analysis of the BpJOS C69A mutant in complex with ubiquitin disclosed its contact sites to the modifier (Figure 11A).

BpJOS interacts with the Ile44- and Ile36-patches in ubiquitin, which resembles the contacts initiated by regular DUBs. Ubiquitin binding by BpJOS is determined by the S1 site, which provides a structural reasoning for the linkage promiscuity. As universal, structural determinants for the clippase activity were yet unclear, the contact sites at the ubiquitin C-terminus were examined. As for regular DUBs, BpJOS interacts with Arg72 and Arg74 within ubiquitin (Figure 11B). It was shown that the R74A di-ubiquitin

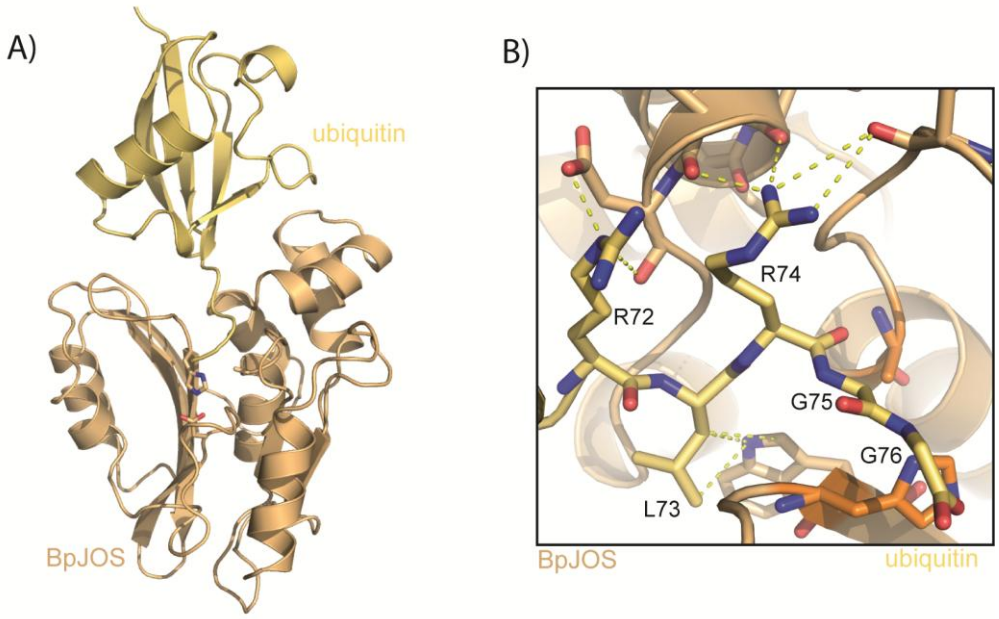

Figure 11: Structure of the BpJOS clippase in complex with ubiquitin. A) BpJOS (orange) in complex with ubiquitin (yellow). The catalytic residues Cys69 (Ala69 in the structure), His166, and Asp182 in BpJOS are shown as sticks. **B)** Close-up of the ubiquitin C-terminus contacted by BpJOS. Arg72, Leu73 and Arg74 of ubiquitin are contacted by BpJOS. Interaction with Leu73 is proposed to be a structural determinant for clippase activity. Both figures were taken from and are published in Hermanns et al. 2025, see Fig. 3B and Fig.4K.

mutant was hardly cleaved by BpJOS, while the R72A di-ubiquitin was processed comparably to the wild-type (Hermanns et al., 2025). This result demonstrated the importance for BpJOS interaction with ubiquitin at Arg74.

However, the shifted cleavage mode is a consequence of the differing interaction sites. While regular DUBs mainly form salt bridges with the Arg residues, BpJOS was shown to also use mainchain interactions. Furthermore, BpJOS interacts with Leu73 in the ubiquitin C-terminus, which was not observed for the characterized, regular DUB PaJOS from *Pigmentiphaga aceris* (Hermanns et al., 2025). The additional interaction at Leu73 is proposed to be a clippase-specific determinant for the cleavage mode. This finding is line with the importance of the Leu154 residue in ISG15 (corresponding to Leu73 in ubiquitin) for Lbpro clippase activity (Swatek et al., 2018)

This unusual cleavage mode exerted by BpJOS and Lbpro resembles the GlyGly-motif left at modified sites after proteolysis by Trypsin, which is most often employed for mass spectrometry studies.

1.9 Mass spectrometry-based studies of Ubl-modifications

The holistic, proteome-wide investigation of post-translational modifications by ubiquitin or Ubls and their implications for the cell is an emerging research field. The identification of the entirety of ubiquitin-targets (ubiquitome) and Ubl-targets (Ublome) was facilitated by the developments of advanced mass spectrometry (MS)-based strategies. A plethora of different approaches were utilized to study the ubiquitome and Ublome in recent years.
Many ubiquitin substrates, for instance, were targeted by use of ubiquitin-binding domains to enrich ubiquitinated proteins (Akimov et al., 2011), ectopic expression of ubiquitin (Danielsen et al., 2011; Kliza et al., 2017) or the exchange of endogenous ubiquitin with tagged ubiquitin-fusions (Akimov et al., 2014). The gold standard in many cases for the preparation for mass spectrometry analysis still is the protein breakdown by digestion with Trypsin. This enzyme cleaves C-terminally of Arg and Lys residues. Thereby, short peptides are generated, which are suitable for the analysis via MS (Olsen et al., 2004). For ubiquitinated, ISGylated and neddylated substrates, Trypsin digestion creates a GlyGly-remnant at the modified site by processing their C-terminus (-LR↓**GG-K**).

One breakthrough in the field was the development of GlyGly-(K)-antibodies. These specifically recognize these trypsin-generated GlyGly-motifs at lysine residues. By employing the antibody in an immune-precipitation (IP), these GlyGly-sites can be specifically enriched and later analyzed by MS. This method not only allows for substrate profiling, but site-resolved mapping of the modifications. One of the first studies to employ the GlyGly-enrichment approach combined the method with the expression of tagged ubiquitin and a quantitative MS measurement using SILAC (stable isotope labeling by amino acids in cell culture). They could identify around 380 ubiquitination sites in HEK293 cells (G. Xu et al., 2010). Studies like the one conducted by Udeshi et al. refined this method. They coupled the GlyGly-enrichment to Tandem Mass Tags (TMT) before MS analysis to achieve quantitative ubiquitination profiling (Udeshi et al., 2020). By this method termed ‘UbiFast’, they identified around 10.000 ubiquitination sites. Both methods, amongst many others, rely on trypsin-generated GlyGly-K-peptides. However, by this, the conflation of ubiquitin-, ISG15- and Nedd8-modifications based on their shared (LRGG) C-terminus is disregarded. Most often all identified sites are attributed to be ubiquitin-derived.

To overcome this challenge, some studies employ ectopic over-expression of the modifier Nedd8 (Enchev et al., 2015) or ISG15 (Radoshevich et al., 2015; Yan et al., 2021). However, these manipulations at proteomic level may lead to artefacts. Other strategies include the generation of mutants, as reported for the Nedd8 R74K mutant (Lobato-Gil et al., 2021). Alternatively, knock-out organisms are employed, as reported for ISG15 to discern between the modifiers (Yifeng Zhang et al., 2019). For targeting ubiquitination sites specifically, the ‘UbiSite’ approach was developed (Akimov et al., 2018). This method uses LysC for peptide generation instead of Trypsin. LysC cleaves only after Lys residues, which results in different C-terminal peptides for ubiquitin,

Nedd8 and ISG15. The peptide produced only by ubiquitin is then enriched by a specific ‘UbiSite’ antibody.

The investigation of cellular ubiquitin chain lengths and architectures were addressed in recent years as well. In an approach termed ‘Ub-ProT’, cellular ubiquitin chains are enriched by tandem Ub-binding entities (TUBEs; Tsuchiya et al., 2018). The utilized TUBE variant was engineered to be Trypsin-resistant, TR-TUBE. These artificial protein structures are designed to bind and enrich polyubiquitin chains from complex samples, while protecting them from Trypsin digestion. By Trypsin digestion at lower concentrations, the modified substrates, but not TR-TUBE-bound ubiquitin chains are broken down into peptides. TR-TUBE-pulled ubiquitin chains are then treated with high concentrations of Trypsin and the peptides are subjected to tandem MS (MS/MS)-based absolute quantitation (AQUA).
A recent approach conceptualized by Swatek et al. is based on the Lbpro* (L102W) variant of Lbpro (Swatek et al., 2019). Lbpro* exhibits higher activity against ubiquitin compared to its parent enzyme. By ‘clipping’ ubiquitin chains with Lbpro*, the generated single ubiquitin moieties are marked with the GlyGly-motif of the adjacent ubiquitin. In case of branched chains, one ubiquitin carries multiple GlyGly-remnants. Analysis with intact protein MS (intact mass) allows for insights into ubiquitin chain architectures (Swatek et al., 2019). Coupling a TUBE-pulldown of ubiquitin chains with Lbpro* treatment and later AQUA MS enables the estimation of average chain length and identification of cellular linkage compositions (Swatek et al., 2019). This clippase-based method was baptized ‘Ub-clipping’.
In sum, a multitude of methods for the investigation of ubiquitin and Ubl modifications were developed in the past years. The approaches take on different angles, and all come with their individual advantages and limitations. However, all these studies heavily contributed to the current available knowledge of the ubiquitome and Ublome.

1.10 Aim of the thesis

The overarching goal of this study was to explore the potential of bacterial C-terminal clippases (UCCs) as tools to investigate the eukaryotic ubiquitination system. One major aim was to use the specificity of clippases to discriminate between modifications by ubiquitin, Nedd8 and ISG15, which all leave indistinguishable GlyGly(K)-remnants in conventional proteomics studies. BpJOS is a clippase that appeared to be highly active against ubiquitin and to a lesser extent Nedd8 but inert towards ISG15 modifications. Consequently, BpJOS is a prime candidate for studying ubiquitination during an ongoing interferon response. Clippases also allow the investigation of chain branching, since multiply-modified ubiquitin moieties will - after clipping - retain multiple GlyGly-remnants, which can be identified and quantified by mass spectrometry (MS).

The first part of the thesis describes the search for novel clippases with useful modifier- and/or linkage-specificities, which would allow novel types of MS-based analyses. In the second part, the highly active BpJOS clippase is characterized for its discrimination between ubiquitin and ISG15. A ‘clippomics-based’ method is established, in which a combination of BpJOS and Lbpro clipping is used to separately identify ubiquitin- and ISG15-modification sites. Moreover, BpJOS was used to specifically identify interferon-stimulated ubiquitination sites. In the third part of the thesis, a method reminiscent of the published ‘Ub-clipping’ is developed to elucidate the linkage-specificity of ubiquitin ligases, potentially in a semi-quantitative way.

2 Material and Methods

2.1 Molecular biology

2.1.1 Cloning

DNA fragments were amplified by polymerase chain reaction (PCR) using the Phusion High Fidelity DNA Polymerase (New England Biolabs). The reaction composition and used PCR program are listed in Table 1 and Table 2. Amplified products were cleaned on a 1% agarose gel, excised with a scalpel and purified using the NucleoSpin Gel and PCR Clean-up kit (Macherey Nagel). Circular target vector pcDNA5 FRT/TO was linearized with BamHi and HindIII and gel purified. Generated PCR products (Table 3) and synthesized gBlocks obtained from Integrated Technologies (Table 4) harbored 5'-3' and 3'-5' overhangs compatible with the pcDNA5 FRT/TO vector for In-Fusion cloning (Takara Bio). The In-Fusion ligation reaction was conducted for 15min at 50°C with the composition listed in Table 5.

Table 1: PCR reaction mix used in this study.

Reagent	Volume[µl]
5x Phusion buffer (New England Biolabs)	5
Template DNA	0.5
10µM forward primer	1.25
10µM reverse primer	1.25
10mM dNTPs	1
Phusion DNA Polymerase (New England Biolabs)	0.5
H_2O	15.5

Table 2: PCR program for amplification of DNA fragments used in this study.

Step	Time [s]	Temperature [°C]	Cycles
Hot Start	Infinite	98	n/a
Denaturation	45	98	34x
Annealing	30	65	
Elongation	30s/kb	72	
Final Elongation	300	72	n/a

Table 3: List of primers used for PCR amplification in this study. All target sequences were cloned into the pcDNA5 FRT/TO backbone. The overhangs for pcDNA5 FRT/TO for In-Fusion cloning are shown in blue, the start and stop codons in red and the 1xFLAG-tag in green.

Primer	Sequence 5‘- 3‘
FLAG-OTULIN fwd	TACCGAGCTCGGATCATGGACTACAAGGATGACGATGACAAG ATGTCAAGAGGCACCATGCCGCAACCTGAAG
OTULIN rev	TAGACTCGAGCGGCCTTACAAAGACGTTTCCTCGCACACCCT CACAGG
FLAG-HOIL1L fwd	TACCGAGCTCGGATCATGGACTACAAGGATGACGATGACAAG ATGGACGAGAAGACCAAGAAAGCAGAGGAAATGGC
HOIL1L rev	TAGACTCGAGCGGCCTTAGTGGCAGTTCTGACAGCTTGGGT GGCAAG
FLAG-HOIP fwd	TACCGAGCTCGGATCATGGACTACAAGGATGACGATGACAAG AGGCTGTGGGTGAGCGTGGAGGATGC
HOIP rev	TAGACTCGAGCGGCCTTAGTGGCAGTTCTGACAGCTTGGGT GGCAAG
FLAG-Sharpin fwd	TACCGAGCTCGGATCATGGACTACAAGGATGACGATGACAAG ATGGCGCCGCCAGCGGGCGG
Sharpin rev	TAGACTCGAGCGGCCTTATGTGGAAGCTGCAGCAAGGGGGT CCC

Table 4: Codon optimized sequences of gBlocks (Integrated DNA Technologies). The extensions for In-Fusion cloning into the pcDNA5 FRT/TO backbone are marked in blue. The start and stop codons are indicated in red and the 1xFLAG tag are highlighted in green.

Name	Sequence 5’-3’
OTULIN pOPINBov	AAGTTCTGTTTCAGGGCCCGATGTCAAGAGGCACCATGCCGCAACCTGA AGCCTGGCCAGGTGCTTCCTGTGCAGAGACACCCGCTCGCGAAGCCGC TGCTACCGCTCGCGACGGCGGTAAAGCTGCGGCATCTGGTCAGCCGCG GCCTGAGATGCAATGTCCCGCCGAACACGAAGAGGACATGTACCGAGCC GCCGATGAAATAGAGAAAGAGAAAGAGCTGCTCATTCATGAGCGCGGAG CTTCAGAACCGCGCCTCTCCGTCGCGCCAGAGATGGACATTATGGACTA CTGTAAGAAGGAGTGGAGGGGTAATACACAAAAAGCAACTTGCATGAAAA TGGGTTACGAGGAGGTCTCTCAGAAGTTTACTTCCATCCGACGCGTGAG AGGGGACAACTATTGTGCTCTCAGAGCGACACTTTTCCAAGCCATGTCC CAAGCCGTCGGTCTGCCGCCCTGGTTGCAAGACCCAGAATTGATGCTTC TTCCAGAGAAGCTGATCAGTAAATATAACTGGATAAAACAATGGAAACTGG GCCTCAAATTCGACGGTAAAAATGAGGATCTGGTCGATAAAATCAAGGAA TCTCTGACCCTCCTGCGCAAGAAATGGGCCGGGCTGGCCGAAATGAGA ACTGCAGAGGCACGGCAAATTGCATGCGATGAGCTTTTCACGAACGAAG CGGAAGAGTATAGTTTGTATGAAGCTGTTAAATTTCTTATGCTGAACCGAG CTATCGAACTTTATAATGATAAAGAGAAGGGAAAGGAGGTACCTTTTTTTT CCGTGCTCTTGTTCGCGCGCGATACCAGTAATGATCCAGGTCAACTCCT

	GCGCAATCATCTTAACCAGGTTGGCCACACTGGAGGACTGGAACAGGTG GAGATGTTTCTTCTCGCGTACGCCGTGCGGCATACCATACAAGTGTATCG ACTCAGCAAATACAATACCGAAGAATTTATCACCGTCTACCCGACCGACC CACCTAAAGATTGGCCGGTAGTGACACTTATAGCAGAAGACGACCGGCAT TACAATATACCTGTGAGGGTGTGCGAGGAAACGTCTTTGTGATAAAGCTT TCTAGACCAT
PcJOS 70-325	TACCGAGCTCGGATCATGGACTACAAGGATGACGATGACAAG AAAACCCAGCCGAGTACGACGCAAAAGGTCGAGAACACGGCGAAAACC TTGTTCAAGCCGGATCTTAAAAGCCCGCCGATGAACCCACAATGGCTTAC AGAAGAACAGATCAAGAAGATGTCACCCGACGAGCAAGGGAATCTCATA GACACCTATGCAGCTCGCAAGATTAACGCGGCCTCTGATCTCACACACG CTCAACTGCGAGGAATGATCGGCAGTACAGCGGCATCCCACATTGCGAT CGTGAACGCACAAGAGACCGGCTTGGGTCATTGCGGCCGATATGCGATA AACAATGCGCTTCAGCAAGAGGCGTTGTCACAGAATGAATTCCTCTCACT GACAGGGCAAATATTCAGCAATCAACTCGGGATGTCACTTGCCGACGTAA AGAACCTCATTCAAAATCAAGACGATTTTGGGATCGACACGGGGGTCCTT GCCCAGATTCTGAAACAAAAATTCAACCAACCCGTGAAGGAATCAAAAAT ATGTGATCTTCCCGACTGTGCGTTGAGCAAGCAGCAAGCTGTTGAAAATT ATATAGGGAAAGCGAAGTGGGTAATTGTAGCAAACATCGGAACAGAGGTC TTCGACATGCCATCATCAACTCACGCTGTATATCCTCTCACGAGGGGACA CTTCGTAGCCCTTAGACGGGATGCCGATAACAGGTGGTGGTATCTGGAC TCCCGAGGAAAAAACCCCGTGAACATTGCTCTCGCAATTATACCGAGGAC CTGTACCCTCATAGTTCCCTTGTAAGGCCGCTCGAGTCTA

Table 5: In-Fusion reaction mix used in this study.

Component	Volume [µl]
gBlock/ DNA fragment (75ng/µl / 1-5µg/µl)	1.5
Vector (1-5µg/µl)	0.5
In-Fusion reagent (Takara Bio)	0.5

2.1.2 Site-directed mutagenesis

Point mutations were introduced to ORFs coding for PcJOS by site-directed mutagenesis (SDM) PCR using the Pfu Turbo Polymerase (Agilent Technologies). Used PCR reaction, PCR protocol and SDM primers are listed in Table 6, Table 7 and Table 8. Wildtype template DNA was degraded by DpnI treatment for 2h at 37°C.

Table 6: PCR reaction mix (25µl) used for SDM in this study.

Component	Volume [µl]
10x PfuTurbo buffer (Agilent Technologies)	2.5
Template DNA (1µg/µl)	0.25
10µm forward primer	1.25
10µm reverse primer	1.25
10mM dNTP	0.5
2.5U/µl PfuTurbo DNA polymerase (Agilent Technologies)	0.5
H_2O	18.75

Table 7: PCR protocol used for SDM in this study.

Step	Time [s]	Temperature [°C]	Cycles
Initial Denaturation	180	95	n/a
Denaturation	45	95	18x
Annealing	60	57	
Elongation	120/kb	72	
Final Elongation	300	72	n/a

Table 8: List of primers used for SDM in this study.

Name	Primer sequence 5'-3'
PcJOS C162A fwd	catatcggccggcatgacccaagccggtctctt
PcJOS C162A rev	aagagaccggcttgggtcatgccggccgatatg

2.1.3 *E. coli* transformation

Plasmids were propagated by transformation into chemically competent *Escherichia coli* strain DH5α after (Hanahan, 1983). Bacterial aliquots were supplemented with 1µl of plasmid for re-transformation or 2µl of In-Fusion reaction and incubated on ice for 30 minutes. The DNA uptake was facilitated by heat shock treatment at 42°C for 2 minutes. For recovery, 400µl of chilled Lysogeny Broth (LB) medium (1% tryptone, 0.5% yeast extract, 1% NaCl) was added and bacteria were incubated for 1h at 37°C

to allow for expression of the ampicillin selection marker. The bacteria were plated onto LB medium +2% agar plates supplemented with 100 µg/ml ampicillin. Plates were incubated invertedly at 37°C overnight.

2.1.4 DNA isolation and purification

Single colonies were picked with a pipette tip and transferred into 5ml LB medium for mini preps or 20ml for midi preps used for transfection (see 2.3.3). Bacteria were grown at 37°C overnight and pelleted at 11.000xg for 1 minute the following day. Plasmids were purified using the NucleoSpin Plasmid kit or NucleoBond Xtra Midi kit (both Macherey Nagel) for endotoxin-free plasmid preparation according to the manufacturer's protocol. Sequencing of isolated plasmids was conducted by Eurofins Genomics. Sequences obtained were analyzed using CLC Main Workbench 6.8.2 (Qiagen). The comprehensive list of used constructs is given in Table 9.

Table 9: List of constructs used in this study. All constructs were codon optimized for human codon usage. All listed constructs are full-length, if not indicated otherwise. Truncation borders refer to the amino acid positions.

Construct	Backbone	Origin species	Source
FLAG-HOIL1L	pcDNA5 FRT/TO	human	This study
FLAG-HOIP	pcDNA5 FRT/TO	human	This study
FLAG-OTULIN	pcDNA5 FRT/TO	human	This study
FLAG-PcJOS$^{70-325}$	pcDNA5 FRT/TO	*Parachlamydia sp.*	This study
FLAG-PcJOS$^{70-325}$ C162A	pcDNA5 FRT/TO	*Parachlamydia sp.*	This study
FLAG-Sharpin	pcDNA5 FRT/TO	human	This study

2.2 Protein biochemistry

2.2.1 Purified proteins used in this study

Proteins were purified and di-ubiquitin chains were generated according to (Hermanns et al., 2025). Purified proteins used in this study were kindly provided by Dr. Thomas Hermanns and Dr. Vanessa Lachmayer (Institute for Genetics, Cologne) or prepared during the master's thesis (Kolek, 2021). All purified proteins and di-ubiquitin chains used are listed in Table 10.

Table 10: List of purified proteins used in this study and their respective sources.
All listed constructs are full-length, if not indicated otherwise. Truncation borders refer to the amino acid positions.

Protein	Source
BpJOS	Thomas Hermanns
BpJOS$^{12\text{-}218}$	Thomas Hermanns
PcJOS$^{70\text{-}325}$	Thomas Hermanns
PvJOS$^{764\text{-}1098}$	Thomas Hermanns
CsJOS$^{56\text{-}289}$	Thomas Hermanns
BcJOS	Thomas Hermanns
USP21$^{196\text{-}565}$	Thomas Hermanns
ATX3L	Thomas Hermanns
JOSD2	Thomas Hermanns
ChNJCl$^{468\text{-}725}$	Thomas Hermanns
SnJOS1	Vanessa Lachmayer
SnJOS2	Vanessa Lachmayer
PaJOS$^{1881\text{-}2146}$	Thomas Hermanns
HeJOS	Master thesis (Kolek, 2021)
Lbpro$^{29\text{-}195}$	Thomas Hermanns
Lbpro*(L102W)$^{29\text{-}195}$	Thomas Hermanns
NEDP1	Thomas Hermanns
SnUSP1$^{167–529}$	Vanessa Lachmayer
NleL$^{170\text{-}782}$ E705A	Vanessa Lachmayer
di-Ubiquitin M1/K6/11/48/63	Thomas Hermanns
di-Ubiquitin K6/29/33	Boston Biochem
di-Ubiquitin K27	UbiQ

2.2.2 Ubiquitin chain cleavage

Di-ubiquitin chains (50µM) were incubated with 50nM BpJOS or PcJOS in reaction buffer (20mM Tris pH7.5, 150mM NaCl, 10mM DTT) for the indicated timepoints. The reactions were quenched by addition of 2x Lämmli buffer (Table 11) and were analyzed by SDS-PAGE.

Table 11: Recipe for 2x Lämmli buffer.

Component	Concentration
Tris pH 6.8	125mM
SDS	2% (w/v)
Glycerol	20% (v/v)
Bromophenol blue	0.03% (w/v)
β-mercaptoethanol	2% (v/v)

2.2.3 Activity-based probe assay

Activity-based probes (ABPs) were chemically synthesized and the testing of BpJOS for reaction with Ub^{1-73} , $Nedd8^{1-73}$ $ISG15^{79-154}$-PA probes were conducted by Thomas Herrmanns according to Hermanns et al., 2025. The propargylamine (PA) group, which acts as a reactive warhead, reacts with the catalytic cysteine of tested protease and forms a covalent bond. The reaction was monitored by SDS-PAGE.

2.2.4 Generation of NleL chains

The *in vitro* ubiquitin chain assembly assay using bacterial E3 ligase $NleL^{170-782}$ E705A (Franklin et al., 2023) was conducted by Dr. Vanessa Lachmayer according to (Park et al., 2015). The produced chains were tested in proof-of-concept experiment using ‘Ubi clipping with BpJOS’.

2.2.5 Parkin chain generation

For testing by ‘Ubi clipping with BpJOS’, PARKIN chains were generated by collaboration partner Dr. Maria Georgina Herrera from the Winklhofer lab, Ruhr University Bochum. All purified proteins and the reaction were prepared by the Winklhofer lab and kindly provided for this study together with the following information in this chapter for their preparation (a-d).

a. Protein expression and purification of Parkin

BL21 pLys (DE3) were transformed with the plasmid (ampicillin resistance). Precultures were produced overnight and 4 liters LB cultures were grown to OD around 0.9. Then they were taken to 20 °C and induced overnight with 50 µM IPTG and 50 µM ZnCl2. The pellets were harvested and resuspended in Lysis buffer: 20mM Tris-HCl pH 7.4, 120mM NaCl, 0.5mM TCEP with protease inhibitor and DNase I, $MgCl_2$ and RNAse I. The cells were lysed using a French press, and 2% triton was added to the lysate, and it was incubated for 1 hour at 4°C under rotation. Then, the lysate was centrifuged at 45.000 g for 45 minutes. The purification was carried out using a GST-TRAP 16/100 column. The equilibration and washing buffer were 20mM Tris-HCl pH 7.4, 120mM NaCl, 0.5mM TCEP. The protein was eluted with 20mM Tris-HCl pH 7.4, 120mM NaCl, 0.5mM TCEP, 20mM glutathione. GST-precision protease was added to the eluted protein and dialyzed in buffer 20mM Tris-HCl, pH 7.4, 120 mM NaCl, 0.5mM TCEP. The dialyzed protein was passed again through the GST-TRAP (Cytiva) column to bind GST, GST-precision protease, and the uncleaved protein, yielding untagged FL-Parkin.

b. Parkin phosphorylation by Pink1

Parkin was mixed with GST-PINK1 at a 1:10 protein kinase ratio. The phosphorylation was carried out by adding 1 mM ATP and Mg^{+2} and incubating the sample for 2 hours at 37°C. After the reaction was produced, PINK1 was removed using a GST-TRAP column. Then, the ATP was removed using a Zeba spin desalting column, and the protein was rebuffered in 20 mM Tris-HCl, 200 mM NaCl, 1 mM DTT using a Vivaspin (Sartorius) desalting collum. The protein purity was checked by SDS-PAGE and the concentration was determined using absorbance at 280 nm and the extinction coefficient of each construct by Nanodrop (Thermo Fisher).

c. Purification of GST-M1-linked tetra-ubiquitin

GST-M1-linked tetra-ubiquitin was expressed in E. coli Rossetta (pLysS). Cells were grown at 37°C to an OD (600 nm) of 0.6–1.0. Protein expression induction 300 µM IPTG ON at 16°C. The bacteria were centrifuged, and the pellet was resuspended in lysis buffer and frozen.

Purification of GST-M1-linked tetra-ubiquitin was performed by standardized methods (Wu et al., 2022). After centrifugation for 40 min at 38,000 g, the protein was purified by glutathione Sepharose 4B resin (GE Healthcare). The elution was dialyzed and treated with precision protease. Another purification step to remove the tag and the protease was implemented using anion exchange chromatography (Hi-Trap Capto Q, Cytiva), where the protein is obtained in the flow-through. The protein purity was checked by SDS-PAGE and the concentration was determined using absorbance at 280 nm and the extinction coefficient of each construct by Nanodrop (Thermo Fisher).

d. Reaction:

The reaction was carried out in 20 mM Tris-HCl, 200 mM NaCl in the presence of 1 µM E1, 2 µM E2 (UBE2L3), 4 µM phospho-Parkin and 50 µM 4xM1-ub. The reaction was initiated by adding ATP/Mg^{+2} and incubated for 2 h at 37°C. Then the reaction was stopped by adding Laemmli buffer and heating for 5 minutes at 95°C.

2.2.6 Ubi clipping of *in vitro* ubiquitin chains

For 'Ubi clipping with BpJOS', 20µg of 2K48 and 2K63 di-ubiquitin chains or NleL chain mix (2.2.4) were incubated with 10µM BpJOS for 1h on ice. Proteins were denatured by addition of 8M Urea (6M Urea, 2M Thiourea in 50mM TEAB, MS-grade). Samples were reduced and alkylated by supplementation with 5mM DTT (Dithiothreitol) f.c. (1h, RT) and 40mM CAA (Chloroacetamide) f.c. (45min, RT, dark), respectively. Urea, DTT and CAA were provided by the CECAD proteomics facility, Cologne. In preparation for enzymatic digest, the urea concentration was diluted to >1M with buffers appropriate for used protein digestion enzyme. The enzyme GluC used is sensitive to chloride ions, therefore salt concentrations for these samples were reduced using the Zeba™ Spin Desalting Columns (7K MWCO, #89887, ThermoFischer) according to the manufacturer's protocol prior to GluC digestion. For GluC or AspN digest, 50mM ammonium bicarbonate buffer (ABC buffer, Proteomics facility) was added to the samples. For digestion with Chymotrypsin, the samples were supplemented with 100mM Tris-HCl pH8.0, 10mM$CaCl_2$ in accordance with the manufacturer's protocol. The site-specific proteases used for protein digestion in the bottom-up mass spectrometry approach and the appropriate incubation temperatures are listed in Table 12. Samples were incubated with the respective enzyme at a 1:40 substrate: enzyme ratio gently shaking for 16h. The reactions were quenched by addition of 1% trifluoroacetic acid (TFA). The preparation of samples for Liquid chromatography–mass spectrometry (LC-MS/MS) is described in chapter 2.4.1.

Table 12: Protein digestion enzymes used for bottom-up proteomics in this study.

Enzyme	Source	Incubation temperature [°C]
GluC	Promega, V1651	37
Chymotrypsin	Roche, 11418467001	25
AspN	Promega, V1621	37

2.2.7 SDS-PAGE

Mixtures of purified protein or clarified cell lysates (see 2.3.5) were resolved using denaturing polyacrylamide gel electrophoresis (PAGE) supplemented with sodium dodecyl sulfate (SDS). Purified protein mixtures were supplemented with 2xLämmli buffer and separated on a 12% polyacrylamide gel (Table 13) in a Mini-PROTEAN Tetra vertical electrophoresis cell (Bio-Rad Laboratories). Running buffer in the inner chamber (25 mM Tris, 190 mM glycine, 0.1% SDS) was supplemented with 100mM sodium acetate for the outer chamber to enhance the resolution of smaller proteins. Gels were stained by Coomassie staining with Instant*Blue* solution (Sigma-Aldrich) or subjected to western blotting.
For large-scale experiments with more than 16 samples, the Criterion Vertical Electrophoresis Cell (BioRad) was used in combination with commercially available Criterion TGX Pre-cast gels and the appropriate running buffer (25mM Tris, 192mM glycine, 0.1% SDS, pH 8.3).
Preparation of samples from cell lysates are described in chapter 2.3.6.

Table 13: Recipe for six 12% SDS gels.

Component	Stacking gel [ml]	Separating gel [ml]
Rotiphorese Gel 40 (Roth)	1.275	9
1.5 M Tris pH 8.8	n/a	7.8
1 M Tris pH 6.8	1.25	n/a
10 % SDS	0.1	0.25
H_2O	7.265	12.676
10 % Ammonium persulfate (APS)	0.1	0.25
Tetramethyl ethylenediamine (TEMED, Roth)	0.01	0.024

2.2.8 Western blotting

Proteins separated by SDS-PAGE were transferred onto polyvinylidene fluoride (PVDF) membranes via semi-dry blotting using the TransBlot Turbo system (Biorad) according to the manufacturer's protocol. BioRad TGX Pre-cast gels were blotted using the Scie-Plas V20-SDB blotting system. The western blotting stack was assembled according to standard procedure. In brief, Whatman paper were pre-soaked in transfer buffer (25mM Tris, 192mM glycine, 10% (v/v) methanol, 0.1% SDS) and layered with the methanol pre-soaked PVDF membrane and polyacrylamide gel followed by a second layer of Whatman paper. Transfers were conducted at 98mA for 1-1.5h (Scie-Plas system) or 1A for 30 minutes (BioRad TransBlot system).

2.2.9 Immunoblot analysis

Membranes were handled in PBS buffer (Table 14) supplemented by 0.05% Tween20 (PBS-T). After transfer, membranes were blocked in blocking solution (1xPBS-T, 5% (w/v) milk powder) for 1h to reduce unspecific antibody binding. Membranes were then incubated with primary antibodies diluted in blocking solution for 16h at 4°C. The list of used primary antibodies and the respective dilutions is given in Table 15. After incubation, membranes were washed three times for 5-10 minutes with PBS-T by gentle rocking followed by, if applicable, the incubation with the appropriate secondary antibody coupled to horseradish peroxidase (HRP) for 1h at room temperature (RT, Table 16). Unbound secondary antibodies were removed by washing three times with PBS-T. The analysis was conducted using enhanced chemiluminescence (ECL). Chemiluminescent signals were developed using an ECL substrate (Advansta WesternBright ECL) according to the supplier's instructions and recorded using a digital imaging system (Gel Doc XR+ system or GelDoc Go system, BioRad Laboratories). The exposure times were adjusted to avoid oversaturation. Image files obtained were analyzed using the ImageLab software version 5.2.1 (BioRad).

Table 14: Recipe for 10x PBS in H_2O.

Ingredient	Concentration [M]
NaCl	1.37
Na_2HPO_4	0.1
KCl	0.027
KH_2PO_4	0.019

Table 15: List of primary antibodies used in this study.

Antibody	Manufacturer	Product No.	Species	Dilution
α-FLAG-HRP	Miltenyi Biotec	130-101-572	human	1:5000
α-GAPDH	Invitrogen	39-8600	mouse	1:1000
α-ISG15	Proteintech	15981	rabbit	1:500
α-K-ε-GG	Lucerna	30-0100	mouse	1:500
α-M1-Ubiquitin	Sigma-Adrich	ZRB2114	rabbit	1:1000
α-M1-Ubiquitin	AG Walczak, Univ. Cologne	n/a	rabbit	1:1000
α-NEDD8	Abcam	ab81264	rabbit	1:500
α-Tubulin	Millipore Sigma	T6074	mouse	1:1000

α-Ubiquitin	Sigma-Aldrich	05-944	mouse	1:3000
α-β-Actin	Santa Cruz	sc-81178	mouse	1:1000

Table 16: List of secondary antibodies used in this study.

Antibody	Manufacturer	Product No.	Dilution
HRP α-mouse	Cell Signaling Technology	7076	1:3000
HRP α-rabbit	Cell Signaling Technology	7074	1:3000

2.3 Cell biology

2.3.1 Cultivation of human cells

Cell lines HEK293T and HEK-Blue™ IFN-α/β cells were maintained in Dulbecco's modified eagle medium (DMEM; Gibco) supplemented with 10% fetal bovine serum (FBS; PAN-Biotech) and 1% Penicillin-Streptomycin (100U/ml penicillin, 0.1mg/ml streptomycin; Sigma Aldrich). Used cell lines were maintained in 10cm dishes as adherent cultures at 37°C and 5% CO_2 in a humidified incubator. Cultures were routinely inspected under an inverted light microscope (Zeiss Primovert) for cell confluence and morphology. Used cell lines and their sources are listed in Table 17.

Table 17: Human cells lines used in this study.

Cell line	Source
HEK293T	ATCC
HEK-Blue™ IFN-α/β	Invivogen, kind gift by Prof Dr. K.P. Knobeloch, University Medical Center Freiburg

2.3.2 Cell passaging and seeding

Cells were passaged at a 70-90% confluency by aspiration of the medium, washing with sterile 1xPBS and treatment with Trypsin-EDTA in PBS (Biowest) for cell

dissociation. The enzymatic reaction was neutralized by added medium, and the solution was centrifuged at 150xg for 5 minutes. The supernatant was discarded, the pellet resolubilized in fresh medium and plated onto new culture dishes in a split ratio of 1:10 (HEK-Blue™ IFN-α/β) or 1:30 (HEK293T). Seeding densities used for different experiments varied across cell lines and purpose and are listed in Table 18. Cells were counted using a cell counter chamber (CytoSmart) and an automated cell counter (Corning) with visualization in the Axis Vue software (Axion Biosystems).

Table 18: Seeded cell numbers for used cell lines and the respective experiment.
The time of harvest refers to the time after seeding. Cell no., Number of seeded cells.

Cell line	Experiment type	Cell No.	Harvest	Vessel
HEK293T	Clippase-treatment on cell lysate	$4.5x10^6$	24h	10cm dish
HEK-Blue™ IFN-α/β	IFNβ-treatment in culture & Clippase-treatment on cell lysate	$2x10^6$	48h	10cm dish

2.3.3 Transfection

Cells were transfected one day after seeding at a confluency of 70-90%. HEK293T cells were transiently transfected using polyethylenimine (Boussif et al., 1995). For each condition the plasmid was diluted in serum-free and antibiotics-free DMEM and supplemented with the PEI reagent in a PEI:DNA ratio of 2.5:1. The transfection mix was incubated for 15 minutes to allow for PEI:DNA complex formation. The culture medium was removed and cells were washed with sterile PBS before replenishment with FBS-reduced (50%) DMEM. The transfection mix was then drop-wise added to the cells followed by incubation at 5% CO2 and 37°C. After 4 to 5 hours, the medium was replaced with fresh regular FBS DMEM medium. The cells were harvested 24h after transfection. Volumes and solutions used for PEI transfection for 6-well plates are shown in Table 19. All experiments include a PEI-treated negative control without a transfected plasmid.

Table 19: Volume and quantity used for PEI transfection of HEK293T cells.

Culture plate	Serum-free medium [µl]	DNA [µg]	PEI (1µg/µl) [µl]
6-well	250	2	5

2.3.4 Cell treatments in culture

HEK-Blue™ IFN-α/β cells were treated with Ubiquitin-activating enzyme (UAE; UBA1) inhibitor TAK243 (Cayman) at 500nM for 4h to diminish ubiquitination events in the cells. For the reduction of basal neddylation levels, Nedd8-activating enzyme (NAE) inhibitor MLN4924 (Merck Millipore) was supplemented to cultures at 1µM for 5h. Concentrations used for TAK243 and MLN4924 were titrated to target the levels of the intended modifier, but to omit cross-reactions against ISG15 (Brownell et al., 2010; Hyer et al., 2018). Vehicle (DMSO) and compound-treated plates were handled identically.
For induction of Interferon-stimulated gene expression (ISGs) in HEK-Blue™ IFN-α/β cells, cultures were treated with $1x10^3$ U/ml human Interferon-beta (IFNβ) for 24h or 48h, as indicated at the respective figure. The IFNβ (Proteintech) stock was prepared by reconstitution of 50µg lyophilized IFNβ in 50µl sterile H_2O and further dilution with 450µl sterile 0.1% bovine serum albumin (BSA, Gibco) in PBS solution. Cell treatments were stopped by cell harvest.

2.3.5 Cell harvest and lysis

For cell harvest, the culture medium was aspirated the cells were washed with ice-cold 1xPBS. The cells were then scraped in 1ml of PBS using a cell scraper and transferred into a fresh Eppendorf tube. Cell suspension was centrifuged for 5 minutes, 500xg and 4°C. The PBS supernatant was removed, and cell pellets were resuspended in an appropriate volume of lysis buffer (20mM Tris, 150mM NaCl, 0.5% NP-40, 2mM Ethylenediaminetetraacetic acid (EDTA), 5mM N-Ethylmaleinimid (NEM)). Cysteine protease inhibitor NEM and divalent cation chelator EDTA, which prevents metalloprotease activity, were added to preserve protein integrity and present modifications (Beyer et al., 2013; Green & Sambrook, 2012). After brief sonication at 30% amplitude with 3x 10s pulses the cell debris was cleared by centrifugation at 13.000xg for 15 minutes. Total protein concentration of the supernatant was measured by using a Bradford protein assay.

2.3.6 Bradford assay

Protein concentrations of lysates were determined by employing a Bradford protein assay using ROTI-Quant (Roth) according to the manufacturer's protocol. Samples were measured at a spectrophotometer. The BSA dilutions used for the standard curve and the measured dilutions of lysates were prepared in lysis buffer (chapter 2.3.5) lacking NP-40. The detergent could distort protein measurement resulting in an inaccurate reflection of protein concentration (Compton & Jones, 1985). The protein concentration of lysates was interpolated from the BSA standard curve. Lysates were

measured in triplicates and the measurements were averaged. Protein concentrations were adjusted to 5µg/µl, if not indicated otherwise. Samples were either mixed with 5x Lämmli buffer (Table 20), denatured at 95°C for 5 minutes and analyzed by SDS-PAGE and immunoblot analysis or were further processed by in-lysate treatments.

Table 20: Recipe for 5xLämmli buffer used for cell lysates.

Component	Concentration
Tris pH 6.8	300mM
SDS	10% (w/v)
Glycerol	50% (v/v)
Bromophenol blue	0.03% (w/v)
β-mercaptoethanol	25% (v/v)

2.3.7 Cell lysate treatment with Clippases and DUBs

For enzymatic treatment of cell lysates, unreacted cysteine inhibitor NEM in the lysis buffer was quenched by addition of 10mM DTT and incubation for 10 minutes on ice (G. Shen et al., 2018). Tested proteins and incubation times vary and are indicated at the respective figure. If not subjected to the Clippomics protocol including mass spectrometry analysis, samples were prepared for SDS-PAGE and immunoblot analysis (2.2.7, 2.2.9).
For the Clippomics methodology test, lysates were pre-treated with purified pan-DUB SnUSP1 or deneddylase NEDP1 for removal of residual ubiquitination or neddylation (Boll et al., 2023; Mendoza et al., 2003; L. Shen et al., 2005). After incubation with DTT, samples were supplemented with 10µM SnUSP1 or 10µM NEDP1 for 1h on ice. The generation of GlyGly-sites on present modifiers was conducted by incubation with 10µM BpJOS or 40µM Lbpro WT for 1h or 2h on ice, as indicated at the figures. All enzymes where pre-diluted in reaction buffer (2.2.2), if necessary.

2.3.8 Clippomics sample preparation for mass spectrometry

For the Clippomics method, pre-treated cell lysates (2mg protein per sample) were precipitated by addition of 4 times the sample volume 100% MS-grade acetone, cooling at -80°C for 15 minutes and over 120 minutes at -20°C. The samples were centrifuged at 6000xg for 15 minutes at 4°C before removal of the acetone and air-drying for 20 minutes at RT. The proteins pellets were further denatured by resuspension in 8M MS-grade Urea for a concentration of 25µg/µl. Samples were reduced by addition of

DTT (4.5mM f.c.) for 1h at RT and alkylated by treatment with CAA (40mM f.c.) under light-protected conditions for 30 minutes at RT. In preparation for enzymatic protein digestion, the urea concentration was diluted by addition of buffers or left undiluted. Enzymes used and the respective buffers used for dilution are listed in Table 21. Digestion was conducted at an enzyme:substrate ratio of 1:200 for the initial clippomics establishment (3.2.1), which was conducted during the master thesis (Kolek, 2021) or at a Lysarginase:substrate ratio of 1:50 for all following Clippomics studies for 18h. Prior to C18 purification and GlyGly-enrichment, efficient Lysarginase digestion of proteomic samples was tested by LC-MS/MS measurement of 10µl lysate (2.4.1, 2.4.2).

Table 21: Used digestion enzymes for the Clippomics method.

Digestion enzyme	Source	Used buffer	Incubation temperature [°C]
Lysarginase	Merck Millipore, EMS0008	50mM HEPES pH7.5, 5mM $CaCl_2$	37
Chymotrypsin	Roche, 11418467001	100mM Tris pH8, 10mM $CaCl_2$	25
LysC	Promega, VA1170	no dilution required	37

2.3.9 C18 purification and GlyGly-enrichment

For the Clippomics method, digested proteins were cleared from salts and concentrated by C18 purification using C18 cartridges SepPak® 3cc 200mg (Waters, WAT054945) columns. The purification was conducted according to the protocol of used PTMScan® HS Ubiquitin/SUMO Remnant Motif (K-ε-GG) Kit (Cell Signaling Technologies, #59322). After desalting, purified peptides were eluted in 0.1% Trifluoroacetic acid (TFA), 50% acetonitrile solution. The solvent was removed under vacuum using a SpeedVac instrument. The drying of peptides was kindly conducted by members of the Neundorf lab (Biochemistry Institute, University of Cologne) using a XcelVap® Automated Concentration/Evaporation System at 1200mbar and 23°C for ~6h. The information was kindly provided by M.Sc. Melina Ruppel, Neundorf lab.
Dry peptides were stored at -80°C until subsequent immunoaffinity purification (IAP) of GlyGly(K)-sites using the PTMScan® HS Ubiquitin/SUMO Remnant Motif (K-ε-GG) kit according to the manufacturer's protocol. After the enrichment, the peptide eluate was present in 50µl IAP buffer and stored at -20°C until preparation for mass spectrometry.

2.4 Mass spectrometry

2.4.1 Stage tip purification of peptides

Digested peptides were purified using Stage tips containing two layers of Styrenedivinylbenzene–Reversed Phase Sulfonate (SDB-RPS) disks. All buffers and the protocol used were provided by the Proteomics Core Facility Cologne. In brief, the disks were equilibrated by addition of 20µl methanol, 20µl 0.1% formic acid in 80% Acetonitrile (Buffer B) and two washes with 20µl 0.1% formic acid in water (Buffer A) Each step was followed by centrifugation 2.600 rpm for 1 minute at RT. If samples have not been acidified at this step, samples were supplemented with 0.1% formic acid (FA) in water for a f.c. of 1% (FA) and cleared by centrifugation at 13.000xg for 5 minutes before loading onto the Stage tips. After centrifugation for 5 minutes, disks were washed with two times 30µl Buffer A followed by one wash with 30µl of buffer B. Stage tips were dried by passing air through the tip with a syringe after the last wash step and stored at 4°C until measurement by the Core Facility.

2.4.2 LC-MS/MS

Peptide samples were measured by liquid chromatography tandem mass spectrometry (LC-MS/MS) by the Proteomics Core Facility Cologne, which kindly provided the following measurement information.
Samples were analyzed by the CECAD Proteomics Facility on an Orbitrap Exploris 480 (Thermo Scientific, granted by the German Research Foundation under INST 216/1163-1 FUGG and INST 1856/71-1 FUGG) mass spectrometer that was coupled to an Vanquish neo in trap-and-elute setup (Thermo Scientific). Samples were loaded onto a precolumn (Acclaim 5µm PepMap 300 µ Cartridge) with a flow of 60 µl/min before reverse-flushed onto an in-house packed analytical column (30 cm length, 75 µm inner diameter, filled with 2.7 µm Poroshell EC120 C18, Agilent). Peptides were chromatographically separated with an initial flow rate of 400 nL/min and the following gradient: initial 2% B (0.1% formic acid in 80 % acetonitrile), up to 6 % in 3 min. Then, flow was reduced to 300 nl/min and B increased to 20% B in 26 min, up to 35% B within 15 min and up to 98% solvent B within 1.0 min while again increasing the flow to 400 nl/min, followed by column wash with 95% solvent B and re-equilibration to initial condition. The mass spectrometer was operated in data-dependent acquisition with a cycle time of 1 s with MS1 scans acquired from 350 m/z to 1400 m/z at 60k resolution and an AGC target of 300%. MS2 scans were acquired at 15 k resolution with a maximum injection time of 118 ms (whole proteome samples: 52ms) and a normalized AGC target of 50% (whole proteome samples:100%) in a 2 Th window and a fixed first mass of 110 m/z. All MS1 scans were stored as profile, all MS2 scans as centroid.

The raw data obtained was autonomously analyzed using MaxQuant (v1.6.12, v2.6.4) and visualized using Perseus (v1.6.15.0 and v2.1.2.0(Cox & Mann, 2008; Tyanova et al., 2016). For the analysis by MaxQuant, the tables ‘proteingroups’, ‘GlyGly(K)modifications’ and ‘modificationSpecificPeptides’ were employed depending on the experiment type.

2.4.3 Intact mass

For analysis of potential clippase activity by intact mass, 10µM PcJOS in reaction buffer (see 2.2.2) was mixed 1:1 with 500mM 2M1 ubiquitin chains. The reaction was quenched after a 2h incubation time at RT by addition of 13,2µl inhibitor solution (0.1% formic acid, 4mM NEM) and submitted to the Proteomics Core Facility Cologne. The following paragraph was provided by the Core Facility and Dr. Thomas Hermanns:

The PcJOS reaction was analyzed on a Q Exactive Plus Orbitrap (Thermo Scientific) mass spectrometer that was coupled to an EASY nLC (Thermo Scientific). Proteins were diluted in solvent A (0.1% formic acid in water) and loaded onto an in-house packed pulled tip column (18 cm length, 75 µm I.D., filled with MABPac™ RP polymeric resin, 4 µm, 1.500 Å, Thermo Scientific). The column was operated at 50 °C and proteins were separated at a constant flow rate of 600 nL/min using the following gradient: 3-15% solvent B (0.1% formic acid in 80 % acetonitrile) within 1.0 min, 15-60% solvent B within 15.0 min, 60-95% solvent B within 1.0 min, followed by washing and column equilibration. Full MS1 scans were acquired from 600-2000 m/z combining 2 microscans at a resolution of 140,000. The AGC target was set to 3E6 and the maximum injection time to 200 ms. Combined exact mass spectra of selected scans were exported from Excalibur 3.1 (Thermo Scientific).

Obtained raw data were analyzed using the opensource mass spectrometry tool mMass v5.5 (Niedermeyer & Strohalm, 2012) by Dr. Thomas Hermanns (Hofmann lab, Cologne).

3 Results

3.1 Identification and characterization of novel clippases

Clippases are a newly found class of de-modifying enzymes, which were shown to cleave ubiquitin and ubiquitin-like modifiers before their C-terminal GlyGly-motif. This newly discovered cleavage mode was first shown to be employed by viral leader protease of foot-and-mouth disease virus Lbpro (Swatek et al., 2018). Recent studies using bioinformatical database searches revealed the existence of a multitude of ubiquitin C-terminal clippases (UCCs) in bacterial genomes of various genera (Hermanns et al., 2025). Biochemical *in vitro* characterization of the UCCs demonstrated varying cleavage activities in terms of ubiquitin chain specificity and speed. Among the discovered UCCs are BpJOS from *Burkholderia pyrrocinia,* BcJOS from *Burkholderia catarinensis* and PcJOS from *Parachlamydia sp*. To deepen the understanding of clippase activity and specificity, these UCCs were, amongst additional UCC candidates, tested on endogenous ubiquitination levels as found in cell lysates.

3.1.1 BpJOS, BcJOS and SnJOS1/2 show clippase activity in cell lysate

Bioinformatical database searches (Hermanns and Hofmann 2023) had led to the identification of multiple UCC candidates in several bacterial genera (Kay Hofmann, personal communication; Hermanns et al., 2025). The goal was to potentially identify candidates, which employ clippase activity on ubiquitin and, ideally, would show modifier- or linkage-specificity in later biochemical characterizations. As solely sequence-based determinants for clippase activity have not been identified yet, representative candidates of potential bacterial Josephin members were selected for activity tests. These candidates include enzymes from *Burkholderia pyrrocinia*, *Simkania negevensis*, *Burkholderia catarinensis*, *Pseudovibrio sp*., *Chlamydiales sp*., *Pigmentiphaga aceris*, *Herbaspirillium sp.,* and *Parachlamydia* (Hermanns et al., 2025). One single candidate, ChNJC from *Chlamydiales bacterium STE3* does not belong to the Josephin family but harbored a predicted clippase-like active site and was therefore included in the test panel as a ‘non-Josephin clippase candidate’ (NJC). The comprehensive list of assessed enzymes and their origin is given in Table 22.

Table 22: Enzymes characterized for ubiquitin C-terminal clippase (UCC) activity.

UCC Candidate	Origin species	Uniprot Accession No.
BpJOS	*Burkholderia pyrrocinia*	A0A118Q714
BcJOS	*Burkholderia catarinensis*	A0A1J9PQV4
SnJOS1	*Simkania negevensis*	F8L436
SnJOS2	*Simkania negevensis*	F8L650
PcJOS	*Parachlamydia sp.*	A0A2H9SU66
PvJOS	*Pseudovibrio sp.*	A0A165MKT0
PaJOS	*Pigmentiphaga aceris*	A0A5C0B1L0
HeJOS	*Herbaspirillium sp.*	J3HRE0
CsJOS	*Chlamydiales bacterium STE3*	KAF3361746.1
ChNJC	*Chlamydiales sp.*	A0A1M3CS75

A multiple sequence alignment of the selected Josephin candidates revealed the conservation of the predicted active-site residues Cys, His and Asp/Asn and multiple conserved residues surrounding the active site when compared to two the human Josephins ATXN3L and JOSD2 (Figure 12, Kay Hofmann). The aromatic gatekeeper motif, shown to direct the ubiquitin cleavage position in several regular DUBs, was present in five of nine candidates (Figure 12, highlighted in blue; Hermanns et al., 2020). The presence of the proposed catalytic triads and the alignment of several amino acid positions warranted the testing of the identified candidates in biochemical experiments for potential clippase activity.

Figure 12: Multiple sequence alignment of bacterial Josephin-family members. Multiple-sequence alignment of all bacterial Josephin ubiquitin C-terminal clippase (UCC) candidates covered in this study. Sequences are aligned and compared to two human Josephins (bottom lines). Residues printed in black or grey background are invariant or conservatively replaced in at least 50% of all considered bacterial Josephin sequences. The active site residues are highlighted in red and the conserved aromatic motif is highlighted in blue (Kay Hofmann, personal communication).

Depending on the presence of transmembrane and unstructured regions, either full-length proteins or predicted catalytic domains were expressed by Dr. Thomas Hermanns (Institute for Genetics, Cologne). Most candidates were characterized biochemically in *in vitro* assays using purified ubiquitin substrates and activity-based probes in a collaborative publication of the Hofmann group (Hermanns et al., 2025). The publication contains some of the data generated in this thesis project.

To assess the catalytic properties of tested UCCs and UCC candidates in a complex environment, their activity was comprehensively tested on HEK293T cell lysate and analyzed by western blotting. Potential deubiquitination activity was monitored with an anti-ubiquitin antibody. In parallel, potential clippase activity was tested using an anti-K-ε-GG antibody, which specifically detects GlyGly-remnants on the epsilon-amino-group of lysine residues (G. Xu et al., 2010).

HEK293T cell lysate incubated with purified N-terminally truncated BpJOS$^{12\text{-}218}$ showed complete deconjugation of cellular ubiquitination when compared to the untreated control (Figure 13A). Only the band at around 10kDa corresponding to monomeric ubiquitin remained detectable. Simultaneously, BpJOS generated strong signals across all molecular weights detected with the anti-K-ε-GG antibody. As ubiquitination was cleaved down including the last moiety, the GlyGly-remnants reflected former ubiquitinated substrates carrying the GlyGly-marking. This result evidently demonstrated clippase-activity by BpJOS. Incubation of lysate with the purified catalytic active domain of USP21$^{196\text{-}565}$ was used as a control and resulted in complete removal of substrate ubiquitination but failed to generate signal with the K-ε-GG-antibody (Figure 13A). USP21 belongs to the USP class and is known as a highly active conventional DUB cleaving all ubiquitin chain types (Hospenthal et al., 2015; Ye et al., 2011) underlining the specificity of the K-ε-GG-antibody and its suitability for detection of clippase products in complex samples. The two eukaryotic Josephins ATX3L and JOSD2 showed moderate reduction of general ubiquitination levels when tested on lysate (Figure 13A). As for the catalytic domain of USP21, lysate treatment with ATX3L and JOSD2 did not generate GlyGly-signals.

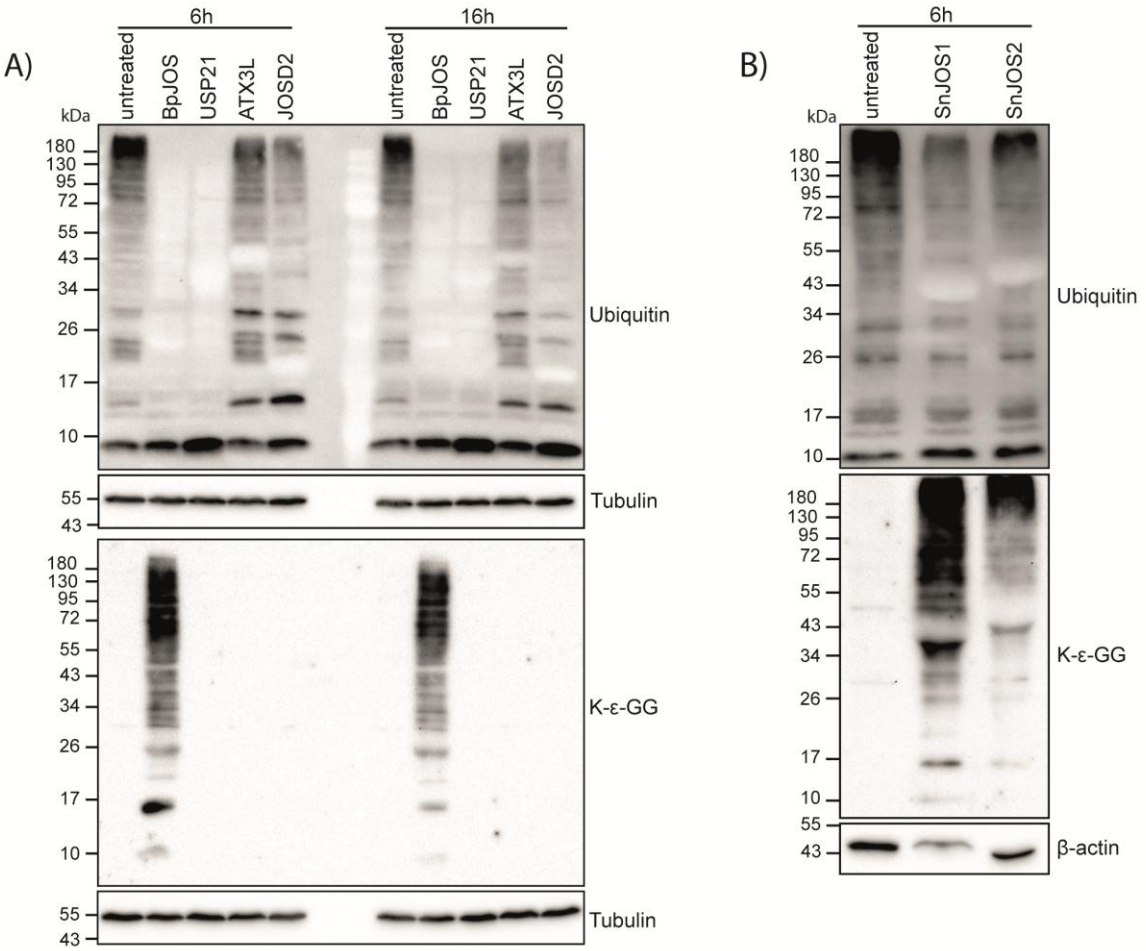

Figure 13: BpJOS, SnJOS1 and SnJOS2 clip ubiquitin in cell lysate. HEK293T cell lysates were left untreated or were treated with the indicated purified proteins at 10µM f.c. followed by incubation on ice. Samples were analyzed by western blotting and detection with antibodies against ubiquitin and GlyGly-remnants on lysine residues (K-ε-GG). **A)** Cell lysate was treated with purified BpJOS$^{12-218}$, USP21$^{196-565}$, ATX3L or JOSD2 for 6h or 16h. Tubulin was detected as a loading control. **B)** Cell lysate was treated with SnJOS1 or SnJOS2 for 6h. Beta-actin was detected as loading control. K-ε-GG, Diglycyl-epsilon-aminogroup-lysine; β-actin, beta-actin.

Treatment of HEK29T lysates with SnJOS1 and SnJOS2 from *Simkania negevensis* demonstrated generation of GlyGly-markings with SnJOS1 showing higher activity compared to SnJOS2 (Figure 13B). The SnJOS enzymes were less active than BpJOS, considering that 6h incubation with SnJOS1/2 only partially cleared HMW-ubiquitination, while 6h incubation with BpJOS removed all ubiquitination (Figure 13A).

Purified catalytic domain of UCC candidates PvJOS$^{764-1098}$ from *Pseudovibrio sp*. showed moderate deubiquitinase activity when added to lysate, while GlyGly-signals remained undetectable, suggesting regular DUB activity (Figure 14A).

The two candidates from *Chlamydiales sp*., CsJOS$^{56-289}$ and ChNJC$^{56-289}$ as well as PcJOS$^{70-324}$ from *Parachlamydia sp*. appeared inactive in this experimental approach

as neither a decrease of ubiquitination levels nor the production of GlyGly-remnants were observed for all three candidates (Figure 14A,B).

Full-length BcJOS from *Burkholderia catarinensis* displayed major ubiquitin deconjugation activity in cell lysate cleaving all ubiquitination within 1 hour incubation on ice (Figure 14B). BcJOS resembled the activity of BpJOS as both were able to efficiently cleave ubiquitin moieties down to the GlyGly-motif remaining on former substrates (Figure 14B). UCC candidates PaJOS from *Pigmentiphaga aceris* and HeJOS from *Herbasprillium* sp. demonstrated lower activity against cellular ubiquitination when compared to BcJOS and BpJOS. The absence of detectable GlyGly-remnant production suggested PaJOS and HeJOS to be conventional DUBs, while PcJOS was seemingly inactive.

Based on this characterization using the anti-K-ε-GG antibody, BpJOS, SnJOS1 SnJOS2 and BcJOS could be verified as UCCs, with BpJOS and BcJOS demonstrating the highest activity when tested on HEK293T cell lysates.

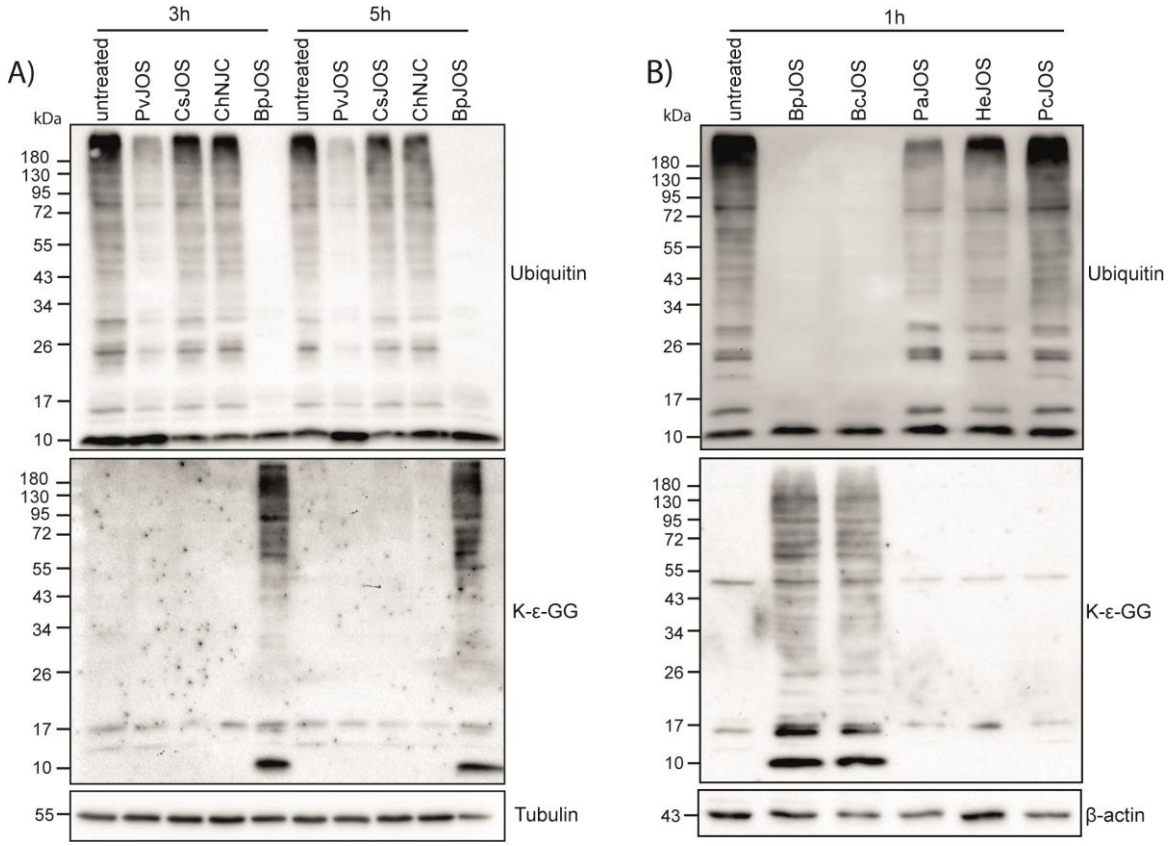

Figure 14: Candidates PvJOS, BcJOS, PaJOS and HeJOS show ubiquitin-deconjugating activity in cell lysate. HEK293T cell lysates were left untreated or were incubated with 10µM of the indicated purified proteins and incubated on ice**.** Samples were analyzed by western blotting and detection with antibodies against ubiquitin and GlyGly-sites on lysine residues (K-ε-GG). **A)** Cell lysates were treated with PvJOS$^{764-1098}$, CsJOS$^{56-289}$, ChNJC$^{56-289}$ or BpJOS$^{12-218}$ for 3h or 5h. Tubulin was detected as a loading control. **B)** Cell lysate was incubated with BpJOS$^{12-218}$, BcJOS, PaJOS$^{1881-2146}$, HeJOS or PcJOS$^{70-324}$ for 1h. Beta-actin was detected as loading control. K-ε-GG, Diglycyl-epsilon-aminogroup-lysine; β-actin, beta-actin. Figure B) was published in Hermanns et al. 2025, see figure 1E.

3.1.2 PcJOS is an M1-specific clippase

PcJOS from *Parachlamydia sp*. showed no visible activity when tested on lysate of HEK293T cells (Figure 14B). Bacteria of the *Parachlamydia* genus, such as *Parachlamydia acanthamoebae* are obligate intracellular bacteria that naturally infect amoeba (Greub, Mege, & Raoult, 2003). However, studies with human macrophages have shown that the bacteria can enter these cells under experimental conditions rendering it a potential human pathogen (Greub, Mege, & Raoult, 2003). Bacterial invasion into human cells triggers defense responses leading to a unique subset of expressed proteins and ratios of specific ubiquitin chain topologies, which are less prevalent in unstressed cells. One example is the absence or low basal levels of linear chains in most unperturbed cells (Tsuchiya et al., 2018; P. Xu et al., 2009).

To investigate whether PcJOS inactivity in lysate of HEK293T cells was based on the absence of the appropriate substrate, PcJOS was probed against a panel of purified di-ubiquitin of all chain types. PcJOS cleaved linear di-ubiquitin chains at nano-molar concentrations demonstrating its specificity for M1 chains (Figure 15A). Linear chains are present at only low levels in unstressed cells providing an explanation for the absence of activity in HEK293T cell lysate (Figure 14B). To test whether PcJOS exhibits conventional DUB or clippase activity, linear di-ubiquitin chains were incubated with PcJOS and analyzed by intact mass analysis (Figure 15B). The products of the reaction corresponded to m/z ratios for one ubiquitin moiety lacking a GlyGly-motif (UbΔGG) and one moiety harboring an additional GlyGly-motif (GG-Ub) confirming clippase activity by PcJOS. The m/z ratio for an intact moiety (Ub) equals the ratio for a moiety for with an N-terminal GlyGly-motif while simultaneously lacking the C-terminal GlyGly-motif (GG-UbΔGG). The model for PcJOS cleavage of linear di-ubiquitin with its products is displayed in Figure 15C.

To assess whether PcJOS activity on linear chains *in vitro* extends to activity *in vivo,* a suitable cell model was generated. HEK293T cells were transfected with components of the LUBAC complex (HOIL1L, HOIP, Sharpin) for the generation of linear chains *in vivo* (Figure 15D). In a quadruple transfection approach, cells were co-transfected with the LUBAC components together with PcJOS, the catalytic cysteine mutant PcJOS C162A or the M1-chain specific DUB OTULIN (Keusekotten et al., 2013). All used constructs harbored an N-terminal FLAG tag for detection by the α-DYKDDDDK-antibody and were successfully expressed. LUBAC-generated linear chains detected with a linear ubiquitin-specific antibody (α-Ub M1) became undetectable upon co-expression of PcJOS or OTULIN (Figure 15D). By contract, levels of linear ubiquitination remained stable upon expression of PcJOS C162A mutant, demonstrating the deconjugation activity relies on the catalytic cysteine at position 162. Clippase activity could not be monitored by the priorly used anti-K-ε-GG-antibody as the antibody does not detect the GlyGly(M)-motif produced by PcJOS-clipping of linear chains.

Total ubiquitin levels decreased upon LUBAC expression, but no further reduction was observed when cells were co-expressed with PcJOS, PcJOS CA or OTULIN. Flag-tagged Sharpin (40.95 kDa) and FLAG-tagged OTULIN (41.26 kDa) ran at similar molecular weights within the gel resulting in overlapping DYKDDDDK-antibody-signals for both constructs. Efficient expression of Sharpin was demonstrated by the decrease of total ubiquitination comparable to all other LUBAC-transfected samples. OTULIN expression was displayed by the loss of linear chains when co-transfected with LUBAC components (Figure 15D).
Based on the characterization activity *in vitro* and *in vivo*, PcJOS could be verified as the first clippase with a specificity for linear ubiquitin chains.

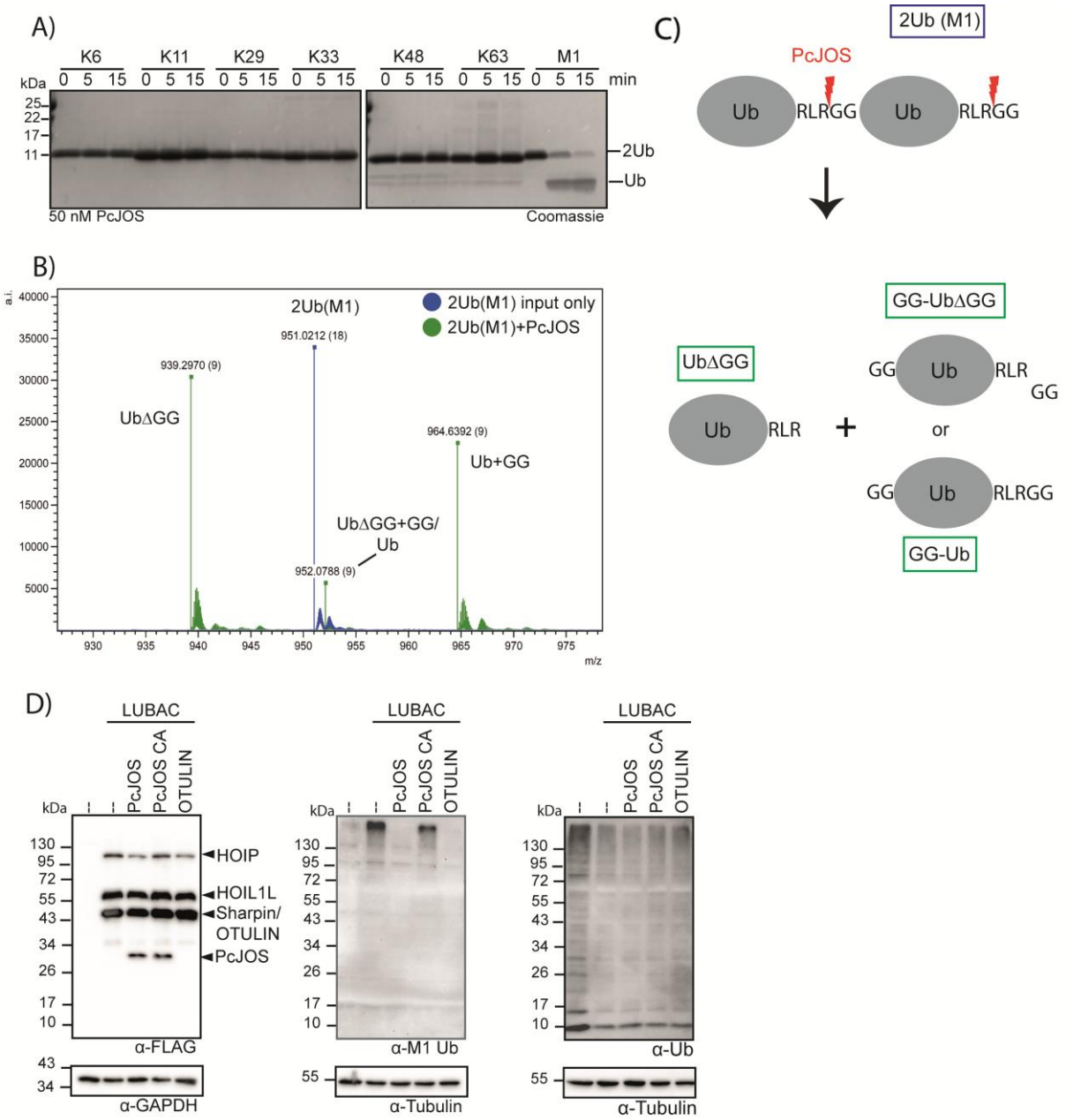

Figure 15: PcJOS cleaves M1 ubiquitin chains *in vitro* and *in vivo*. A) Ubiquitin chain cleavage assay with purified PcJOS$^{70\text{-}324}$ for determination of chain specificity. Di-ubiquitin of all chain types (50µM) were incubated with 50nM PcJOS$^{70\text{-}324}$ for the indicate timepoints, analyzed by SDS-PAGE and visualized by Coomassie staining. **B)** Analysis of PcJOS cleavage mode by intact mass spectrometry. M1-linked di-ubiquitin was incubated with 5µM (f.c.) PcJOS$^{70\text{-}324}$ for 2h at RT. Indicated peaks represent arbitrary intensities (a.i.) over the mass/charge (m/z) ratio of the measured molecules. Peaks for the uncleaved linear di-ubiquitin (2Ub(M1)) input are shown in blue. Measured peaks of the reaction products are given in green. **C)** Schematic representation of possible cleavage products (green borders) of linear di-ubiquitin (blue border) processed by PcJOS. **D)** HEK293T cells were transfected with Flag-tagged LUBAC components HOIP, HOIL1 and Sharpin alone or simultaneous with FLAG-PcJOS$^{70\text{-}324}$, FLAG-PcJOS$^{70\text{-}324}$C172A or FLAG-OTULIN. Samples were analyzed by western blotting and decoration with antibodies against FLAG, linear ubiquitin (M1 Ub) and total ubiquitin (Ub). GAPDH and tubulin were detected as loading controls. m/z, mass over charge; CA, cysteine to alanine mutant.
Experiments shown in A) and B) were conducted during the master's thesis (Kolek 2021) and were published in Hermanns et al. 2025, see Figures 1I&1K.

3.1.3 BpJOS is a highly active, chain-promiscuous ubiquitin clippase

BpJOS exhibited clippase activity when added to HEK293T cell lysate cleaving all cellular ubiquitination within 1h on ice indicating chain promiscuity (Figure 13B). To validate this observation, di-ubiquitin chains of all linkages were incubated with purified full-length BpJOS. Apart from K27-linked di-ubiquitin, BpJOS was able to cleave all ubiquitin chain types in completion at a nanomolar concentration within 30 minutes (Thomas Hermanns, Figure 16A, Hermanns et al., 2025).

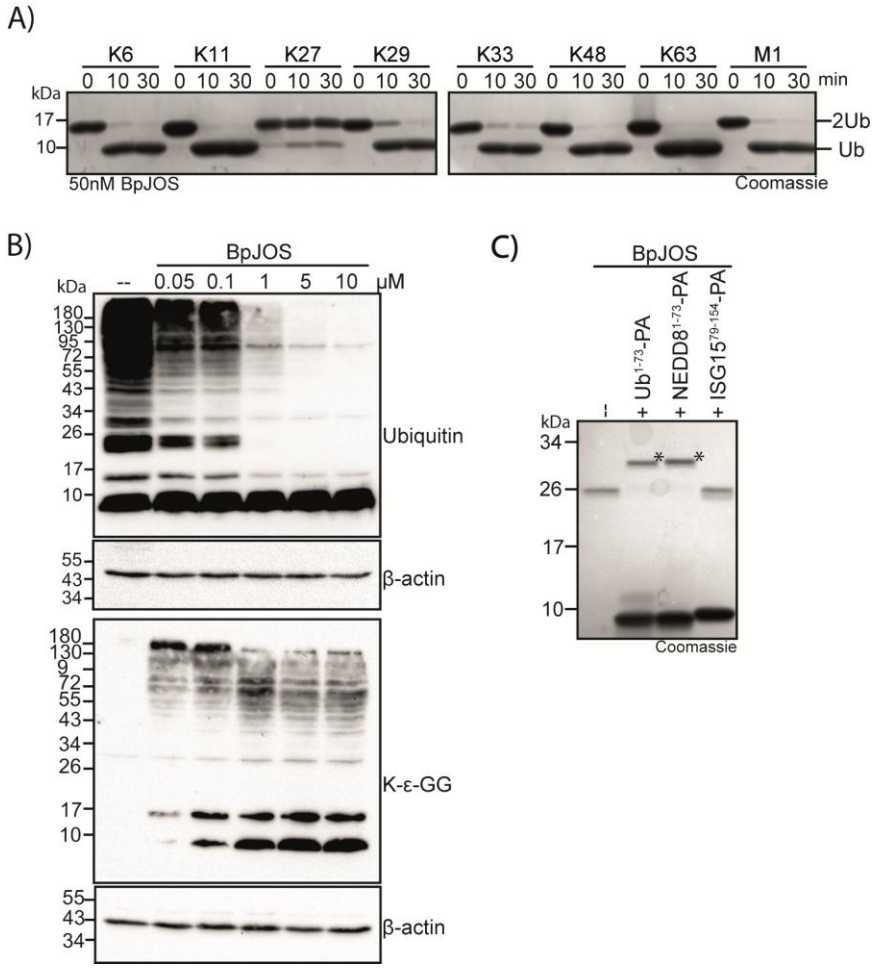

Figure 16: Characterization of BpJOS activity. A) Ubiquitin chain cleavage assay with BpJOS. Chain specificity was tested by incubation of 50µM di-ubiquitin chains of all chain types with 50nM BpJOS for the indicated timepoints. Analysis was conducted by SDS-PAGE and visualization by Coomassie staining. **B)** BpJOS activity test in HEK293T cell lysate. Cell lysate samples were left untreated or were treated with increasing amounts of BpJOS$^{12-218}$ for 1h on ice. Ubiquitination levels and the generation of GlyGly-remnants were monitored by western blotting and α-ubiquitin and α-K-ε-GG detection. Beta-actin (β-actin) was detected as loading controls. Per lane 50µl of protein cell lysate was probed (10µl of 5ug/ul lysate) **C)** Activity-based probe assay for modifier specificity tests of BpJOS. Propargylamine (PA-)-coupled, C-terminally truncated ubiquitin (ubiquitin$^{1-73}$-PA), Nedd8 (Nedd8$^{1-73}$-PA) and ISG15 (C-terminal moiety, ISG15$^{79-154}$-PA) probes (50µM) were incubated with 5µM BpJOS for 18h at 20°C. Asterisks (*) mark the shifted bands after reaction. Reactions were analyzed by SDS-PAGE and Coomassie staining. K-ε-GG, Diglycyl-epsilon-aminogroup-lysine Experiments shown in A) and C) were conducted by Thomas Hermanns (Institute for Genetics, Cologne) and published in Hermanns et al. 2025, see figures 1F and S2B. Experiment shown in B) was included in the master thesis (Kolek 2021).

This result demonstrated BpJOS high efficiency in chain cleavage without displaying linkage specificity. To titrate BpJOS deconjugation activity speed in a semi-quantitative manner, HEK293T lysate was treated with purified BpJOS for 1h on ice at different concentrations ranging from 50nM to 10µM (Figure 16B). A minor reduction in ubiquitination was observed at the lowest BpJOS concentration of 50nM. Simultaneously, GlyGly-remnants of primarily high-molecular weight (HMW) were detected with the K-ε-GG-antibody. This observation indicated that BpJOS might first collapse ubiquitin chains before completely removing them off substrates at lower enzyme:substrate concentrations, since GlyGly-signals migrated from a higher to a lower molecular weight with increasing BpJOS concentration (Figure 16B). At 5µM, BpJOS disassembled nearly all detectable ubiquitination with only minor further reduction at twice the concertation (10µM). Bands appearing close to the 10kDa marker in samples treated with >100nM BpJOS are suggested to be single ubiquitin moieties carrying a GlyGly-remnant at one more multiple lysine residues within ubiquitin. These remnants are proposed to arise from initial inner-chain ubiquitin moieties modified by a more distal ubiquitin.

To investigate whether BpJOS exhibits modifier-selectivity, an activity-based probe assay was performed.

The probes harbored a propargylamine (PA) group, which acts as a reactive warhead, at the C-terminus. In general, the catalytic cysteine residue of a protease attacks the electrophilic carbon, which is positioned towards the protease active site upon substrate binding. In case of the PA probe, the propargylamine warhead forms a covalent bond with the attacking catalytic cysteine residue upon reaction (Borodovsky et al., 2002). A positive reaction is visualized by the mass shift of the protease-probe reaction compared to the mass of the protease alone. A shortened mono ubiquitin-based model substrate (ubiquitin$^{1-73}$-PA) was used, in which Arg74 was replaced with the reactive propargylamine warhead. To assess, whether BpJOS shows reactivity against ubiquitin-like modifiers Nedd8 and ISG15, C-terminally truncated Nedd8- (Nedd8$^{1-73}$-PA) and the C-terminal moiety of ISG15 (ISG15$^{79-154}$-PA) were tested.

In agreement with the prior results on purified di-ubiquitin and cellular ubiquitination cleavage, BpJOS reacted with the ubiquitin$^{1-73}$-PA probe resulting in an upward mass shift (Figure 16C). These results indicated that BpJOS required only one ubiquitin moiety for successful recognition and processing in contrast to some DUBs that necessitate the binding of two or multiple adjacent ubiquitins via their S1 and S1' sites. BpJOS also reacted with the Nedd8$^{1-73}$-PA probe, as indicated by the mass shift demonstrating reactivity towards Nedd8. Despite the long incubation time of 18h at 20°C, BpJOS showed no reaction with the ISG15$^{79-154}$-PA probe indicating inactivity against the Ubl. Taken together, BpJOS was characterized as a highly active, ubiquitin chain promiscuous clippase, that only requires one ubiquitin for recognition and shows cross-reactivity against Nedd8, but not ISG15.

3.1.4 BpJOS is inactive against ISG15

BpJOS was shown to react with activity-based probes based on ubiquitin$^{1-73}$ and Nedd8$^{1-73}$, but not the C-terminal moiety of ISG15$^{79-154}$ (Figure 16C). To elucidate, whether BpJOS might require the complete ISG15 entity for recognition and, if the inactivity against ISG15 would be reproducible in cell lysates, BpJOS was tested against cell lysates with abundant ISGylation targets. Standardized cell culture lines such as HEK293T cells express little, if any detectable endogenous levels of interferon-stimulated genes such as ISG15 and its conjugation enzymes. Consequently, most studies reconstitute the ISG15 system by ectopic expression of interferon-stimulated genes since even under interferon-stimulation HEK293T cells hardly show ISG expression (Durfee & Huibregtse, 2010, 2012). To avoid the need for cell transfection, the commercially available HEK blue Interferon (IFN)-α/β reporter cell line was selected for the subsequent tests. The cells are derived from HEK293 human embryonic kidney cells, which were generated to stably express STAT2 and IRF9 to achieve a fully active IFN type I signaling pathway (Invivogen, kind gift of Prof. Dr. K.P. Knobeloch, Freiburg).
HEK blue IFN-α/β reporter cell line will be hereon after referred to as HEK blue cells.

Stimulation of HEK blue cells using human interferon-beta (IFNβ) results in the expression of ISG15 and stable ISGylation levels as monitored by western blotting and detection with an α-ISG15 antibody (Figure 17A). Monomeric ISG15 was visible at around 17 kDa with a ladder of ISG15 signals in the HMW range representing ISG15-conjugated substrates. Induction of ISGylation levels by IFNβ treatment for 24h or 48h harbored similar results with no major increase in detectable ISGylation targets for the longer timepoint (Figure 17A). As shown in Figure 17A, the anti-ISG15 antibody produced unspecific bands at around 19kDa, 35kDa and 60kDa, which are visible even in the untreated control.
The first ever published clippase is Lbpro, the leader protease from foot-and-mouth-disease-virus. Lbpro was shown to act on ISGylated targets in transfected and virus-infected HeLa cells, thereby producing the clippase-characteristic GlyGly-sites detectable with the K-ε-GG-antibody (Swatek et al., 2018).
To test, whether BpJOS would act on ISGylated targets in cell lysate, HEK blue cells were induced by IFNβ treatment and lysates of those cells were incubated with 10µM purified BpJOS. In parallel, samples were treated with 40µM purified Lbpro clippase targeting ISG15.

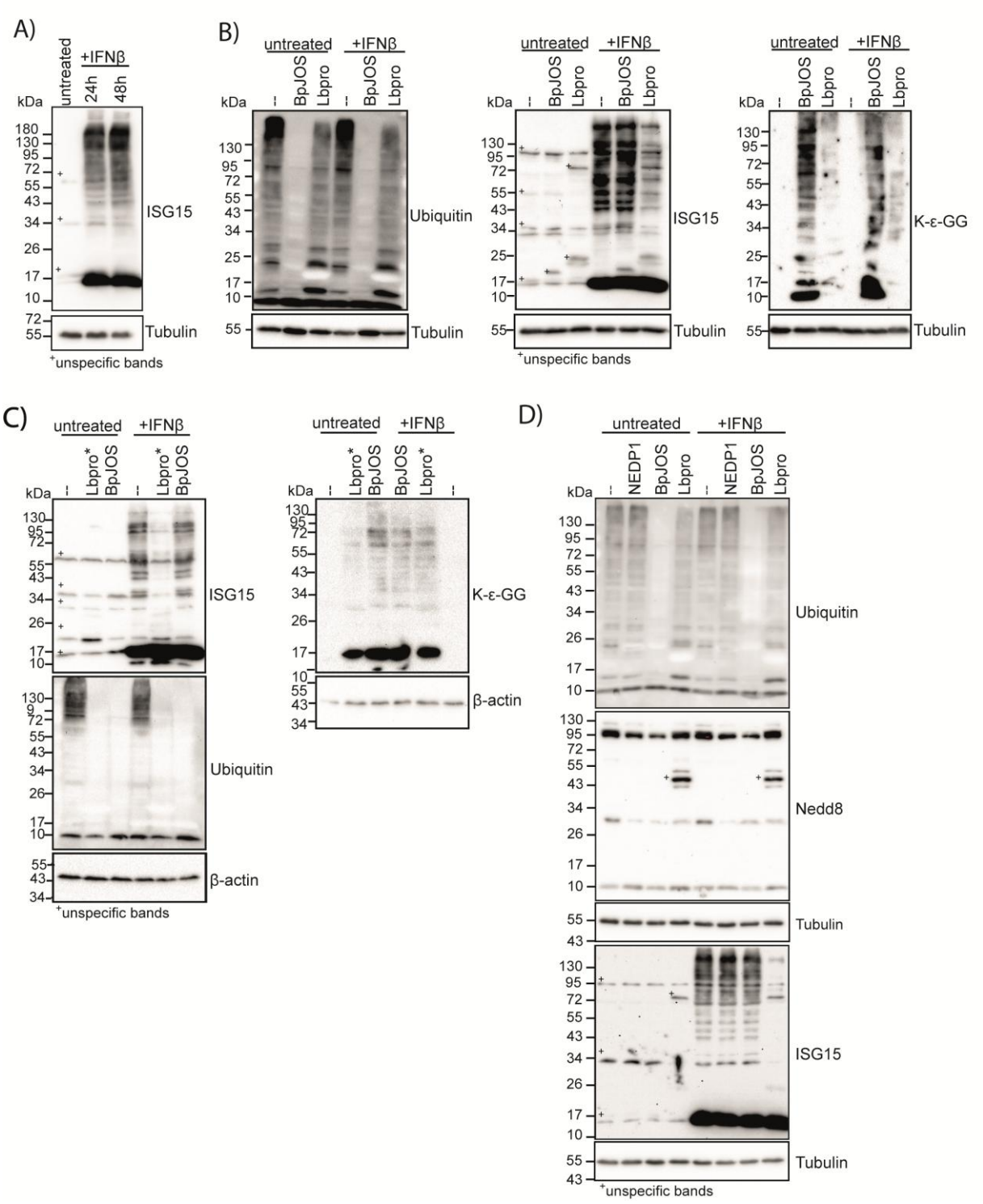

Figure 17: BpJOS is inert against ISG15 in cell lysate. HEK blue IFN-α/β reporter cells were treated with 1000U/ml human IFNβ for 24h (D), 48h (B,C) or the indicated time before lysis. All samples were adjusted to 5µg/µl to equalize substrate concentrations across experiments. If applicable, cell lysates were treated with the indicated purified proteins. All proteins were incubated for 2h on ice. Samples were analyzed by western blotting and decoration with α-ISG15, α-ubiquitin, α-K-ε-GG or α-Nedd8 antibodies. Antibodies against Tubulin or β-actin were used as loading controls. Crosses (+) mark unspecific bands recognized by the α-ISG15 antibody. **A)** ISGylation test in HEK blue reporter cells. Cells were induced with IFNβ for 24h or 48h to test for ISGylation response in an incubation time dependent manner.

Legend continued on next page

Conforming with previous results obtained from tests in cell lysate, BpJOS was able to remove all detectable ubiquitination independent of IFN stimulation (Figure 17B, left panel). Lbpro showed minor activity against the ubiquitination pattern with a moderate reduction in HMW ubiquitination compared to the control lacking clippase treatment. Treatment with Lbpro produced stronger bands detected with the anti-ubiquitin antibody at around 17kDa and 25kDa compared to the control indicating the increased generation of specific ubiquitin species. The observed heights of these two bands correlated with the molecular weight of di-ubiquitin (~17kDa) and tri-ubiquitin (~25kDa). These results could indicate Lbpro cleavage of longer ubiquitin chains (>3Ub) into shorter chains (di-/tri-Ub) under the given experimental conditions leading to loss of HMW ubiquitin signal and simultaneous generation of shorter chains (Figure 17B, left).

ISGylation levels generated by IFNβ treatment remained unchanged in the BpJOS treated sample compared to the control (Figure 17B, center panel). This result established BpJOS' inactivity against ISGylated proteins in cell lysates and conforms with the prior result of the ABP assay with ISG15$^{79-154}$-PA (Figure 16C). BpJOS therefore does not act on ISG15 even if the complete ISG15 moiety or ISG15-conjugated proteins are present. Treatment with Lbpro resulted in a moderate decrease in ISGylated substrates despite the comparably high concentration of supplemented purified protein with 40μM (Figure 17B, center panel). Suspected unspecific bands in the uninduced lysates detected with the anti-ISG15 antibody at around 19kDa, 35kDa, 60kDa and 100kDa appeared in all samples and did not fade under Lbpro treatment, indicating these are indeed unspecific non-ISG15 targets (Figure 17B, center panel). Additional bands in untreated lysates treated with BpJOS or Lbpro are proposed to derive from protein purification impurities.
Both BpJOS and Lbpro generated detectable levels of GlyGly-signals, despite production of GlyGly-marked substrates by Lbpro occurred to a lesser extent compared to BpJOS (Figure 17B, right panel).

Legend continued from previous page

Figure 17: BpJOS is inert against ISG15 in cell lysate. **B)** BpJOS and Lbpro activity test in lysates of stimulated HEK blue cells. HEK blue cells lysates stimulated for 48h or left untreated were treated with 10μM BpJOS$^{12-218}$ or 40μM Lbpro$^{29-195}$ purified protein. Samples were tested for reduction in ubiquitin levels (A, left), ISGylation levels (A, center) and generation of GlyGly-sites (A, right) by use of the corresponding antibodies. **C)** BpJOS and Lbpro* activity test in lysates of stimulated HEK blue cells. Equivalent to B) but testing 10μM BpJOS$^{12-218}$ against 100μM of the Lbpro variant Lbpro* (STAR, L102W$^{29-195}$) harboring heightened activity against ubiquitin. ISGylation and ubiquitination levels (C, right) and the production of GlyGly-sites (C, left) were monitored with the corresponding antibodies. **D)** Activity test of BpJOS and Lbpro against neddylation in IFNβ-treated and untreated HEK blue cell lysate. Lysates of stimulated HEK blue cells (24h) or of unstimulated cells were treated with 10μM BpJOS$^{12-218}$, 10μM NEDP1 or 40μM Lbpro$^{29-195}$ purified protein. Reductions in Ubl levels were monitored with α-ubiquitin, α-Nedd8 and α-ISG15 antibodies. K-ε-GG, Diglycyl-epsilon-aminogroup-lysine.

GlyGly-signals produced by Lbpro reflected the culminated clipped substrate subjected to ubiquitination and ISGylation in IFNβ-treated cell lysate (Figure 17B, right and center panel). This instance demonstrated the lower activity of Lbpro compared to BpJOS, which solely clipped ubiquitinated substrates. This observation was supported by the differences in used enzyme concentration as 4-fold the amount of Lbpro was employed compared to BpJOS (40µM vs 10µM) emphasizing BpJOS efficiency in cleaving ubiquitination and its simultaneous modifier selectivity.

The Lbpro variant Lbpro* was engineered to display higher activity against ubiquitin compared to the wildtype by introducing a single point mutant L102W (Swatek et al., 2019). To test Lbpro* activity against ubiquitin and ISG15, HEK blue lysates of IFNβ-induced and uninduced cells were treated with 100µM Lbpro* or 10µM BpJOS for comparison (Figure 17C). Lbpro* treatment resulted in complete collapse of all ubiquitination independent of ISG15 presence (Figure 17C, left panel). ISGylation was moderately reduced by Lbpro* with residual ISGylated substrates visible across all molecular weights. BpJOS did not alter ISGylation levels in agreement with prior results. The detected pattern of GlyGly-marked substrates by Lbpro* appeared similar to those generated by BpJOS in IFN-induced cell lysate (Figure 17C, right). Lower GlyGly-remnant amounts were observed for the untreated cells compared to lysates from induced cells due to the absence of ISGylated targets (Figure 17C, right). These observations presented Lbpro* as more active against ubiquitination than ISGylation and demonstrated its lack of modifier specificity in contrast to the ubiquitin-targeting and ISG15-inert BpJOS clippase.

Beyond activity against ubiquitin, BpJOS was shown to react with the Nedd8$^{1-73}$-PA activity-based probe (Figure 16C). To test, whether BpJOS displays activity against Nedd8 in lysate, HEK blue cell lysates were used. Interferon-treated or untreated cell lysate was incubated with BpJOS or Lbpro (Figure 17D). Lbpro was reported to show activity against Nedd8 at higher enzyme concentrations when tested in ABP assays (Swatek et al., 2018). As a control, lysates were in-parallel incubated with purified protein of the deneddylase NEDP1 (Mendoza et al., 2003). Ubiquitination and ISG15 levels were detected with specific antibodies to demonstrate successful ISG induction by IFNβ treatment and clippase activity by BpJOS and Lbpro.
Neddylation in HEK blue cells, as detected by use of an anti-Nedd8 antibody, occurred in low prevalence. Monomeric Nedd8 ran at around the 10kDa mark and three additional bands at 30kDa, one strong band at 95kDa and a fainter band at around 120kDa were detected (Figure 17D). All three bands show a minor reduction in signal upon NEDP1, BpJOS or Lbpro treatment compared to the untreated control. BpJOS treatment displayed the highest decrease for the band at 95kDa. Monomeric Nedd8 levels show small fluctuations across samples. The reduction of Nedd8 signal in the HMW bands did not correlate with increased mono Nedd8 signal (Figure 17D).
A band at around 50kDa, which is visible in the Lbpro-treated samples (marked with a cross) was suggested to stem from cross reactions of the Nedd8-antibody with remaining impurifications of the Lbpro protein purification as the signal solely is

detectable in these samples. Despite the already low basal level of detectable neddylation, BpJOS and Lbpro only showed minor activity against Nedd8 suggesting the modifier may not be the preferred targets. Alternatively, deneddylation was prevented by other factors. Lbpro was reported to have a strong preference for ISG15 over ubiquitin and Nedd8 in biochemical assays (Swatek et al., 2018).
Collectively, these characterizations in HEK blue cell lysates of IFNβ-stimulated and unstimulated cells disclose Lbpro and Lbpro* activity against ubiquitin, ISG15 and moderate activity against Nedd8. The tests emphasized BpJOS high activity against ubiquitin even in presence of other modifiers and its complete inactivity against ISG15 and conjugated targets.

3.2 The Clippomics method

Of all tested and characterized clippase candidates, BpJOS was the most interesting, verified ubiquitin C-terminal clippase (UCC) to follow up on. In previous biochemical tests, BpJOS was identified as a highly active clippase, capable of completely cleaving mono ubiquitin and ubiquitin chains from substrates. By this, former ubiquitinated substrates were left decorated with GlyGly-remnants. This instance rendered BpJOS a useful tool in the identification of these substrates. The novel cleavage mode presented an opportunity to exploit BpJOS activity for the systematic investigation of former ubiquitin substrates. Efforts were directed towards establishing an innovative mass spectrometry-based protocol for comprehensive studies on the ubiquitome and other Ublomes. The following chapters detail the various steps of the conceptualization and development of the novel BpJOS-based proteomics method, termed Clippomics. The method was subsequently refined for the disentanglement of ISG15 and ubiquitin substrates as well as targeting shifts in the ubiquitome upon interferon treatment in cells providing two examples of useful applications for this method.

3.2.1 Conceptualization and development of the Clippomics method

The discrimination of ubiquitin and ubiquitin-like modifications on substrates provides a challenge for mass-spectrometry (MS) studies of ISG15, Nedd8 and ubiquitin due to their identical C-termini (Figure 18A). Most conventional MS-based protocols rely on the serine peptidase Trypsin for peptide generation, which cleaves on the C-terminal side of arginine (R) and lysine (K) residues. Modifications residing on lysine residues are spared by Trypsin, leading to the occupancy of small remnants at that site. In case of modifications by ISG15, Nedd8 and ubiquitin, Trypsin digestion produces the same GlyGly-remnant at the modification site based on their shared -LRGG C-terminal peptide sequence (Figure 18B). Ubiquitinated, ISGylated and NEDDylated sites are then equally marked with the GlyGly-remnant. Studies interested in assessing ubiquitination often conduct a GlyGly-enrichment of these modified sites with disregard of the Ubl conflation and assign them to ubiquitin.
To provide a solution for this Ubl entanglement, an updated MS-based protocol was conceptualized. The basis for the novel protocol is the modifier-selectivity exhibited by BpJOS: pre-treatment of the Ublome with BpJOS selects for formerly ubiquitinated and neddylated sites by production of GlyGly-remnants. ISGylated sites remain unprocessed by this treatment, thereby selecting against them. Intact proteins are then digested with a protease different from Trypsin to circumvent conflation of BpJOS- and Trypsin-generated GlyGly-remnants. Clippase-produced GlyGly-remnants are then specifically enriched and analyzed by MS (Figure 19).

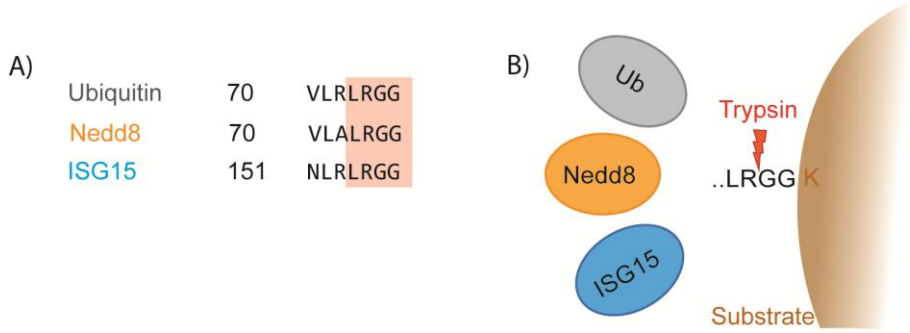

Figure 18: Comparison of ubiquitin, Nedd8 and ISG15 C-terminus sequences. A) Sequence comparison of ubiquitin, Nedd8 and ISG15 for their C-terminal peptides. Given are the last seven amino acids with their respective starting position (Ubiquitin/Nedd8 V70, ISG15 N151). All three modifiers share their four last amino acids highlighted in the red box. **B)** Schematic representation of possible modifications on a substrate lysine residue (K). The four shared amino acids in ubiquitin, Nedd8 and ISG15 C-terminus are depicted with the canonical trypsin cleavage site. Trypsin cleaves the sequence between the Arg (R) and the Gly (G) residue, which is depicted by the lightning symbol in red. The generation of the GlyGly-remnant leads to the loss of information which modifier was initially present.

For the investigation of suitable Trypsin alternatives, three enzymes were selected and tested in a preliminary Clippomics test. The criteria for the selected enzymes included the efficient generation of MS suitable peptides without interfering with or coinciding with the clippase cleavage site within the modifiers C-terminus. The criteria were met by the three commercially available digestion enzymes LysC, Chymotrypsin and Lysarginase. LysC cleaves peptides C-terminally of Lys residues (K), but in comparison to Trypsin not after Arg (R) residues. Chymotrypsin cleaves peptide bonds C-terminally of aromatic residues (Phe, Tyr, Trp) and large hydrophobic residues (Leu, Met). Lastly, Lysarginase mirrors the Trypsin cleavage sites by cleaving N-terminally, but not C-terminally of Lys and Arg residues. The enzymes cleavage patterns are depicted in Figure 19A.

The initial phase of establishing the Clippomics protocol and testing the fragmentation enzymes were conducted during the master thesis (Kolek, 2021) and are included here for the sake of completeness, as the experimental conditions were further refined and optimized during this study.

The Clippomics method comprises the following general steps: lysis of cells, clipping with BpJOS, digestion with an enzyme in preparation for MS, the enrichment of GlyGly-sites and their measurement by LC-MS/MS (see method chapters 2.3.5 to 2.3.9 for details). For the initial digestion enzyme test, untreated HEK blue cells were lyzed and the lysates were treated with BpJOS for production of GlyGly-sites. Samples were then digested with either LysC, Chymotrypsin or Lysarginase. GlyGly-sites were enriched using the PTMScan Ubiquitin Remnant Motif-kit (Cell Signaling Technologies), which employs antibody-coated beads directed against GlyGly(K)-sites. The raw data from LC-MS/MS measurement were analyzed using

MaxQuant. The total number of GlyGly-sites and identified protein within each obtained data set was compared and assessed for the largest quantity.
Digestion with Lysarginase generated the most identified proteins and detected GlyGly-modified sites with 874 and 1857, respectively (Figure 19B,C). The data set comprised 506 proteins and 1507 sites exclusively found with Lysarginase and not detected with LysC and Chymotrypsin. The lowest amount of data was generated by LysC digestion: only 404 proteins were identified, none of which were exclusive to LysC digest as all proteins were also found with Chymotrypsin. Chymotrypsin digested samples detected 111 proteins and 391 sites exclusive to this data set compared to 436 exclusive sites to LysC. The summary of detected GlyGly-sites and identified proteins by LysC, Chymotrypsin and Lysarginase is given in Table 23.

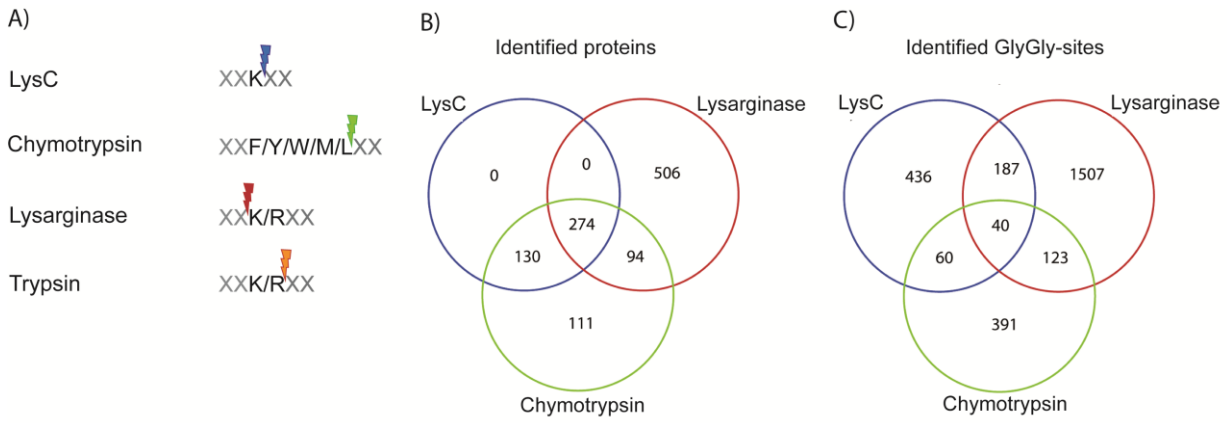

Figure 19: Comparison of enzyme cleavage sites and obtained number in sites and identified proteins in a preliminary Clippomics test. A) The cleavage sites of digestion enzymes LysC, Chymotrypsin and Lysarginase in comparison to the cleavage sites employed by Trypsin. The corresponding specific cleavage positions are marked with differently colored lightning bolts. Given is an arbitrary peptide sequence represented by the grey X symbols. **B)** Venn diagram of the total number of identified proteins in a preliminary Clippomics test using LysC, Chymotrypsin or Trypsin as digestive enzymes used for peptide generation in preparation for measurement by LC-MS/MS. C) Venn diagram of identified enriched GlyGly-carrying peptides digested with LysC, Chymotrypsin or Lysarginase using the Clippomics method.

Table 23: Total number of identified proteins and GlyGly-sites given for the three tested digestion enzymes.

Digestion enzyme	Total No. identified proteins	Total No. identified GlyGly-sites
LysC	404	723
Chymotrypsin	609	614
Lysarginase	874	1857

Overall, treatment with Lysarginase for MS samples preparation generated the most comprehensive data set with the highest number of identified proteins and GlyGly-sites. Applied to the Clippomics method, in complex samples with ubiquitinated, neddylated and ISGylated proteins only ubiquitin and Nedd8 are targeted by BpJOS treatment. For ISGylated sites, which remain intact upon BpJOS treatement, Lysarginase digestion generates a -RGG remnant at the modified site (see Figure 19A). It is rationalized that these remnants are not enriched by the employed GlyGly-enrichment method, thereby ISG15 sites are negatively selected for (Figure 20).
Based on these results, Lysarginase was the enzyme of choice for peptide generation in the Clippomics method. The overview of the steps for the Clippomics approach and the direct comparison with conventional protocols is depicted in Figure 20.

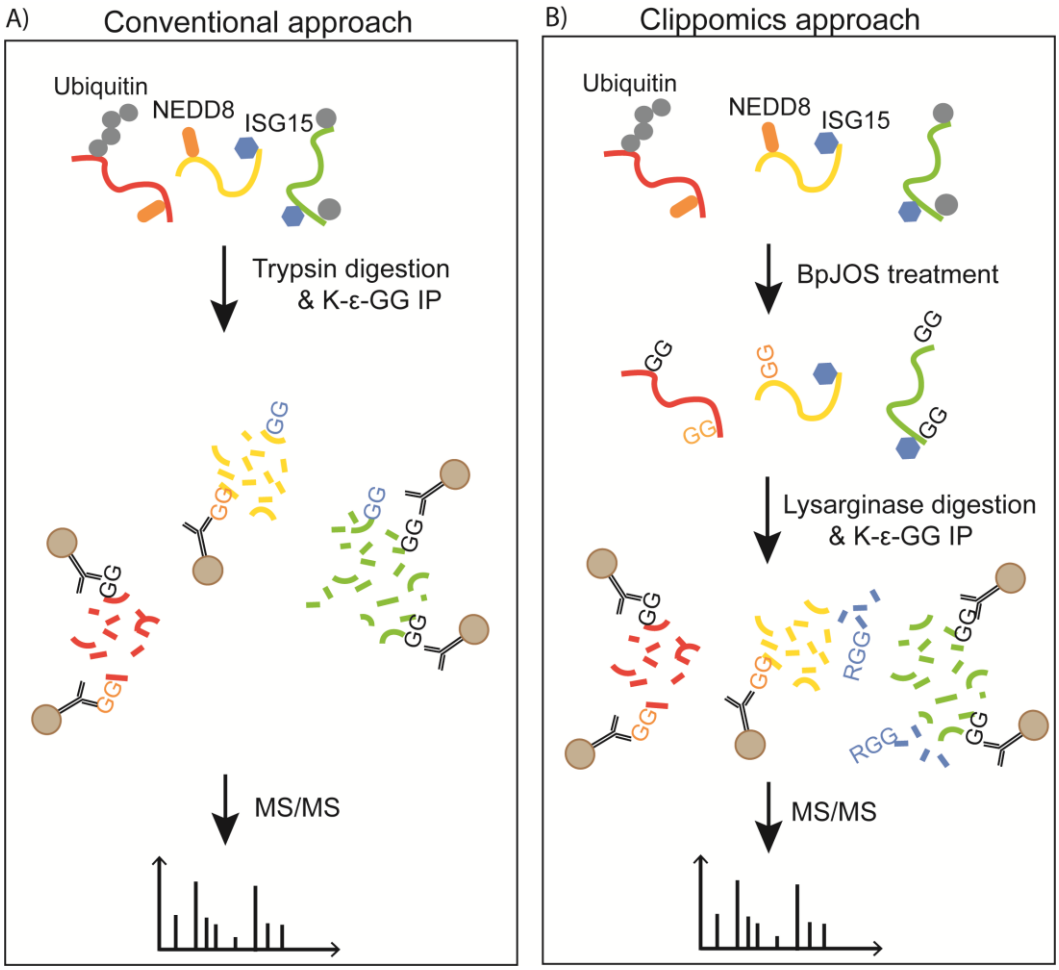

Figure 20: Comparison of conventional protocols for studying the Ublome and the Clippomics method. A) The conventional approach. Complex sample mixtures, in which ubiquitinated, neddylated and ISGylated proteins are present are digested with Trypsin. Generated GlyGly-sites are enriched by an GlyGly-IP leading to a conflation of sites modified by ubiquitin (grey), Nedd8 (orange) and ISG15 (blue). The obtained MS data set does not allow for modification distinguishment. **B)** The Clippomics approach. Complex sample mixtures as in A) are treated with BpJOS. Ubiquitinated (grey) and neddylated (orange) sites are clipped with BpJOS leading to GlyGly-remnant generation. ISGylated (blue) sites are not targeted by BpJOS. Proteins are digested with Lysarginase and GlyGly-sites are enriched by an GlyGly-IP allowing for the distinguishment of ubiquitin/ Nedd8 sites from ISG15 sites.

3.2.2 First proof-of-concept Clippomics test

BpJOS showed rather modifier-selectivity than -specificity in biochemical assays *in vitro* by targeting ubiquitin and to a lower extent Nedd8 (Figure 16C, Figure 17D). To demonstrate its suitability for the modifier disentanglement by the Clippomics method, a first test focusing on substrate profiling was conducted. The aim was to demonstrate that BpJOS is completely inactive against ISG15 on a mass-spectrometry level, and to assess the scope of its activity against Nedd8. Furthermore, the ISG15-targeting clippase Lbpro was incorporated to evaluate its applicability for the Clippomics method for targeting ISGylated substrates. Lbpro was shown to favor ISG15 over ubiquitin and Nedd8 (Figure 17D, Swatek et al., 2018). The chosen approach for the evaluation of BpJOS and Lbpro specificity comprised the depletion of one of multiple modifiers in different samples.
HEK blue cells were left uninduced or treated with IFNβ for ISG expression. Levels of conjugated ubiquitin and Nedd8 in the selected samples were reduced by a two-fold procedure. On the one hand, inhibitors for the respective activating enzyme in cell culture were used to stall ubiquitination/neddylation events in the cell. To that end, the ubiquitin E1 (Ube1)-inhibitor TAK243 and the Nedd8 E1 (NAE)-inhibitor MLN4924 were employed (Brownell et al., 2010; Hyer et al., 2018). On the other hand, these samples were treated with the corresponding purified deconjugating enzymes after cell lysis to remove residual ubiquitination/neddylation not caught by the E1 treatment. To remove ubiquitination, lysates were treated with SnUSP1, which was reported to act on all ubiquitin chains in regular DUB manner while being inert against ISG15- and Nedd8-activity probes (Boll et al., 2023). Residual neddylation was diminished by in-lysate treatment with purified deneddylase NEDP1 (Mendoza et al., 2003). The overview of used treatments for and against modifications and their respective consequences are schematically depicted in Figure 21.

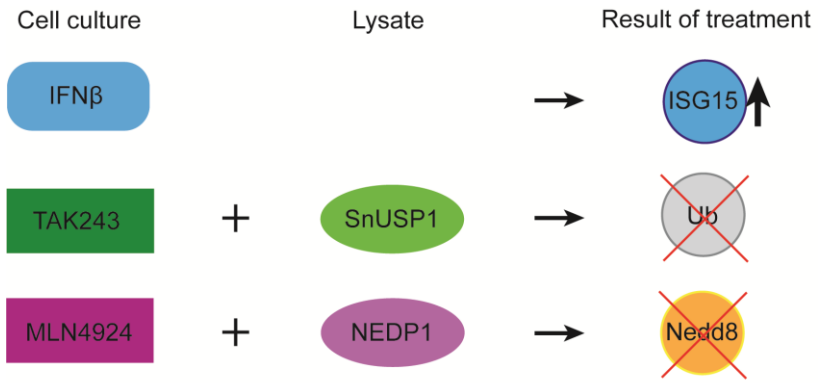

Figure 21: Treatments used to modulate modifier presence. The treatments are given with their corresponding stage of samples preparation (cell culture/lysate). Interferon-β (IFNβ) treatment induced expression of ISG15 and its conjugating enzymes in cells. Ubiquitination was abolished by treatment with ubiquitin E1-inhibitor TAK243 and subsequent incubation of cell lysate with purified SnUSP1. Neddylation was diminished by cell treatment with Nedd8 E1-inhibitor MLN4924 and lysate incubation with purified NEDP1.

In total, nine different samples were prepared for GlyGly-enrichment with different combinations of present modifiers. These samples were later either clipped with BpJOS or Lbpro for GlyGly-remnant production and subjected to GlyGly-enrichment followed by MS measurement. One sample was not treated with either clippase and used as a control for GlyGly-bead enrichtment. The full summary of all samples is listed in Table 24. Three samples were prepared in duplicates and were divided before clippase treatments: samples 3+5, samples 4+6, samples 7+8 (Table 24). Based on the previous characterizations, it was expected that BpJOS targets ubiquitin and Nedd8, but not ISG15. Conversely, Lbpro was assumed to act on all three modifiers.

Table 24: List of samples prepared for the Clippomics test. Given are the induction (ISG15) or depletion (ubiquitin/Nedd8) of modifiers within each sample, the used clippase (BpJOS/Lbpro) and expected modifier GlyGly-sites.

#	ISG15-induction (IFNβ)	Ub-depletion (TAK243+ SnUSP1)	Nedd8-depletion (MLN4924+ NEDP1)	Present modifier	Clippase	Expected sites
1	-	-	+	Ub	BpJOS	Ub
2	-	+	-	Nedd8	BpJOS	Nedd8
3	+	+	-	ISG15/Nedd8	BpJOS	Nedd8
4	+	-	+	ISG15/ Ub	BpJOS	Ub
5	+	+	-	ISG15/Nedd8	Lbpro	ISG15/Nedd8
6	+	-	+	ISG15/ Ub	Lbpro	ISG15/Ub
7	+	+	+	ISG15	BpJOS	-
8	+	+	+	ISG15	Lbpro	ISG15
9	+	-	-	all	-	-

Prior to GlyGly-enrichment and MS analysis, successful preparation of samples and modifier modulation was tested after each treatment step by western blotting. Occupancy of ISGylation, ubiquitination and neddylation were monitored using the corresponding specific antibodies for samples taken after cell lysis, after additional de-modification by SnUSP1/NEDP1 treatment and after clippase treatment with BpJOS and Lbpro (Figure 22).
Lysate samples taken after lysis and before treatment with purified proteins (‘untreated’) showed presence of monomeric ISG15 and a strong ISGylation pattern after *in cellulo* IFNβ treatment (samples 3-8, lanes 3-6, Figure 22). For HEK blue cells left untreated by IFNβ no ISGylation was detected with the exception of two faint bands

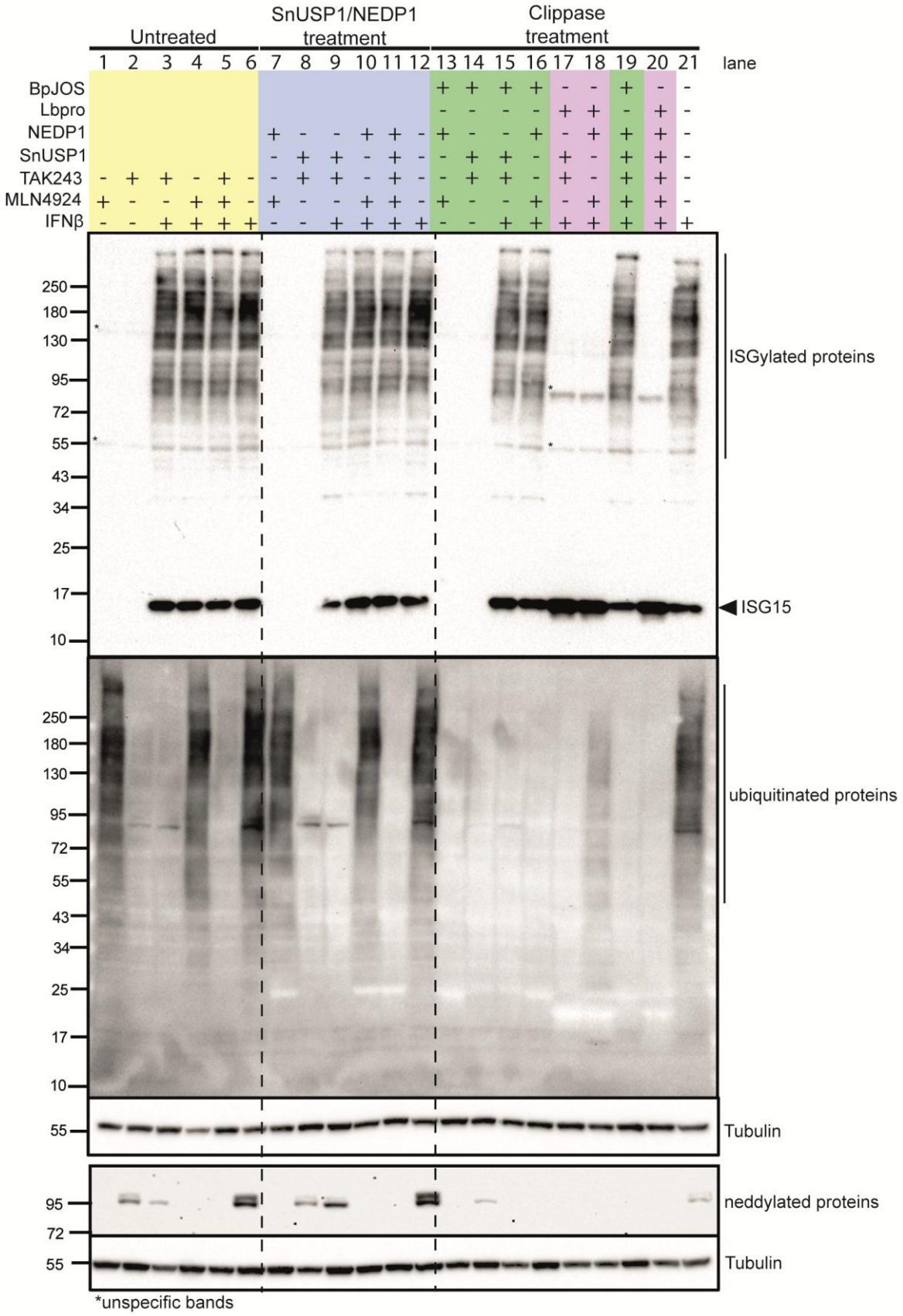

Figure 22: Western blot analysis of samples used for the proof-of-concept Clippomics test. Samples were taken after each step of the protocol and assessed for modifier presence.
Legend continued on next page

at around 55kDa and 130kDa, which were observed in previous western blots as well (Figure 17D). It is assumed that these bands represent unspecific cross-reactions by the used ISG15-antibody (lanes 1-2). Lysates of TAK243-treated cells displayed a major decrease in ubiquitination smear compared to untreated samples (lanes 2,3,5) with no detectable ubiquitination remaining after additional treatment with SnUSP1 (lanes 8,9,11, Figure 22). Monomeric ubiquitin could not be detected with used commercial gels and employed western blotting conditions. Treatment with TAK243 did not interfere with ISGylation levels as treated sample displayed a similar ISGylation pattern as untreated samples (lanes 3,5 vs. lane 6).
Inhibition of the Nedd8-E1 enzyme by MLN4924 resulted in diminished neddylation of suspected Cullins at around 95kDa (lanes 1,4,5). Apart from suggested Cullins, no neddylation targets or monomeric Nedd8 could be detected across all samples. Consequently, MLN4924-treated samples showed no further reduction in neddylation upon NEDP1 treatment (lanes 7,10,11). NEDP1 was reported as being able to deneddylate selected Cullins besides non-Cullin neddylated substrates (Chan et al., 2008; Mendoza et al., 2003). However, the principle deneddylase of Cullins is the COP9 signalosome protein complex (Pick et al., 2012), which was not used for treatment in this study.
Treatment with purified BpJOS in the corresponding samples caused complete collapse of ubiquitination (lanes 13-16, 19) with a minor reduction in neddylation in lane 14, in which neddylation had not been prevented by MLN4924 and NEDP1 incubation. ISGylation patterns remained unchanged upon BpJOS treatment (lanes 15,16,19). Lbpro efficiently removed ISGylation and neddylation while showing moderate activity against the ubiquitination smear (lanes 17,18,20). Clippase activity exhibited by BpJOS and Lbpro was implied by the decrease of observed modifications but was additionally demonstrated by use of the K-ε-GG-antibody (Appendix Figure 30). The western blot analysis matched the expectations for modification abundances and absences. Therefore, samples were further processed by Lysarginase digestion. Used criteria for efficient digestion was the number of missed cleavages (MC) by Lysarginase as reported by MaxQuant: 4% of identified peptides harbored 2 MC sites, 26% had 1 MC and 70% had no MC. As efficient protein digestion was ascertained, samples were subjected to GlyGly-IP and MS measurement.

Legend continued from previous page
Figure 22: Western blot analysis of samples used for the proof-of-concept Clippomics test. Samples were taken after each step of the protocol and assessed for modifier presence monitored with α-ISG15, α-ubiquitin and α-Nedd8 antibodies. Tubulin was detected as loading control. Unspecific bands detected by the ISG15 antibody are marked with a star (*). Sample treatments are indicated with a plus (+) symbol above the figure. Treatment with ubiquitin E1-inhibitor TAK243, Nedd8 E1-inhibitor MLN4924 and interferonβ (IFNβ) was conducted *in cellulo.* Samples taken after cell lysis are highlighted in the yellow box. E1-inhibitor treatment for ubiquitin and neddylation reduction was complemented with SnUSP1 and NEDP1 treatment (each 10µM, 1h) and is highlighted by the blue box. Duplicate samples (lanes 9, 10, 11) were divided for BpJOS or Lbpro treatment (9→ 15/17, 10→ 16/18, 11→19/20). $BpJOS^{12-218}$ (10µM) and $Lbpro^{29-195}$ (40µM) purified proteins were incubated for 2.5h on ice. BpJOS-treated lanes are given in green; samples treated with Lbpro are given in purple. Samples tested in lanes 13-21 were subsequently subjected to GlyGly-enrichment and MS analysis.

The number of enriched GlyGly-sites per sample along with the respective lane in Figure 22 is listed in Table 25.
Analysis of the mass spectrometry data with MaxQuant revealed a total of 627 GlyGly-modified sites obtained from the table 'GlyGly(K) peptides' and 392 modified proteins across all samples. Another 442 identified proteins were listed as unmodified according to the 'proteinGroups' table. The highest number of sites was detected in BpJOS-clipped lysate in which ISGylation and ubiquitination was present with 411 sites (sample 4, Table 25) followed by the lysate of cells lacking ISG15 with 292 sites (sample 1). For Lbpro, most sites were identified in samples containing both ubiquitin and ISG15 (151 sites, sample 6), followed by the ISG15-only sample (100 sites, sample 8) and the ISG15 and Nedd8 containing sample (77 sites, sample 5).
Nedd8-only and ISG15-only comprising data sets clipped with BpJOS revealed solely 10 and 7 identified GlyGly-sites, respectively (samples 2, 8). The unclipped negative control yielded 7 GlyGly-sites (sample 9).

Table 25: Clippomics test samples with detected GlyGly-sites in MS. Given are the respective lanes in the western blot in figure 12. The table is complementary to table 25 expanded by the number of identified GlyGly-sites in MS. Untr.,untreated; treatm., treatment, clipp., clippase.

	Lanes in figure 12						
#	Lysate (untr.)	SnUSP1 /NEDP1 treatm.	Clipp. treatm.	Present modifier	Clippase	Expected sites	Number of detected GlyGly-sites
1	1	7	13	**Ub**	**BpJOS**	**Ub**	**292**
2	2	8	14	**Nedd8**	**BpJOS**	**Nedd8**	**10**
3	3	9	15	**ISG15/Nedd8**	**BpJOS**	**Nedd8**	**16**
4	4	10	16	**ISG15/ Ub**	**BpJOS**	**Ub**	**411**
5	3	9	17	**ISG15/Nedd8**	**Lbpro**	**ISG15/Nedd8**	**77**
6	4	10	18	**ISG15/ Ub**	**Lbpro**	**ISG15/Ub**	**151**
7	5	11	19	**ISG15**	**BpJOS**	**-**	**7**
8	5	11	20	**ISG15**	**Lbpro**	**ISG15**	**100**
9	6	12	21	**all**	**-**	**-**	**7**

Of the 627 GlyGly-sites across all samples, around 70% of sites were identified in two or more data sets. In order to systematically compare detected GlyGly-sites by clipping with BpJOS and Lbpro, the data was further processed using the Perseus software. The causative Ubl of identified GlyGly-modifications was reviewed against the verified clippase specificities. For that, two selected data sets were compared to each other by scatter plot analysis (Figure 23). Samples treated with TAK243 and SnUSP1 were proposed to harbor only neddylation in IFNβ-untreated cells and neddylation together

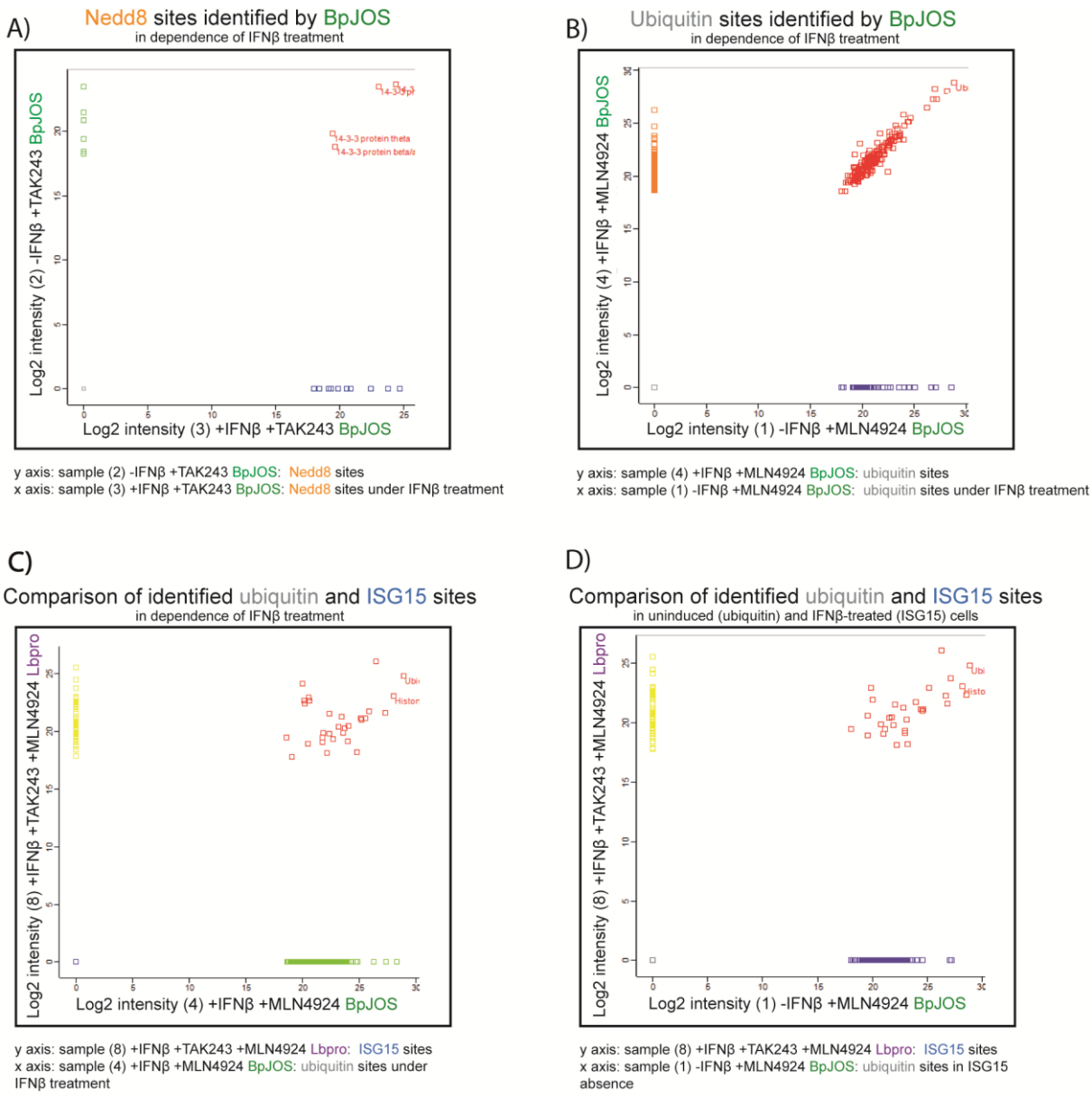

Figure 23: Comparison of modifier GlyGly-sites by BpJOS and Lbpro. Scatter plot analysis of log2 transformed intensities for identified GlyGly-sites using Perseus. Detailed descriptions of applied samples with the respective treatments and expected modifier origin as consequence are given below the panels. Exclusive sites to one data set are marked in different colors: green (sample 2), blue (sample 3), yellow (sample 8), orange (B) /light green (C; sample 4) and purple (sample 1). Matching sites found in both data sets are highlighted in red. Referenced sample numbers are equal to sample numbers listed in tables 25 and 26. IFNβ-treatment resulted in ISG15 expression TAK243 treatments was conducted in combination with SnUSP1 incubation to diminish ubiquitination. MLN4924 treatment was conducted in combination with NEDP1 incubation to remove neddylation from samples. **A)** Analysis of identified proposed Nedd8 sites by BpJOS in lysates of IFNβ-treated and untreated cells (sample 3 vs 2). **B)** Ubiquitin sites identified by BpJOS in IFNβ-treated and untreated cells (samples 1 vs 4). **C)** Identified ubiquitin sites by BpJOS and ISG15 sites by Lbpro in lysates of IFNβ-treated cells (samples 4 vs 8). **D)** Identified ubiquitin sites by BpJOS in untreated cells and ISG15 sites by Lbpro in lysates of IFNβ-treated cells (samples 1 vs 8).

with ISG15 in IFNβ-induced cells (samples 3 and 2). Clipping with BpJOS resulted in 6 exclusive sites to the untreated samples, while the IFNβ-treated sample gathered 12 exclusive sites (Figure 23A).

Both data sets shared 4 reported sites all assigned to position K9/11 in multiple isoforms of the 14-3-3 protein (YWHAB, YWHAQ, YWHAZ) listed individually. The 14-3-3 protein is an adaptor protein involved in various processes such as apoptotic cell death and cell cycle control (Fu et al., 2000). Besides these samples, the reported position was also found in samples 1 and 6, which both contain ubiquitin but presumably no neddylation based on used treatments (Table 24,Table 25). It is speculated that the K9/11 position in 14-3-3 was rather ubiquitinated than neddylated due to is presence in multiple data sets. This result indicated that neddylation might not be highly prevalent in the cells used, which is in accordance with few observed bands in western blotting and Nedd8-antibody detection in previous experiments (Figure 17D). Therefore, limited information about BpJOS activity against Nedd8 could be concluded. As the following studies focused on ubiquitin and ISG15 sites, the relevance of Nedd8 sites and potential targeting by BpJOS was subordinated.

The investigation of ubiquitin sites under IFNβ-treatment revealed 199 shared sites between the uninduced and IFNβ-induced data sets (Figure 23B). Among the reported data, a plethora of sites derived from putative ubiquitination targets and members of the ubiquitin machinery including several DUBs, E3 ligases and E2 enzymes. Top hit with highest measured intensities were GlyGly-decorated K48 residues in ubiquitin proposed to stem from K48-linked polyubiquitin chains. Second highest shared intensities were identified for positions K4 and K8 in ribosomal protein RPS20, which were validated as ubiquitinated by additional literature (Garzia et al., 2017). The first 20 hits sorted by highest intensity are listed in Table 31(Appendix). The gathered data indicated specific targeting of ubiquitin by BpJOS in the given samples.
The GlyGly-IP from untreated cell lysates gathered 50 exclusive sites compared to 164 exclusive sites in lysate of IFNβ-treated cells (samples 1vs4, Table 25, Figure 23B). This result suggested that interferon-treatment leads to a shift in the ubiquitome.

In order to examine BpJOS inactivity against ISG15, proposed ISG15 sites identified by Lbpro (sample 8; IFNβ, TAK243, MLN4924 treatments) and proposed ubiquitin sites identified by BpJOS (sample 4; IFNβ, MLN4924 treatments) were compared (Figure 23C). Sample 8 contained 61 exclusive GlyGly-sites proposed to derive from ISGylation and sample 4 contained 331 exclusive suggested ubiquitination sites. Between both data sets, 32 GlyGly-sites in 28 proteins were shared.
When the assumed ISG15 sites from sample 8 were compared to the ubiquitin-derived sites found in sample 1 (IFNβ-untreated, MLN4924), 33 shared sites were observed (Figure 23D). As sample 1 lacked IFNβ-treatment, no ISGylation was present. Therefore, a direct comparison of ubiquitin- and ISG15-derived sites under interferon-treatment is shown in Figure 23D. It is likely that the 33 shared sites are due to residual ubiquitination caused by incomplete inhibition. However, it cannot be formally excluded that the same sites can be detected in both ubiquitinated and ISGylated form.

Comparison of the 32 (sample 8 vs 4) and 33 (sample 8 vs 1) shared sites among the samples revealed that 24 sites with additional duplicate hits were identical in modified position and reported protein. Among those sites were K48 in ubiquitin, K4 and K8 in RPS20 and multiple sites in several histones, which are proposed to be highly abundant ubiquitin-derived GlyGly-sites. Additionally, the ubiquitin and RPS20 modifications amongst others were observed in the ubiquitin-derived modification data as well (samples 1vs4, Figure 23B). The comprehensive list of all 24 identical sites is provided in Table 32 (Appendix). It is concluded that observed matching sites in the ISG15 and ubiquitin sets (Figure 23C, D) can most likely be assigned to ubiquitin, which was not sufficiently removed by TAK243 and SnUSP1 treatment.
The GlyGly-sites identified as ISG15-derived (sample 8) by clipping with Lbpro included 100 sites across 75 proteins, of which 23 proteins have been previously shown to be ISGylated (Thery et al., 2021; Yifeng Zhang et al., 2019). Among those reported ISG15 targets are the pyruvate kinase PKM, the chaperone HSPA8 and the enolase ENO1.

Taken together, these results show that BpJOS is well suited to specifically detect ubiquitination sites, even in the presence of ISGylation. Lbpro, on the other hand, detects ISGylated sites with some cross-reactivity towards ubiquitin-derived sites. The proof-of-concept test using E1 inhibitors and additional SnUSP1/NEDP1 treatment served as a methodological basis to validate the clippase specificities and will not be employed in ensuing studies. Hence, a combination of BpJOS and Lbpro can be used to detect both modification types in parallel, as will be demonstrated in the following experiment.

3.2.3 Identification of ISG15 targets by the clippomics approach

The Clippomics method was used to comprehensively determine the ISGylome in IFNβ-treated HEK blue cells. As BpJOS and Lbpro were established as suitable tools, both clippases were employed to identify ISG15 targets. The experimental design was based on the clippase specificities: BpJOS targets ubiquitin and to a lesser extent Nedd8, while Lbpro targets ISG15, ubiquitin and to a lesser extent Nedd8. The testing methodology included two conditions, in which half of the samples were treated with BpJOS while the other half was clipped with Lbpro. The rationale is based on the exclusion of ISG15 sites by BpJOS: following the Clippomics protocol and later comparison of obtained data sets, sites identified by Lbpro but not BpJOS were proposed to be ISGylated (Figure 24). Hence, the protocol is based on a negative selection of ISG15 sites by BpJOS.
To increase robustness of the acquired data sets, three technical triplicates were prepared in parallel. Six plates of HEK blue cells were induced with IFNβ, lyzed and treated with the respective clippase. Induction of ISGylation as well as clippase activity was monitored by western blotting preceding the GlyGly-IP (Figure 25A). Ubiquitination levels were equal in all tested lysates. Stable ISGylation was observed for all

IFNβ-induced samples (samples 1-6) in comparison to the untreated control (sample C), which was only used as a ISG15-antibody control in western blotting (Figure 25A). BpJOS treatment removed all ubiquitination but was inactive against ISGylation. Treatment with Lbpro collapsed the majority of ISGylation with few faint bands remaining in the higher MW range (Figure 25A).

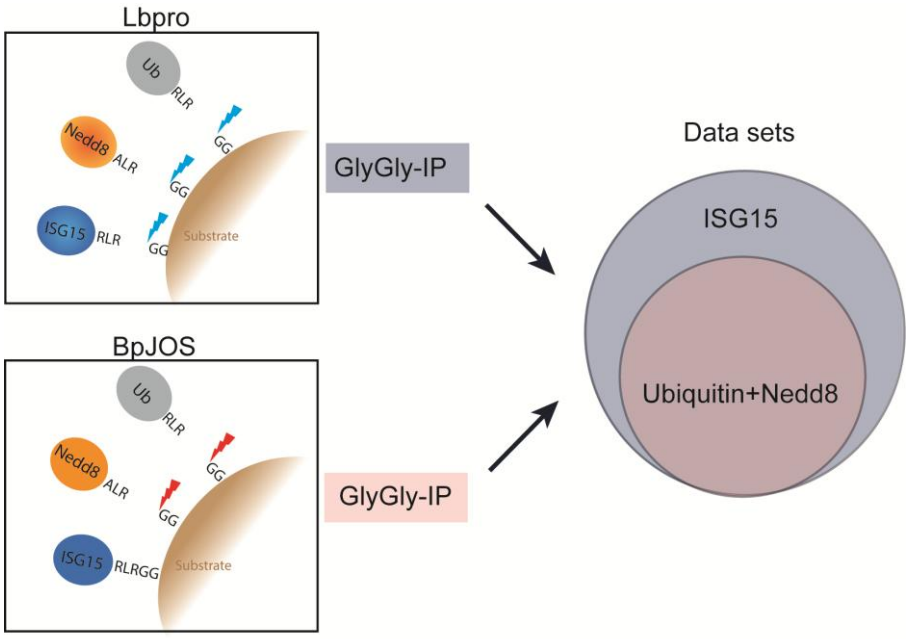

Figure 24: Research design for the investigation of ISG15 sites. Schematic representation of the conceptual design to discern ubiquitin/Nedd8 sites from ISG15-derived sites. The comparison of Lbpro-generated GlyGly-sites and BpJOS generated GlyGly-sites allows for the identification of ISG15-derived modification. Sites obtained with Lbpro, but not BpJOS are assigned to ISG15.

Lbpro partially removed the ubiquitination pattern as a reduction across all molecular weights was observed compared to the pre-treatment lysate samples (Samples 4-6, Figure 25A). BpJOS treatment generated detectable levels of GlyGly-remnants on substrates in western blotting (Figure 25B). Lbpro-generated GlyGly-signals were visibly weaker compared to those generated by BpJOS in accordance with the lower amount of clipped ubiquitination and remaining of residual ISGylation.

Prior to GlyGly-enrichment, a small amount (20µg) of clippase-treated and Lysarginase-digested proteomic samples were analyzed by LC-MS/MS to examine the digestion efficiency. In total, 2057 proteins were found across all samples. Despite the lack of GlyGly-enrichment at this step, 76 GlyGly-modfied peptides were detected. According to the table ‘modificationSpecificPeptides’ generated by MaxQuant, of all ~12.000 detected modified and unmodified peptides, 70% showed no missed

cleavage. This result demonstrated that the majority of detected peptides were adequately processed by Lysarginase. Only 30% of peptides harbored one or two missed cleavages. After the efficient digestion by Lysarginase was determined, the samples were further processed by the Clippomics method and subjected to GlyGly-enrichment. The analysis of LC-MS/MS measurement after the enrichment revealed a total of 1067 GG-marked peptides across the six samples. Overall, peptides of 1105 proteins were listed by the table ‘proteingroups’ of MaxQuant.

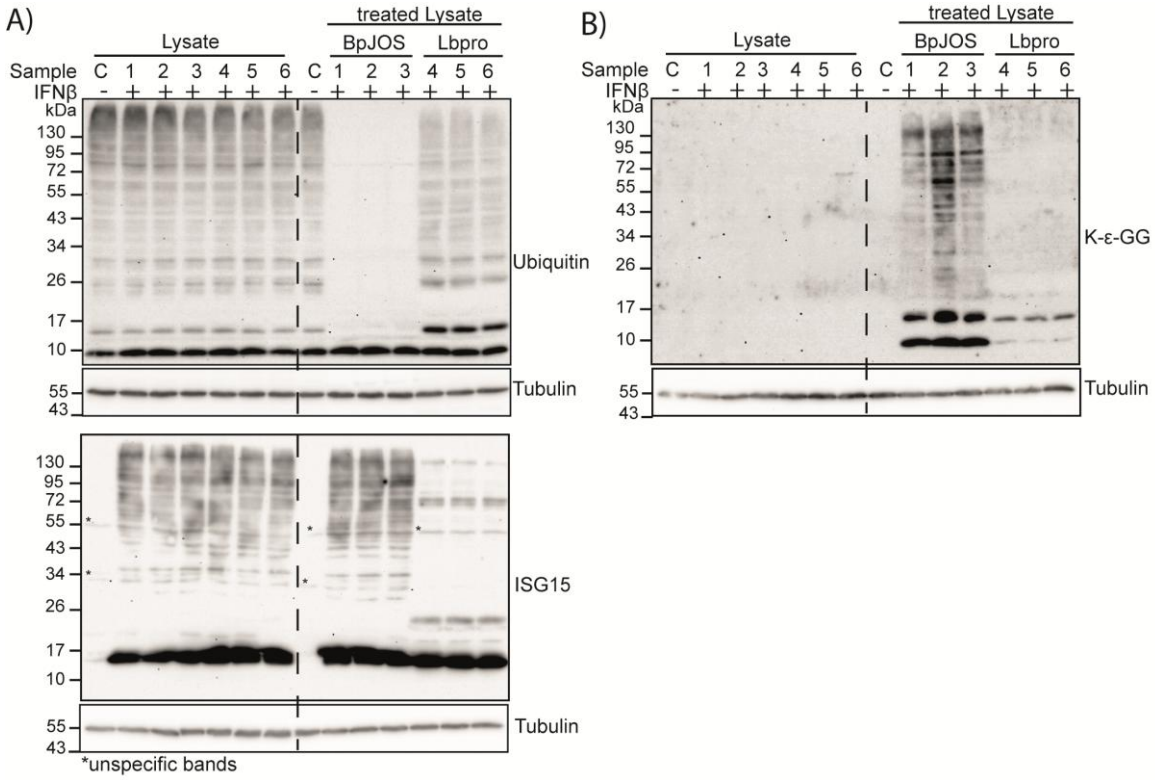

Figure 25: Western blot analysis of samples used for ISG15 substrate profiling. Six individual HEK blue cell plates were induced by treatment with 1000U/ml human IFNβ for 24h and lysates were monitored for presence of **A)** ubiquitination, ISGyaltion and **B)** GlyGly-production by use of the corresponding specific antibodies. One control sample (C) of uninduced HEK blue cells were incorporated as a control for the ISG15-antibody. Samples were tested after lysis (left of separation line) and after in-lysate treatments with purified BpJOS$^{12\text{-}218}$ (10µM) or Lbpro$^{29\text{-}195}$ (40µM) for 2h on ice (right of separation line). Unspecific bands generated by the ISG15 antibody are marked with a star (*). IFNβ, Interferon-β

Analyzed MS data were categorized into three levels of confidence for the assignment to being ISG15-derived. The sites within these levels were characterized by being all simultaneously not found by BpJOS and found in one, two or all three data sets produced by clipping with Lbpro (Table 26).

Table 26: Categories of confidence levels for GlyGly-sites derived from ISG15. The confidence level was based on peptides being detected by clipping with Lbpro but not BpJOS. The levels were defined by GlyGly-carrying peptides being identified in all three technical replicates (high), in two (medium) or one replicate (low) processed with Lbpro.

Confidence level	Number of GlyGly-peptides
High (3 samples)	19
Medium (2 samples)	41
Low (1 sample)	73

In total, 133 GlyGly(K)-modified peptides were found in the data set produced by Lbpro but were absent in the data gathered with BpJOS. It was proposed that GlyGly-carrying peptides assigned to the high confidence level (19 sites) were *bona fide* targets of ISGylation with declining certainty for the medium and low confidence categories. A high number of GlyGly-sites have been identified in both data sets generated with BpJOS and Lbpro, respectively. A big subset of these GlyGly-sites were identified with high intensities but can most likely be attributed to be ubiquitin-derived.
Here, the modification sites in the high confidence level were focused on. The comprehensive list of all sites within the 'high confidence' category is attached in the Appendix (Table 33).

The obtained ISG15 sites and identified ISGylated proteins were compared to other resources to examine their validity. A review by Thery et al. gathered all ISGylated sites and corresponding proteins reported in three different studies (Thery et al., 2021). These studies applied various approaches by using *Isg15*$^{-/-}$ mice (Yifeng Zhang et al., 2019), *Usp18*$^{-/-}$ human-derived cells (Pinto-Fernandez et al., 2021) or porcine macrophage cell lines (Zhu et al., 2021). For the verification of ISG15 sites identified in the present study, the study by Pinto-Fernandez was focused on. Cell lines used in the two studies differed but were both human-derived and therefore most suitable for the comparison of data sets. An automated script was written for the computational matching of reported ISG15 sites in this study with those from the Pinto-Fernandez study (Ruslan Ibragimov, Institute for Genetics, University of Cologne). Of the 19 high confidence ISG15 sites identified in IFNβ-induced HEK blue cells, 6 positions were matching with the external source (Table 27). For another 8 ISGylated substrates, the proteins have been reported to be ISGylated, but at different positions than identified in the present study.

Table 27: Matching ISG15 sites of the present study compared to external resource (Pinto-Fernandez et al., 2021). Given are the ISG15 sites (lysine positions) in proteins reported by both studies.

Protein name	Gene name	Lysine position
Bifunctional glutamate/proline--tRNA ligase	EPRS1	435
Heat shock protein HSP 90-alpha	HSP90AA1	84
ATP synthase subunit alpha, mitochondrial	ATP5F1A	117
Cytosol aminopeptidase	LAP3	48
Regulator of nonsense transcripts 1	UPF1	915
Protein PRRC2C	PRRC2C	671

No information could be retrieved for 5 of the 19 high confidence level sites when searching for reported ISGylation of the proteins using databases such as PhosphoSitePlus or Uniprot and additional search engines for publications (Table 28). To my knowledge these proteins have not been published yet as being ISG15 targets.

Table 28: Potential novel targets of ISGylation revealed by Clippomics. Listed are the ISGylated proteins with the respective modified lysine position (given for isoforms), which have not been reported yet.

Protein name	Gene name	Lysine position
Ubiquitin-associated protein 2-like	UBAP2L	413;420
YTH domain-containing family protein 1/3	YTHDF1; YTHDF3	240;244
Sorting nexin-2	SNX2	131;248
Myomesin-2	MYOM2	11
Transcriptional regulator QRICH1	QRICH1	246

Overall, these results demonstrated that a subset of Clippomics-identified ISG15 sites using Lbpro could be validated using external resources. Further, yet undescribed ISG15 targets could be identified by using the Clippomics approach underlining its feasibility for the identification of ISGylation sites.

3.2.4 Interferon-dependent shifts in the ubiquitome identified by Clippomics

The proof-of-concept Clippomics test revealed the induction of 164 ubiquitin sites detectable exclusively upon IFNβ treatment (chapter 3.2.2. Figure 23B). This result indicated a shift in the ubiquitome in induced cells. To investigate these changes in the ubiquitome, the Clippomics method was tailored to profile ubiquitin sites in uninduced and IFNβ-induced HEK blue cells. The analysis was expanded to three technical replicates for both conditions of which all were clipped by BpJOS.

As for all Clippomics experiments, lysates before and after clipping treatment were analyzed by western blotting. Levels of ubiquitination and ISGylation were monitored by the respective modifier-specific antibodies and production of GlyGly-remnants was visualized by detection with the K-ε-GG antibody (Figure 26A). Ubiquitination levels were equal across all six samples (lysates 1-6) with complete removal under BpJOS treatment for the uninduced lysates (lysates+BpJOS 1-3). Amounts of ubiquitination in lysates of IFNβ-treated cells showed a sharp decrease for samples 5 and 6 with shadows of residual ubiquitination observed for sample 4 (lysate+BpJOS, Figure 26A, upper panel). ISGylation abundance was identical independent of BpJOS treatment (Figure 26A, middle panel). Generation of GlyGly-remnants showed some variety in signal patterns and observed band width for GlyGly-decorated mono ubiquitin. These observations implied a slightly lower amount of GlyGly-marked substrates in lysates if the IFNβ-treated compared to the control (Figure 26A, lowest panel).

Small amounts of BpJOS-treated lysate samples were subjected to MS analysis prior to the GlyGly-enrichment. The analysis was conducted to test, whether the IFNβ-induction facilitated major changes in the proteome compared to the untreated control. In total, 3200 proteins were identified across all samples. The measured mean intensities of the two groups (untreated/ IFN-treated) amounted to $8.33x10^8$ for the untreated control group and $8.45x10^8$ for IFNβ-treated samples. This result indicated that comparable protein amounts were present between both groups before the GlyGly-enrichment. Vulcano plot analysis of the proteomic samples showed a similar distribution of detected protein intensities between groups (Figure 26B). In the IFNβ-stimulated samples several proteins were upregulated compared to the control (selected proteins are marked in blue in Figure 26B). All of the proteins over a 2xlog2 fold-change-threshold compared to the untreated control were reported as IFN-stimulated genes according to the Interferome database (Hertzog et al., 2011). A selection of the enriched interferon-stimulated proteins and their respective functions are listed in Table 29. In comparison to the untreated control, the Ubl Nedd8 and the small GTPase Rab10, which regulates intracellular membrane trafficking (Hutagalung & Novick, 2011) were 3.5- and 4-fold downregulated in the IFNβ-treated sample (marked in red, Figure 26B).

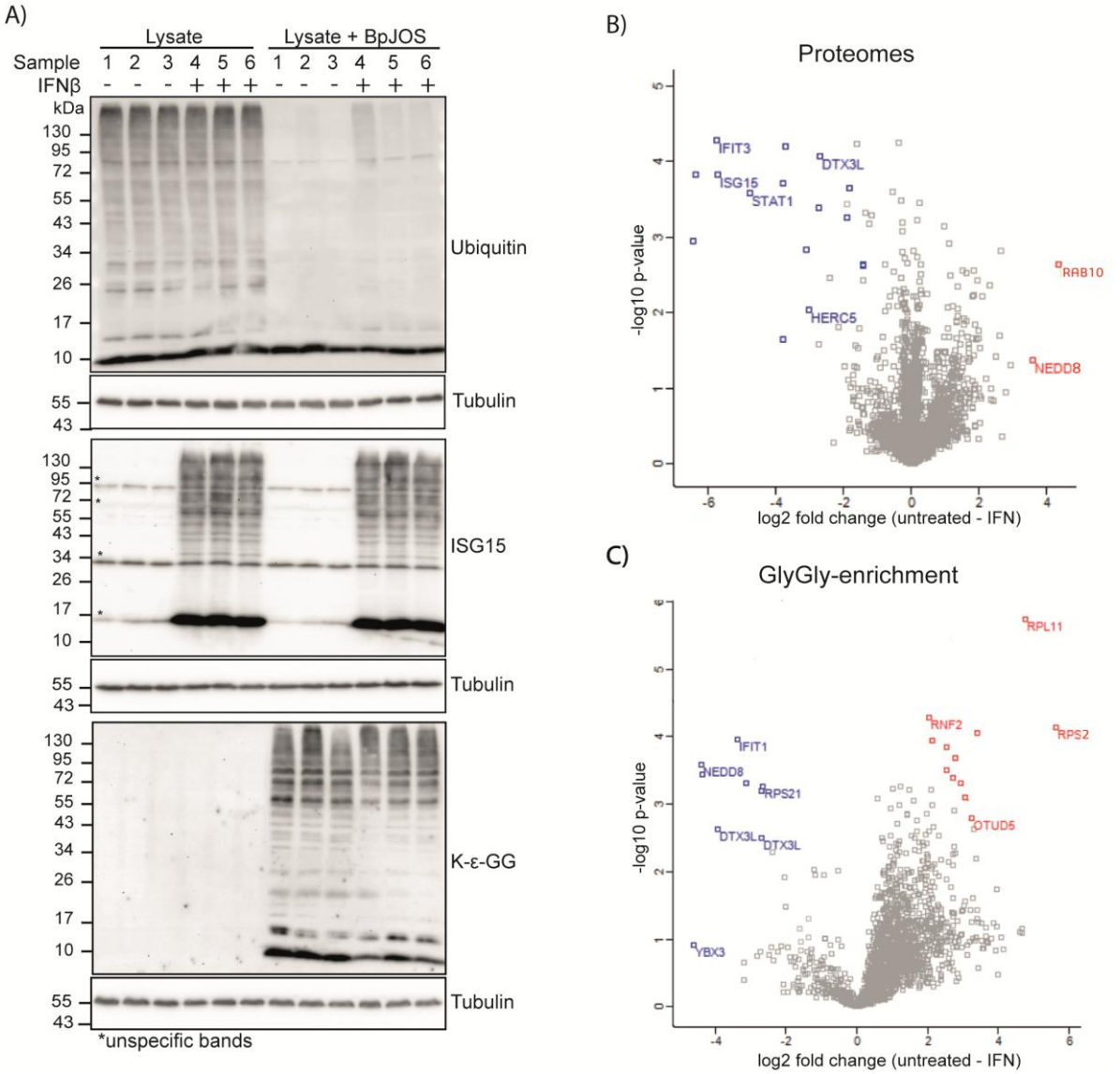

Figure 26: Investigation of IFNβ-induced shifts in the ubiquitome by Clippomics. A) Western blot analysis of samples used for Clippomics. Samples of uninduced and IFNβ-treated HEK blue cells were tested for modifier abundance (ubiquitin, ISG15) and presence of GlyGly-remnants after lysis (Lysate) and after clipping with BpJOS (Lysate+BpJOS) with the respective, specific antibodies. Tubulin was detected as loading control. **B)** Vulcano plot of proteomic samples taken before the GlyGly-IP. BpJOS-treated lysate samples as shown in A) were digested and analyzed by LC-MS/MS. The plot shows the differential abundance between proteins detected in lysates of the untreated control and IFNβ-treated sample. As input the measured intensities of identified proteins reported in the table 'proteingroups' by MaxQuant were used and analyzed with Perseus. The x-axis shows the log2 fold change and the y-axis the -log10 p-value of detected proteins. Selected, enriched proteins in the IFNβ-treated samples are marked in blue. Selected, enriched proteins in the untreated control are highlighted in red. **C)** Vulcano plot of GlyGly(K)-modified sites identified after GlyGly-enrichment. BpJOS-treated lysates samples as shown in A) (Lysate+BpJOS) were processed according to the Clippomics protocol and measured by LC-MS/MS. The plot displays the differential abundance between GlyGly(K)-modified sites in lysates of the untreated control and IFNβ-treated sample. As input, the measured intensities of identified GlyGly(K) sites reported in the 'GlyGly(K)Sites' table by MaxQuant were used and analyzed with Perseus. Selected, enriched sites in the IFNβ-treated samples are marked in blue. Selected, enriched sites in the untreated control are highlighted in red. LC-MS/MS, liquid chromatography–tandem mass spectrometry.

Table 29: Selected IFN-stimulated genes (ISGs) identified upon IFN-treatment. Listed are enriched, selected proteins, which were identified in the proteomic samples of interferon-stimulated cells before the GlyGly-enrichment. The subset of identified IFN-stimulated genes is given with their respective functions as reported by the Uniprot database.

ISG	Function
IFIT1	recognizes and sequesters viral RNAs
IFIT3	acts as an inhibitor of cellular and viral processes
IFIT5	RNA recognition in antiviral defense
ISG15	Ubl, innate immune response to viral infection
Herc5	Major E3 ligase for ISG15 conjugation
DTX3L	E3 ubiquitin-protein ligase, IFN-mediated antiviral response
STAT1	Signal transducer and transcription activator, mediates cellular responses to interferons

GlyGly-enrichment of the untreated triplicates harbored 1604 different GlyGly-modified sites and the IFNβ-treated data set reported 1154 GlyGly-sites. Of all sites, 1032 detected GlyGly-sites were matching between both groups. Vulcano plot analysis of the enrichment demonstrated an overall lower amount of enriched GlyGly-sites in the IFNβ-treated samples compared to untreated control (Figure 26C). This observation matched with the precedingly observed lower amount of GlyGly-carrying proteins visualized by western blotting (Figure 26A, lower panel).

The 20 GlyGly-sites enriched under IFN-stimulation (log2 fold change >2) belong mainly to putative Interferon-stimulated genes (ISGs) as 14 sites were identified in 13 proteins. A selection of these proteins is listed in Table 30 and is highlighted and labeled in blue in Figure 26C. Six of the 20 GlyGly-sites were found in non-ISG proteins, in specific Histone 2B, PSMA3 (proteasomal α3 subunit), Nedd8, DDI2 (ubiquitin shuttling factor), BCORP1 (potential pseudogene) and NSFL1C (adaptor protein; functions were retrieved from the Uniprot database). For the untreated control, 11 GlyGly-sites were identified as upregulated (log2 fold change >2.5) compared to the IFN-treated samples (marked in red in Figure 26C). Selected sites were identified proteins of the ISG and E3 ligase OTUD5, the E3 ligase RNF2 and ribosomal proteins RPS2 and RPL11 (marked and labeled in red in Figure 26C).

Table 30: Selected top hits of GlyGly-modified proteins upregulated upon IFN-treatment. Given are selected top hits of BpJOS-produced GlyGly-sites identified after GlyGly-enrichment. Sites were selected based on highest measured intensities by MS and a log2 fold change >2.5 compared to the untreated control. The modified lysine residue positions are given for multiple isoforms divided by a semicolon for the respective protein. For DTX3L two modification sites matched the given criteria and are listed with a plus sign.

Protein names	Gene name	Lysine position
Interferon-induced protein with tetratricopeptide repeats 1	IFIT1	376;407
Y-box-binding protein 3	YBX3	124;92;127
Nedd8	NEDD8	54
E3 ubiquitin-protein ligase DTX3L	DTX3L	209+456
40S ribosomal protein S21	RPS21	81

Overall, the Clippomics method using BpJOS for the identification of shifts in the ubiquitome in dependence of IFNβ-treatment elucidated several up- and downregulated ubiquitinated sites within several proteins. This experiment demonstrated the feasibility of the method to be applied to physiological relevant specimens.

3.3 Ubi clipping with BpJOS

Swatek et al. introduced a quantitative methodology to study polyubiquitin architectures and the prevalence of branched chains by employing the Lbpro variant Lbpro* (Swatek et al., 2019). The engineered Lbpro* clippase harbors a point mutation (L102W) rendering its more active against ubiquitin compared to its parent enzyme Lbpro (Swatek et al., 2018). The conceptual rationale is based on Lbpro* clipping of enriched polyubiquitin chains, which collapses them to GlyGly-modified monoubiquitin species (Swatek et al., 2019). These species can carry one or multiple GlyGly-remnants in case of branched chains and their abundance can be analyzed by intact mass MS analysis or robustly quantified by AQUA MS measurement.
Inspired by this method, we conceptualized a simplified method to study ubiquitin modifications by exploiting BpJOS activity. BpJOS exceeds cleavage activity exhibited by Lbpro* as less enzyme concentrations and shorter incubation times are needed for total disassembly of ubiquitin chains (Hermanns et al., 2025, see Fig.S2D). In the approach termed ‘Ubi clipping with BpJOS’ several applications were tested. By that, the potential of BpJOS as a powerful tool for studying ubiquitin modifications was assessed.

3.3.1 Semi-quantitative analysis of ubiquitin modifications by BpJOS

The investigation of ubiquitin site occupancy in ubiquitin chains presents a challenge to current studies. For simple modifications like phosphorylation, the corresponding modified and unmodified peptides can be detected by MS and a site occupancy can be estimated from the modified/unmodified signal ratios. For ubiquitination, such an approach would fail since modified lysine residues are not cleaved by Trypsin. As a consequence, modified lysines generate much longer tryptic peptides that do not really correspond to the peptides derived from unmodified lysines.
To address this challenge, a BpJOS-based methodology was proposed for studying ubiquitin chain architecture. First, clipping with BpJOS converts ubiquitin chains into single ubiquitin moieties with GlyGly-remnants at the modified site. Second, the moieties are digested with an enzyme that omits lysine residues for cleavage. The modified and unmodified generated peptides are suggested to differ only in the small GlyGly-remnant between different moieties. GluC and Asp-N were tested as Trypsin substitutions, which cleave C-terminally of Glu>>Asp (GluC) and N-terminally of Asp>>Glu (AspN), respectively (Drapeau, 1976; Ingrosso et al., 1989). The cleavage sites employed by GluC and AspN on the amino sequence of mono ubiquitin and the respective generated peptide are depicted in Figure 27A. In a first proof-of-concept test, K48- and K63-linked di-ubiquitin chains were used as a model substrate (Figure 27B). Di-ubiquitin was clipped with BpJOS and subjected to digestion with GluC or Asp-N prior to LC-MS/MS analysis. It was assessed, if formerly modified and BpJOS-clipped peptides behave similarly to the unmodified form in terms of measured MS/MS intensities.

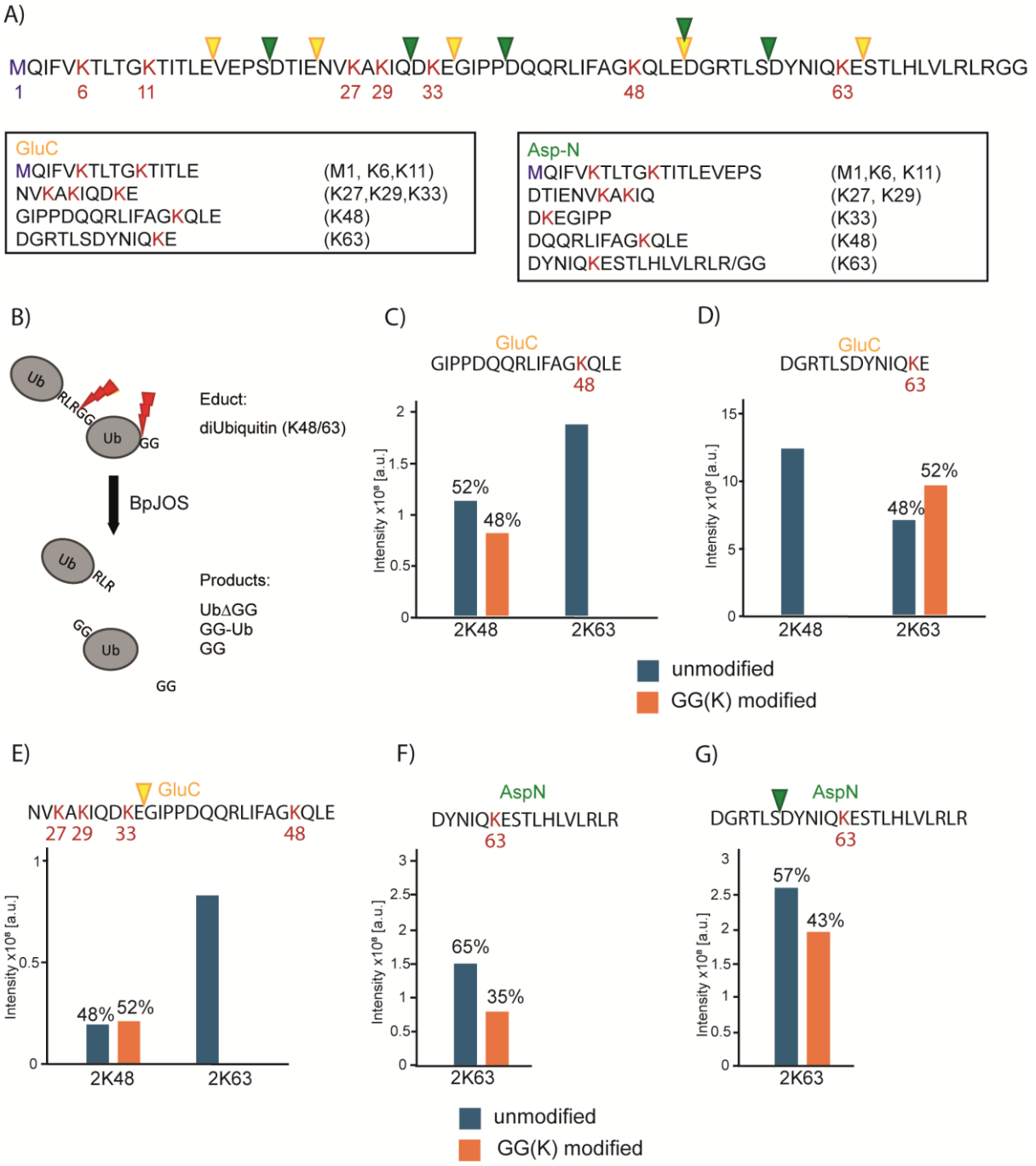

Figure 27: Testing GluC and AspN for a semi-quantitative analysis of ubiquitin occupancy in chains. A) Sequence of mono-ubiquitin with highlighted ubiquitin modification sites at Met1 (blue) and Lys residues (red). The arrows indicate cleavage sites of GluC (yellow) and Asp-N (green). The tables below contain the relevant peptides carrying the respective modification sites. **B)** Schematic representation of used substrate (K48/K63-linked di-ubiquitin) and products generated after clipping with BpJOS. The BpJOS cleavage sites are indicated with a red lightning bolt. **C-E)** K48- and K63-linked purified di-ubiquitin was clipped with BpJOS (1h, 4°C), digested with GluC (16h, 37°C) and analyzed by MS/MS. The obtained intensities of the unmodified peptide (blue) are compared to the GG-modified counterpart (orange) at position C) K48, D) K63 or E) K27/K29/K33/K48 detected in purified 2K48 and 2K63 purified di-ubiquitin. The peptide in D) contains one missed cleavage site indicated by the yellow arrow. **F-G)** As for C-E) 2K63 purified di-ubiquitin was digested with Asp-N (16h, 37°C) showing the intensities of the unmodified and GG-modified peptides at position K63 for F) the expected K63-carrying peptide and G) a K63 peptide with one missed cleavage (green arrow).

It was tested whether an estimated 50:50 intensity ratio of the peptide carrying the GlyGly-motif and its unmodified version originating from the two ubiquitin moieties would be observed. Peptides produced by GluC digestion showed intensity ratios close to the expected 50% distribution with 52% unmodified to 48% GG-modified K48-carrying peptide (GIPPDQQRLIFAGK(48)QLE; Figure 27C). Similar results were obtained for the K63-peptide (DGRTLSDYNIQK(63)E) with 48% unmodified to 52% modified peptide intensities (Figure 27D). Despite the high enzyme:substrate concentration of 1:40, GluC peptides harbored up to three missed cleavages leading to long peptides with up to 35 amino acids. Missed cleavage at E24 within ubiquitin resulted in a combined K27/K29/K33- and K48-carrying peptide (Figure 27E).
Intensities of unmodified and GlyGly-modified peptides for the K27/K29/K33/K48-harboring fraction were low compared to the expected K48- peptide (Figure 27C) but showed a good 48% to 52% ratio (Figure 27E). Multiple entries of peptides with missed cleavage sites indicated a less-than-optimal digest but all share their approximate 50:50 ratio.
Digestion with Asp-N resulted in greater deviation in unmodified and modified peptide intensities, such as 65% to 35% for the K63-carrying peptide and 57% to 43% for the peptide with one missing cleavage site (Figure 27F,G). In Comparison to GluC digestion, an overall higher number of peptides with missed cleavages was detected. This observation complicated the estimation of ubiquitin site occupancy even in simple samples as the di-ubiquitin used. The low digestion efficiency employed by Asp-N rendered it less suitable for the Ubi clipping with BpJOS approach.

The test using di-ubiquitin as a simple substrate demonstrated that digestion with GluC was more suitable for the ‘Ubi clipping with BpJOS’ approach compared to Asp-N to estimate ubiquitin modification occupancy. Minding the need for optimization of digestion efficiency, next tests were conducted in more complex samples.

3.3.2 Testing Ubi clipping with BpJOS on *in vitro* NleL chains

Following the promising results of the first test on dissecting ubiquitin occupancy by ‘Ubi clipping with BpJOS’ of di-ubiquitin, the method was tested on longer ubiquitin chains. The aim was to test a more complex ubiquitin chain composition in a semi-quantitative manner. For that, the approach was tested on *in vitro* generated chains of the bacterial E3 ligase NleL. The protein purification of used constructs and the chain assembly assay was conducted by Dr. Vanessa Lachmayer, University of Cologne.
NleL is a HECT-like E3 ligases encoded by Enterohemorrhagic *Escherichia coli* (EHEC) and builds in equal parts K6 and K48-linked polyubiquitin chains (Franklin et al., 2023; Sheng et al., 2017). By directed mutagenesis of the wild-type to the NleL

E705A variant, the reported specificity was driven towards the generation of K6-linked polyubiquitin chains (Franklin et al., 2023).
The NleL E705A *in vitro* chain assembly assay was conducted using pre-activated mono ubiquitin-MesNa, which allows chain generation in a E1- and E2-less reaction (Park et al., 2015). The assembled chains were subjected to western blot analysis to demonstrate efficient chain generation (Figure 28A). Ubiquitin modifications were clipped with BpJOS and digested with GluC. To enhance digestion efficiency of GluC, the salt concentration in the sample was reduced as GluC suffers from chloride ion sensitivity (see methods 2.2.6). Measurement by LC-MS/MS and subsequent analysis with MaxQuant revealed the presence of three types of GlyGly-modified peptides according to the table 'modificationSpecificPeptides' (Figure 28B). Highest intensities were reported for the peptide carrying the GlyGly-modification at K6. In comparison, intensities for GlyGly-modified peptides at K48 or K63 amounted to an order of magnitude less.

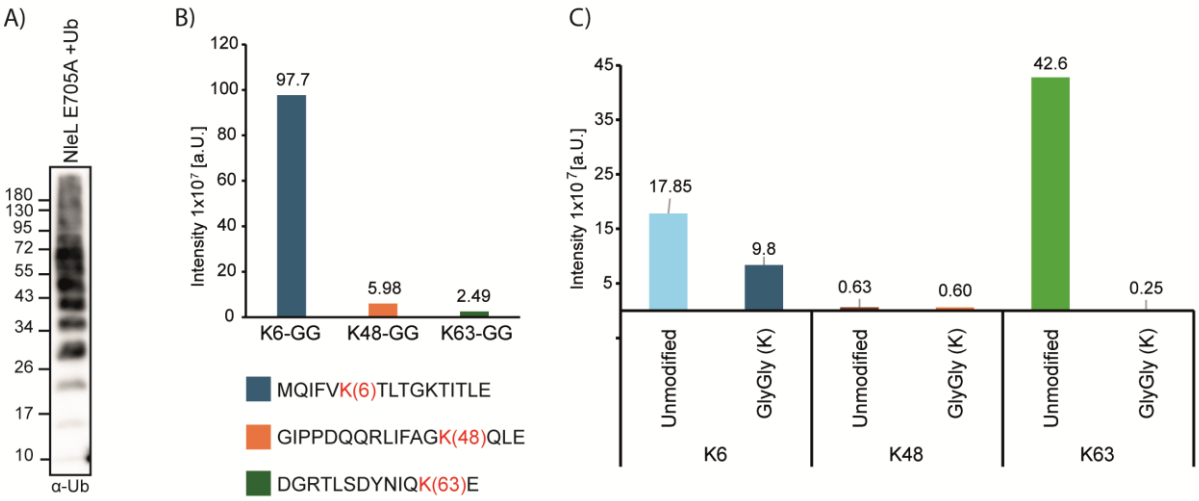

Figure 28: Ubi clipping with BpJOS on NleL E705A *in vitro* ubiquitin chains. Ubiquitin chains were generated using NleL170-782 E705A and Ubiquitin-MesNa. **A)** Western blot analysis of NleL-generated ubiquitin chains monitored by use of a α-Ubiquitin antibody. **B)** Bar chart of measured intensities of identified ubiquitin GlyGly-modified peptides generated by digestion with GluC. NleL chain mix was clipped with purified BpJOS$^{12\text{-}218}$ and digested with GluC before LC-MS/MS. Intensities are given in arbitrary unit [a.U.]. The sequence and GlyGly-modified lysine residue (red) of the respective peptides are listed below the bar chart with the corresponding bar color. **C)** Bar chart of reported intensities of GlyGly-modified peptides as in B) with the measured intensities of their respective unmodified counterpart. The peptides carrying K6 are given in light and dark blue, the K48-peptides are given in light and dark orange, and the K63-peptides are displayed in light and dark green. The intensities values ($1x10^7$) are given above the respective bar. a.U., arbitrary Unit

Reported intensities for the GlyGly-modified peptides and their unmodified counterparts displayed some variability (Figure 28C). For the K6-peptide a deviation of 45% was observed between the modified and unmodified form. The peptides containing K48 were detected equally low intensities independent of the GlyGly-modification. Unmodified K63-haboring peptides showed the highest reported intensities. The GlyGly-modified counterpart was detected but in low intensity ($2.5x10^6$ a.U.; Figure 28C). The stark difference in collectively measured intensities for the K48 peptides (modified & unmodified) to the high intensity given for the unmodified K63-peptide indicated a lack of relative quantifiability between different peptides. These results implied that a calculation of ubiquitin site occupancy and dissection of chain architecture in a quantitative manner is not feasible. If measured intensities can be roughly extrapolated to abundance, K6-linkages were the dominant chain type generated by NleL E705A. This results was in agreement with the published preferences of the NleL variant for K6 chains (Franklin et al., 2023). Proposed low prevalence of K48-linked and K63-linked chains are not necessarily in conflict with the published results: the highly sensitive MS/MS analysis conducted here might report low abundance linkages not observable in chain assays tested by SDS gels as employed by the referenced study.

Despite the absence of quantifiability, the qualitative presence of ubiquitin chain linkages of NleL E705A-generated chains could be determined by Ubi clipping with BpJOS.

3.3.3 Ubi clipping with BpJOS on PARKIN chains

The ‘Ubi clipping with BpJOS’ method was utilized to study the types of chains generated by PARKIN. The PARKIN E3 ligase is known to build K6-, K11-, K48- and K63-linked ubiquitin chains upon mitochondrial depolarization and plays a vital role in mitophagy and mitochondrial quality control (Narendra et al., 2008; Ordureau et al., 2014). Mitochondrial damage is sensed by the kinase PINK1 which phosphorylates the effector PARKIN at Ser65 to facilitate its active state by releasing PARKIN autoinhibition (Chaugule et al., 2011; Kondapalli et al., 2012; Ordureau et al., 2014).

In a collaborative effort together with the Winklhofer Lab (Ruhr University Bochum) it was aimed to uncover novel PARKIN activities. The protein purifications, PARKIN activation by phosphorylation and the reaction mixtures were all prepared by Dr. Maria Georgina Herrera (Winklhofer Lab) and the finished reactions were kindly provided for this study (see methods chapter 2.2.5)
To our knowledge, it was yet unknown if PARKIN can assemble ubiquitin chains *en block,* meaning the modification of a pre-existing ubiquitin chain with another ubiquitin chain. Furthermore, it was unclear which types of modifications could be produced in this process by PARKIN.

Here, phosphorylated and thereby activated PARKIN (pPARKIN) was incubated with tetra linear ubiquitin chains together with E1 and the E2 UbcH7 (Dr. Maria Georgina Herrera). The final reactions before and after clipping with BpJOS were analyzed by SDS-PAGE and western blotting (Figure 29A).

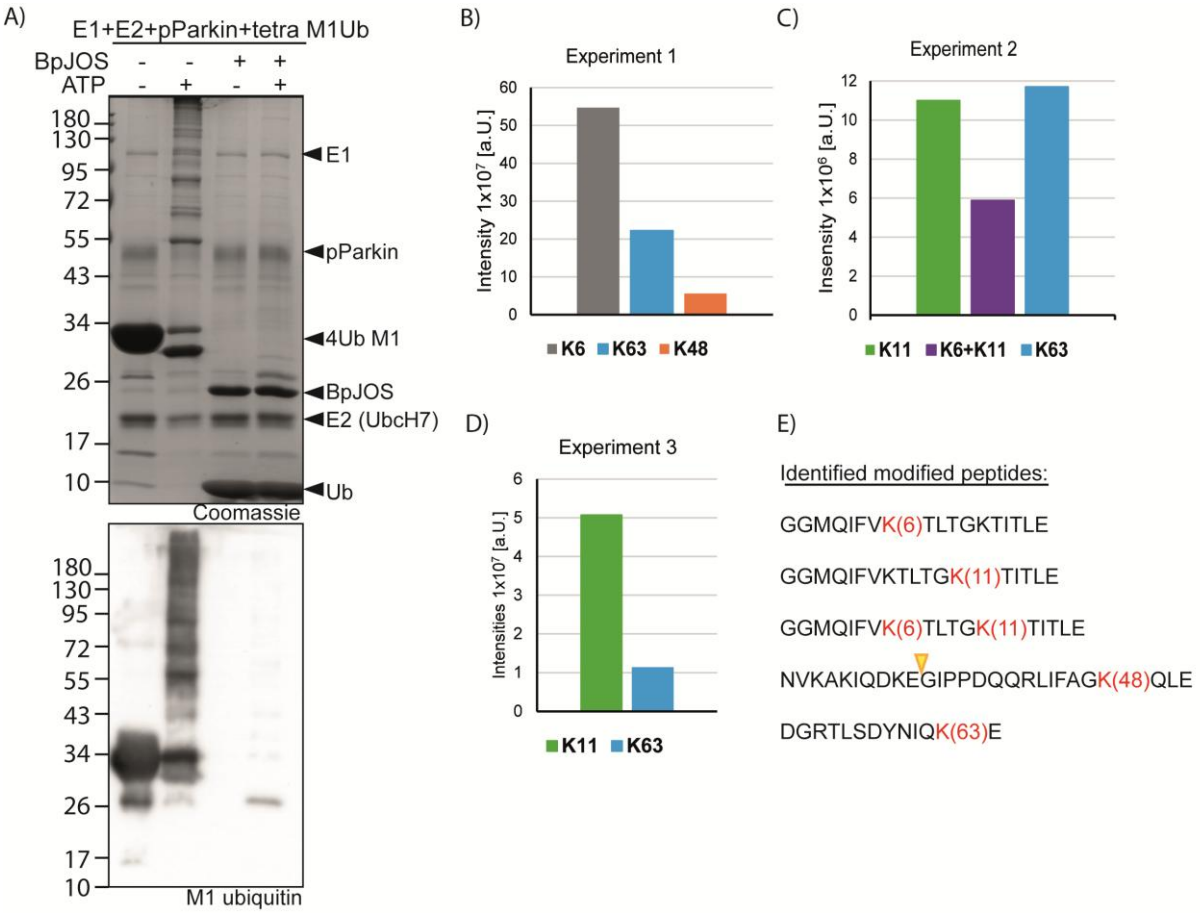

Figure 29: Ubi clipping with BpJOS on PARKIN *en block* assembled ubiquitin chains. Ubiquitin chains generated by pPARKIN were prepared by Dr. Maria Georgina Herrera (Winklhofer Lab, RUB) and tested by Ubi clipping with BpJOS. **A)** Representative gel and western blot of pPARKIN ubiquitin chains by reaction with E1, UbcH7, tetra linear (M1) ubiquitin chains with and without ATP. Samples were analyzed unprocessed and after clipping with purified BpJOS$^{12-218}$. Reactions were analyzed by Coomassie-stained SDS PAGE (upper panel) and western blotting (lower panel). Linear chains were detected using a M1-ubiquitin antibody. n=3. **B)-D**) Measured intensities by LC-MS/MS of generated ubiquitin GlyGly-modified peptides after digestion with GluC per experiment (n=3). Given are the respective reported intensities in arbitrary Units (a.U.). **E)** Summary of identified GlyGly-modified ubiquitin peptides of experiments B)-D). Experiment shown in B) detected a K48-GlyGly-modified peptides with a missed GluC cleavage site (yellow arrow).

As a negative control, a chain assembly reaction without ATP supplementation was prepared. In absence of ATP, a strong band at around 30kDa was visible in the Coomassie-stained SDS gel corresponding to the tetra linear chain input. This result was validated by western blotting as the same band was recognized by an antibody directed specifically against linear chains (anti-M1 ubiquitin; Figure 29A). The sample supplemented with ATP showed the appearance of a pattern produced by linear chains as monitored by the M1-specific antibody. The ubiquitin pattern was demonstrated to derive from the tetra linear chains used as substrates as simultaneously the respective 30kDa band was reduced. This result demonstrated PARKIN chain assembly activity using the tetra linear chain as substrate. Clipping with BpJOS collapsed the present ubiquitin chains in the samples with and without supplemented ATP. Thereby, both the tetra linear chain substrates in the negative control as well as the PARKIN-generated HMW chains were converted into mono ubiquitin. Both samples were desalted and digested with GluC before LC-MS/MS measurement.

In total, the ‘Ubi clipping with BpJOS’ method was utilized on three individual replicates of the *in vitro* reactions. Measured intensities of GlyGly-modified ubiquitin peptides varied across samples (Figure 29B-D). Overall, modifications at K6, K11, K6&K11, K48 and K63 within ubiquitin were identified (Figure 29E). All K6/K11-modified ubiquitin peptides simultaneously carried a GlyGly-motif at their N-terminus. No modified peptides were reported lacking the N-terminal GlyGly. The most distal ubiquitin moiety within the tetra M1 chain used as substrates lacks this GlyGly-motif at its N-terminus as it represents the end of the chain. This result demonstrated that PARKIN - at least when modifying K6/K11- targeted one of the proximal units in the M1 chain and spares the most distal unit, thus creating a branched chain. This instance implied that one or more ubiquitin moieties being part of the pre-existing ubiquitin block were further modified by another block. The data obtained demonstrated that modifications of these ubiquitin moieties were occurring on K6 or K11. Notably, in experiment 2, a doubly-modified peptide with GlyGly-motifs at K6 and K11 was detected additionally to the N-terminal GlyGly (Figure 29C,E). This observation gave another indication for branched chains. An inner-chain ubiquitin was simultaneously modified at K6 and K11, each with tetra M1 ubiquitin blocks.

By testing with ‘Ubi clipping with BpJOS’, it could be shown that the pPARKIN E3 ligase produced a novel chain architecture by *en block* assembly of tetra M1 chains *in vitro.* Thereby several different ubiquitin linkages (K6/K11/K48/K63) were produced amongst the generation of branched chains. These results render BpJOS a powerful tool to dissect ubiquitin chain topologies by Ubi clipping.

4 Discussion

Recent advances in the ubiquitin field uncovered the existence of a novel DUB-like family of enzymes, which cleave ubiquitin and ubiquitin-like modifiers N-terminally of the C-terminal GlyGly-motif called clippases. Several members of this novel class were identified and biochemically characterized by the Hofmann group (Hermanns et al., 2025). One candidate from *Burkholderia pyrrocinia*, termed BpJOS, was shown to cleave mono ubiquitin and ubiquitin chains including the last moiety with high efficiency, leading to its classification as one of the first described ubiquitin C-terminal clippase (UCC). The unique clippase cleavage mode renders ubiquitin unrecyclable for another modification cycle and marks the former substrate with the GlyGly-remnant. This instance renders BpJOS an interesting new tool for studies on ubiquitin chain architecture and the ubiquitome by proteomics. Exploiting BpJOS activity, the Clippomics method was developed to separately study changes in ubiquitome and the the ISGylome. Furthermore, a modified protocol of the published 'Ub- clipping' method was established for the investigation of ubiquitin chain topologies.
Aspects of the characterization of clippase candidates in cell lysates and both developed proteomics tools based on BpJOS will be discussed in the following chapters and contextualized with current state-of-the-art publications.

4.1 Identification and characterization of novel clippases

4.1.1 BpJOS, BcJOS and SnJOS1/2 show clippase activity in cell lysate

In the bioinformatical search for clippases with certain specificities, such as against K48 or K63 only, several candidates from different clusters of the Josephin family were selected for further investigation and experimental validation.
During the characterization of clippase activity on cellular ubiquitination BpJOS and BcJOS were shown to harbor the highest and most holistic activity (Figure 13A). Both were able to cleave all ubiquitination within 1 hour including the most proximal ubiquitin off substrates. In contrast to that, known conventional Josephin DUBs ATX3L and JOSD2 exhibited moderate deubiquitinating activity despite long incubation hours resulting in a portion of intact cellular ubiquitination. Both DUBs were reported to harbor regular DUB activity with a preference for K48- and K63-linked polyubiquitin chains (Grasty et al., 2019; Mao et al., 2005). In addition, JOSD2 was found to cleave K11 chains (Weeks et al., 2011). The preference for longer ubiquitin chains by ATX3L was in agreement with observed residual ubiquitination across all molecular weights as presumably remaining proximal ubiquitination was detected (Figure 13B). Despite ATX3L' reported faster DUB activity compared to JOSD2, cellular ubiquitination showed higher decrease for JOSD2 (Weeks et al., 2011; Figure 13B). This instance could be based on JOSD2's ability to also cleave shorter K11 chains when compared to ATX3L activity.

Beyond BpJOS and BcJOS, two additional UCCs were identified with SnJOS1 and SnJOS2 albeit with slower activity against cellular ubiquitination. SnJOS1 and SnJOS2 were characterized as being active against di-ubiquitin of all chain types with lower preference for K27, K29 and linear chains and did not exert autoinhibition (Boll et al., 2023). The predominant ubiquitin chain linkages in unstressed cells are K48 and K63 as reported for yeast cells (Tsuchiya et al., 2018; P. Xu et al., 2009), suggesting that SnJOS1 and SnJOS2 are indeed less efficient than BpJOS in deubiquitinating substrates. Both enzymes are able to process single ubiquitin moieties demonstrated by their reaction with activity-based-probes using ubiquitin$^{1\text{-}73}$ as bait (Hermanns et al., 2025). Furthermore, mass spectrometry analysis of SnJOS1-treated K63-linked di-ubiquitin resulted in C-terminally truncated proximal ubiquitin demonstrating its clippase activity (Hermanns et al., 2025). These observations hint at SnJOS1 ability to cleave off the proximal ubiquitin off substrates but might be inefficient in doing so compared to the observed strong BpJOS cleavage activity of ubiquitination down to the last moiety.

PvJOS from *Pseudovibrios sp*. showed moderate to high activity against cellular ubiquitination but failed to generate GlyGly signals (Figure 14A). The absence of GlyGly-signals pointed to conventional DUB activity. However, recent unpublished studies revealed PvJOS being the first member of a new class of UCCs (Thomas Hermanns, personal communication). PvJOS acts as a clippase, but in comparison to conventional clippases, hydrolyzes the peptide bond not N-terminally but between the Gly-Gly-motif in the ubiquitin C-terminus (RLRG↓G) in all linkage types. This novel mode of action was determined via intact mass spectrometry (unpublished) and cannot be detected by the commercial K-ε-GG-antibody. Thus, the activity remains unnoticed when potential clippase activity is only detected by the use of the GlyGly-antibody. This result presented one limitation of identifying novel clippases with the K-ε-GG-antibody. Solely clippase activity acting on the C-terminal GlyGly-motif modified to a lysine residue can be detected by this antibody. This underlines the necessity to pursue further testing of clippase candidates upon the observation of activity with additional methods such as intact mass spectrometry. By employing such methods, a potentially novel cleavage mode can be elucidated and prevents the false characterization of these enzymes to the class of regular DUBs.

The non-Josephin clippase candidate ChNJC showed close to no deubiquitinating activity when tested on cell lysate (Figure 14A). The enzyme does not belong to the Josephin-family but is predicted bioinformatically to harbor two separate catalytic domains (Kay Hofmann, personal communication). One of them is of a novel type and appears to recognize ubiquitin in a clippase-like orientation, as modelled by Alphafold-3. The other catalytic domain shows sequence similarities to the ATG4-proteases (Kay Hofmann, personal communication). The function of neither domain has been characterized, but the combination of a clippase-like domain with an ATG4-like domain suggests a role of this enzyme in helping bacteria to evade autophagic clearance. The four ATG4 isoforms in humans are reported to act on the Ubl ATG8, which itself is divided into two the subclasses LC3 and GABARAP in

mammals (Agrotis et al., 2019). ATG4 is one key player in autophagy as it lipidates newly synthesized pro-LC3/ GABARAP, which leads to the recruitment other autophagy machinery components at the formed phagophore promoting autophagosome formation (Birgisdottir et al., 2013; Nieto-Torres et al., 2021). ATG4 then deconjugates the lipidated LC3/GABARAP form off the phagophore. This process recycles it to their free form and thereby promotes autophagosome maturation and elongation (Agrotis et al., 2019). As ChNJC harbors an ATG4-like domain, it could be speculated that the expression of ChNJC by *Chlamydiales sp*. might serve the purpose to counteract potential autophagic clearance of the bacteria upon infection, which is termed xenophagy (Deretic et al., 2013). Purely speculatively, the bacterial ChNJC could target host cell ATG8/LC3/GABARAP, thereby deconjugating it prematurely from the phagophore and interfering with autophagosome formation.
Most constructs of the UCC candidates used in this study were designed as a truncation with the exception of BcJOS. The truncations were designed to harbor the predicted catalytically active domain but to leave out transmembrane regions and unstructured regions to aid successful protein purification. Therefore, constructs were chosen to focus on catalytic activity and to relegate potential regulatory functions. The investigation of these functions was not prioritized in order to narrow down the search of highly active enzymes potentially exhibiting modifier-specificity, which could be utilized in other experimental approaches, such as the Clippomics method (See chapters 3.2 and 4.2).
The lack of activity in truncated ChNJC might be based on the lack of potential protein-binding domains, which could be required for interaction with the substrate or binding partners mediating the substrate-DUB interaction. Furthermore, it was not assayed whether ChNJC might rather act on LC3/GABARAP than on ubiquitin. Due to the abundance of multiple other interesting UCC candidates, the characterization of ChNJC was no longer pursued.

PaJOS from *Pigmentiphaga aceris* and HeJOS from *Herbaspirillium sp*. displayed minor to moderate activity against cellular ubiquitination (Figure 14B). The absence of generated GlyGly-signal with the K-ε-GG-antibody hinted at conventional DUB activity just as for PvJOS. In contrast to PvJOS, both enzymes could be validated as regular DUBs as PaJOS was shown to react with the full-length Ub-PA probe and was able to process the C-terminal GlyGly-motif of mono ubiquitin demonstrated by intact mass spectrometry (Hermanns et al., 2025). Tests against the entire panel of di-ubiquitin linkages displayed its specificity for K63-linked chains (Hermanns et al., 2025). HeJOS was demonstrated to also cleave K63-linked chains with minor activity against K11 chains and was shown remain inactive against mono ubiquitin in intact mass analysis. Together with the observation, that HeJOS did not react with the C-terminally truncated (Ub^{1-73}) or full-length (Ub^{1-75}) ubiquitin-PA probe, it could be speculated that HeJOS requires binding of more than one ubiquitin moiety as linkage-specific DUBs often do not react with probes (Hermanns et al., 2025). It is assumed that at least two ubiquitins might be bound at HeJOS potential S1 and S1’ site for effective hydrolysis as this

instance is shown for most linkage-specific DUBs, such as the member Zup1 of the ZUFSP DUB family and its specificity for K63 chains (Hermanns et al., 2022).

The two remaining candidates CsJOS from *Chlamydiales bacterium STE3* and PcJOS from *Parachlamydia sp*. were seemingly devoid of deubiquitinating activity in cell lysates of HEK293T cells. To answer the question, whether the lysates lacked a suitable substrate for both candidates, their activity was investigated by additional methods. In unstressed cells, linear chains are only present at very low basal levels (Tsuchiya et al., 2018). CsJOS was recently shown to specifically cleave linear chains employing clippase activity as demonstrated by intact mass analysis (Hermanns et al., 2025). This result stressed the requirement for using of suitable substrates and analysis methods to elucidate clippase activity, equivalent to the priorly discussed results of PvJOS. Apart from CsJOS, PcJOS was the first linear specific clippase to be uncovered and its comprehensive activity analysis will be focused on in the following chapter.

Taken together, the characterization of the bacterial UCC candidates revealed the existence of two linkage-specific UCCs (CsJOS, PcJOS), three linkage-promiscuous UCCs (BpJOS, BcJOS, PvJOS) and two linkage-specific DUBs (HeJOS, PaJOS) in the batch of tested Josephins while their eukaryotic counterparts JOSD2 and ATX3Nl lack chain specificity demonstrating the diversity in action within this family.

4.1.2 PcJOS is an M1-specific clippase

PcJOS was characterized as a clippase with specificity against linear chains (Figure 15). Validation of clippase activity was achieved by intact mass analysis of linear di-ubiquitin incubated with PcJOS and the interpretation of acquired m/z ratios of generated products (Figure 15B). The m/z ratio for an intact moiety (Ub) equals the ratio for a moiety with an N-terminal GlyGly motif while simultaneously lacking the C-terminal GlyGly motif (GG-UbΔGG). Despite that conflation, it is assumed that those peaks can be rather assigned to the GG-UbΔGG product than PcJOS employing conventional DUB activity in parallel to clippase activity.
Prior studies on PcJOS involved solving of the PcJOS structure in complex with linear di-ubiquitin (Thomas Herrmanns, data not shown). The structure revealed how di-ubiquitin is bound by PcJOS enabling further investigation of linkage-determining interaction sites, which were focused on in experiments incorporated in the master thesis (Kolek, 2021). Point-mutations within the interaction sites and corresponding mutation sites in di-ubiquitin elucidated that both the S1 and S1’ site binding of the M1 chains are required for activity (Kolek, 2021). Despite these results, it is assumed that PcJOS was able to cleave the proximal ubiquitin unit to a lower degree, presumably caused by the experimental conditions using high amounts of enzyme (10µM PcJOS on 500mM linear di-ubiquitin).

The binding mode by PcJOS is reminiscent of eukaryotic M1-specific DUB OTULIN, which also requires S1 and S1' site binding and exhibits a ubiquitin-assisted catalysis. Oversimplified, the OTULIN catalytic triad exerts auto-inhibition in absence of a substrate but is released upon M1-ubiquitin binding pushing it into an active conformation (Keusekotten et al., 2013). Main driver of this conformational change was shown to be Glu16 in the proximal ubiquitin inserted into the catalytic center (Keusekotten et al., 2013). For PcJOS binding of linear chains, Glu16 in the proximal ubiquitin was equivalently important for ubiquitin processing as mutation of the Glu16-contacting site R302A in PcJOS led to drastic decrease in activity (Kolek, 2021). Whether PcJOS mimics OTULINs mode of action could not be fully dissected due to lack of a PcJOS apo-structure without a linear di-ubiquitin as substrate.
PcJOS derives from the genome of bacteria of the *Parachlamydia* genus, which are obligate intracellular bacteria (Amann et al., 1997; Greub & Raoult, 2002). Their natural niche was reported to infecting free-living amoebae but show zoonotic potential. For example, for one member of the genus, *Parachlamydia acanthamoebae*, it was shown that the bacteria were able to invade human macrophages (Greub, Mege, & Raoult, 2003). Moreover, *P. acanthamoebae* was identified in nasal mucosa samples of healthy volunteers but also was detected in serological samples of patients suffering from pneumonia rendering it an emerging respiratory pathogen (Corsaro & Greub, 2006; Greub, Boyadjiev, et al., 2003). Studies on macrophage infection with *P. acanthamoebae* demonstrated the bacteria resided in an intracellular vacuole used as a replication niche and at a later infection stage induced apoptosis (Greub, Mege, & Raoult, 2003). In response to bacterial infection, bacteria containing vacuoles are often decorated with linear chains by LUBAC triggering autophagic responses as shown for *S. typhimurium* as a first line of defense in higher eukaryotic cells (Tripathi-Giesgen et al., 2021). These vacuoles are then referred to autophagic clearance. Hypothetically, PcJOS expression upon *Parachlamydia* infection of human cells could counteract this defense mechanism by collapsing linear chains used for immune signaling by the host cells. This hypothesis is still under investigation and is purely speculative. Due to amoebae not harboring linear ubiquitin chains and the yet limited available data on *Parachlamydia* infection of human cells, it remains unclear how this cleavage mode evolved.

When PcJOS activity was assayed in LUBAC-transfected HEK293T cells, a decrease of total ubiquitination pattern was observed independent of PcJOS or OTULIN expression (Figure 15D). Albeit not being crucial for PcJOS characterization on LUBAC-produced linear chains *in vivo*, this observation indicated a shift in the ubiquitinome worth noting. Despite lack of further investigation, it is speculated that the expression of the LUBAC components led to a deduction of free ubiquitin used for regular chains present in HEK293T cells under basal condition, which are primarily K48- and K63 chains, and a redirection of free ubiquitin for the generation of linear chains.

By the extended characterization of PcJOS, the existence and function of the first linear chain specific clippase could be elucidated, which was followed by the identification of the second linear-specific clippase CsJOS. These findings imply the existence of more, yet undiscovered clippases with diverse ubiquitin chain-specificities.

4.1.3 BpJOS is a highly active, chain-promiscuous ubiquitin clippase

BpJOS was characterized in this study as well as in the first clippase publication by Hermanns et al. as a highly active clippase targeting mono ubiquitin and ubiquitin chains of all linkage types (2025). When tested against a di-ubiquitin panel of all linkage types, BpJOS cleaved all linkages with high efficiency with the exception of K27-linked di-ubiquitin (Figure 16A). Studies have shown that ubiquitin K27-linkages display resistance to disassembly by USP2, USP5, and Ubp6, which are all able to efficiently cleave all other chain topologies (Castañeda et al., 2016). Ubiquitin linkages via K27 harbor a unique architecture and distinct properties as they suffer from lower solvent-accessibility and less mobility compared to all other chain types (Castañeda et al., 2016). These results are in concordance with BpJOS decreased ability to hydrolyze K27 di-ubiquitin albeit being linkage-promiscuous.

The BpJOS titration in HEK293T cell lysate revealed the production of a distinct band at around 17kDa detected with the K-ε-GG-antibody (Figure 16B). It was assumed that this band represents a rather specific, formerly ubiquitinated substrate than GlyGly-marked di-ubiquitin, which would run at around the same molecular weight. This assumption is based on the observation that BpJOS efficiently hydrolyzes di- to mono ubiquitin within minutes (Figure 16A). To answer the question which substrate would be prevalent in such high amounts, an in-gel digest was performed and analyzed by LC-MS/MS (data not shown). The obtained MS data listed several GlyGly-marked lysine residues within core histones such as multiple variants of histone H2B in the samples, which is in line with the numerous reports on strong regulation of histones by ubiquitination serving as a signaling platform (Cao & Yan, 2012; Goldknopf & Busch, 1977).

This micro identification of former ubiquitin targets by BpJOS gave insight into BpJOS potential to be used a proteomics tool for studying the ubiquitome in a greater scale as pursued in chapters 3.2 (Clippmics) and 3.3 (Ubi clipping).

4.1.4 BpJOS is inactive against ISG15

BpJOS' high activity against ubiquitin came in stark contrast to its complete inactivity against ISG15 (Figure 16C, Figure 17B,C,D). Compared to Nedd8, other Ubls like ISG15 share less sequence conservation with ubiquitin (Ronau et al., 2016). This instance is demonstrated by the conservation of both the Ile36 and Ile44 hydrophobic patches in ubiquitin and Nedd8, which both are absent in ISG15. One of the most crucial determinants in DUBs and clippases, is the interaction with modifiers via the Ile44-patch and Ile36-patch recognition (Beal et al., 1996; Hermanns et al., 2025; Ronau et al., 2016; Sloper-Mould et al., 2001). Upon single mutation of the respective contact sites interacting with the Il44- and Ile36-patches, BpJOS activity against di-ubiquitin was highly diminished or abrogated (Hermanns et al., 2025).

BpJOS inactivity against ISG15 was rationalized by the solved BpJOS structure in complex with mono ubiquitin (Hermanns et al., 2025). BpJOS in complex with ubiquitin was superimposed with a hypothetical BpJOS-ISG15 complex (data not shown). The superimposed complex revealed the lack of sufficient interaction of BpJOS with ISG15. Therefore, BpJOS can interact with ubiquitin or Nedd8 via their Ile44 patches but does not interact with ISG15 due to the absence of crucial interaction sites giving a structural reasoning for BpJOS lack of activity.

Apart from activity against ubiquitin, BpJOS was shown to react with C-terminally truncated Nedd8($^{1-73}$) probe. The activity of BpJOS against Nedd8 can be explained by findings made for di-ubiquitin tested with BpJOS. When tested against a R74A mutant of di-ubiquitin, BpJOS activity was abolished, but activity was hardly decreased against the R72A mutant (Hermanns et al., 2025). This result demonstrated that BpJOS interaction at R72 is dispensable for its clippase activity. Nedd8 harbors an Ala residue at position 72, but in line with the findings, this sequence difference to ubiquitin does not affect BpJOS activity. Furthermore, Nedd8 comprises the conserved Ile44 patch. Both implications support the observed activity of BpJOS against Nedd8.
However, BpJOS showed only minor activity against cellular neddylation (Figure 16C, Figure 17D). The detection with the anti-Nedd8 antibody showed a relatively low prevalence of neddylation in unstressed HEK293T cells with three to four distinct bands visible (Figure 17D). The low amounts of detectable neddylation under basal conditions is reflected by studies showing the main Nedd8 substrate (>90% of neddylation targets) are all eight Cullin ring ligases (Cul-1, -2, -3, -4A, -4B, -5, -7, and Cul9/Parc) with traces of non-Cullin neddylation substrates (Jones et al., 2008; Vijayasimha & Dolan, 2021). Cullin ring ligases (CRLs) are multi-protein complexes comprised of a Cullin scaffold as a core component interacting with a catalytic RING-containing protein (RBX1/RBX2) at the Cullin C-terminus and binding a substrate receptor (e.g. Skp1) at the Cullin N-terminus (Duda et al., 2011; Petroski & Deshaies, 2005; Zheng et al., 2002). Neddylation of the Cullin C-terminus stimulates a conformational change within the complex resulting in a shift from a closed to an open conformation. This allows for the RBX1/2-bound ubiquitin E2 to reach the substrate recruited at the Cullins opposing

end (Duda et al., 2011). Thereby, Cullin neddylation facilitates ubiquitination of targeted substrates.
Monomeric Cullins can be roughly categorized into three different size ranges with ~87-90kDa (Cul-1,-2,-3,-4A,-5), ~105-114kDa (Cul-4B,-7) and ~183kDa (Cul9/PARC). The size of assembled CRL complexes amounts to ~200-700kDa depending on the composition (Duda et al., 2011).
The bands observed in HEK293T cell lysate using the Nedd8-antibody revealed two bands at around 95kDa and 120kDa, which are assumed to belong to monomeric Cullins, albeit no further assignment is possible by western blot alone (Figure 17D). Suspected Cullin bands showed only a minor reduction upon NEDP1 or BpJOS treatment indicating both were able to deneddylate Cullins notwithstanding to a very low degree (Figure 17D). NEDP1 is reported as a Nedd8-specific protease, which is able to deneddylate a wide variety of substrate including Cullins Cul-1,-2, -3 and -4A *in vitro* (Chan et al., 2008; Mendoza et al., 2003). Assumed Cullin-neddylation, which remained intact upon incubation with NEDP1, might be based on the presence of Cullins apart from those which are reported to be deneddylated by NEDP1. However, missing data on deneddylation of specific Cullins does not have to correlate with missing NEDP1 cleavage ability. More than NEDP1, the principle deneddylase of Cullins is the major multi-subunit complex termed COP9 signalosome with its CSN5 catalytic core (Pick et al., 2012). NEDP1 might rather exhibit activity against their non-Cullin targets under experimental conditions *in vitro* compared to the cellular environment, where the COP9 signalosome is proposed to act as the major Cullin deneddylator.

Studies have shown that bacterial deamidases CHBP from *Burkholderia pseudomallei* and Cif from *Escherichia coli* can deamidate Nedd8 at position Gln40 to Glu40 (Crow et al., 2012; Cui et al., 2010). The deamidation reaction corrupts the Nedd8~CRL interaction site, which diminishes the stabilization of the open conformation and greatly reduces ubiquitination activity (Duda et al., 2011; Yao et al., 2012). It is hypothesized that the changed interaction surface might impair Nedd8 removal. During the deamidation reaction an amino acid amino (NH_2) group is replaced by a hydroxyl (OH) group. This reaction can occur in enzyme-free settings and spontaneously in cell lysates depending on multiple factors. These factors include the ionic strength and type of buffer used, the pH of the solution and is facilitated by high temperatures (Boudier-Lemosquet et al., 2022). If this deamidation mechanism rationalizes the impairment on BpJOS and NEDP1 deneddylation activity on Cullins is not clear. This hypothesis would require validation by analysis of Nedd8 modifications in the given experimental conditions in a native SDS gel. Alternatively, mass spectrometry analysis specifically focusing on the occurrence of amino acid replacements in Nedd8 could be pursued.

The more ubiquitin-targeting Lbpro* (L102W) variant was generated on the basis of the Lbpro wild-type enzyme acting mainly on ISG15 (Swatek et al., 2018; Swatek et al., 2019). Reminiscent of the Lbpro* variant, the generation of a more modifier-specific

BpJOS variant was attempted (Thomas Hermanns, personal communication). The solved structure of BpJOS in complex with ubiquitin allowed for the identification of potential mutation sites driving modifier selectivity towards ubiquitin or Nedd8 (Hermanns et al., 2025). Although no structural feature could be identified for increasing ubiquitin specificity, the D110 residue in BpJOS harbored potential for blocking ubiquitin interaction (data not shown, Thomas Hermmans). The BpJOS D110R mutant was assumed to repel ubiquitin at position R72 due to static repulsion. Nedd8 harbors an alanine (A72) at this position potentially allowing for BpJOS D110R binding. Extensive biochemical characterization of the BpJOS D110R variant demonstrated a sharp decrease in activity against ubiquitin in cell lysate (data not shown). However, activity against Nedd8 was also slightly impaired. The remaining minor activity against ubiquitin at longer time points visualized by western blotting and in mass spectrometry-based analysis revealed lack of absolute specificity (data not shown). This specificity was aimed at for use in the Clippomics method, which will be discussed in the following chapters, but was discarded due to residual conflation of ubiquitin and Nedd8 modifications.

4.2 The Clippomics method

4.2.1 Conceptualization and development of the Clippomics method

The Clippomics method was developed to disentangle the modifiers ubiquitin, Nedd8 and ISG15 in complex samples. The conflation of the modifiers based on their shared -RGG C-terminal motif is most often disregarded in studies profiling modified substrates. By employing the Clippomics method, ubiquitin and potentially Nedd8 sites are positively selected for by clipping with BpJOS before GlyGly-enrichment. ISG15 is not targeted by BpJOS and escapes enrichment.
In order to assess a digestion enzyme apart from Trypsin for peptide generation, LysC, Chymotrypsin and Lysarginase were tested for the scale of generated data sets in a preliminary clippomics test. Of the tested enzymes, Lysarginase generated the biggest set of identified proteins and detected GlyGly-carrying peptides (3.2.1).
Trypsin is considered the gold standard for generation of peptide fragments in preparation for tandem MS. It creates relatively short peptides with an average length of 14 amino acids by cleaving C-terminally of Arg and Lys residues (Burkhart et al., 2012; Olsen et al., 2004). Further, the peptides carry at least two defined positive charges: one at the N-terminus and one at the C-terminal Lys/Arg residue (Burkhart et al., 2012). The positive charges facilitate peptide ionization generating precursors well suited for later fragmentation in the collision cell (Dongré et al., 1996). These properties render Trypsin-produced peptides optimal for measurement by CID (collision-induced dissociation)-based LC-MS/MS (Burkhart et al., 2012). Lysarginase mirrors the cleavage positions of Trypsin by cleaving N-terminally and not C-terminally of Lys and

Arg residues. This instance leads to the generation of peptide with similar characteristics, providing an explanation for the good performance in the digestion enzyme test.
Chymotrypsin exhibits a broader specificity compared to Trypsin and Lysarginase as it hydrolyzes proteins at the aromatic residues Phe, Trp, Tyr and to a lower extent at Met and Leu (Hudáky et al., 1999; Vreeke et al., 2023). Chymotrypsin-generated peptides are longer compared to Trypsin due to sparser cleavage sites (Vreeke et al., 2023). Together with the proposed lower ionization capability due to the absence of additional charges, it serves as a rational for the lower number of identified proteins in the enzyme test. LysC is most often used in combination with Trypsin to enhance cleavage at Lys residues (van der Hoeven et al., 2026; Wiśniewski et al., 2009). Again, due to scarcity in cleavage sites as it cleaves only Lys produced peptides are too long for optimal behavior during tandem MS.
Taken together, Lysarginase was found to be most suitable digestion enzyme for the Clippomics method and was incorporated into the protocol for further proof-of-concept test.

4.2.2 First proof-of-concept Clippomics test

The first Clippomics test including an array of controls validated BpJOS and Lbpro suitability to profile ubiquitinated and ISGylated proteins in complex samples. It was expected that a minor amount of unspecific sites could be detected due to the high sensitivity of MS measurement and potential co-enrichment of single, unmodified peptides. The included negative control lacking clippase treatment yielded 7 seven sites after GlyGly-enrichment despite the absence of endogenous clippases in human cells. The ‘GlyGly(K)’ table generated by MaxQuant listed three sites with high intensities defined by a $1x10^6$ cutoff. The three reported GlyGly-sites included peptides from Nesprin-2 (SYNE2), Spermatogenesis-associated protein 17 (SPATA17) and K48-modified ubiquitin. It is likely that the sites of SYNE2 and SPATA17 are a false assignment of measured peptides to the GlyGly-modified peptides by MaxQuant.
If not based on experimental circumstances, speculatively, detected GlyGly-sites could derive from an endogenous, putative cell mechanism. Lysine-48-linked ubiquitin chains convey the modified substrate to proteasomal degradation (Grice & Nathan, 2016; Thrower et al., 2000). The β-subunits of the 20S proteasome exhibit protein breakdown into peptides in a chymotrypsin-like and trypsin-like manner (Kisselev et al., 1999). Possibly, proteasomal degradation produced peptides by chance, that were suitable to be recognized by the GlyGly-antibody beads. Speculatively, in some cases proximal ubiquitination might not have been removed efficiently from the substrate prior to degradation leading to the generation of the GlyGly-remnant. As the overall amount of these sites were low, the data gathered did not invalidate the use of the GlyGly-beads for specific enrichment of GlyGly-carrying, formerly modified peptides.

The absence of ubiquitination and neddylation in the samples was ensured by the combination of E1-inhibitors (TAK243/MLN4924) and treatment of the lysates with purified de-modifiers (SnUSP1/NEDP1) to the lysates. As both E1-inhibitor exert rather strong selectivity for the targeted modifier than absolute specificity, dosages and incubation times were titrated in experiments prior to the Clippomics test. Conditions were selected to limit crosstalk to other modifiers, which supposedly led to insufficient removal of the unwanted modifiers in the given experiment. The treatment with E1-inhibitors might not have stalled all modification events due to short incubation times (4/5h). Modification events might also have a lower turn-over rate and could have sustained despite the treatment. Additional SnUSP1/NEDP1 treatment might potentially not have compensated for removal of residual modifications to escape detection by the sensitive MS analysis. The presence of residual modifications provides an explanation for the presence of supposed ubiquitination sites in samples, in which ubiquitination should have been depleted (samples 2,3,7 Table 25, Figure 23). This instance strengthens BpJOS inactivity against ISG15 as the 7 sites found in the sample proposed to harbor only ISGylation supposedly derived from residual ubiquitination (sample 7, Table 25). Reported sites were matching the identified sites in the neddylation test (Figure 23A): position 9 in the 14-3-3 protein, which was assigned to being likely a ubiquitin modification.

The samples designed to harbor only neddylation still included GlyGly-sites supposedly derived from ubiquitination including peptides from the 14-3-3 protein (Samples 2 and 3, Table 25). No canonical Nedd8 sites were identified by BpJOS, which was in line the low prevalence of neddylation in the samples visualized by western blotting and decoration with a Nedd8-antibody (Figure 22). Furthermore, these findings are in line with the comparably low number of *bona fide* neddylation targets apart from Cullins reported by other studies (Jones et al., 2008; Rabut & Peter, 2008; Santonico, 2020; Vijayasimha & Dolan, 2021).

Many proteomic studies on neddylation rely on overexpression of Nedd8-fusion proteins which alters the neddylome due to increase in the cross talk with the ubiquitination machinery, which in turn leads to artifacts (Enchev et al., 2015). This instance demonstrates the technical challenges in deciphering the neddylome under basal conditions and in the de-conflation with the ubiquitome. The investigation of neddylated substrates, the function and prevalence of Nedd8 mixed- and poly-chains remains an obstacle with current strategies. Recent advances in the Nedd8 field display the emerging scope of cellular neddylation and its contribution to the Ubl code. Lobato-Gil et al. employed a GlyGly-antibody-based strategy and investigated the Neddylome by use of a Nedd8 R74K mutant (Lobato-Gil et al., 2021). The study found 1101 neddylation sites on 620 proteins and identified canonical and non-canonical neddylation pathways.

A Nedd8-specifc clippase would negate the requirement for mutant generation. Further, it would allow for the investigation of neddylation targets under basal conditions as manipulation by over-expression or generation of knock-out cells would

be dispensable. The investigation of shifts in the neddylome under controlled stressors could be examined just by addition of purified clippase to lysate.
Such Nedd8-specific clippase has not been identified yet and advances in engineering a Nedd8-specific BpJOS variant (BpJOS D110R, see 4.1.4) did not harbor a specificity high enough for MS-based studies. However, novel clippases are currently being discovered and their activities are subject in ongoing studies at the Hofmann lab (Institute for Genetics, University of Cologne). The opportunity to employ such specific clippases would give rise to a powerful tool in deciphering the neddylome.

For the investigation of ISGylation targets, the overlap of identified ubiquitin and ISG15 sites was initially explained with residual ubiquitination (Figure 23C, D). Despite that, it is proposed that some lysine residues in proteins could be undergoing either ubiquitination or ISGylation depending on the cellular context. ISGylation occurred rapidly as strong ISGylation was detected within 24 hours of IFNβ treatment in this study (Figure 17A) and also other studies (Fan et al., 2015; Y. J. Kim et al., 2016). Quick responses to viral infection are mandatory for cell survival, hence, ISG15 acts antivirally by covalently modifying host and viral proteins which interferes with viral assembly or function (Thery et al., 2021). The main ISG15 E3 ligase Herc5 associates with polyribosomes and modifies newly synthesized viral and host proteins (Durfee et al., 2010; Thery et al., 2021). Due to the rapid nature of ISGylation, it is proposed that ISG15 modification relies more on target accessibility than on site-specificity compared to ubiquitination. As clear evidence is lacking for that assumption, it is more implied by the findings by Zhang et al. using bone-marrow-derived macrophages (BMDMs) of ISG15 deconjugase-dead ($USP18^{C61A/C61A}$) and *Isg15*–/– mice under *Listeria monocytogenes* infection (Yifeng Zhang et al., 2019). The study found a 71% overlap of ubiquitin sites reported by other studies and their identified ISGylation sites in wild-type animals (Yifeng Zhang et al., 2019). Notably, reported ubiquitin sites, which are available on the PhosphoSitePlus PTM database, were acquired by GlyGly-enrichment lacking exclusion of Nedd8 and ISG15 sites (Hornbeck et al., 2015; Yifeng Zhang et al., 2019). Further, no discernable consensus motif for ISG15 modification could be identified by Zhang et al. These data suggest ISG15 could be competing with ubiquitin for site modifications.

Comparison of the 75 identified ISGylated proteins in the present experiment with identified proteins by Zhang et al. revealed that 45 of the proteins were reported in both data sets. This comparably high number despite differences in used cell lines and employed procedures lies in contrast to the number of shared sites: only 5 of the 100 identified sites in this study match with the sites by Zhang et al. This observation further underlined the suspected variation in ISG15 modification sites.
Conclusively, the available data indicates that alternating ubiquitination or ISGlyation at the same site could be possible.

BpJOS generated more GlyGly-sites in the samples containing both ubiquitin and ISG15 (411 sites) compared to ubiquitin alone (292 sites) despite its inactivity against ISG15 (samples 4 vs 1, Table 25). It is assumed that the deviation in the number of

expected and acquired sites could be based on a single batch effect. Furthermore, interferon-stimulation (as in sample 4) could have stimulated ubiquitination or, alternatively, that ISG proteins expressed under the stimulation were additional targets for ubiquitination.

4.2.3 Identification of ISG15 targets by the Clippomics approach

The Clippomics method employing the comparison of BpJOS- and Lbpro-generated triplicate data sets revealed the identification of several high confidence ISG15 modifications, of which a subset could be validated by external resources (chapter 3.2.3, Table 27). Additionally, five ISGylation sites were found to belong to proteins which, to my knowledge, have not yet been proclaimed as ISGylation targets (Table 28). These proteins include UBAP2L, YTHDF1/3, SNX2, MYOM2 and QRICH1. For all proteins, moderate RNA expression levels were reported in HEK cells according to data deposited on the Human Protein Atlas database (Thul & Lindskog, 2018). This instance strengthens the plausibility of the identified proteins being expressed in the given context and being *bona fide* targets of ISGylation. These results could be confirmed by additional orthogonal validation. One example would be the enrichment proposed ISGylation targets from cells undergoing microbial or viral infections to investigate the physiological relevance of the ISG15 modification. This approach would preclude the identified sites as technical artefacts and substantiate the validity of the Clippomics method.

State-of-the-art strategies on profiling the ISGylome while discerning ubiquitin sites often rely on ectopic (over) expression of ISG15 (Bhushan et al., 2020; Radoshevich et al., 2015; Yan et al., 2021) or the generation of ISG15 knock-out mice (Yifeng Zhang et al., 2019). Genetic manipulation can lead to the production of artifacts as overall protein expression levels might shift in response. Further, the generation and breeding of knock-out mice is costly, long-winded and requires a specific skillset not available to all labs.
Other approaches to specifically target ISGylation could include prior treatment with pan-DUB USP2 or USP21 (Hospenthal et al., 2015; Ye et al., 2011) to remove ubiquitination or COP9 signalosome (Lyapina et al., 2001; Pick et al., 2012) and NEDP1 (Mendoza et al., 2003; L. Shen et al., 2005) to remove neddylation as discussed in (Thery et al., 2021). However, residual modifications not caught by the treatment would yet again lead to false assignment of ubiquitin/Nedd8 sites to ISG15. This was demonstrated by prior results in this study, which employed two-fold approaches to remove unwanted modifiers, as most but not all modification was eradicated (see 3.2.2, 4.2.2).

The Clippomics method as applied in this experiment allows for the distinguishment of ubiquitin and ISG15 sites by in-lysate treatment of samples. The protocol negates the requirement for further samples processing for modifier disentanglement. This renders

it a suitable tool for the investigation of ISG15 targets in cells and tissues, potentially samples of patients suffering from viral infections. An ISG15-specifc clippase has not yet been identified but would further simply the process by omitting the comparison to BpJOS-generated GlyGly-sites. Current projects in the Hofmann lab address this search for ISG15-specific clippase with the prospect of uncovering such enzyme, potentially in a viral genome.

4.2.4 Interferon-dependent shifts in the ubiquitome identified by Clippomics

In order to investigate, which ubiquitin sites are up- or down-regulated upon IFNβ-treatment, the Clippomics approach using BpJOS was conducted on untreated and treated HEK blue cells. As a result, several ubiquitination sites have been identified, that were upregulated primarily on Interferon-stimulated genes (ISGs). Interferon treatment of cells simulates an infection condition as the production of Interferons and Interferon-stimulated genes is a defense response to viral infections (S.-Y. Liu et al., 2012).

In the proteomic samples, Nedd8 and Rab10 were highly downregulated in the IFNβ-treated samples compared to the untreated control (Figure 26B). Rab10 is reportedly able to diminish pro-inflammatory signaling and interferon production (Di Wang et al., 2010). In turn, Neddylation activates Cullin-Ring ligases and facilitates ubiquitination, which renders it a potential target of being hijacked by viruses. Suppression of neddylation was reported to negatively regulate viral replication as shown for Influenza A, Herpesviruses and Adenovirus (Han & Zhang, 2018; Sun et al., 2018). Possible interpretations of the downregulation of Rab10 and Nedd8 upon IFN could be that these aid the innate immune response under infection conditions to fight off viral infections and may be physiologically relevant in that context.

In line with the low abundance of Nedd8 in the proteomic sample, the GlyGly-enrichment reported GlyGly-modified Nedd8 as one of the top hits (Figure 26C). It is proposed that Nedd8 could be targeted to proteasomal degradation by ubiquitination to suppress virulence in infection conditions. Alternatively, these sites might derive from another Nedd8 moiety. BpJOS showed moderate activity against Nedd8 in previous experiments (Figure 17C, Figure 22). The production of tri-Nedd8 chains was reported under stress conditions and could be present in the given conditions (Keuss et al., 2019). A lack of detectable Nedd8 chains in Western blotting was observed in several experiments testing Nedd8 abundance in HEK blue cells (untreated/IFNβ-treated; Figure 17D, Figure 22). However, it cannot be excluded that Nedd8-chain levels were too low for antibody-detection but prevalent enough to be measured via MS.

The lower amount of GlyGly-sites detected in the IFN-treated group as visible in the volcano plot raised the question whether it may be based on a technical artefact or does indeed have physiological relevance (Figure 26C). Only 122 exclusive

GlyGly-sites were detected in the IFN-treated samples, which may provide a technical reason for this finding. Western blot analysis of samples used for GlyGly-enrichment showed a moderately lower presence in IFNβ-treated samples when clipped with BpJOS (Figure 26A), which could underline a technical issue. However, increased ubiquitination of ISGs under IFNβ-treatment may potentially lead to lower ubiquitination of non-ISGs in simulated infection conditions. This hypothesis could be tested by producing multiple replicates of the experiments and potentially by employing a different cell line.

Upregulated ubiquitination was primarily observed for multiple IFN-stimulated gene (ISGs) proteins in IFN induced samples. This instance could be based on the choice of the cell line used. The IFN type I HEK blue reporter cells employed here might display enhanced expression of ISGs compared to physiologically more relevant models. These models would include virus-infected cells or tissue material of patients suffering from virus infections. Therefore, the investigation of shifts in the ubiquitome upon IFN treatment in cells serves as test model for the establishment of the methodology to use it in future studies under physiological contexts.

Hypothesizing that the ubiquitination of ISGs was a physiological effect, it may serve the purpose of regulating ISG activity. As viral infections demand an immediate cellular response, ISGs often may be short-lived and require a regulation to prevent extensive inflammation and tissue damage (Schneider et al., 2014; P. Wang et al., 2015; Yang & Li, 2020).
In this regard, it would be interesting to further identify ubiquitination substrates of putative ISG ubiquitin E3 ligases such as DTX3L, which was found be ubiquitinated itself in the present study (Table 30). Beyond DTX3L, other interferon-stimulated E3 ligases were identified in the data sets including TRIM25 and TRIM28. These ligases are upregulated upon IFN induction, from which arises the question which substrates these are targeting. All three ligases have been reported to mediate different processes during interferon presence (Hua et al., 2024; Nakasato et al., 2006; Yong Zhang et al., 2015). Interestingly, TRIM25 is capable of substrate modification with either ubiquitin or ISG15 (Nakasato et al., 2006). This finding renders it an interesting target for the Clippomics approach. Upon testing with BpJOS only or BpJOS and Lbpro, as for the identification of ISG15 targets (3.2.3) one could decipher in which contexts which modifier is used for ligation.

Across all Clippomics studies presented here, the number of identified sites was lower compared to other published studies using the GlyGly-enrichment kit by Cell Signaling Technologies. Detected sites ranged from a few hundred GlyGly-sites (chapter 3.2.2) to a maximum of 1604 GlyGly-sites (chapter 3.2.4). Early, published studies reported around 370 ubiquitinated sites in HEK293 cells (G. Xu et al., 2010). More recent studies report around 11.000 ubiquitin sites (Wagner et al., 2011), 19.000 sites (W. Kim et al., 2011) or even 23.000 sites (van der Wal et al., 2018). Notably, some of these studies do not discern between ubiquitin and ISG15/Nedd8 sites.

In the last years, major advances were made by the development of advanced mass spectrometry techniques, such as data-independent acquisition (DIA) and parallel reaction monitoring (PRM). Different methods were employed for harvesting an increasing amount of ubiquitination sites: some studies used SILAC labeling, some treated tested cells priorly with proteasome inhibitor MG-132 and the protein input varied, if disclosed. Some studies employed 20mg of protein input compared to the 2mg used in the present study. Furthermore, some studies use peptide fractionation prior to the GlyGly-enrichment (van der Wal et al., 2018) or prior to MS measurement (Hansen et al., 2021; Ordureau et al., 2015). Taken together, the employed methodology to study ubiquitination sites varies highly and in accordance, the number of identified sites varies as well.
The Clippomics methods presented here serve as methodological bases, which can be further improved by increasing the protein input, incorporation of more advanced MS techniques compared to those used here or additional fractionation. Further, current studies aim to expand the identification from ubiquitin sites on lysine residues onto other ubiquitinated targets, such as modifications at serine or threonine residues or ubiquitination of sugars and other biomolecules. For that end, it would be beneficial to replace the GlyGly(K)-targeting IP Kit (Cell Signaling Technologies) with a more suitable enrichment method. As an alternative, biochemical labeling of newly clippase-generated amino termini at glycine residues is currently being tested. This novel labeling method is based on the specific targeting of the newly introduced amino termini with a small peptide handle fused to Biotin, which can be enriched from the samples by IP. The studies are ongoing in the Hofmann lab but showed first, promising results.
Moreover, GlyGly-sites generated by the linear specific PcJOS clippase could be enriched by utilizing a specific antibody directed against the GG-M-motif, which was published in Davies et al., 2021. By that, potentially new targets of the LUBAC complex, which are decorated with linear chains upon immune signaling, could be identified.

Overall, the Clippomics method was established to decipher ISGylation targets in complex samples (3.2.3) or targeting ubiquitin events in presence of ISG15 without risk of modifier conflation (3.2.4). These render the method a universal tool with prospect to employ it in physiological relevant specimens in the future.

4.3 Ubi clipping with BpJOS

The quantification or stoichiometric analysis of site-specific ubiquitin occupancy and prevalence of ubiquitin chain types remains a hurdle for studies of the ubiquitome. The dynamics of the ubiquitin modification, varying ubiquitination turn-over rates and the production of different modified and unmodified peptides by Trypsin digestion are only few of these challenges.
In recent years few studies have addressed this challenge. These studies are mostly based on SILAC labeling of proteins or IBAQ-labeling of peptides followed by the enrichment of trypsin-generation of GlyGly-remnants (Hristova et al., 2020) or in combination with chemical modifications (Y. Li et al., 2019) and spinking-in of an internal standard for MS measurement (Prus et al., 2024). These procedures are complex, costly and disregard the modifier conflation of ubiquitin, Nedd8 and ISG15 when digesting with Trypsin.

In order to provide a simpler method for the semi-quantitative analysis of ubiquitin chain modifications, the ‘Ubi clipping with BpJOS’ method was presented. The first test using di-ubiquitin chains clipped with BpJOS and digested with GluC or AspN harbored similar intensities for the unmodified and GlyGly-modified peptides (chapter 3.3.1). These results indicated a feasible estimation of ubiquitin modifications. Despite the successful efforts in low complexity samples, it failed to be applicable to more intricate ubiquitin chain architectures when tested on chains generated by NleL E705A (chapter 3.3.2). The calculation for ubiquitin modifications was further complicated by the production of peptides with one or two missed cleavage sites by GluC digestion. On top of that, generated peptides behaved differently in the mass spectrometer independent of the GlyGly-modification as the unmodified K48-peptide (GIPPDQQRLIFAGK(48)QLE) was detected with lower intensities compared the unmodified K63 or K6 peptide throughout experiments (chapters 3.3.2, 3.3.3). Despite not aiming for the comparison of different sites with each other, this instance is worth noting. The use of a spiked-in internal standard for MS measurement could help with the quantification, even those detected with lower intensities.

However, ‘Ubi clipping with BpJOS’ allowed for the identification of generated ubiquitin chain types without claiming for absolute quantification. By using the method, it was confirmed that the bacterial E3 ligase NleL E705A mainly produces K6-linked ubiquitin chains. Further, when used on chains generated by PARKIN, it was elucidated that the E3 ligase *en block*-ubiquitinated present chains via several linkages (K6/11/48/63). Besides these linkages, it was shown that PARKIN produced K6/K11-branched chains on an inner-chain ubiquitin moiety as displayed by peptides simultaneously GlyGly-modified at the Met N-terminus, K6(GG) and/or K11 (GG). These results demonstrated that BpJOS is a powerful tool in dissecting ubiquitin chain architecture.

Notably, the identification of branched chains by the ‘Ubi clipping’ method presented here was only applicable to ubiquitin modifications at K6 and K11 as these lysine residues reside on the same peptide generated by GluC (see Figure 27A). Branched modifications at K27, K29 and K33 could theoretically be identified by the method but

have not been observed in the experiments given. As K48 and K63 are present on different peptides separated by GluC digestion, branched chains could not be identified with used experimental conditions. Use of an alternative digestion enzyme preserving K48 and K63 on one peptide would presumably render it too long for efficient MS measurement.

Hypothetically, the ‘Ubi clipping with BpJOS’ method could be improved by swapping the GluC-based bottom-up proteomics approach by a top-down approach: BpJOS clipping would convert ubiquitin chains into single moieties carrying GlyGly-remnants at one or multiple sites. This could be followed up with intact mass analysis. Thereby, single moieties could be identified as single or multiply modified. Subsequently, these moieties could separately be converted into peptide fragments by fragmentation for MS2, which would allow for site-identification.
The initial ‘Ub-clipping’ method using Lbpro* published by Swatek et al. employs TUBE-enrichment of ubiquitin chains and subsequent intact mass analysis. Further, they used quantitative AQUA MS of Lbpro*-clipped and Trypsin-digested monoubiquitin moieties (Swatek et al., 2019). Using these methods, they demonstrated that 4-7% of TUBE-pulled ubiquitin chains from HCTT16 whole cell lysates were present as branched chains. By coupling the TUBE-pulldown to AQUA MS, they investigated *in vitro* generated chains by PARKIN. Similar to the results presented in the given study, PARKIN was found to build K6, K11, K48 and K63-linked ubiquitin chains. Furthermore, it was found that PARKIN generated branched chains as measured by intact mass. As analysis by intact mass alone does not allow for site-specific identification of branching, it could not be determined which branched linkage types were produced by PARKIN (Swatek et al., 2019). This strengthens the applicability of ‘Ubi clipping with BpJOS’ on the identification of ubiquitin branches at the N-terminal internal ubiquitin lysine residues.

The versatility of BpJOS in the elucidation of ubiquitin substrates or chain types was recently acknowledged by two emerging applications. One group used BpJOS to investigate the ubiquitin chain types and production of branched chains by the Varicella Zoster Virus encoded E3 ligase ORF16 (Puri et al., 2026). Intriguingly, the Komander lab was able to identify ubiquitination of glycogen and other biomolecules employing BpJOS in a non-protein Ub-clipping approach termed ‘NoPro-clipping’ (yet unpublished). These studies solidify BpJOS as a potent instrument in unraveling the copious ubiquitin substrates and intricate ubiquitin chain architectures.

Despite several limitations to the ‘Ubi clipping with BpJOS’ method, one application could be addressed which is not easily met by current strategies. Hybrid chains such as SUMOylated ubiquitin or ubiquitinated SUMO moieties predominantly occur upon different stressor and are associated to DNA damage responses and proteasomal degradation (Guzzo & Matunis, 2013; Hendriks et al., 2014; Hendriks et al., 2017). Trypsin digestion for the investigation of hybrid chains generates the GlyGly-remnant for ubiquitin. In contrast, human SUMO paralogs have a threonine preceding the

C-terminal GlyGly-sequence and no other tryptic cleavage sites near the C terminus (Lumpkin et al., 2017). Trypsin digestion would harbor the following C-terminal SUMO peptide: FDGQPINETDTPAQLEMEDEDTIDVFQQQTGG-K(modified)-X.
This renders the peptide presumably too long for efficient flight properties in the mass spectrometer. Studies often rely on manipulation by mutations of the SUMO C-terminus to make it more amenable to trypsin-based cleavage (Blomster et al., 2010; Knuesel et al., 2005; Lumpkin et al., 2017).
'Ubi clipping with BpJOS' could be employed to discern SUMO-Ub chains from Ub-SUMO chains. BpJOS does not target SUMOylation (data not shown). If a hybrid chain is clipped with BpJOS, GlyGly-remnants are generated only by the initial ubiquitin modification. As SUMO contains several glutamic acids residues within its C-terminus, digestion with GluC would produce the C-terminal SUMO peptide DTIDVFQQQTGG-K-X. Digestion with AspN would even generate a shorter peptide with DVFQQQTGG-K at the initial modification sites. This would allow for the disentanglement of whether ubiquitin was SUMOylated or SUMO was ubiquitinated at a lysine residue.

Taken together, the gathered results in this and other studies exemplify BpJOS as a powerful incentive in the studies of the ubiquitome. BpJOS can be utilized as a Swiss knife in various contexts and samples to dissect novel ubiquitin substrates and harbors the potential to be employed on branched and hybrid ubiquitin chains.

5 Appendix

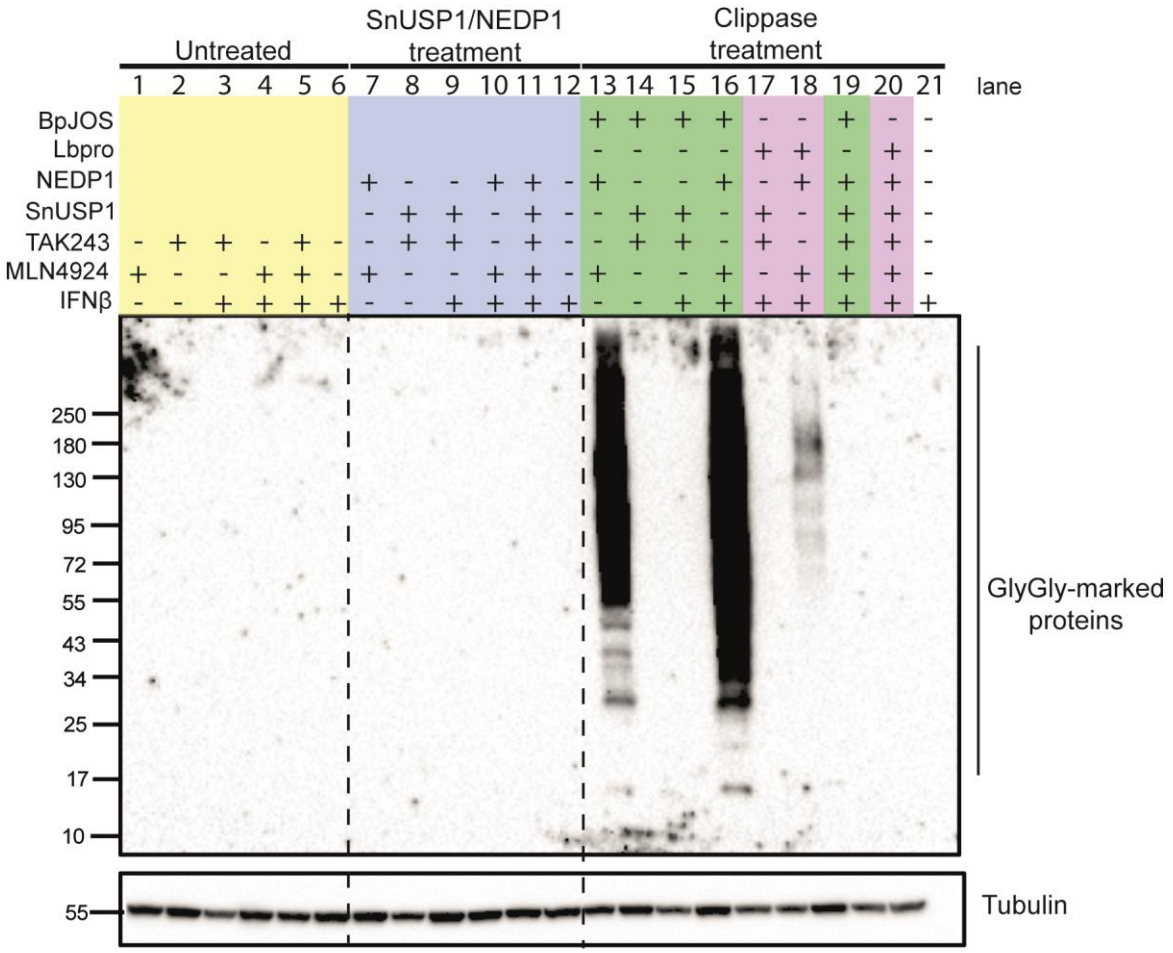

Figure 30: Western blot analysis of samples used for the proof-of-concept Clippomics test. Samples were taken after each step of the protocol and assessed for presence of GlyGly(K)-remnants monitored with α-K-ε-GG antibody. Tubulin was detected as a loading control. Sample treatments are indicated with a plus (+) symbol above the figure. Treatment with ubiquitin E1-inhibitor TAK243, Nedd8 E1-inhibitor MLN4924 and Interferonβ (IFNβ) was conducted *in cellulo.* Samples taken after cell lysis are highlighted in the yellow box. E1-inhibitor treatment for ubiquitin and neddylation reduction was complemented with SnUSP1 and NEDP1 treatment (each 10µM, 1h) and is highlighted by the blue box. Duplicate samples (lanes 9, 10, 11) were divided for BpJOS or Lbpro treatment (9→ 15/17, 10→ 16/18, 11→19/20). BpJOS$^{12-218}$ (10µM) and Lbpro$^{29-195}$ (40µM) purified proteins were incubated for 2.5h on ice. BpJOS-treated lanes are given in green; samples treated with Lbpro are given in purple. Samples tested in lanes 13-21 were subsequently subjected to GlyGly-enrichment and MS analysis.

Table 31: Selected top 20 hits of GlyGly-sites shared among samples 4 (assumed to only harbor ubiquitin sites in presence of ISGylation;+IFN, +MLN4924/NEDP1) **and sample 1** (assumed to only harbor ubiquitin sites in absence of ISGylation; -IFN, +MLN4924/NEDP1). Multiple positions correspond to positions in isoforms. The GlyGly-sites are given in order of decreasing intensity.

Positions within proteins	Protein names	Gene names
48;50	Ubiquitin-40S ribosomal protein S27a	RPS27A; UBB
8	40S ribosomal protein S20	RPS20
121	Histone H2B type	HIST1H2B
148	Spermatogenesis-associated protein 17	SPATA17
4	40S ribosomal protein S20	RPS20
113	Ubiquitin-40S ribosomal protein S27a	RPS27A
138;149	40S ribosomal protein S10	RPS10
507;510	Heat shock cognate 71 kDa protein	HSPA8
9	14-3-3 protein beta/alpha	YWHAB
2307	Nesprin-2	SYNE2
72;119	T-complex protein 1 subunit beta	CCT6A
117	Histone H2B type 1	HIST1H2BJ
9; 11	14-3-3 protein beta/alpha/zeta/delta	YWHAZ
60; 63	Zinc finger protein 516	ZNF516
92	Ubiquitin-conjugating enzyme E2 N	UBE2N
524;469;524	Heat shock 70 kDa protein 1A	HSPA1A
214;230	40S ribosomal protein S3	RPS3
119	Histone H2A type 1	HIST1H2AJ
1363;1408;1426;1460;1493	BCL-6 corepressor-like protein 1	BCORL1
34	Proteasomal ubiquitin receptor ADRM1	ADRM1

Table 32: List of all 24 GlyGly-sites proposed to stem from residual ubiquitination and not from BpJOS targeted ISGylation. Sites derived from the comparison of proposed ISG15-only data sets and ubiquitin only data sets in absence or presence of ISG15 (Samples 8 vs 4 + Samples 8 vs 1). The sites are given in alphabetical order by protein name. Listed positions correspond to positions in isoforms.

Positions within proteins	Protein names	Gene names
9	14-3-3 protein zeta/delta	YWHAZ
138;149	40S ribosomal protein S10	RPS10
4	40S ribosomal protein S20	RPS20
8	40S ribosomal protein S20	RPS20
214;230	40S ribosomal protein S3	RPS3
52;51	60S ribosomal protein L11	RPL11
93	60S ribosomal protein L24	RPL24
1363;1408;1426;1460;1493	BCL-6 corepressor-like protein 1	BCORL1
71	Heat shock 70 kDa protein 1A	HSPA1A
524;469;524	Heat shock 70 kDa protein 1A	HSPA1A
119	Histone H2A type 1/3	HIST1H2AC
121	Histone H2B type 1-J	HIST1H2BO
251;307	Melanoma-associated antigen D1	MAGED1
309;335;537	Neutral amino acid transporter B(0)	SLC1A5
56;127	Proteasome subunit alpha type-4	PSMA4
206;191	Pyruvate kinase PKM	PKM
148	Spermatogenesis-associated protein 17	SPATA17
182;275	T-complex protein 1 subunit epsilon	CCT5
5;5	T-complex protein 1 subunit zeta	CCT8
315	Transmembrane protein 59	TMEM59
48	Ubiquitin-40S ribosomal protein S27a	RPS27A;UBB
92	Ubiquitin-conjugating enzyme E2 N	UBE2N
83;83	UBX domain-containing protein 1	UBXN7
99	UBX domain-containing protein 7	UBXN7

Table 33: All high confidence ISG15 sites identified by Clippomics. Listed are all 19 GlyGly-sites of ISGylated proteins in the high confidence category. These sites were identified in all three Lbpro-generated data sets, but in BpJOS-generated data sets. Listed positions correspond to positions in isoforms.

Positions within proteins	Proteins	Gene names
413;420	Ubiquitin-associated protein 2-like	UBAP2L
240;244	YTH domain-containing family protein 1	YTHDF1
389;468	Probable ATP-dependent RNA helicase DDX17	DDX17
915;926	Regulator of nonsense transcripts 1	UPF1
399;440	Interferon-induced, double-stranded RNA-activated protein kinase	EIF2AK2
48;79	Cytosol aminopeptidase	LAP3
84;206;84	Heat shock protein HSP 90-alpha	HSP90AA1
447;479;556 ;603;643;650	Eukaryotic translation initiation factor 4 gamma 1	EIF4G1
435	Bifunctional glutamate/proline--tRNA ligase	EPRS1
58;180;58	Heat shock protein HSP 90-alpha	HSP90AA1
594	Elongation factor 2	EEF2
131;248	Sorting nexin-2	SNX2
11	Myomesin-2	MYOM2
246	Transcriptional regulator QRICH1	QRICH1
38;38;71	Caspase-7	CASP7
185	Coiled-coil domain-containing protein 124	CCDC124
117;167	ATP synthase subunit alpha, mitochondrial	ATP5F1A
219;219	Protein-L-isoaspartate(D-aspartate) O-methyltransferase	PCMT1
426;669;671	Protein PRRC2C	PRRC2C

6 List of abbreviations

°C	Degree celsius
a.U.	Arbitrary Units
APS	Ammonium persulfate
AspN	Aspartic acid-specific protease N-terminal
ATG	Autophagy-related protein
ATP	Adenosintriphosphate
BcJOS	Josephin-like from *Burkholderia catarinensis*
BpJOS	Josephin-like from *Burkholderia pyrrocinia*
C18	Octadecyl functional group
CAA	Chloroacetic acid
CsJOS	Josephin-like enzyme from *Chlamdiales bacterium STE3*
PvJOS	Josephin-like enzyme from *Pseudovibrio*
DNA	Deoxyribonucleic acid
dNTP	Deoxyribonucleotide triphosphate
DTT	Dithiothreitol
DUB	Deubiquitinase
ECL	Enhanced chemiluminescence
f.c.	Final concentration
FA	Formic acid
FAT10	Human leukocyte antigen F locus adjacent transcript 10
FBS	Fetal bovine serum
fwd	Forward
GluC	Glutamic/ aspartic acid specific protease C-terminal
GlyGly	Glycine glycine
HeJOS	Josephin-like enzyme from *Herbasprillium*
HEK	human embryonic kidney
HRP	horseradish peroxidase
IFNβ	Interferon-beta
IP	Immune precipitation

ISG	Interferon-stimulated gene
kb	Kilo base pairs
KCl	Potassium chloride
KH_2PO_4	Potassium dihydrogen phosphate
l	Liter
LC-MS/MS	Liquid chromatography-tandem mass spectrometry
Lysarginase	Lysine/ arginine specific protease
LysC	Lysyl endopeptidase
min	Minutes
MJD	Machado-Joseph disease protease
ms	Milli seconds
Na_2HPO_4	Disodium hydrogen phosphate
NaCl	Sodium chloride
NAE	Nedd8-activating enzyme
PA	Propargylamide
PaJOS	Josephin-like enzyme from *Pigmentiphaga aceris*
PBS	Phosphate buffer saline
PcJOS	Josephin-like enzyme from *Parachlamydia*
PCR	Polymerase chain reaction
PEI	Polyethylenimine
PVDF	Polyvinylidene fluoride
RBR	RING-between-RING
RCR	RING-Cys-Relay
rev	Reverse
RING	Really-interesting-new-gene
rpm	Rotations per minute
s	Seconds
SDM	Site-directed mutagenesis
SDS-PAGE	Sodium dodecyl sulphate – polyacrylamide gel electrophoresis
STUbL	SUMO-targeted ubiquitin ligase
SUMO	Small ubiquitin-like modifier

TEAB	Triethylammonium bicarbonate
TEMED	Tetramethylethylenediamine
TFA	Trifluoroacetic acid
Tris	Tris(hydroxymethyl)aminomethan
UAE	Ubiquitin-activating enzyme
Ub	Ubiquitin
UBD	Ubiquitin-binding domain
Ubl	Ubiquitin-like protein
UCH	Ubiquitin C-terminal hydrolase
UFM1	Ubiquitin-fold modifier 1
UIM	Ubiquitin-interacting motif
UPS	Ubiquitin proteasome system
USP	Ubiquitin-specific protease
WT	wild type

7 List of figures

8 List of tables

9 References

Abdul Rehman, S. A., Kristariyanto, Y. A., Choi, S.-Y., Nkosi, P. J., Weidlich, S., Labib, K., Hofmann, K., & Kulathu, Y. (2016). Mindy-1 Is a Member of an Evolutionarily Conserved and Structurally Distinct New Family of Deubiquitinating Enzymes. *Molecular Cell*, *63*(1), 146–155. https://doi.org/10.1016/j.molcel.2016.05.009

Agrotis, A., Pengo, N., Burden, J. J., & Ketteler, R. (2019). Redundancy of human ATG4 protease isoforms in autophagy and LC3/GABARAP processing revealed in cells. *Autophagy*, *15*(6), 976–997. https://doi.org/10.1080/15548627.2019.1569925

Akimov, V., Barrio-Hernandez, I., Hansen, S. V. F., Hallenborg, P., Pedersen, A.-K., Bekker-Jensen, D. B., Puglia, M., Christensen, S. D. K., Vanselow, J. T., Nielsen, M. M., Kratchmarova, I., Kelstrup, C. D., Olsen, J. V., & Blagoev, B. (2018). Ubisite approach for comprehensive mapping of lysine and N-terminal ubiquitination sites. *Nature Structural & Molecular Biology*, *25*(7), 631–640. https://doi.org/10.1038/s41594-018-0084-y

Akimov, V., Henningsen, J., Hallenborg, P., Rigbolt, K. T. G., Jensen, S. S., Nielsen, M. M., Kratchmarova, I., & Blagoev, B. (2014). Stubex: Stable tagged ubiquitin exchange system for the global investigation of cellular ubiquitination. *Journal of Proteome Research*, *13*(9), 4192–4204. https://doi.org/10.1021/pr500549h

Akimov, V., Rigbolt, K. T. G., Nielsen, M. M., & Blagoev, B. (2011). Characterization of ubiquitination dependent dynamics in growth factor receptor signaling by quantitative proteomics. *Molecular BioSystems*, *7*(12), 3223–3233. https://doi.org/10.1039/c1mb05185g

Amann, R., Springer, N., Schönhuber, W., Ludwig, W., Schmid, E. N., Müller, K. D., & Michel, R. (1997). Obligate intracellular bacterial parasites of acanthamoebae related to Chlamydia spp. *Applied and Environmental Microbiology*, *63*(1), 115–121. https://doi.org/10.1128/aem.63.1.115-121.1997

Arroyo-Gomez, J., Murray, M. J., Guérillon, C., Wang, J [Juanjuan], Isaakova, E., Reverón-Gómez, N., Koutrouli, M., Suryo Rahmanto, A., Mitrofanov, K., Ingham, A., Schovsbo, S., Weischenfeldt, K., Coscia, F., Typas, D., Völker-Albert, M., Solis, V., Jensen, L. J [Lars Juhl], Groth, A., Mund, A., . . . Mailand, N. (2025). Functional landscape of ubiquitin linkages couples K29-linked ubiquitylation to epigenome integrity. *The EMBO Journal*, *44*(23), 6944–6978. https://doi.org/10.1038/s44318-025-00599-7

Bachmair, A [A.], Finley, D [D.], & Varshavsky, A. (1986). In vivo half-life of a protein is a function of its amino-terminal residue. *Science (New York, N.Y.)*, *234*(4773), 179–186. https://doi.org/10.1126/science.3018930

Barriere, H., Nemes, C., Du, K., & Lukacs, G. L. (2007). Plasticity of polyubiquitin recognition as lysosomal targeting signals by the endosomal sorting machinery. *Molecular Biology of the Cell*, *18*(10), 3952–3965. https://doi.org/10.1091/mbc.E07-07-0678

Beal, R., Deveraux, Q., Xia, G., Rechsteiner, M., & Pickart, C. (1996). Surface hydrophobic residues of multiubiquitin chains essential for proteolytic targeting. *Proceedings of the National Academy of Sciences of the United States of America*, *93*(2), 861–866. https://doi.org/10.1073/pnas.93.2.861

Bergink, S., Salomons, F. A., Hoogstraten, D., Groothuis, T. A. M., Waard, H. de, Wu, J., Yuan, L., Citterio, E., Houtsmuller, A. B., Neefjes, J., Hoeijmakers, J. H. J., Vermeulen, W., & Dantuma, N. P. (2006). Dna damage triggers nucleotide excision repair-dependent monoubiquitylation of histone H2A. *Genes & Development*, *20*(10), 1343–1352. https://doi.org/10.1101/gad.373706

Beyer, S. R., Mallmann, R. T., Jaenecke, I., Habermeier, A., Boissel, J.-P., & Closs, E. I. (2013). Identification of cysteine residues in human cationic amino acid transporter hCAT-2A that are targets for inhibition by N-ethylmaleimide. *The Journal of Biological Chemistry*, *288*(42), 30411–30419. https://doi.org/10.1074/jbc.M113.490698

Bhushan, J., Radke, J. B., Perng, Y.-C., Mcallaster, M., Lenschow, D. J., Virgin, H. W., & Sibley, L. D. (2020). Isg15 Connects Autophagy and IFN-γ-Dependent Control of Toxoplasma gondii Infection in Human Cells. *MBio*, *11*(5). https://doi.org/10.1128/mBio.00852-20

Birgisdottir, Å. B., Lamark, T., & Johansen, T. (2013). The LIR motif - crucial for selective autophagy. *Journal of Cell Science*, *126*(Pt 15), 3237–3247. https://doi.org/10.1242/jcs.126128

Blomster, H. A., Imanishi, S. Y., Siimes, J., Kastu, J., Morrice, N. A., Eriksson, J. E., & Sistonen, L. (2010). In vivo identification of sumoylation sites by a signature tag and cysteine-targeted affinity purification. *The Journal of Biological Chemistry*, *285*(25), 19324–19329. https://doi.org/10.1074/jbc.M110.106955

Boll, V., Hermanns, T., Uthoff, M., Erven, I., Hörner, E.-M., Kozjak-Pavlovic, V., Baumann, U., & Hofmann, K. (2023). Functional and structural diversity in deubiquitinases of the Chlamydia-like bacterium Simkania negevensis. *Nature Communications*, *14*(1), 7335. https://doi.org/10.1038/s41467-023-43144-y

Borodovsky, A., Ovaa, H., Kolli, N., Gan-Erdene, T., Wilkinson, K. D., Ploegh, H. L., & Kessler, B. M. (2002). Chemistry-based functional proteomics reveals novel members of the deubiquitinating enzyme family. *Chemistry & Biology*, *9*(10), 1149–1159. https://doi.org/10.1016/S1074-5521(02)00248-X

Boudier-Lemosquet, A., Mahler, A., Bobo, C., Dufossée, M., & Priault, M. (2022). Introducing protein deamidation: Landmark discoveries, societal outreach, and tentative priming workflow to address deamidation. *Methods*, *200*, 3–14. https://doi.org/10.1016/j.ymeth.2021.11.012

Boughton, A. J., Krueger, S., & Fushman, D. (2020). Branching via K11 and K48 Bestows Ubiquitin Chains with a Unique Interdomain Interface and Enhanced Affinity for Proteasomal Subunit Rpn1. *Structure (London, England : 1993)*, *28*(1), 29-43.e6. https://doi.org/10.1016/j.str.2019.10.008

Boussif, O., Lezoualc'h, F., Zanta, M. A., Mergny, M. D., Scherman, D., Demeneix, B., & Behr, J. P. (1995). A versatile vector for gene and oligonucleotide transfer

into cells in culture and in vivo: Polyethylenimine. *Proceedings of the National Academy of Sciences of the United States of America*, *92*(16), 7297–7301. https://doi.org/10.1073/pnas.92.16.7297

Brownell, J. E., Sintchak, M. D., Gavin, J. M., Liao, H., Bruzzese, F. J., Bump, N. J., Soucy, T. A., Milhollen, M. A., Yang, X., Burkhardt, A. L., Ma, J., Loke, H.-K., Lingaraj, T., Wu, D., Hamman, K. B., Spelman, J. J., Cullis, C. A., Langston, S. P., Vyskocil, S., . . . Dick, L. R. (2010). Substrate-assisted inhibition of ubiquitin-like protein-activating enzymes: The NEDD8 E1 inhibitor MLN4924 forms a NEDD8-AMP mimetic in situ. *Molecular Cell*, *37*(1), 102–111. https://doi.org/10.1016/j.molcel.2009.12.024

Burkhart, J. M., Schumbrutzki, C., Wortelkamp, S., Sickmann, A., & Zahedi, R. P. (2012). Systematic and quantitative comparison of digest efficiency and specificity reveals the impact of trypsin quality on MS-based proteomics. *Journal of Proteomics*, *75*(4), 1454–1462. https://doi.org/10.1016/j.jprot.2011.11.016

Cao, J., & Yan, Q [Qin] (2012). Histone ubiquitination and deubiquitination in transcription, DNA damage response, and cancer. *Frontiers in Oncology*, *2*, 26. https://doi.org/10.3389/fonc.2012.00026

Cappadocia, L., & Lima, C. D. (2018). Ubiquitin-like Protein Conjugation: Structures, Chemistry, and Mechanism. *Chemical Reviews*, *118*(3), 889–918. https://doi.org/10.1021/acs.chemrev.6b00737

Castañeda, C. A., Dixon, E. K., Walker, O., Chaturvedi, A., Nakasone, M. A., Curtis, J. E., Reed, M. R., Krueger, S., Cropp, T. A., & Fushman, D. (2016). Linkage via K27 Bestows Ubiquitin Chains with Unique Properties among Polyubiquitins. *Structure (London, England : 1993)*, *24*(3), 423–436. https://doi.org/10.1016/j.str.2016.01.007

Cesare, V. de, Carbajo Lopez, D., Mabbitt, P. D., Fletcher, A. J., Soetens, M., Antico, O., Wood, N. T., & Virdee, S. (2021). Deubiquitinating enzyme amino acid profiling reveals a class of ubiquitin esterases. *Proceedings of the National Academy of Sciences of the United States of America*, *118*(4), e2006947118. https://doi.org/10.1073/pnas.2006947118

Chan, Y., Yoon, J., Wu, J.-T., Kim, H.-J., Pan, K.-T., Yim, J., & Chien, C.-T. (2008). Den1 deneddylates non-cullin proteins in vivo. *Journal of Cell Science*, *121*(Pt 19), 3218–3223. https://doi.org/10.1242/jcs.030445

Chang, Y.-Y., Stévenin, V., Duchateau, M., Giai Gianetto, Q., Hourdel, V., Rodrigues, C. D., Matondo, M., Reiling, N., & Enninga, J. (2020). Shigella hijacks the exocyst to cluster macropinosomes for efficient vacuolar escape. *PLoS Pathogens*, *16*(8), e1008822. https://doi.org/10.1371/journal.ppat.1008822

Chau, V., Tobias, J. W., Bachmair, A [A.], Marriott, D., Ecker, D. J., Gonda, D. K., & Varshavsky, A. (1989). A multiubiquitin chain is confined to specific lysine in a targeted short-lived protein. *Science (New York, N.Y.)*, *243*(4898), 1576–1583. https://doi.org/10.1126/science.2538923

Chaugule, V. K., Burchell, L., Barber, K. R., Sidhu, A., Leslie, S. J., Shaw, G. S., & Walden, H. (2011). Autoregulation of Parkin activity through its ubiquitin-like domain. *The EMBO Journal*, *30*(14), 2853–2867. https://doi.org/10.1038/emboj.2011.204

Ciechanover, A., Finley, D [D.], & Varshavsky, A. (1984). Ubiquitin dependence of selective protein degradation demonstrated in the mammalian cell cycle mutant ts85. *Cell*, *37*(1), 57–66. https://doi.org/10.1016/0092-8674(84)90300-3

Ciechanover, A., Heller, H., Elias, S., Haas, A. L., & Hershko, A. (1980). Atp-dependent conjugation of reticulocyte proteins with the polypeptide required for protein degradation. *Proceedings of the National Academy of Sciences of the United States of America*, *77*(3), 1365–1368. https://doi.org/10.1073/pnas.77.3.1365

Ciechanover, A., & Schwartz, A. L. (1998). The ubiquitin-proteasome pathway: The complexity and myriad functions of proteins death. *Proceedings of the National Academy of Sciences of the United States of America*, *95*(6), 2727–2730. https://doi.org/10.1073/pnas.95.6.2727

Ciehanover, A., Hod, Y., & Hershko, A. (1978). A heat-stable polypeptide component of an ATP-dependent proteolytic system from reticulocytes. *Biochemical and Biophysical Research Communications*, *81*(4), 1100–1105. https://doi.org/10.1016/0006-291X(78)91249-4

Clague, M. J., Heride, C., & Urbé, S. (2015). The demographics of the ubiquitin system. *Trends in Cell Biology*, *25*(7), 417–426. https://doi.org/10.1016/j.tcb.2015.03.002

Compton, S. J., & Jones, C. G. (1985). Mechanism of dye response and interference in the Bradford protein assay. *Analytical Biochemistry*, *151*(2), 369–374. https://doi.org/10.1016/0003-2697(85)90190-3

Corsaro, D., & Greub, G. (2006). Pathogenic potential of novel Chlamydiae and diagnostic approaches to infections due to these obligate intracellular bacteria. *Clinical Microbiology Reviews*, *19*(2), 283–297. https://doi.org/10.1128/CMR.19.2.283-297.2006

Cox, J., & Mann, M. (2008). Maxquant enables high peptide identification rates, individualized p.P.B.-range mass accuracies and proteome-wide protein quantification. *Nature Biotechnology*, *26*(12), 1367–1372. https://doi.org/10.1038/nbt.1511

Crow, A., Hughes, R. K., Taieb, F., Oswald, E., & Banfield, M. J. (2012). The molecular basis of ubiquitin-like protein NEDD8 deamidation by the bacterial effector protein Cif. *Proceedings of the National Academy of Sciences of the United States of America*, *109*(27), E1830-8. https://doi.org/10.1073/pnas.1112107109

Cui, J., Yao, Q., Li, S [Shan], Ding, X., Lu, Q., Mao, H., Liu, L [Liping], Zheng, N., Chen, S., & Shao, F. (2010). Glutamine deamidation and dysfunction of ubiquitin/NEDD8 induced by a bacterial effector family. *Science (New York, N.Y.)*, *329*(5996), 1215–1218. https://doi.org/10.1126/science.1193844

Danielsen, J. M. R., Sylvestersen, K. B., Bekker-Jensen, S., Szklarczyk, D., Poulsen, J. W., Horn, H., Jensen, L. J [Lars J.], Mailand, N., & Nielsen, M. L. (2011). Mass spectrometric analysis of lysine ubiquitylation reveals promiscuity at site level. *Molecular & Cellular Proteomics*, *10*(3), M110.003590. https://doi.org/10.1074/mcp.M110.003590

Davies, C. W., Vidal, S. E., Phu, L., Sudhamsu, J., Hinkle, T. B., Chan Rosenberg, S., Schumacher, F.-R., Zeng, Y. J., Schwerdtfeger, C., Peterson, A. S., Lill, J. R., Rose, C. M., Shaw, A. S., Wertz, I. E., Kirkpatrick, D. S., & Koerber, J. T. (2021). Antibody toolkit reveals N-terminally ubiquitinated substrates of UBE2W. *Nature Communications*, *12*(1), 4608. https://doi.org/10.1038/s41467-021-24669-6

Deng, L., Wang, C [C.], Spencer, E., Yang, L., Braun, A., You, J., Slaughter, C., Pickart, C., & Chen, Z. J. (2000). Activation of the IkappaB kinase complex by TRAF6 requires a dimeric ubiquitin-conjugating enzyme complex and a unique polyubiquitin chain. *Cell*, *103*(2), 351–361. https://doi.org/10.1016/S0092-8674(00)00126-4

Deretic, V., Saitoh, T., & Akira, S. (2013). Autophagy in infection, inflammation and immunity. *Nature Reviews. Immunology*, *13*(10), 722–737. https://doi.org/10.1038/nri3532

Di Wang, Lou, J., Ouyang, C., Chen, W., Liu, Y., Liu, X [Xinyuan], Cao, X., Wang, J [Jianli], & Lu, L [Linrong] (2010). Ras-related protein Rab10 facilitates TLR4 signaling by promoting replenishment of TLR4 onto the plasma membrane. *Proceedings of the National Academy of Sciences of the United States of America*, *107*(31), 13806–13811. https://doi.org/10.1073/pnas.1009428107

Dongré, A. R., Jones, J. L., Somogyi, Á., & Wysocki, V. H. (1996). Influence of Peptide Composition, Gas-Phase Basicity, and Chemical Modification on Fragmentation Efficiency: Evidence for the Mobile Proton Model. *Journal of the American Chemical Society*, *118*(35), 8365–8374. https://doi.org/10.1021/ja9542193

Dos Santos, P. F., & Mansur, D. S. (2017). Beyond ISGlylation: Functions of Free Intracellular and Extracellular ISG15. *Journal of Interferon & Cytokine Research : The Official Journal of the International Society for Interferon and Cytokine Research*, *37*(6), 246–253. https://doi.org/10.1089/jir.2016.0103

Drapeau, G. R. (1976) [21] Cleavage at glutamic acid with staphylococcal protease. In *Methods in Enzymology : Part B: Proteolytic Enzymes* (Vol. 47, pp. 189–191). Academic Press. https://doi.org/10.1016/0076-6879(77)47023-X

Duda, D. M., Scott, D. C., Calabrese, M. F., Zimmerman, E. S., Zheng, N., & Schulman, B. A. (2011). Structural regulation of cullin-RING ubiquitin ligase complexes. *Current Opinion in Structural Biology*, *21*(2), 257–264. https://doi.org/10.1016/j.sbi.2011.01.003

Durcan, T. M., Kontogiannea, M., Bedard, N., Wing, S. S., & Fon, E. A. (2012). Ataxin-3 deubiquitination is coupled to Parkin ubiquitination via E2 ubiquitin-conjugating enzyme. *The Journal of Biological Chemistry*, *287*(1), 531–541. https://doi.org/10.1074/jbc.M111.288449

Durfee, L. A., & Huibregtse, J. M. (2010). Identification and Validation of ISG15 Target Proteins. *Sub-Cellular Biochemistry*, *54*, 228–237. https://doi.org/10.1007/978-1-4419-6676-6_18

Durfee, L. A., & Huibregtse, J. M. (2012). The ISG15 conjugation system. *Methods in Molecular Biology (Clifton, N.J.)*, *832*, 141–149. https://doi.org/10.1007/978-1-61779-474-2_9

Durfee, L. A., Lyon, N., Seo, K., & Huibregtse, J. M. (2010). The ISG15 conjugation system broadly targets newly synthesized proteins: Implications for the antiviral function of ISG15. *Molecular Cell*, *38*(5), 722–732. https://doi.org/10.1016/j.molcel.2010.05.002

Dzimianski, J. V., Scholte, F. E. M., Bergeron, É., & Pegan, S. D. (2019). Isg15: It's Complicated. *Journal of Molecular Biology*, *431*(21), 4203–4216. https://doi.org/10.1016/j.jmb.2019.03.013

Ebadi, P., Stratton, C. M., & Olsen, S. K. (2025). E3 ubiquitin ligases in signaling, disease, and therapeutics. *Trends in Biochemical Sciences*, *50*(11), 960–976. https://doi.org/10.1016/j.tibs.2025.07.009

Elliott, P. R [Paul R.], Leske, D., Hrdinka, M., Bagola, K., Fiil, B. K [Berthe K.], McLaughlin, S. H., Wagstaff, J., Volkmar, N., Christianson, J. C., Kessler, B. M., Freund, S. M. V., Komander, D., & Gyrd-Hansen, M. (2016). Spata2 Links CYLD to LUBAC, Activates CYLD, and Controls LUBAC Signaling. *Molecular Cell*, *63*(6), 990–1005. https://doi.org/10.1016/j.molcel.2016.08.001

Emmerich, C. H., Ordureau, A., Strickson, S., Arthur, J. S. C., Pedrioli, P. G. A., Komander, D., & Cohen, P. (2013). Activation of the canonical IKK complex by K63/M1-linked hybrid ubiquitin chains. *Proceedings of the National Academy of Sciences of the United States of America*, *110*(38), 15247–15252. https://doi.org/10.1073/pnas.1314715110

Enchev, R. I., Schulman, B. A., & Peter, M. (2015). Protein neddylation: Beyond cullin-RING ligases. *Nature Reviews. Molecular Cell Biology*, *16*(1), 30–44. https://doi.org/10.1038/nrm3919

Erven, I., Abraham, E., Hermanns, T., Baumann, U., & Hofmann, K. (2022). A widely distributed family of eukaryotic and bacterial deubiquitinases related to herpesviral large tegument proteins. *Nature Communications*, *13*(1), 7643. https://doi.org/10.1038/s41467-022-35244-y

Fan, J.-B., Miyauchi-Ishida, S., Arimoto, K., Liu, D., Yan, M., Liu, C.-W., Győrffy, B., & Zhang, D.-E. (2015). Type I IFN induces protein ISGylation to enhance cytokine expression and augments colonic inflammation. *Proceedings of the National Academy of Sciences of the United States of America*, *112*(46), 14313–14318. https://doi.org/10.1073/pnas.1505690112

Feldman, R. M., Correll, C. C., Kaplan, K. B., & Deshaies, R. J [R. J.] (1997). A complex of Cdc4p, Skp1p, and Cdc53p/cullin catalyzes ubiquitination of the phosphorylated CDK inhibitor Sic1p. *Cell*, *91*(2), 221–230. https://doi.org/10.1016/s0092-8674(00)80404-3

Fels, U., Willems, P., Meyer, M. de, Gevaert, K., & van Damme, P. (2023). Shift in vacuolar to cytosolic regime of infecting Salmonella from a dual proteome perspective. *PLoS Pathogens*, *19*(8), e1011183. https://doi.org/10.1371/journal.ppat.1011183

Finley, D [D.], Bartel, B., & Varshavsky, A. (1989). The tails of ubiquitin precursors are ribosomal proteins whose fusion to ubiquitin facilitates ribosome biogenesis. *Nature*, *338*(6214), 394–401. https://doi.org/10.1038/338394a0

Finley, D [D.], Ciechanover, A., & Varshavsky, A. (1984). Thermolability of ubiquitin-activating enzyme from the mammalian cell cycle mutant ts85. *Cell*, *37*(1), 43–55. https://doi.org/10.1016/0092-8674(84)90299-x

Franklin, T. G., Brzovic, P. S., & Pruneda, J. N. (2023). Bacterial ligases reveal fundamental principles of polyubiquitin specificity. *Molecular Cell*, *83*(24), 4538-4554.e4. https://doi.org/10.1016/j.molcel.2023.11.017

Fu, H., Subramanian, R. R., & Masters, S. C. (2000). 14-3-3 proteins: Structure, function, and regulation. *Annual Review of Pharmacology and Toxicology*, *40*, 617–647. https://doi.org/10.1146/annurev.pharmtox.40.1.617

Fuseya, Y., Fujita, H., Kim, M., Ohtake, F., Nishide, A., Sasaki, K., Saeki, Y., Tanaka, K., Takahashi, R., & Iwai, K. (2020). The HOIL-1L ligase modulates immune signalling and cell death via monoubiquitination of LUBAC. *Nature Cell Biology*, *22*(6), 663–673. https://doi.org/10.1038/s41556-020-0517-9

Ganesan, M., Poluektova, L. Y., Tuma, D. J., Kharbanda, K. K., & Osna, N. A. (2016). Acetaldehyde Disrupts Interferon Alpha Signaling in Hepatitis C Virus-Infected Liver Cells by Up-Regulating USP18. *Alcoholism, Clinical and Experimental Research*, *40*(11), 2329–2338. https://doi.org/10.1111/acer.13226

Garzia, A., Jafarnejad, S. M., Meyer, C., Chapat, C., Gogakos, T., Morozov, P., Amiri, M., Shapiro, M., Molina, H., Tuschl, T., & Sonenberg, N. (2017). The E3 ubiquitin ligase and RNA-binding protein ZNF598 orchestrates ribosome quality control of premature polyadenylated mRNAs. *Nature Communications*, *8*(1), 16056. https://doi.org/10.1038/ncomms16056

Goebl, M. G., Yochem, J., Jentsch, S [S.], McGrath, J. P., Varshavsky, A., & Byers, B. (1988). The yeast cell cycle gene CDC34 encodes a ubiquitin-conjugating enzyme. *Science (New York, N.Y.)*, *241*(4871), 1331–1335. https://doi.org/10.1126/science.2842867

Goel, S., Oliva, R., Jeganathan, S., Bader, V., Krause, L. J., Kriegler, S., Stender, I. D., Christine, C. W., Nakamura, K., Hoffmann, J.-E., Winter, R., Tatzelt, J., & Winklhofer, K. F. (2023). Linear ubiquitination induces NEMO phase separation to activate NF-κB signaling. *Life Science Alliance*, *6*(4). https://doi.org/10.26508/lsa.202201607

Goldknopf, I. L., & Busch, H. (1977). Isopeptide linkage between nonhistone and histone 2A polypeptides of chromosomal conjugate-protein A24. *Proceedings of the National Academy of Sciences of the United States of America*, *74*(3), 864–868. https://doi.org/10.1073/pnas.74.3.864

Goldstein, G., Scheid, M., Hammerling, U., Schlesinger, D. H., Niall, H. D., & Boyse, E. A. (1975). Isolation of a polypeptide that has lymphocyte-

differentiating properties and is probably represented universally in living cells. *Proceedings of the National Academy of Sciences of the United States of America*, *72*(1), 11–15. https://doi.org/10.1073/pnas.72.1.11

Grasty, K. C., Weeks, S. D., & Loll, P. J. (2019). Structural insights into the activity and regulation of human Josephin-2. *Journal of Structural Biology: X*, *3*, 100011. https://doi.org/10.1016/j.yjsbx.2019.100011

Green, M. R., & Sambrook, J. (2012). *Molecular cloning: A laboratory manual* (4th ed.). Cold Spring Harbor Laboratory Press.

Greub, G., Boyadjiev, I., La Scola, B., Raoult, D., & Martin, C. (2003). Serological hint suggesting that Parachlamydiaceae are agents of pneumonia in polytraumatized intensive care patients. *Annals of the New York Academy of Sciences*, *990*(1), 311–319. https://doi.org/10.1111/j.1749-6632.2003.tb07381.x

Greub, G., Mege, J.-L., & Raoult, D. (2003). Parachlamydia acanthamoebae enters and multiplies within human macrophages and induces their apoptosis corrected. *Infection and Immunity*, *71*(10), 5979–5985. https://doi.org/10.1128/IAI.71.10.5979-5985.2003

Greub, G., & Raoult, D. (2002). Parachlamydiaceae: Potential emerging pathogens. *Emerging Infectious Diseases*, *8*(6), 625–630. https://doi.org/10.3201/eid0806.010210

Grice, G. L., & Nathan, J. A. (2016). The recognition of ubiquitinated proteins by the proteasome. *Cellular and Molecular Life Sciences : CMLS*, *73*(18), 3497–3506. https://doi.org/10.1007/s00018-016-2255-5

Guzzo, C. M., & Matunis, M. J [Michael J.] (2013). Expanding SUMO and ubiquitin-mediated signaling through hybrid SUMO-ubiquitin chains and their receptors. *Cell Cycle*, *12*(7), 1015–1017. https://doi.org/10.4161/cc.24332

Haas, A. L., & Rose, I. A. (1982). The mechanism of ubiquitin activating enzyme. A kinetic and equilibrium analysis. *Journal of Biological Chemistry*, *257*(17), 10329–10337. https://pubmed.ncbi.nlm.nih.gov/6286650/

Haglund, K., Sigismund, S., Polo, S., Szymkiewicz, I., Di Fiore, P. P., & Dikic, I. (2003). Multiple monoubiquitination of RTKs is sufficient for their endocytosis and degradation. *Nature Cell Biology*, *5*(5), 461–466. https://doi.org/10.1038/ncb983

Han, K., & Zhang, J [Jiyan] (2018). Roles of neddylation against viral infections. *Cellular & Molecular Immunology*, *15*(3), 292–294. https://doi.org/10.1038/cmi.2017.100

Hanahan, D. (1983). Studies on transformation of Escherichia coli with plasmids. *Journal of Molecular Biology*, *166*(4), 557–580. https://doi.org/10.1016/S0022-2836(83)80284-8

Hansen, F. M., Tanzer, M. C., Brüning, F., Bludau, I., Stafford, C., Schulman, B. A., Robles, M. S., Karayel, O., & Mann, M. (2021). Data-independent acquisition method for ubiquitinome analysis reveals regulation of circadian biology. *Nature Communications*, *12*(1), 254. https://doi.org/10.1038/s41467-020-20509-1

Hendriks, I. A., D'Souza, R. C. J., Yang, B., Verlaan-de Vries, M., Mann, M., & Vertegaal, A. C. O. (2014). Uncovering global SUMOylation signaling networks in a site-specific manner. *Nature Structural & Molecular Biology*, *21*(10), 927–936. https://doi.org/10.1038/nsmb.2890

Hendriks, I. A., Lyon, D., Young, C., Jensen, L. J [Lars J.], Vertegaal, A. C. O., & Nielsen, M. L. (2017). Site-specific mapping of the human SUMO proteome reveals co-modification with phosphorylation. *Nature Structural & Molecular Biology*, *24*(3), 325–336. https://doi.org/10.1038/nsmb.3366

Hermanns, T., & Hofmann, K. (2019). Bacterial DUBs: Deubiquitination beyond the seven classes. *Biochemical Society Transactions*, *47*(6), 1857–1866. https://doi.org/10.1042/BST20190526

Hermanns, T., & Hofmann, K. (2023). Bioinformatical Approaches to the Discovery and Classification of Novel Deubiquitinases. *Methods in Molecular Biology (Clifton, N.J.)*, *2591*, 135–149. https://doi.org/10.1007/978-1-0716-2803-4_9

Hermanns, T., Kolek, S., Uthoff, M., Heiden, R. A. de, Mulder, M. P. C., Baumann, U., & Hofmann, K. (2025). A family of bacterial Josephin-like deubiquitinases with an irreversible cleavage mode. *Molecular Cell*, *85*(6), 1202-1215.e5. https://doi.org/10.1016/j.molcel.2025.02.002

Hermanns, T., Pichlo, C., Baumann, U., & Hofmann, K. (2022). A structural basis for the diverse linkage specificities within the ZUFSP deubiquitinase family. *Nature Communications*, *13*(1), 401. https://doi.org/10.1038/s41467-022-28049-6

Hermanns, T., Pichlo, C., Woiwode, I., Klopffleisch, K., Witting, K. F., Ovaa, H., Baumann, U., & Hofmann, K. (2018). A family of unconventional deubiquitinases with modular chain specificity determinants. *Nature Communications*, *9*(1), 799. https://doi.org/10.1038/s41467-018-03148-5

Hermanns, T., Woiwode, I., Guerreiro, R. F., Vogt, R., Lammers, M., & Hofmann, K. (2020). An evolutionary approach to systematic discovery of novel deubiquitinases, applied to Legionella. *Life Science Alliance*, *3*(9). https://doi.org/10.26508/lsa.202000838

Hershko, A., & Heller, H. (1985). Occurrence of a polyubiquitin structure in ubiquitin-protein conjugates. *Biochemical and Biophysical Research Communications*, *128*(3), 1079–1086. https://doi.org/10.1016/0006-291X(85)91050-2

Hershko, A., Heller, H., Elias, S., & Ciechanover, A. (1983). Components of ubiquitin-protein ligase system. Resolution, affinity purification, and role in protein breakdown. *Journal of Biological Chemistry*, *258*(13), 8206–8214. https://pubmed.ncbi.nlm.nih.gov/6305978/

Hertzog, P., Forster, S., & Samarajiwa, S. (2011). Systems biology of interferon responses. *Journal of Interferon & Cytokine Research : The Official Journal of the International Society for Interferon and Cytokine Research*, *31*(1), 5–11. https://doi.org/10.1089/jir.2010.0126

Hipp, M. S., Kalveram, B., Raasi, S [Shahri], Groettrup, M [Marcus], & Schmidtke, G [Gunter] (2005). Fat10, a ubiquitin-independent signal for proteasomal

degradation. *Molecular and Cellular Biology*, *25*(9), 3483–3491. https://doi.org/10.1128/MCB.25.9.3483-3491.2005

Hochstrasser, M [M.], & Varshavsky, A. (1990). In vivo degradation of a transcriptional regulator: The yeast alpha 2 repressor. *Cell*, *61*(4), 697–708. https://doi.org/10.1016/0092-8674(90)90481-S

Hoege, C., Pfander, B., Moldovan, G.-L., Pyrowolakis, G., & Jentsch, S [Stefan] (2002). Rad6-dependent DNA repair is linked to modification of PCNA by ubiquitin and SUMO. *Nature*, *419*(6903), 135–141. https://doi.org/10.1038/nature00991

Hornbeck, P. V., Zhang, B., Murray, B., Kornhauser, J. M., Latham, V., & Skrzypek, E. (2015). Phosphositeplus, 2014: Mutations, PTMs and recalibrations. *Nucleic Acids Research*, *43*(Database issue), D512-20. https://doi.org/10.1093/nar/gku1267

Hospenthal, M. K [Manuela K.], Mevissen, T. E. T., & Komander, D. (2015). Deubiquitinase-based analysis of ubiquitin chain architecture using Ubiquitin Chain Restriction (UbiCRest). *Nature Protocols*, *10*(2), 349–361. https://doi.org/10.1038/nprot.2015.018

Hristova, V., Sun, S., Zhang, H., & Chan, D. W. (2020). Proteomic analysis of degradation ubiquitin signaling by ubiquitin occupancy changes responding to 26S proteasome inhibition. *Clinical Proteomics*, *17*, 2. https://doi.org/10.1186/s12014-020-9265-x

Hu, W., Chan, H., Lu, L [Lan], Wong, K. T., Wong, S. H., Li, M. X., Xiao, Z. G., Cho, C. H., Gin, T., Chan, M. T. V., Wu, W. K. K., & Zhang, L [Lin] (2020). Autophagy in intracellular bacterial infection. *Seminars in Cell & Developmental Biology*, *101*, 41–50. https://doi.org/10.1016/j.semcdb.2019.07.014

Hua, F., Nass, T., & Parvatiyar, K. (2024). Trim28 facilitates type I interferon activation by targeting TBK1. *Frontiers in Immunology*, *15*, 1279920. https://doi.org/10.3389/fimmu.2024.1279920

Huang, D. T., Ayrault, O., Hunt, H. W., Taherbhoy, A. M., Duda, D. M., Scott, D. C., Borg, L. A., Neale, G., Murray, P. J., Roussel, M. F., & Schulman, B. A. (2009). E2-RING expansion of the NEDD8 cascade confers specificity to cullin modification. *Molecular Cell*, *33*(4), 483–495. https://doi.org/10.1016/j.molcel.2009.01.011

Huang, D. T., & Schulman, B. A. (2005). Expression, purification, and characterization of the E1 for human NEDD8, the heterodimeric APPBP1-UBA3 complex. *Methods in Enzymology*, *398*, 9–20. https://doi.org/10.1016/S0076-6879(05)98002-6

Huang, H., Jeon, M.-S., Liao, L., Yang, C., Elly, C., Yates, J. R., & Liu, Y.-C. (2010). K33-linked polyubiquitination of T cell receptor-zeta regulates proteolysis-independent T cell signaling. *Immunity*, *33*(1), 60–70. https://doi.org/10.1016/j.immuni.2010.07.002

Huang, L., Kinnucan, E., Wang, G., Beaudenon, S., Howley, P. M., Huibregtse, J. M., & Pavletich, N. P. (1999, November 12). Structure of an E6AP-UbcH7

Complex: Insights into Ubiquitination by the E2-E3 Enzyme Cascade. *American Association for the Advancement of Science*. https://www.science.org/doi/10.1126/science.286.5443.1321

Hudáky, P., Kaslik, G., Venekei, I., & Gráf, L. (1999). The differential specificity of chymotrypsin A and B is determined by amino acid 226. *European Journal of Biochemistry*, *259*(1-2), 528–533. https://doi.org/10.1046/j.1432-1327.1999.00075.x

Huen, M. S. Y., Grant, R., Manke, I., Minn, K., Yu, X., Yaffe, M. B., & Chen, J [Junjie] (2007). Rnf8 transduces the DNA-damage signal via histone ubiquitylation and checkpoint protein assembly. *Cell*, *131*(5), 901–914. https://doi.org/10.1016/j.cell.2007.09.041

Huett, A., Heath, R. J., Begun, J., Sassi, S. O., Baxt, L. A., Vyas, J. M., Goldberg, M. B., & Xavier, R. J. (2012). The LRR and RING domain protein LRSAM1 is an E3 ligase crucial for ubiquitin-dependent autophagy of intracellular Salmonella Typhimurium. *Cell Host & Microbe*, *12*(6), 778–790. https://doi.org/10.1016/j.chom.2012.10.019

Hunt, L. T., & Dayhoff, M. O. (1977). Amino-terminal sequence identity of ubiquitin and the nonhistone component of nuclear protein A24. *Biochemical and Biophysical Research Communications*, *74*(2), 650–655. https://doi.org/10.1016/0006-291X(77)90352-7

Husnjak, K., Elsasser, S., Zhang, N [Naixia], Chen, X., Randles, L., Shi, Y., Hofmann, K., Walters, K. J., Finley, D [Daniel], & Dikic, I. (2008). Proteasome subunit Rpn13 is a novel ubiquitin receptor. *Nature*, *453*(7194), 481–488. https://doi.org/10.1038/nature06926

Hutagalung, A. H., & Novick, P. J. (2011). Role of Rab GTPases in membrane traffic and cell physiology. *Physiological Reviews*, *91*(1), 119–149. https://doi.org/10.1152/physrev.00059.2009

Hyer, M. L., Milhollen, M. A., Ciavarri, J., Fleming, P., Traore, T., Sappal, D., Huck, J., Shi, J., Gavin, J., Brownell, J., Yang, Y [Yu], Stringer, B., Griffin, R., Bruzzese, F., Soucy, T., Duffy, J., Rabino, C., Riceberg, J., Hoar, K., . . . Bence, N. F. (2018). A small-molecule inhibitor of the ubiquitin activating enzyme for cancer treatment. *Nature Medicine*, *24*(2), 186–193. https://doi.org/10.1038/nm.4474

Ichimura, Y., Kirisako, T [T.], Takao, T., Satomi, Y., Shimonishi, Y., Ishihara, N., Mizushima, N., Tanida, I., Kominami, E., Ohsumi, M., Noda, T., & Ohsumi, Y. (2000). A ubiquitin-like system mediates protein lipidation. *Nature*, *408*(6811), 488–492. https://doi.org/10.1038/35044114

Ingrosso, D., Fowler, A. V., Bleibaum, J., & Clarke, S. (1989). Specificity of endoproteinase Asp-N (Pseudomonas fragi): Cleavage at glutamyl residues in two proteins. *Biochemical and Biophysical Research Communications*, *162*(3), 1528–1534. https://doi.org/10.1016/0006-291X(89)90848-6

Jentsch, S [S.], McGrath, J. P., & Varshavsky, A. (1987). The yeast DNA repair gene RAD6 encodes a ubiquitin-conjugating enzyme. *Nature*, *329*(6135), 131–134. https://doi.org/10.1038/329131a0

Jin, L., Williamson, A., Banerjee, S., Philipp, I., & Rape, M. (2008). Mechanism of ubiquitin-chain formation by the human anaphase-promoting complex. *Cell*, *133*(4), 653–665. https://doi.org/10.1016/j.cell.2008.04.012

Jones, J., Wu, K., Yang, Y [Yingying], Guerrero, C., Nillegoda, N., Pan, Z.-Q., & Huang, L. (2008). A targeted proteomic analysis of the ubiquitin-like modifier nedd8 and associated proteins. *Journal of Proteome Research*, *7*(3), 1274–1287. https://doi.org/10.1021/pr700749v

Jong, M. F. de, Liu, Z., Chen, D., & Alto, N. M. (2016). Shigella flexneri suppresses NF-κB activation by inhibiting linear ubiquitin chain ligation. *Nature Microbiology*, *1*(7), 16084. https://doi.org/10.1038/nmicrobiol.2016.84

Kaiser, S. E., Riley, B. E., Shaler, T. A., Trevino, R. S., Becker, C. H., Schulman, H., & Kopito, R. R. (2011). Protein standard absolute quantification (PSAQ) method for the measurement of cellular ubiquitin pools. *Nature Methods*, *8*(8), 691–696. https://doi.org/10.1038/nmeth.1649

Kamadurai, H. B., Qiu, Y., Deng, A., Harrison, J. S., Macdonald, C., Actis, M., Rodrigues, P., Miller, D. J., Souphron, J., Lewis, S. M., Kurinov, I., Fujii, N., Hammel, M., Piper, R., Kuhlman, B., & Schulman, B. A. (2013, August 8). Mechanism of ubiquitin ligation and lysine prioritization by a HECT E3. *ELife Sciences Publications, Ltd*. https://elifesciences.org/articles/00828

Kamadurai, H. B., Souphron, J., Scott, D. C., Duda, D. M., Miller, D. J., Stringer, D., Piper, R. C., & Schulman, B. A. (2009). Insights into ubiquitin transfer cascades from a structure of a UbcH5B approximately ubiquitin-HECT(NEDD4L) complex. *Molecular Cell*, *36*(6), 1095–1102. https://doi.org/10.1016/j.molcel.2009.11.010

Kamitani, T., Kito, K., Nguyen, H. P., & Yeh, E. T. (1997). Characterization of NEDD8, a developmentally down-regulated ubiquitin-like protein. *Journal of Biological Chemistry*, *272*(45), 28557–28562. https://doi.org/10.1074/jbc.272.45.28557

Kamura, T., Conrad, M. N., Yan, Q [Q.], Conaway, R. C [R. C.], & Conaway, J. W [J. W.] (1999). The Rbx1 subunit of SCF and VHL E3 ubiquitin ligase activates Rub1 modification of cullins Cdc53 and Cul2. *Genes & Development*, *13*(22), 2928–2933. https://doi.org/10.1101/gad.13.22.2928

Kang, J. an, Kim, Y. J [Yoon Jung], & Jeon, Y. J. (2022). The diverse repertoire of ISG15: More intricate than initially thought. *Experimental & Molecular Medicine*, *54*(11), 1779–1792. https://doi.org/10.1038/s12276-022-00872-3

Kelsall, I. R. (2022). Non-lysine ubiquitylation: Doing things differently. *Frontiers in Molecular Biosciences*, *9*, 1008175. https://doi.org/10.3389/fmolb.2022.1008175

Kelsall, I. R., McCrory, E. H., Xu, Y [Yingqi], Scudamore, C. L., Nanda, S. K., Mancebo-Gamella, P., Wood, N. T., Knebel, A., Matthews, S. J., & Cohen, P. (2022). Hoil-1 ubiquitin ligase activity targets unbranched glucosaccharides and is required to prevent polyglucosan accumulation. *The EMBO Journal*, *41*(8), e109700. https://doi.org/10.15252/embj.2021109700

Kelsall, I. R., Zhang, J [Jiazhen], Knebel, A., Arthur, J. S. C., & Cohen, P. (2019). The E3 ligase HOIL-1 catalyses ester bond formation between ubiquitin and

components of the Myddosome in mammalian cells. *Proceedings of the National Academy of Sciences of the United States of America*, *116*(27), 13293–13298. https://doi.org/10.1073/pnas.1905873116

Keusekotten, K., Elliott, P. R [Paul Ronald], Glockner, L., Fiil, B. K [Berthe Katrine], Damgaard, R. B., Kulathu, Y., Wauer, T., Hospenthal, M. K [Manuela Kathrin], Gyrd-Hansen, M., Krappmann, D., Hofmann, K., & Komander, D. (2013). Otulin antagonizes LUBAC signaling by specifically hydrolyzing Met1-linked polyubiquitin. *Cell*, *153*(6), 1312–1326. https://doi.org/10.1016/j.cell.2013.05.014

Keuss, M. J., Hjerpe, R., Hsia, O., Gourlay, R., Burchmore, R., Trost, M., & Kurz, T. (2019). Unanchored tri-NEDD8 inhibits PARP-1 to protect from oxidative stress-induced cell death. *The EMBO Journal*, *38*(6), EMBJ2018100024. https://doi.org/10.15252/embj.2018100024

Kim, J., Guermah, M., McGinty, R. K., Lee, J.-S., Tang, Z., Milne, T. A., Shilatifard, A., Muir, T. W., & Roeder, R. G. (2009). Rad6-Mediated transcription-coupled H2B ubiquitylation directly stimulates H3K4 methylation in human cells. *Cell*, *137*(3), 459–471. https://doi.org/10.1016/j.cell.2009.02.027

Kim, W., Bennett, E. J., Huttlin, E. L., Guo, A., Li, J [Jing], Possemato, A., Sowa, M. E., Rad, R., Rush, J., Comb, M. J., Harper, J. W [J. Wade], & Gygi, S. P. (2011). Systematic and quantitative assessment of the ubiquitin-modified proteome. *Molecular Cell*, *44*(2), 325–340. https://doi.org/10.1016/j.molcel.2011.08.025

Kim, Y. J [Ye Ji], Kim, E. T., Kim, Y.-E., Lee, M. K., Kwon, K. M., Kim, K. I., Stamminger, T., & Ahn, J.-H. (2016). Consecutive Inhibition of ISG15 Expression and ISGylation by Cytomegalovirus Regulators. *PLOS Pathogens*, *12*(8), e1005850. https://doi.org/10.1371/journal.ppat.1005850

Kirisako, T [Takayoshi], Kamei, K., Murata, S., Kato, M., Fukumoto, H., Kanie, M., Sano, S., Tokunaga, F., Tanaka, K., & Iwai, K. (2006). A ubiquitin ligase complex assembles linear polyubiquitin chains. *The EMBO Journal*, *25*(20), 4877–4887. https://doi.org/10.1038/sj.emboj.7601360

Kisselev, A. F., Akopian, T. N., Castillo, V., & Goldberg, A. L [A. L.] (1999). Proteasome active sites allosterically regulate each other, suggesting a cyclical bite-chew mechanism for protein breakdown. *Molecular Cell*, *4*(3), 395–402. https://doi.org/10.1016/S1097-2765(00)80341-X

Kliza, K., Taumer, C., Pinzuti, I., Franz-Wachtel, M., Kunzelmann, S., Stieglitz, B., Macek, B., & Husnjak, K. (2017). Internally tagged ubiquitin: A tool to identify linear polyubiquitin-modified proteins by mass spectrometry. *Nature Methods*, *14*(5), 504–512. https://doi.org/10.1038/nmeth.4228

Knuesel, M., Cheung, H. T., Hamady, M., Barthel, K. K. B., & Liu, X [Xuedong] (2005). A method of mapping protein sumoylation sites by mass spectrometry using a modified small ubiquitin-like modifier 1 (SUMO-1) and a computational program. *Molecular & Cellular Proteomics*, *4*(10), 1626–1636. https://doi.org/10.1074/mcp.T500011-MCP200

Kolek, S. (2021). *Analysis of cleavage properties of bacterial ATX3-like clippases.: Master thesis*.

Komander, D., Clague, M. J., & Urbé, S. (2009). Breaking the chains: Structure and function of the deubiquitinases. *Nature Reviews Molecular Cell Biology*, *10*(8), 550–563. https://doi.org/10.1038/nrm2731

Komander, D., Lord, C. J., Scheel, H., Swift, S., Hofmann, K., Ashworth, A., & Barford, D. (2008). The structure of the CYLD USP domain explains its specificity for Lys63-linked polyubiquitin and reveals a B box module. *Molecular Cell*, *29*(4), 451–464. https://doi.org/10.1016/j.molcel.2007.12.018

Komander, D., & Rape, M. (2012). The ubiquitin code. *Annual Review of Biochemistry*, *81*(Volume 81, 2012), 203–229. https://doi.org/10.1146/annurev-biochem-060310-170328

Komatsu, M., Inada, T., & Noda, N. N. (2024). The UFM1 system: Working principles, cellular functions, and pathophysiology. *Molecular Cell*, *84*(1), 156–169. https://doi.org/10.1016/j.molcel.2023.11.034

Kondapalli, C., Kazlauskaite, A., Zhang, N [Ning], Woodroof, H. I., Campbell, D. G., Gourlay, R., Burchell, L., Walden, H., Macartney, T. J., Deak, M., Knebel, A., Alessi, D. R., & Muqit, M. M. K. (2012). Pink1 is activated by mitochondrial membrane potential depolarization and stimulates Parkin E3 ligase activity by phosphorylating Serine 65. *Open Biology*, *2*(5), 120080. https://doi.org/10.1098/rsob.120080

Kortebi, M., Milohanic, E., Mitchell, G., Péchoux, C., Prevost, M.-C., Cossart, P., & Bierne, H. (2017). Listeria monocytogenes switches from dissemination to persistence by adopting a vacuolar lifestyle in epithelial cells. *PLoS Pathogens*, *13*(11), e1006734. https://doi.org/10.1371/journal.ppat.1006734

Lauwers, E., Jacob, C., & André, B. (2009). K63-linked ubiquitin chains as a specific signal for protein sorting into the multivesicular body pathway. *Journal of Cell Biology*, *185*(3), 493–502. https://doi.org/10.1083/jcb.200810114

Le Negrate, G., Krieg, A., Faustin, B., Loeffler, M., Godzik, A., Krajewski, S., & Reed, J. C. (2008). Chladub1 of Chlamydia trachomatis suppresses NF-kappaB activation and inhibits IkappaBalpha ubiquitination and degradation. *Cellular Microbiology*, *10*(9), 1879–1892. https://doi.org/10.1111/j.1462-5822.2008.01178.x

Lenschow, D. J., Giannakopoulos, N. V., Gunn, L. J., Johnston, C., O'Guin, A. K., Schmidt, R. E., Levine, B., & Virgin, H. W. (2005). Identification of interferon-stimulated gene 15 as an antiviral molecule during Sindbis virus infection in vivo. *Journal of Virology*, *79*(22), 13974–13983. https://doi.org/10.1128/JVI.79.22.13974-13983.2005

Levinger, L., & Varshavsky, A. (1980). High-resolution fractionation of nucleosomes: Minor particles, "whiskers," and separation of mononucleosomes containing and lacking A24 semihistone. *Proceedings of the National Academy of Sciences of the United States of America*, *77*(6), 3244–3248. https://doi.org/10.1073/pnas.77.6.3244

Li, J [Jie], Zou, J., Littlejohn, R., Liu, J [Jinbao], & Su, H. (2020). Neddylation, an Emerging Mechanism Regulating Cardiac Development and Function. *Frontiers in Physiology*, *11*, 612927. https://doi.org/10.3389/fphys.2020.612927

Li, Y., Evers, J., Luo, A., Erber, L., Postler, Z., & Chen, Y. (2019). A Quantitative Chemical Proteomics Approach for Site-specific Stoichiometry Analysis of Ubiquitination. *Angewandte Chemie International Edition*, *58*(2), 537–541. https://doi.org/10.1002/anie.201810569

Liang, Y.-C., Lee, C.-C., Yao, Y.-L., Lai, C.-C., Schmitz, M. L., & Yang, W.-M. (2016). Sumo5, a Novel Poly-SUMO Isoform, Regulates PML Nuclear Bodies. *Scientific Reports*, *6*, 26509. https://doi.org/10.1038/srep26509

Lin, D. Y., Diao, J., & Chen, J [Jue] (2012). Crystal structures of two bacterial HECT-like E3 ligases in complex with a human E2 reveal atomic details of pathogen-host interactions. *Proceedings of the National Academy of Sciences of the United States of America*, *109*(6), 1925–1930. https://doi.org/10.1073/pnas.1115025109

Liu, A., Zhang, P [Pengfei], Bai, B., Bai, F., Jin, T., & Ren, J. (2020). Volatile Organic Compounds of Endophytic Burkholderia pyrrocinia Strain JK-SH007 Promote Disease Resistance in Poplar. *Plant Disease*, *104*(6), 1610–1620. https://doi.org/10.1094/PDIS-11-19-2366-RE

Liu, S.-Y., Sanchez, D. J., Aliyari, R., Lu, S., & Cheng, G. (2012). Systematic identification of type I and type II interferon-induced antiviral factors. *Proceedings of the National Academy of Sciences of the United States of America*, *109*(11), 4239–4244. https://doi.org/10.1073/pnas.1114981109

Liu, Y. C., Pan, J., Zhang, C., Fan, W., Collinge, M., Bender, J. R., & Weissman, S. M. (1999). A MHC-encoded ubiquitin-like protein (FAT10) binds noncovalently to the spindle assembly checkpoint protein MAD2. *Proceedings of the National Academy of Sciences of the United States of America*, *96*(8), 4313–4318. https://doi.org/10.1073/pnas.96.8.4313

Lobato-Gil, S., Heidelberger, J. B., Maghames, C., Bailly, A., Brunello, L., Rodriguez, M. S., Beli, P., & Xirodimas, D. P. (2021). Proteome-wide identification of NEDD8 modification sites reveals distinct proteomes for canonical and atypical NEDDylation. *Cell Reports*, *34*(3), 108635. https://doi.org/10.1016/j.celrep.2020.108635

Lüders, J., Pyrowolakis, G., & Jentsch, S [Stefan] (2003). The ubiquitin-like protein HUB1 forms SDS-resistant complexes with cellular proteins in the absence of ATP. *EMBO Reports*, *4*(12), 1169–1174. https://doi.org/10.1038/sj.embor.7400025

Lumpkin, R. J., Gu, H., Zhu, Y [Yiying], Leonard, M., Ahmad, A. S., Clauser, K. R., Meyer, J. G., Bennett, E. J., & Komives, E. A. (2017). Site-specific identification and quantitation of endogenous SUMO modifications under native conditions. *Nature Communications*, *8*(1), 1171. https://doi.org/10.1038/s41467-017-01271-3

Lyapina, S., Cope, G., Shevchenko, A [Anna], Serino, G., Tsuge, T., Zhou, C., Wolf, D. A., Wei, N., Shevchenko, A [Andrej], & Deshaies, R. J [Raymond J.] (2001, May 3). Promotion of NEDD8-CUL1 Conjugate Cleavage by COP9 Signalosome. *American Association for the Advancement of Science*. https://www.science.org/doi/full/10.1126/science.1059780?casa_token=cGXim2UOU0sAAAAA%3Ac4bnDbYS44zxy-X41gaJNABbL0662_lz7vwK1Bf6xBA7-fpEgK2c5nDYMXsxBMWIQFnF6FHV-eO-oA

Ma, T., Keller, J. A., & Yu, X. (2011). Rnf8-dependent histone ubiquitination during DNA damage response and spermatogenesis. *Acta Biochimica Et Biophysica Sinica*, *43*(5), 339–345. https://doi.org/10.1093/abbs/gmr016

Mabbitt, P. D., Loreto, A., Déry, M.-A., Fletcher, A. J., Stanley, M., Pao, K.-C., Wood, N. T., Coleman, M. P., & Virdee, S. (2020). Structural basis for RING-Cys-Relay E3 ligase activity and its role in axon integrity. *Nature Chemical Biology*, *16*(11), 1227–1236. https://doi.org/10.1038/s41589-020-0598-6

Malakhov, M. P., Malakhova, O. A., Kim, K. I., Ritchie, K. J., & Zhang, D.-E. (2002). Ubp43 (USP18) specifically removes ISG15 from conjugated proteins. *Journal of Biological Chemistry*, *277*(12), 9976–9981. https://doi.org/10.1074/jbc.M109078200

Mao, Y., Senic-Matuglia, F., Di Fiore, P. P., Polo, S., Hodsdon, M. E., & Camilli, P. de (2005). Deubiquitinating function of ataxin-3: Insights from the solution structure of the Josephin domain. *Proceedings of the National Academy of Sciences of the United States of America*, *102*(36), 12700–12705. https://doi.org/10.1073/pnas.0506344102

Matic, I., van Hagen, M., Schimmel, J., Macek, B., Ogg, S. C., Tatham, M. H [Michael H.], Hay, R. T [Ronald T.], Lamond, A. I., Mann, M., & Vertegaal, A. C. O. (2008). In vivo identification of human small ubiquitin-like modifier polymerization sites by high accuracy mass spectrometry and an in vitro to in vivo strategy. *Molecular & Cellular Proteomics*, *7*(1), 132–144. https://doi.org/10.1074/mcp.M700173-MCP200

Matsumoto, M. L., Wickliffe, K. E., Dong, K. C., Yu, C., Bosanac, I., Bustos, D., Phu, L., Kirkpatrick, D. S., Hymowitz, S. G., Rape, M., Kelley, R. F., & Dixit, V. M. (2010). K11-linked polyubiquitination in cell cycle control revealed by a K11 linkage-specific antibody. *Molecular Cell*, *39*(3), 477–484. https://doi.org/10.1016/j.molcel.2010.07.001

Matunis, M. J [M. J.], Coutavas, E., & Blobel, G. (1996). A novel ubiquitin-like modification modulates the partitioning of the Ran-GTPase-activating protein RanGAP1 between the cytosol and the nuclear pore complex. *The Journal of Cell Biology*, *135*(6 Pt 1), 1457–1470. https://doi.org/10.1083/jcb.135.6.1457

McCrory, E. H., Akimov, V., Cohen, P., & Blagoev, B. (2022). Identification of ester-linked ubiquitylation sites during TLR7 signalling increases the number of inter-ubiquitin linkages from 8 to 12. *The Biochemical Journal*, *479*(23), 2419–2431. https://doi.org/10.1042/BCJ20220510

McCullough, J., Clague, M. J., & Urbé, S. (2004). Amsh is an endosome-associated ubiquitin isopeptidase. *Journal of Cell Biology*, *166*(4), 487–492. https://doi.org/10.1083/jcb.200401141

Mendoza, H. M., Shen, L., Botting, C., Lewis, A., Chen, J [Jingwen], Ink, B., & Hay, R. T [Ronald T.] (2003). Nedp1, a highly conserved cysteine protease that deNEDDylates Cullins. *The Journal of Biological Chemistry*, *278*(28), 25637–25643. https://doi.org/10.1074/jbc.M212948200

Meszka, I., Polanowska, J., & Xirodimas, D. P. (2022). Mixed in chains: Nedd8 polymers in the Protein Quality Control system. *Seminars in Cell & Developmental Biology*, *132*, 27–37. https://doi.org/10.1016/j.semcdb.2022.01.005

Metlagel, Z., Otomo, C., Takaesu, G., & Otomo, T. (2013). Structural basis of ATG3 recognition by the autophagic ubiquitin-like protein ATG12. *Proceedings of the National Academy of Sciences of the United States of America*, *110*(47), 18844–18849. https://doi.org/10.1073/pnas.1314755110

Michel, M. A., Swatek, K. N., Hospenthal, M. K [Manuela K.], & Komander, D. (2017). Ubiquitin Linkage-Specific Affimers Reveal Insights into K6-Linked Ubiquitin Signaling. *Molecular Cell*, *68*(1), 233-246.e5. https://doi.org/10.1016/j.molcel.2017.08.020

Middleton, A. J., & Day, C. L. (2023). From seeds to trees: How E2 enzymes grow ubiquitin chains. *Biochemical Society Transactions*, *51*(1), 353–362. https://doi.org/10.1042/BST20220880

Mueller, R. D., Yasuda, H., Hatch, C. L., Bonner, W. M., & Bradbury, E. M. (1985). Identification of ubiquitinated histones 2A and 2B in Physarum polycephalum. Disappearance of these proteins at metaphase and reappearance at anaphase. *Journal of Biological Chemistry*, *260*(8), 5147–5153. https://pubmed.ncbi.nlm.nih.gov/2985575/

Nakasato, N., Ikeda, K., Urano, T., Horie-Inoue, K., Takeda, S., & Inoue, S. (2006). A ubiquitin E3 ligase Efp is up-regulated by interferons and conjugated with ISG15. *Biochemical and Biophysical Research Communications*, *351*(2), 540–546. https://doi.org/10.1016/j.bbrc.2006.10.061

Narendra, D., Tanaka, A., Suen, D.-F., & Youle, R. J. (2008). Parkin is recruited selectively to impaired mitochondria and promotes their autophagy. *The Journal of Cell Biology*, *183*(5), 795–803. https://doi.org/10.1083/jcb.200809125

Niedermeyer, T. H. J., & Strohalm, M. (2012). Mmass as a software tool for the annotation of cyclic peptide tandem mass spectra. *PloS One*, *7*(9), e44913. https://doi.org/10.1371/journal.pone.0044913

Nieto-Torres, J. L., Leidal, A. M., Debnath, J., & Hansen, M. (2021). Beyond Autophagy: The Expanding Roles of ATG8 Proteins. *Trends in Biochemical Sciences*, *46*(8), 673–686. https://doi.org/10.1016/j.tibs.2021.01.004

Novatchkova, M., Bachmair, A [Andreas], Eisenhaber, B., & Eisenhaber, F. (2005). Proteins with two SUMO-like domains in chromatin-associated complexes:

The RENi (Rad60-Esc2-NIP45) family. *BMC Bioinformatics*, *6*, 22. https://doi.org/10.1186/1471-2105-6-22

Ohki, Y., Funatsu, N., Konishi, N., & Chiba, T. (2009). The mechanism of poly-NEDD8 chain formation in vitro. *Biochemical and Biophysical Research Communications*, *381*(3), 443–447. https://doi.org/10.1016/j.bbrc.2009.02.090

Ohtake, F., Saeki, Y., Ishido, S., Kanno, J., & Tanaka, K. (2016). The K48-K63 Branched Ubiquitin Chain Regulates NF-κB Signaling. *Molecular Cell*, *64*(2), 251–266. https://doi.org/10.1016/j.molcel.2016.09.014

Okumoto, K., Misono, S., Miyata, N., Matsumoto, Y., Mukai, S., & Fujiki, Y. (2011). Cysteine ubiquitination of PTS1 receptor Pex5p regulates Pex5p recycling. *Traffic (Copenhagen, Denmark)*, *12*(8), 1067–1083. https://doi.org/10.1111/j.1600-0854.2011.01217.x

Okumura, A., Lu, G., Pitha-Rowe, I., & Pitha, P. M. (2006). Innate antiviral response targets HIV-1 release by the induction of ubiquitin-like protein ISG15. *Proceedings of the National Academy of Sciences of the United States of America*, *103*(5), 1440–1445. https://doi.org/10.1073/pnas.0510518103

Olsen, J. V., Ong, S.-E., & Mann, M. (2004). Trypsin cleaves exclusively C-terminal to arginine and lysine residues. *Molecular & Cellular Proteomics*, *3*(6), 608–614. https://doi.org/10.1074/mcp.T400003-MCP200

Ordureau, A., Münch, C., & Harper, J. W [J. Wade] (2015). Quantifying ubiquitin signaling. *Molecular Cell*, *58*(4), 660–676. https://doi.org/10.1016/j.molcel.2015.02.020

Ordureau, A., Sarraf, S. A., Duda, D. M., Heo, J.-M., Jedrychowski, M. P., Sviderskiy, V. O., Olszewski, J. L., Koerber, J. T., Xie, T., Beausoleil, S. A., Wells, J. A., Gygi, S. P., Schulman, B. A., & Harper, J. W [J. Wade] (2014). Quantitative proteomics reveal a feedforward mechanism for mitochondrial PARKIN translocation and ubiquitin chain synthesis. *Molecular Cell*, *56*(3), 360–375. https://doi.org/10.1016/j.molcel.2014.09.007

Otten, E. G., Werner, E., Crespillo-Casado, A., Boyle, K. B., Dharamdasani, V., Pathe, C., Santhanam, B., & Randow, F. (2021). Ubiquitylation of lipopolysaccharide by RNF213 during bacterial infection. *Nature*, *594*(7861), 111–116. https://doi.org/10.1038/s41586-021-03566-4

Ozkan, E., Yu, H., & Deisenhofer, J. (2005). Mechanistic insight into the allosteric activation of a ubiquitin-conjugating enzyme by RING-type ubiquitin ligases. *Proceedings of the National Academy of Sciences of the United States of America*, *102*(52), 18890–18895. https://doi.org/10.1073/pnas.0509418102

Ozkaynak, E., Finley, D [D.], Solomon, M. J., & Varshavsky, A. (1987). The yeast ubiquitin genes: A family of natural gene fusions. *The EMBO Journal*, *6*(5), 1429–1439. https://doi.org/10.1002/j.1460-2075.1987.tb02384.x

Pao, K.-C., Wood, N. T., Knebel, A., Rafie, K., Stanley, M., Mabbitt, P. D., Sundaramoorthy, R., Hofmann, K., van Aalten, D. M. F., & Virdee, S. (2018). Activity-based E3 ligase profiling uncovers an E3 ligase with esterification activity. *Nature*, *556*(7701), 381–385. https://doi.org/10.1038/s41586-018-0026-1

Park, S., Krist, D. T., & Statsyuk, A. V. (2015). Protein ubiquitination and formation of polyubiquitin chains without ATP, E1 and E2 enzymes. *Chemical Science*, *6*(3), 1770–1779. https://doi.org/10.1039/C4SC02340D

Peng, J., Schwartz, D., Elias, J. E., Thoreen, C. C., Cheng, D., Marsischky, G., Roelofs, J., Finley, D [Daniel], & Gygi, S. P. (2003). A proteomics approach to understanding protein ubiquitination. *Nature Biotechnology*, *21*(8), 921–926. https://doi.org/10.1038/nbt849

Perng, Y.-C., & Lenschow, D. J. (2018). Isg15 in antiviral immunity and beyond. *Nature Reviews. Microbiology*, *16*(7), 423–439. https://doi.org/10.1038/s41579-018-0020-5

Peth, A., Uchiki, T., & Goldberg, A. L [Alfred L.] (2010). Atp-dependent steps in the binding of ubiquitin conjugates to the 26S proteasome that commit to degradation. *Molecular Cell*, *40*(4), 671–681. https://doi.org/10.1016/j.molcel.2010.11.002

Petroski, M. D., & Deshaies, R. J [Raymond J.] (2005). Function and regulation of cullin-RING ubiquitin ligases. *Nature Reviews. Molecular Cell Biology*, *6*(1), 9–20. https://doi.org/10.1038/nrm1547

Phillips, A. R., Suttangkakul, A., & Vierstra, R. D. (2008). The ATG12-conjugating enzyme ATG10 Is essential for autophagic vesicle formation in Arabidopsis thaliana. *Genetics*, *178*(3), 1339–1353. https://doi.org/10.1534/genetics.107.086199

Pick, E., Golan, A., Zimbler, J. Z., Guo, L., Sharaby, Y., Tsuge, T., Hofmann, K., & Wei, N. (2012). The minimal deneddylase core of the COP9 signalosome excludes the Csn6 MPN- domain. *PloS One*, *7*(8), e43980. https://doi.org/10.1371/journal.pone.0043980

Pinto-Fernandez, A., Salio, M., Partridge, T., Chen, J [Jianzhou], Vere, G., Greenwood, H., Olie, C. S., Damianou, A., Scott, H. C [Hannah Claire], Pegg, H. J., Chiarenza, A., Díaz-Saez, L., Smith, P., Gonzalez-Lopez, C., Patel, B., Anderton, E., Jones, N., Hammonds, T. R., Huber, K., . . . Kessler, B. M. (2021). Deletion of the deISGylating enzyme USP18 enhances tumour cell antigenicity and radiosensitivity. *British Journal of Cancer*, *124*(4), 817–830. https://doi.org/10.1038/s41416-020-01167-y

Pinto-Fernández, A., Davis, S., Schofield, A. B., Scott, H. C [Hannah C.], Zhang, P [Ping], Salah, E., Mathea, S., Charles, P. D., Damianou, A., Bond, G., Fischer, R., & Kessler, B. M. (2019). Comprehensive Landscape of Active Deubiquitinating Enzymes Profiled by Advanced Chemoproteomics. *Frontiers in Chemistry*, *7*, Article 592, 592. https://doi.org/10.3389/fchem.2019.00592

Potter, J. L., Narasimhan, J., Mende-Mueller, L., & Haas, A. L. (1999). Precursor processing of pro-ISG15/UCRP, an interferon-beta-induced ubiquitin-like protein. *Journal of Biological Chemistry*, *274*(35), 25061–25068. https://doi.org/10.1074/jbc.274.35.25061

Pruneda, J. N., Bastidas, R. J., Bertsoulaki, E., Swatek, K. N., Santhanam, B., Clague, M. J., Valdivia, R. H., Urbé, S., & Komander, D. (2018). A Chlamydia effector combining deubiquitination and acetylation activities induces Golgi

fragmentation. *Nature Microbiology*, *3*(12), 1377–1384. https://doi.org/10.1038/s41564-018-0271-y

Prus, G., Satpathy, S., Weinert, B. T., Narita, T., & Choudhary, C. (2024). Global, site-resolved analysis of ubiquitylation occupancy and turnover rate reveals systems properties. *Cell*, *187*(11), 2875-2892.e21. https://doi.org/10.1016/j.cell.2024.03.024

Puri, A., Hembram, D. S., Aravind, R., & Das, R. (2026). *Investigating the activity of Varicella Zoster Virus (VZV) SUMO-targeted Ubiquitin Ligase ORF61.* https://doi.org/10.64898/2026.03.11.710994

Purser, N., Tripathi-Giesgen, I., Li, J [Jerry], Scott, D. C., Horn-Ghetko, D., Baek, K., Schulman, B. A., Alpi, A. F., & Kleiger, G. (2023). Catalysis of non-canonical protein ubiquitylation by the ARIH1 ubiquitin ligase. *The Biochemical Journal*, *480*(22), 1817–1831. https://doi.org/10.1042/BCJ20230373

Raasi, S [S.], Schmidtke, G [G.], & Groettrup, M [M.] (2001). The ubiquitin-like protein FAT10 forms covalent conjugates and induces apoptosis. *Journal of Biological Chemistry*, *276*(38), 35334–35343. https://doi.org/10.1074/jbc.M105139200

Rabut, G., & Peter, M. (2008). Function and regulation of protein neddylation. 'protein modifications: Beyond the usual suspects' review series. *EMBO Reports*, *9*(10), 969–976. https://doi.org/10.1038/embor.2008.183

Radoshevich, L., Impens, F., Ribet, D., Quereda, J. J., Tham, T. N., Nahori, M., Bierne, H., Dussurget, O., Pizarro-cerdá, J., Knobeloch, K.-P., & Cossart, P. (2015, August 11). ISG15 counteracts Listeria monocytogenes infection. *ELife Sciences Publications, Ltd*. https://elifesciences.org/articles/06848

Rahighi, S., Ikeda, F., Kawasaki, M., Akutsu, M., Suzuki, N., Kato, R., Kensche, T., Uejima, T., Bloor, S., Komander, D., Randow, F., Wakatsuki, S., & Dikic, I. (2009). Specific recognition of linear ubiquitin chains by NEMO is important for NF-kappaB activation. *Cell*, *136*(6), 1098–1109. https://doi.org/10.1016/j.cell.2009.03.007

Randles, L., & Walters, K. J. (2012). Ubiquitin and its binding domains. *Frontiers in Bioscience-Landmark*, *17*(6), 2140–2157. https://doi.org/10.2741/4042

Recht, M., Borden, E. C., & Knight, E. (1991). A human 15-kDa IFN-induced protein induces the secretion of IFN-gamma. *Journal of Immunology (Baltimore, Md. : 1950)*, *147*(8), 2617–2623. https://pubmed.ncbi.nlm.nih.gov/1717569/

Reyes-Turcu, F. E., Horton, J. R., Mullally, J. E., Heroux, A., Cheng, X., & Wilkinson, K. D. (2006). The ubiquitin binding domain ZnF UBP recognizes the C-terminal diglycine motif of unanchored ubiquitin. *Cell*, *124*(6), 1197–1208. https://doi.org/10.1016/j.cell.2006.02.038

Rogov, V., Dötsch, V., Johansen, T., & Kirkin, V. (2014). Interactions between autophagy receptors and ubiquitin-like proteins form the molecular basis for selective autophagy. *Molecular Cell*, *53*(2), 167–178. https://doi.org/10.1016/j.molcel.2013.12.014

Ronau, J. A., Beckmann, J. F., & Hochstrasser, M [Mark] (2016). Substrate specificity of the ubiquitin and Ubl proteases. *Cell Research*, *26*(4), 441–456. https://doi.org/10.1038/cr.2016.38

Saavedra-Sanchez, L., Dickinson, M. S., Apte, S., Zhang, Y [Yifeng], Jong, M. de, Skavicus, S., Heaton, N. S., Alto, N. M., & Coers, J. (2025). The Shigella flexneri effector IpaH1.4 facilitates RNF213 degradation and protects cytosolic bacteria against interferon-induced ubiquitylation. *BioRxiv*, 2024.09.05.611450. https://doi.org/10.1101/2024.09.05.611450

Santonico, E. (2020). Old and New Concepts in Ubiquitin and NEDD8 Recognition. *Biomolecules*, *10*(4), 566. https://doi.org/10.3390/biom10040566

Scaglione, K. M., Zavodszky, E., Todi, S. V., Patury, S., Xu, P., Rodríguez-Lebrón, E., Fischer, S., Konen, J., Djarmati, A., Peng, J., Gestwicki, J. E., & Paulson, H. L. (2011). Ube2w and ataxin-3 coordinately regulate the ubiquitin ligase CHIP. *Molecular Cell*, *43*(4), 599–612. https://doi.org/10.1016/j.molcel.2011.05.036

Schneider, W. M., Chevillotte, M. D., & Rice, C. M. (2014). Interferon-stimulated genes: A complex web of host defenses. *Annual Review of Immunology*, *32*, 513–545. https://doi.org/10.1146/annurev-immunol-032713-120231

Schwickart, M., Huang, X., Lill, J. R., Liu, J [Jinfeng], Ferrando, R., French, D. M., Maecker, H., O'Rourke, K., Bazan, F., Eastham-Anderson, J., Yue, P., Dornan, D., Huang, D. C. S., & Dixit, V. M. (2010). Deubiquitinase USP9X stabilizes MCL1 and promotes tumour cell survival. *Nature*, *463*(7277), 103–107. https://doi.org/10.1038/nature08646

Shen, G., Li, S [Shuang], Cui, W., Liu, S., Yang, Y [Yihu], Gross, M., & Li, W. (2018). Membrane Protein Structure in Live Cells: Methodology for Studying Drug Interaction by Mass Spectrometry-Based Footprinting. *Biochemistry*, *57*(3), 286–294. https://doi.org/10.1021/acs.biochem.7b00874

Shen, L., Liu, H., Dong, C., Xirodimas, D., Naismith, J. H [James H.], & Hay, R. T [Ronald T.] (2005). Structural basis of NEDD8 ubiquitin discrimination by the deNEDDylating enzyme NEDP1. *The EMBO Journal*, *24*(7), 1341–1351. https://doi.org/10.1038/sj.emboj.7600628

Shen, Z., Pardington-Purtymun, P. E., Comeaux, J. C., Moyzis, R. K., & Chen, D. J. (1996). Ubl1, a human ubiquitin-like protein associating with human RAD51/RAD52 proteins. *Genomics*, *36*(2), 271–279. https://doi.org/10.1006/geno.1996.0462

Sheng, X., You, Q., Zhu, H., Chang, Z., Li, Q., Wang, H [Haifeng], Wang, C [Chen], Wang, H [Hongyan], Hui, L., Du, C., Xie, X., Zeng, R., Lin, A., Shi, D., Ruan, K., Yan, J., Gao, G. F., Shao, F., & Hu, R. (2017). Bacterial effector NleL promotes enterohemorrhagic E. Coli-induced attaching and effacing lesions by ubiquitylating and inactivating JNK. *PLoS Pathogens*, *13*(7), e1006534. https://doi.org/10.1371/journal.ppat.1006534

Shi, H.-X., Yang, K., Liu, X [Xing], Liu, X.-Y., Wei, B., Shan, Y.-F., Zhu, L.-H., & Wang, C [Chen] (2010). Positive regulation of interferon regulatory factor 3 activation by Herc5 via ISG15 modification. *Molecular and Cellular Biology*, *30*(10), 2424–2436. https://doi.org/10.1128/MCB.01466-09

Shimohata, T., Nakajima, T., Yamada, M., Uchida, C., Onodera, O., Naruse, S., Kimura, T., Koide, R., Nozaki, K., Sano, Y., Ishiguro, H., Sakoe, K., Ooshima, T., Sato, A., Ikeuchi, T., Oyake, M., Sato, T., Aoyagi, Y.,

Hozumi, I., . . . Tsuji, S. (2000). Expanded polyglutamine stretches interact with TAFII130, interfering with CREB-dependent transcription. *Nature Genetics*, *26*(1), 29–36. https://doi.org/10.1038/79139

Shrestha, R. K., Ronau, J. A., Davies, C. W., Guenette, R. G., Strieter, E. R., Paul, L. N., & Das, C. (2014). Insights into the Mechanism of Deubiquitination by JAMM Deubiquitinases from Cocrystal Structures of the Enzyme with the Substrate and Product. *Biochemistry*, *53*(19), 3199–3217. https://doi.org/10.1021/bi5003162

Skowyra, D., Craig, K. L., Tyers, M., Elledge, S. J [S. J.], & Harper, J. W [J. W.] (1997). F-box proteins are receptors that recruit phosphorylated substrates to the SCF ubiquitin-ligase complex. *Cell*, *91*(2), 209–219. https://doi.org/10.1016/s0092-8674(00)80403-1

Sloper-Mould, K. E., Jemc, J. C., Pickart, C. M., & Hicke, L. (2001). Distinct functional surface regions on ubiquitin. *Journal of Biological Chemistry*, *276*(32), 30483–30489. https://doi.org/10.1074/jbc.M103248200

Smit, J. J., van Dijk, W. J., El Atmioui, D., Merkx, R., Ovaa, H., & Sixma, T. K. (2013). Target specificity of the E3 ligase LUBAC for ubiquitin and NEMO relies on different minimal requirements. *The Journal of Biological Chemistry*, *288*(44), 31728–31737. https://doi.org/10.1074/jbc.M113.495846

Soucy, T. A., Dick, L. R., Smith, P. G., Milhollen, M. A., & Brownell, J. E. (2010). The NEDD8 Conjugation Pathway and Its Relevance in Cancer Biology and Therapy. *Genes & Cancer*, *1*(7), 708–716. https://doi.org/10.1177/1947601910382898

Soucy, T. A., Smith, P. G., Milhollen, M. A., Berger, A. J., Gavin, J. M., Adhikari, S., Brownell, J. E., Burke, K. E., Cardin, D. P., Critchley, S., Cullis, C. A., Doucette, A., Garnsey, J. J., Gaulin, J. L., Gershman, R. E., Lublinsky, A. R., McDonald, A., Mizutani, H., Narayanan, U., . . . Langston, S. P. (2009). An inhibitor of NEDD8-activating enzyme as a new approach to treat cancer. *Nature*, *458*(7239), 732–736. https://doi.org/10.1038/nature07884

Sturgill-Koszycki, S., & Swanson, M. S. (2000). Legionella pneumophila replication vacuoles mature into acidic, endocytic organelles. *The Journal of Experimental Medicine*, *192*(9), 1261–1272. https://doi.org/10.1084/jem.192.9.1261

Sun, H., Yao, W., Wang, K., Qian, Y., Chen, H [Hongjun], & Jung, Y.-S. (2018). Inhibition of neddylation pathway represses influenza virus replication and pro-inflammatory responses. *Virology*, *514*, 230–239. https://doi.org/10.1016/j.virol.2017.11.004

Suresh, H. G., Pascoe, N., & Andrews, B. (2020). The structure and function of deubiquitinases: Lessons from budding yeast. *Open Biology*, *10*(10), 200279. https://doi.org/10.1098/rsob.200279

Swatek, K. N., Aumayr, M., Pruneda, J. N., Visser, L. J., Berryman, S., Kueck, A. F., Geurink, P. P., Ovaa, H., van Kuppeveld, F. J. M., Tuthill, T. J., Skern, T., & Komander, D. (2018). Irreversible inactivation of ISG15 by a viral leader protease enables alternative infection detection strategies. *Proceedings of the*

National Academy of Sciences of the United States of America, *115*(10), 2371–2376. https://doi.org/10.1073/pnas.1710617115

Swatek, K. N., Usher, J. L., Kueck, A. F., Gladkova, C., Mevissen, T. E. T., Pruneda, J. N., Skern, T., & Komander, D. (2019). Insights into ubiquitin chain architecture using Ub-clipping. *Nature*, *572*(7770), 533–537. https://doi.org/10.1038/s41586-019-1482-y

Tatham, M. H [M. H.], Jaffray, E., Vaughan, O. A., Desterro, J. M., Botting, C. H., Naismith, J. H [J. H.], & Hay, R. T [R. T.] (2001). Polymeric chains of SUMO-2 and SUMO-3 are conjugated to protein substrates by SAE1/SAE2 and Ubc9. *Journal of Biological Chemistry*, *276*(38), 35368–35374. https://doi.org/10.1074/jbc.M104214200

Thery, F., Eggermont, D., & Impens, F. (2021). Proteomics Mapping of the ISGylation Landscape in Innate Immunity. *Frontiers in Immunology*, *12*, 720765. https://doi.org/10.3389/fimmu.2021.720765

Thrower, J. S., Hoffman, L., Rechsteiner, M., & Pickart, C. M. (2000). Recognition of the polyubiquitin proteolytic signal. *The EMBO Journal*, *19*(1), 94–102. https://doi.org/10.1093/emboj/19.1.94

Thul, P. J., & Lindskog, C. (2018). The human protein atlas: A spatial map of the human proteome. *Protein Science*, *27*(1), 233–244. https://doi.org/10.1002/pro.3307

Tokunaga, F., & Iwai, K. (2009). Involvement of LUBAC-mediated linear polyubiquitination of NEMO in NF-kappaB activation. *Tanpakushitsu kakusan koso. Protein, nucleic acid, enzyme*, *54*(5), 635–642. https://pubmed.ncbi.nlm.nih.gov/19348259/

Tripathi-Giesgen, I., Behrends, C., & Alpi, A. F. (2021). The ubiquitin ligation machinery in the defense against bacterial pathogens. *EMBO Reports*, *22*(11), e52864. https://doi.org/10.15252/embr.202152864

Tsuchiya, H., Burana, D., Ohtake, F., Arai, N., Kaiho, A., Komada, M., Tanaka, K., & Saeki, Y. (2018). Ub-ProT reveals global length and composition of protein ubiquitylation in cells. *Nature Communications*, *9*(1), 524. https://doi.org/10.1038/s41467-018-02869-x

Tyanova, S., Temu, T., Sinitcyn, P., Carlson, A., Hein, M. Y., Geiger, T., Mann, M., & Cox, J. (2016). The Perseus computational platform for comprehensive analysis of (prote)omics data. *Nature Methods*, *13*(9), 731–740. https://doi.org/10.1038/nmeth.3901

Udeshi, N. D., Mani, D. C., Satpathy, S., Fereshetian, S., Gasser, J. A., Svinkina, T., Olive, M. E., Ebert, B. L., Mertins, P., & Carr, S. A. (2020). Rapid and deep-scale ubiquitylation profiling for biology and translational research. *Nature Communications*, *11*(1), 359. https://doi.org/10.1038/s41467-019-14175-1

Uzunova, K., Göttsche, K., Miteva, M., Weisshaar, S. R., Glanemann, C., Schnellhardt, M., Niessen, M., Scheel, H., Hofmann, K., Johnson, E. S., Praefcke, G. J. K., & Dohmen, R. J. (2007). Ubiquitin-dependent proteolytic control of SUMO conjugates. *Journal of Biological Chemistry*, *282*(47), 34167–34175. https://doi.org/10.1074/jbc.M706505200

van der Hoeven, L. R., Lechner, M., Hernandez-Rollan, C., Batth, T. S., & Olsen, J. V. (2026). Comparative Analysis of Lysine-Specific Peptidases for Optimizing Proteomics Workflows. *Journal of Proteome Research*, *25*(2), 1176–1183. https://doi.org/10.1021/acs.jproteome.5c00872

van der Wal, L., Bezstarosti, K., Sap, K. A., Dekkers, D. H. W., Rijkers, E., Mientjes, E., Elgersma, Y., & Demmers, J. A. A. (2018). Improvement of ubiquitylation site detection by Orbitrap mass spectrometry. *Journal of Proteomics*, *172*, 49–56. https://doi.org/10.1016/j.jprot.2017.10.014

van Wijk, S. J. L., Fricke, F., Herhaus, L., Gupta, J., Hötte, K., Pampaloni, F., Grumati, P., Kaulich, M., Sou, Y., Komatsu, M., Greten, F. R., Fulda, S., Heilemann, M., & Dikic, I. (2017). Linear ubiquitination of cytosolic Salmonella Typhimurium activates NF-κB and restricts bacterial proliferation. *Nature Microbiology*, *2*(7), 17066. https://doi.org/10.1038/nmicrobiol.2017.66

Vijayasimha, K., & Dolan, B. P. (2021). The Many Potential Fates of Non-Canonical Protein Substrates Subject to NEDDylation. *Cells*, *10*(10), 2660. https://doi.org/10.3390/cells10102660

Vijay-Kumar, S., Bugg, C. E., & Cook, W. J. (1987). Structure of ubiquitin refined at 1.8 A resolution. *Journal of Molecular Biology*, *194*(3), 531–544. https://doi.org/10.1016/0022-2836(87)90679-6

Vreeke, G. J. C., Vincken, J.-P., & Wierenga, P. A. (2023). The path of proteolysis by bovine chymotrypsin. *Food Research International (Ottawa, Ont.)*, *165*, 112485. https://doi.org/10.1016/j.foodres.2023.112485

Wagner, S. A., Beli, P., Weinert, B. T., Nielsen, M. L., Cox, J., Mann, M., & Choudhary, C. (2011). A proteome-wide, quantitative survey of in vivo ubiquitylation sites reveals widespread regulatory roles. *Molecular & Cellular Proteomics*, *10*(10), M111.013284. https://doi.org/10.1074/mcp.M111.013284

Walden, H., & Martinez-Torres, R. J. (2012). Regulation of Parkin E3 ubiquitin ligase activity. *Cellular and Molecular Life Sciences : CMLS*, *69*(18), 3053–3067. https://doi.org/10.1007/s00018-012-0978-5

Wan, M., Wang, X [Xiaofei], Huang, C., Xu, D., Wang, Z [Zhao], Zhou, Y., & Zhu, Y [Yongqun] (2019). A bacterial effector deubiquitinase specifically hydrolyses linear ubiquitin chains to inhibit host inflammatory signalling. *Nature Microbiology*, *4*(8), 1282–1293. https://doi.org/10.1038/s41564-019-0454-1

Wang, D., Fang, L., Li, P., Sun, L., Fan, J., Zhang, Q., Luo, R., Liu, X [Xiangtao], Li, K., Chen, H [Huanchun], Chen, Z., & Xiao, S. (2011). The leader proteinase of foot-and-mouth disease virus negatively regulates the type I interferon pathway by acting as a viral deubiquitinase. *Journal of Virology*, *85*(8), 3758–3766. https://doi.org/10.1128/JVI.02589-10

Wang, P [Peng], Zhao, W., Zhao, K., Zhang, L [Lei], & Gao, C. (2015). Trim26 negatively regulates interferon-β production and antiviral response through polyubiquitination and degradation of nuclear IRF3. *PLoS Pathogens*, *11*(3), e1004726. https://doi.org/10.1371/journal.ppat.1004726

Wang, W., Lu, J [Jian], Yang, W.-C., Spear, E. D., Michaelis, S., & Matunis, M. J [Michael J.] (2023). Analysis of a degron-containing reporter protein GFP-CL1

reveals a role for SUMO1 in cytosolic protein quality control. *The Journal of Biological Chemistry*, *299*(2), 102851. https://doi.org/10.1016/j.jbc.2022.102851

Wang, W., & Matunis, M. J [Michael J.] (2023). Paralogue-Specific Roles of SUMO1 and SUMO2/3 in Protein Quality Control and Associated Diseases. *Cells*, *13*(1), 8. https://doi.org/10.3390/cells13010008

Weddle, E., & Agaisse, H. (2018). Principles of intracellular bacterial pathogen spread from cell to cell. *PLoS Pathogens*, *14*(12), e1007380. https://doi.org/10.1371/journal.ppat.1007380

Weeks, S. D., Grasty, K. C., Hernandez-Cuebas, L., & Loll, P. J. (2011). Crystal structure of a Josephin-ubiquitin complex: Evolutionary restraints on ataxin-3 deubiquitinating activity. *The Journal of Biological Chemistry*, *286*(6), 4555–4565. https://doi.org/10.1074/jbc.M110.177360

Wei, W., Yang, P., Pang, J., Zhang, S [Shu], Wang, Y., Wang, M.-H., Dong, Z., She, J.-X., & Wang, C.-Y. (2008). A stress-dependent SUMO4 sumoylation of its substrate proteins. *Biochemical and Biophysical Research Communications*, *375*(3), 454–459. https://doi.org/10.1016/j.bbrc.2008.08.028

Weisshaar, S. R., Keusekotten, K., Krause, A., Horst, C., Springer, H. M., Göttsche, K., Dohmen, R. J., & Praefcke, G. J. K. (2008). Arsenic trioxide stimulates SUMO-2/3 modification leading to RNF4-dependent proteolytic targeting of PML. *FEBS Letters*, *582*(21-22), 3174–3178. https://doi.org/10.1016/j.febslet.2008.08.008

Wenzel, D. M., Lissounov, A., Brzovic, P. S., & Klevit, R. E. (2011). Ubch7 reactivity profile reveals parkin and HHARI to be RING/HECT hybrids. *Nature*, *474*(7349), 105–108. https://doi.org/10.1038/nature09966

Wiborg, O., Pedersen, M. S., Wind, A., Berglund, L. E., Marcker, K. A., & Vuust, J. (1985). The human ubiquitin multigene family: Some genes contain multiple directly repeated ubiquitin coding sequences. *The EMBO Journal*, *4*(3), 755–759. https://doi.org/10.1002/j.1460-2075.1985.tb03693.x

Wiśniewski, J. R., Zougman, A., & Mann, M. (2009). Combination of FASP and StageTip-based fractionation allows in-depth analysis of the hippocampal membrane proteome. *Journal of Proteome Research*, *8*(12), 5674–5678. https://doi.org/10.1021/pr900748n

Wu, Z., Berlemann, L. A., Bader, V., Sehr, D. A., Dawin, E., Covallero, A., Meschede, J., Angersbach, L., Showkat, C., Michaelis, J. B., Münch, C., Rieger, B., Namgaladze, D., Herrera, M. G., Fiesel, F. C., Springer, W., Mendes, M., Stepien, J., Barkovits, K., . . . Winklhofer, K. F. (2022). Lubac assembles a ubiquitin signaling platform at mitochondria for signal amplification and transport of NF-κB to the nucleus. *The EMBO Journal*, *41*(24), e112006. https://doi.org/10.15252/embj.2022112006

Xu, G., Paige, J. S., & Jaffrey, S. R. (2010). Global analysis of lysine ubiquitination by ubiquitin remnant immunoaffinity profiling. *Nature Biotechnology*, *28*(8), 868–873. https://doi.org/10.1038/nbt.1654

Xu, P., Duong, D. M., Seyfried, N. T., Cheng, D., Xie, Y., Robert, J., Rush, J., Hochstrasser, M [Mark], Finley, D [Daniel], & Peng, J. (2009). Quantitative proteomics reveals the function of unconventional ubiquitin chains in proteasomal degradation. *Cell*, *137*(1), 133–145. https://doi.org/10.1016/j.cell.2009.01.041

Yan, S., Kumari, M., Xiao, H., Jacobs, C., Kochumon, S., Jedrychowski, M., Chouchani, E., Ahmad, R., & Rosen, E. D. (2021). Irf3 reduces adipose thermogenesis via ISG15-mediated reprogramming of glycolysis. *The Journal of Clinical Investigation*, *131*(7). https://doi.org/10.1172/JCI144888

Yang, E., & Li, M. M. H. (2020). All About the RNA: Interferon-Stimulated Genes That Interfere With Viral RNA Processes. *Frontiers in Immunology*, *11*, 605024. https://doi.org/10.3389/fimmu.2020.605024

Yao, Q., Cui, J., Wang, J [Jiayi], Li, T., Wan, X., Luo, T., Gong, Y.-N., Xu, Y [Ying], Huang, N., & Shao, F. (2012). Structural mechanism of ubiquitin and NEDD8 deamidation catalyzed by bacterial effectors that induce macrophage-specific apoptosis. *Proceedings of the National Academy of Sciences of the United States of America*, *109*(50), 20395–20400. https://doi.org/10.1073/pnas.1210831109

Yashiroda, H., & Tanaka, K. (2004). Hub1 is an essential ubiquitin-like protein without functioning as a typical modifier in fission yeast. *Genes to Cells : Devoted to Molecular & Cellular Mechanisms*, *9*(12), 1189–1197. https://doi.org/10.1111/j.1365-2443.2004.00807.x

Ye, Y., Akutsu, M., Reyes-Turcu, F., Enchev, R. I., Wilkinson, K. D., & Komander, D. (2011). Polyubiquitin binding and cross-reactivity in the USP domain deubiquitinase USP21. *EMBO Reports*, *12*(4), 350–357. https://doi.org/10.1038/embor.2011.17

Yu, M., Tang, Y., Lu, L [Lanxiang], Kong, W., & Ye, J. (2023). Cysb Is a Key Regulator of the Antifungal Activity of Burkholderia pyrrocinia JK-SH007. *International Journal of Molecular Sciences*, *24*(9), 8067. https://doi.org/10.3390/ijms24098067

Zhang, S [Shengzhe], Zhang, M., Jing, Y., Yin, X., Ma, P., Zhang, Z., Wang, X [Xiaojie], Di, W., & Zhuang, G. (2018). Deubiquitinase USP13 dictates MCL1 stability and sensitivity to BH3 mimetic inhibitors. *Nature Communications*, *9*(1), 215. https://doi.org/10.1038/s41467-017-02693-9

Zhang, Y [Yifeng], Thery, F., Wu, N. C., Luhmann, E. K., Dussurget, O., Foecke, M., Bredow, C., Jiménez-Fernández, D., Leandro, K., Beling, A., Knobeloch, K.-P., Impens, F., Cossart, P., & Radoshevich, L. (2019). The in vivo ISGylome links ISG15 to metabolic pathways and autophagy upon Listeria monocytogenes infection. *Nature Communications*, *10*(1), 5383. https://doi.org/10.1038/s41467-019-13393-x

Zhang, Y [Yong], Mao, D., Roswit, W. T., Jin, X., Patel, A. C., Patel, D. A., Agapov, E., Wang, Z [Zhepeng], Tidwell, R. M., Atkinson, J. J., Huang, G., McCarthy, R., Yu, J [Jinsheng], Yun, N. E., Paessler, S., Lawson, T. G., Omattage, N. S., Brett, T. J., & Holtzman, M. J. (2015). Parp9-DTX3L ubiquitin ligase targets

host histone H2BJ and viral 3C protease to enhance interferon signaling and control viral infection. *Nature Immunology*, *16*(12), 1215–1227. https://doi.org/10.1038/ni.3279

Zhao, C., Sridharan, H., Chen, R., Baker, D. P., Wang, S [Shanshan], & Krug, R. M. (2016). Influenza B virus non-structural protein 1 counteracts ISG15 antiviral activity by sequestering ISGylated viral proteins. *Nature Communications*, *7*(1), 12754. https://doi.org/10.1038/ncomms12754

Zheng, N., Schulman, B. A., Song, L., Miller, J. J., Jeffrey, P. D., Wang, P [Ping], Chu, C., Koepp, D. M., Elledge, S. J [Stephen J.], Pagano, M., Conaway, R. C [Ronald C.], Conaway, J. W [Joan W.], Harper, J. W [J. Wade], & Pavletich, N. P. (2002). Structure of the Cul1-Rbx1-Skp1-F boxSkp2 SCF ubiquitin ligase complex. *Nature*, *416*(6882), 703–709. https://doi.org/10.1038/416703a

Zheng, N., & Shabek, N. (2017). Ubiquitin Ligases: Structure, Function, and Regulation. *Annual Review of Biochemistry*, *86*(Volume 86, 2017), 129–157. https://doi.org/10.1146/annurev-biochem-060815-014922

Zhou, H., Lu, J [Jianfeng], Liu, L [Liu], Bernard, D., Yang, C.-Y., Fernandez-Salas, E., Chinnaswamy, K., Layton, S., Stuckey, J., Yu, Q., Zhou, W [Weihua], Pan, Z., Sun, Y., & Wang, S [Shaomeng] (2017). A potent small-molecule inhibitor of the DCN1-UBC12 interaction that selectively blocks cullin 3 neddylation. *Nature Communications*, *8*(1), 1150. https://doi.org/10.1038/s41467-017-01243-7

Zhou, W [Wenlai], Zhu, P., Wang, J [Jianxun], Pascual, G., Ohgi, K. A., Lozach, J., Glass, C. K., & Rosenfeld, M. G. (2008). Histone H2A monoubiquitination represses transcription by inhibiting RNA polymerase II transcriptional elongation. *Molecular Cell*, *29*(1), 69–80. https://doi.org/10.1016/j.molcel.2007.11.002

Zhu, C., Li, J [Jingrui], Tian, C., Qin, M., Wang, Z [Zhenni], Shi, B., Qu, G., Wu, C., & Nan, Y. (2021). Proteomic Analysis of ISGylation in Immortalized Porcine Alveolar Macrophage Cell Lines Induced by Type I Interferon. *Vaccines*, *9*(2). https://doi.org/10.3390/vaccines9020164

10 Zusammenfassung

Die posttranslationale Modifikation durch das kleine Protein Ubiquitin reguliert nahezu alle zellulären Prozesse und ist unerlässlich für die Proteinhomöostase, die Zellproliferation und das Zellüberleben. In den letzten Jahren wurde eine Vielzahl massenspektrometrischer Methoden entwickelt, um ubiquitinierte Substrate, deren individuelle Modifikationsstellen und die Architektur zellulärer Ubiquitinketten aufzuklären. Darüber hinaus zielten Studien darauf ab, einen umfassenden Einblick in die Modifikationen durch die ubiquitin-ähnlichen Proteine Nedd8, ISG15 und SUMO zu gewinnen. Aktuelle Studien verwenden jedoch entweder sehr komplexe Strategien, um zwischen den Modifikatoren zu unterscheiden, die aufgrund ihrer Ähnlichkeiten in der Primärsequenz oft verwechselt werden, oder ignorieren diese Verwechselung gänzlich. Die Charakterisierung mehrerer Mitglieder einer neuen Klasse von Deubiquitinierungsenzymen bakteriellen Ursprungs ebnete den Weg für deren Einsatz in massenspektrometrischen Studien von Ubiquitin- und ubiquitin-ähnlichen Modifikationssystemen. Diese Enzyme „clippen“ innerhalb des C-Terminus der Modifikatoren und hinterlassen einen GlyGly-Rest an den Modifikationsstellen. Aufgrund ihrer ungewöhnlichen Wirkungsweise wurden diese Enzyme als Clippasen bezeichnet. Eines der charakterisierten Enzyme ist BpJOS aus *Burkholderia pyrrocinia*, das eine außergewöhnlich hohe Aktivität gegenüber Ubiquitin aufweist und dabei unspezifisch auf alle Ubiquitin-Kettentypen wirkt. Darüber hinaus ist BpJOS gegenüber dem Modifikator ISG15 inert. Basierend auf der Aktivität von BpJOS wurden zwei verschiedene massenspektrometrische Methoden entwickelt, um die Lücken der derzeit verfügbaren, etablierten Protokolle zu schließen. Zunächst wurde die einfach anzuwendende Methode „Clippomics“ konzipiert. Diese Methode ermöglicht die Unterscheidung zwischen Ubiquitin- und ISG15-Modifikationen in komplexen Proben durch parallele Behandlung mit der publizierten, ISG15-spezifischen Clippase Lbpro. Darüber hinaus ermöglicht die alleinige Behandlung mit BpJOS die spezifische Identifizierung von Ubiquitinierungsstellen in Gegenwart von ISG15. Dadurch wurden die Veränderungen des Ubiquitoms nach Interferon-Stimulation, wie sie unter Infektionsbedingungen auftreten, untersucht. Beide Anwendungen dienen als Machbarkeitsnachweise für ihren Einsatz in nachfolgenden Studien, da die „Clippomics“-Methode weitere genetische Manipulationen zur Unterscheidung von Ubiquitin und ISG15 entbehrlich macht und auf eine Vielzahl von Proben anwendbar ist. Zweitens wurde BpJOS zur Untersuchung von Ubiquitinkettenverknüpfungen in *In-vitro*-Studien eingesetzt. Die „Ubi-Clipping mit BpJOS“-Methodik ist vom „Ub-Clipping“-Ansatz mit Lbpro inspiriert. Die durch die Clippase erzeugten GlyGly-Reste nach Behandlung von Ubiquitinketten ermöglichen die detaillierte Charakterisierung der vorhandenen Kettenverknüpfungen und -architekturen. Dieser Prozess wird durch die hohe Aktivität von BpJOS gegenüber Ubiquitin im Vergleich zur publizierten Lbpro-Clippase optimiert. Zusammengefasst dient BpJOS als leistungsstarkes, vielseitiges Werkzeug zur Aufklärung von Ubiquitin und ubiquitin-ähnlichen Modifikationen. Beide entwickelten, Massenspektrometrie-basierten Methoden bergen großes Potenzial, einen bedeutenden Beitrag zum Forschungsgebiet der Modifikationssysteme zu leisten.